DOE/NASA/0093--1

DE83 011420

DOE/NASA/0093-1
NASA CR-159773

Advanced Hybrid Vehicle Propulsion System Study

Robert Schwarz
South Coast Technology, Inc.
Ann Arbor, Michigan

May 1982

Prepared for
National Aeronautics and Space Administration
Lewis Research Center
Cleveland, Ohio 44135
Under Contract DEN 3-93

for
U.S. DEPARTMENT OF ENERGY
Conservation and Renewable Energy
Office of Vehicle and Engine R&D
Washington, D.C. 20545
Under Interagency Agreement DE-AI01-77CS51044

PREFACE

The Electric and Hybrid Vehicle Research, Development, and Demonstration Act of 1976 (Public Law 94-413) authorized a federal program of research and development designed to promote electric and hybrid vehicle technologies. The Department of Energy (DOE), which has the responsibility for implementing the Act, established the Electric and Hybrid Vehicle Research, Development, and Demonstration Program within the Office of Transportation Programs to manage the activities required by Public Law 94-413.

The National Aeronautics and Space Administration (NASA) was authorized under an interagency agreement (Number EC-77-A-31-1044) wit.. DOE to undertake research and development of propulsion systems for electric and hybrid vehicles. The Lewis Research Center was made the responsible NASA center for this project. The study presented in this report is an early part of the Lewis Research Center program for propulsion system research and development for hybrid vehicles.

TABLE OF CONTENTS

Table of Contents (cont'd)

1. EXECUTIVE SUMMARY

1.1 Introduction

This report presents the results of a study performed on hybrid heat engine/battery electric-vehicle-propulsion systems. The systems considered all used a rotary stratified-charge engine and an AC motor in a parallel hybrid configuration.

The work involved three major tasks, which are treated in the remainder of this summary. These are:

- o Parametric studies, in which a class of vehicle and a set of propulsion-system design parameters were selected for further study.
- o Design tradeoff studies, which resulted in the selection of design directions for the major components.
- o Conceptual design, in which these design directions were pursued in more detail.

The study was performed by South Coast Technology, Inc., and two major subcontractors, Gould, Inc., and Curtiss-Wright Corporation.

1.2 Parametric Studies

The five vehicle types considered in these studies were:

- o Two-passenger commuter car
- o Four-passenger car (primarily local use)
- o Six-passenger family car (general use)
- o Eight-passenger van
- o Fifty-passenger city bus

Using vehicle weight relationships supplied by LeRC, and component power-to-weight relationships developed by SCT and its subcontractors, propulsion systems were sized for these vehicles to meet performance goals set by LeRC. This analysis was performed for each vehicle type, over a range of heat engine power fractions ranging from 0 (pure electric vehicle) to 1 (conventional heat engine powered vehicle), and for two battery types, nickel-zinc and lead-acid.

In most cases, the critical performance goal was the 0-90 KPH (0-56 MPH) time, which was specified by LeRC as follows:

o Two passenger car	15 sec.
o Four passenger car	12 sec.
o Six passenger car	12 sec.
o Eight passenger van	15 sec.

(No 0-90 KPH time was specified for the bus)

A computer program was developed to analyze the energy consumption of these various vehicle/propulsion system combinations over driving cycles specified by LeRC. The program incorporated a control strategy with a bi-modal structure, which allowed the propulsion battery to discharge to a specified level (discharge limit) on the first mode, and which maintained it at that level in the second mode. This strategy permitted a portion of the vehicle energy requirements normally supplied by on-board fuel to be shifted to wall plug electricity. The control strategy also called for the heat engine to be running only when the power demand was high enough so that it could be operated within an efficient region. This program was exercised for all the vehicle propulsion system combinations to provide estimates of annual fuel and wall plug energy consumption under the usage conditions specified by LeRC. These results, together with estimates of proulsion system acquisition costs, battery life and replacement costs, and maintenance and repair costs, were then used to estimate life cycle costs for the various propulsion systems. (Note: All cost estimates are given in 1976 $, per LeRC guidelines.)

These studies gave the following results:

- For all vehicles, fuel consumption increased and wall plug energy usage decreased as the heat engine power fraction increased from 0 (pure electric) to 1 (pure heat engine). This was expected. However, the life cycle cost steadily decreased over the same range of values of heat engine power fraction. In other words, for all vehicles and missions considered, it is cheaper to buy and operate a conventional vehicle than a hybrid, both of which use the same heat engine technology. This conclusion held true for assumed 1985 energy pricing ($1.50/gal. for gasoline, $.06/KWH for electricity, in 1976 $) and for 1990 pricing ($2.00/gal. and $.07/KWH).

- The application for which a hybrid propulsion system appears to be most nearly competitive with a conventional system is in the large six passenger car. This application had the largest percentage reduction in fuel consumption, and the smallest percentage increase in life cycle cost. Because this application also represents a large segment of the automotive market, it was concluded that it was the most suitable for continued study. LeRC concurred in this conclusion.

- In order to keep the economics of the hybrid system somewhat competitive with a conventional propulsion system, the heat engine power fraction should be at least .7; i.e., the heat engine should be capable of supplying at least 70% of the maximum system power requirement. Moreover, the propulsion battery should be sized so that it operates near its peak power capability when the electric propulsion subsystem is operating at maximum power.

- Based on the battery cost and life assumptions provided by LeRC, the use of lead-acid batteries resulted in a lower life cycle cost than nickel-zinc. However, recognizing the uncertainties involved in any projections regarding cost and life of developmental batteries, both these battery types were kept under study during the subsequent Design Tradeoff Studies task.

1.3 Design Tradeoff Studies

The objective of this task was to develop a design approach for a hybrid propulsion system for the six passenger car application which would provide substantially reduced fuel consumption, compared with a conventional system, and competitive life cycle cost. To this end, variations in design parameters and design approaches were studied at the system, subsystem, and component level. The first step in this effort was the construction (on paper) of a baseline hybrid system, whose design parameters were based on the results of the Parametric Studies Task. A computer simulation of this system was developed which represented the system elements in considerably greater detail than the program used in the Parametric Studies. This simulation, appropriately modified as required by the particular study being done, was used to quantify the variations in fuel and energy consumption which resulted from changes to the baseline system in design parameters, component characteristics, or system configuration.

The design parameters for the baseline hybrid system are summarized below:

Heat Engine - Single rotor, direct-injected stratified charge, 70 KW peak output at 6000 RPM.

Electric Propulsion Subsystem - Induction motor with thristor AC controller, 28.5 KW peak output at 3600 RPM.

Propulsion Battery - Improved state of the art lead-acid, 390 KG weight, 95 W/KG peak utilized specific power.

Transmission - 4 speed automatic with torque converter.

In terms of mechanical configurations, the heat engine and induction motor were in-line with a clutch between them to permit the heat engine to be decoupled from the system and shut down when it is not required. The traction motor drove through the torque converter and drove the accessories (power steering pump, transmission front pump, etc.).

The control strategy used for the baseline hybrid was, again, a bi-modal strategy with the change in mode being determined by battery depth of discharge; and the heat engine operated in an on-off manner. The elements of the strategy were as follows:

Mode 1 (Depth of discharge above a specified discharge limit) - Heat engine is off unless the system power demand is above a minimum level, which was determined from optimization studies to be about 17 KW (22.8 HP). For power demands above this level, the heat engine is brought on-line and operated whenever possible along an optimum power vs. speed line. The traction motor supplies the difference between the power demand and that supplied by the heat engine.

Mode 2 (Depth of discharge held constant at the discharge limit) - In this case, the heat engine must meet the average system power demand, and it operates a much larger fraction of the time than on Mode 1. It is brought on-line whenever the torque demand exceeds a minimum level of 23.8 N-M (17.6 ft.-lb.). Once the heat engine is on-line, the electric motor is operated at zero current draw unless the system demand exceeds the heat engine's capability, in which case the motor makes up the difference. The motor is used for regenerative braking on both Modes 1 and 2.

With this basic control strategy, it was found that it was possible to operate the heat engine at an average brake specific fuel consumption which was only 6.5% higher than its lowest possible value on Mode 1, and 10% higher on Mode 2. Both these results were attained on the Federal Urban Driving Cycle. The battery discharge limit was set, more or less arbitrarily, at 60% of the maximum energy which could be withdrawn from the battery under the discharge pattern experienced in the hybrid. Subsequent analysis indicated that this limit could be set up to 80% without significant loss in performance or battery life.

With the 60% discharge limit, the baseline hybrid met all the performance and gradeability goals set by LeRC. The yearly average fuel consumption was estimated to be .0431 l/km (54.6 mpg) vs. .0881 l/km (26.7 mpg) for a reference conventional propulsion system. The hybrid also consumed .196 kwh/km of wall plug electricity. With regard to costs, it was found that, with $2/gal. for gasoline and 7¢/kwh for electricity, the life cycle cost for the baseline hybrid system was 7.17¢/km vs. 6.11¢/km for the reference conventional system. Major factors in the excess cost of the hybrid system were acquisition costs for the electric propulsion system and battery, and battery replacement costs. At the 7¢/kwh electricity cost level, the break-even fuel price point for the hybrid was about $3/gal. No justification could be found for assuming fuel prices at this level, so the values of $2/gal. and 7¢/kwh were retained.

With the baseline system characterized, a number of computer simulation runs and cost analyses were made to assess the effects of variations in design parameters from the baseline values. The first of these parameters was the heat engine power fraction. This analysis confirmed the findings of the Parametric Studies Task; i.e., fuel consumtpion increased, but life cycle cost decreased with increasing heat engine power fraction. However, it was also found that the rate of increase of fuel consumption got much higher when the power fraction was pushed much past .7, and it was concluded that the best compromise between fuel consumption and life cycle cost was in the .7 to .75 region. Consequently, there was no reason to change from the baseline value of .71.

Variations in design parameters involving the propulsion batteries were also studied. These parameters included:

- o Battery weight (equivalently, maximum battery specific power)
- o Battery type (i.e., lead-acid, nickel-zinc, or nickel-iron*)
- o Battery specific energy

The results of this study included the following:

- o Increasing the maximum battery specific power to permit a reduction in battery weight of 16.7% increased fuel consumption by 7%, decreased wall plug energy consumption by 10%, and decreased life cycle cost by 3.1%.

- o Reducing battery specific energy by 20% (leaving peak specific power and battery weight unchanged) increased fuel consumption by 10%, decreased wall plug energy consumption by 9%, and increased life cycle cost 2.1%.

- o Of the three ISOA battery types, with the batteries sized to take advantage of their respective peak specific power capabilities, the system with nickel-iron batteries achieved slightly lower life cycle cost and slightly lower fuel consumption than the baseline lead-acid system. The nickel-zinc system achieved the lowest fuel consumption (20% lower than the baseline), but the life cycle cost was significantly higher (17% above the baseline) due to high battery cost and frequency of replacement.

It must be noted that these results were obtained under certain assumptions with respect to battery performance, cost and life which may or may not prove to be true in the event the ISOA batteries reach production status. However, it was possible to draw a more general conclusion which is not so highly dependent on these assumptions. This relates to the dependence of life cycle cost on the battery parameters of peak specific power (w/kg), specific energy (wh/kg), and the ratio of specific cost ($/kg) to life. Specifically, what the study results indicate is that, in minimizing the life cycle cost of a hybrid vehicle, the two most important parameters are, first, peak specific power, and, following it very closely, the ratio of specific cost to life. Specific energy, generally considered as being extremely important in electric vehicles, is of secondary importance in a hybrid, at least in terms of life cycle cost.

* Nickel-iron was not included in the scope of work; however, it was included so that all three ISOA (Improved State of the Art) batteries would be represented.

A parameter which affects life cycle cost and fuel economy, and which is also related intimately to the propulsion battery, is the battery discharge limit at which the transition from Mode 1 to Mode 2 is made. Because of the high average rate at which the propulsion battery discharges in Mode 1, the actual depth of discharge (relative to the standard 3-hour rate) at which the discharge limit is reached, is considerably less than the discharge limit itself. In fact, at a discharge limit of .6, the depth of discharge relative to the 3-hour rate was found to be only 31% for the baseline system. Within the range of discharge limits of .6 to .8, it was found that the reduction in battery life at higher values of discharge limit was outweighed, in terms of cost, by savings in fuel. At a value of .8 for the discharge limit, fuel consumption decreased to .0384 l/km and life cycle cost to 7.13¢/km from the baseline values of .0431 l/km and 7.17¢/km, respectively. The change in discharge limit from .6 to .8 was incorporated in the subsequent work in the Conceptual Design Task.

Another area of study in the Design Tradeoff Studies involved variations in vehicle characteristics and design parameters. In particular, the effects of variations in vehicle performance requirements were investigated to determine whether a reduction in these requirements would alleviate the hybrid's problem of high life cycle cost. The effect of a reduction in acceleration performance was, indeed, found to be significant, provided the reduction was fully taken advantage of by holding the peak battery specific constant, thereby reducing the battery size. Holding the heat engine power fraction and the peak battery specific power at the same values as the baseline, and reducing the 0-90 kph acceleration time by about 8% (1 sec.), resulted in a reduction in life cycle cost by 4% to 6.88¢/km. Surprisingly, the lower performance system consumed about 2.6% more fuel than the baseline; this was a result of the fact that the reduction in battery size produced a net decrease in the fraction of the total vehicle energy requirements which was supplied by stored energy. It was concluded from this investigation that the life cycle cost picture for the hybrid could be improved somewhat by backing off on the performance requirements. It would be appropriate to consider this in defining the requirements for a hardware development program; however, for the duration of this program, the requirements as defined by LeRC were adhered to.

Design approaches other than those used in the baseline system were investigated for the system mechanical layout, the transmission, heat engine, and electric propulsion subsystem. An alternative mechanical layout was considered in which the torque converter was interposed between the heat engine and the electric

motor, rather than both components driving through the torque converter. This has the advantage of reducing torque converter losses; however, it also means that a separate accessory drive system is required (since, with this configuration, the electric motor is stopped whenever the vehicle is). It was found that the cost of a separate accessory drive would not be offset by the fuel savings, so no further consideration was given to this layout. It would, however, provide a viable alternative for a system in which the heat engine ran continuously and would thus be available to drive accessories directly. However, simulation of systems with continuously running heat engines indicated substantial fuel consumption penalties (in excess of 20%) over the baseline system and its control strategy. This associated cost is only slightly offset by a reduction in wall plug energy. Consequently, it was concluded the hybrid system's best chance of being cost competitive with a conventional system is to maximize fuel savings by using an on/off heat engine control strategy. The mechanical configuration used for the baseline system appears to offer the most economical way of implementing such a strategy.

Alternative transmissions were also considered, primarily as a means to eliminate torque converter losses. Transmissions considered included an automatically shifted gearbox and continuously variable transmissions (CVT's). These devices all have one major disadvantage: They provide no shock absorbing capability in the driveline to smooth out the transient associated with suddenly coupling the heat engine into the system and starting it when the power demand requires it. With a torque converter in the system, the severity of this transient is reduced by a factor of about 10. In short, for a small improvement in fuel economy, use of a transmission without a torque converter significantly increases the problem of developing adequate driveability in a system using on/off engine operation. In addition, it imposes an additional development task with regard to the transmission itself. Since the development of a system which incorporates on/off engine operation involves considerable risk in the areas of emissions control, driveability, and engine thermal control, and since the largest fuel economy pay-off is associated with the successful implementation of on/off engine operation, the judgment was made to stay with a transmission that does not complicate this task; i.e., the conventional 4-speed automatic used in the baseline was retained.

A similar "keep it simple and concentrate on what is important" philosophy applied to the tradeoffs involving the heat engine. Alternatives considered here included using a downsized, turbocharged single rotor design and a two-rotor,

9

variable displacement design. In conventional systems, both these approaches at improving the specific fuel consumption at light load operation. However, in the hybrid, such operation is effectively eliminated by the control strategy, so the potential fuel economy gains from turbocharging or variable displacement are extremely small relative to the costs involved. Consequently, the simple single rotor, naturally aspirated design used in the baseline was retained.

Design alternatives considered for the electric propulsion subsystem included the following:

- o Type of semiconductor device (thyristor, transistor)
- o Commutation circuit for thyristor case (individual pole, DC-side)
- o Motor type (AC induction, AC permanent magnet synchronous)

These alternatives were investigated in terms of cost, efficiency, and development requirements. The principal results of this study were the following:

- o The most cost effective approach to motor control, in terms of semiconductor device selection, depends not only on the power level to be controlled, but also on the ease with which the basic controller topology can be modified to serve other functions, in particular, battery charging and the supply of 12 V accessory power. When all these factors are taken into account, it was concluded that, in the time frame of interest (1981-1985 for development, post-1985 for production), an SCR based controller using DC-side commutation would probably have a slight advantage over a transistor based controller, for motor output power levels in the 25-30 kw range. Optimistic and conservative cost projections were made for the controller components for both transistor and SCR approaches. These were then used as a basis for estimating the cost of the complete controller. It was found that the optimistic and conservative estimates for the transistor approach were higher than the corresponding estimates for the SCR approach. However, the ranges of subsystem costs for the two approaches overlapped; i.e., the optimistic cost projection for the transistor based controller was less than the conservative estimate for the SCR based controller.

- o The transistor based controller has the potential for somewhat higher combined motor/controller efficiency than the SCR based system (ca. 86% vs. ca. 82%). In terms of life cycle cost, this would tend to minimize

the cost disparities between the two approaches, although, based on the average of optimistic and conservative projections, the SCR system would still have a slight advantage.

- The permanent magnet synchronous motor offers three major advantages over an induction motor: higher efficiency, higher power factor, and reduction in SCR controller complexity by its ability to commutate the main motor SCR's and, thus, reduce commutation circuitry (some is still required for low speed operation). The principal question mark involves its cost in volume production. Two present manufacturers of motors of this type provided estimates of 3 to 4 times the cost of a comparably rated induction motor. Such a cost penalty would outweigh the savings due to the reduction in commutation circuitry and the improvement in efficiency.

Based on these results, it was concluded that an AC drive system using an SCR controller with DC-side commutation and a three-phase induction motor represented a suitable design approach for continued study. However, because of relatively small difference in cost between transistor and SCR design approaches, it was concluded that any future development program should leave open the option of pursuing the transistor approach if information available at the time indicates changes in the cost projections made in this program. Future costs of permanent magnet synchronous motors remains an open question; it was concluded that development of these motors to achieve lower costs was more appropriate to a component level development program, than to a program involving development of a complete hybrid system.

1.4 Conceptual Design

The Design Tradeoff Studies Task indicated that the configuration and design parameters used for the baseline hybrid propulsion system were, in general, suitable as starting points for continued design and development. (The major exception to this was the battery discharge limit, which was raised from .6 to .8 based on tradeoff study results which showed that this would improve fuel consumption and not adversely affect life cycle cost.) The major components and subsystems of the hybrid propulsion system are as follows:

- Heat engine - A single rotor, 72 CID stratified charge rotary engine rated at 70 kw at 6000 rpm. The engine is mounted in-line with the

electric motor and coupled to it by a hydraulically actuated clutch. The engine utilizes a two-stage direct injection system with the pilot stage initiating combustion and the main stage accommodating the varying load requirement. A high energy ignition system is provided which supplies a long duration spark obviating the possibility of misfire. The combustion zone itself is formed by a pocket in an insert bolted to the rotor face. The temperature of this pocket is maintained at high level by an insulating air gap between the insert and rotor; test results show that maintaining such high temperatures reduces exhaust emission levels. Overall, the engine's thermal efficiency is competitive with that of the best automotive pre-chamber diesels, with low raw emission levels and lower particulate emissions than a diesel.

- Electric propulsion subsystem - Consists of a 3-phase AC induction motor powered by an SCR controller. The inverter configuration is a voltage source, force commutated inverter with DC-side commutation used to turn off the main SCR's. The peak shaft output of the system is 28.5 kw at 3600 rpm. The battery charger is integrated with the controller, utilizing the same major power elements (SCR's and commutation inductors and capacitors). The peak charge rate would be on the order of 2-2.5 kw. The topology of the SCR controller also permits a 12 V accessory supply of about 600 W output to be incorporated without much additional circuitry.

- System controller - Implementation of the bi-modal control strategy requires the use of a microprocessor based controller. An 8-bit unit would be used, with a program memory of between 2 and 4 bytes, a data memory of 256 x 8, and a software program execution rate of at least 20 times per second. The controller interfaces with the vehicle and propulsion system components through suitable sensors and electromechanical actuators.

- Transmission/final drive - Four-speed overdrive automatic with transmission ratios of 2.45, 1.45, 1.0, and .75, a final drive ratio of 4.12, and a converter stall torque ratio of 2.1. Torque converter lockup, or a split mechanical/hydrodynamic torque path, could be provided on the upper gears provided this does not result in excessive transmission of engine start transients to the vehicle.

- o Propulsion Battery - Improved state of the art lead-acid, weighing 390 kg. Voltage would be determined primarily by factors of technical convenience during detail design and development of the motor controls, but would be in the 60-120 V range. An alternative which may be more attractive, depending on whether production costs can be brought down to reasonable levels, is a nickel-iron battery of about 275 kg mass. The associated reduction in vehicle mass would permit a reduction in peak motor shaft output to 26.3 kw, with the heat engine output being unchanged.

- o Cooling and Lubrication System - The preferred approach here is to use a conventional radiator and cooling system to handle the bulk of the heat engine's cooling requirements, together with a system utilizing automatic transmission fluid as a combined lubricant and heat transfer medium, which accomplishes the following functions:

  - Lubrication and hydraulic supply for the transmission
  - Cooling of the induction motor and inverter
  - Engine lubrication and temperature maintenance

  This second system controls the fluid temperature at the entry to inverter by means of an oil cooler and bypass thermostat and reduces the packaging requirements on the inverter by providing it with liquid (rather than air) cooling. By utilizing waste heat from the inverter motor and transmission to keep the motor temperature elevated during its off cycle, it reduces the thermal cycling which the heat engine experiences as it cycles on and off. It is expected that this will alleviate problems in the areas of thermal stress fatigue and emissions control resulting from on/off engine operation.

The projected performance, energy consumption, and life cycle cost for the hybrid propulsion system can be summarized as follows:

1. Performance (at 2216 kg (4875 lbs.) vehicle test weight)
   - o Acceleration: 0-90 km/h in 11.6 sec.
0-50 km/h in 4.4 sec.
40-90 km/h in 8.4 sec.
   - o Gradeability: Maintain 90 km/h on 4% grade indefinitely.
Start from rest on 30% grade, minimum.

2. Fuel and Energy Consumption (yearly average)
   - o Fuel (assumed gasoline), .0384 l/km (61.3 mpg)
   - o Wall plug electricity, .221 kwh/km (.356 kwh/mi)

3. Life Cycle Cost (160,000 km (100,000 mi.) life)
   - o 7.13¢/km (11.5¢/mi.) at $2/gal. gasoline and 7¢/kwh electricity

The above fuel consumption and life cycle cost values compare to values of .0881 l/km (26.7 mpg) and 6.11¢/km (9.8¢/mi.) for a conventional propulsion system, providing the same performance in a vehicle of the same accommodations and using the same heat engine technology. Thus, the hybrid system is projected to reduce fuel consumption by about 60% relative to a conventional system, but at a life cycle cost penalty of about 17%. The life cycle cost penalty has a total present value of about $1600. Reduction in this cost penalty will require reductions primarily in acquisition costs of the electric propulsion subsystem and acquisition and replacement costs (or life) of the propulsion battery, which represent disproportionately high costs relative to the power outputs of these subsystems. These could materialize if the cost projections made in this study for semiconductor devices prove to be conservative, or as a result of battery optimization specifically for the hybrid application. However, it is considered unlikely that the hybrid system will reach actual equality with a conventional system in terms of life cycle cost unless fuel prices reach the $3/gal. level.

The critical areas of development for the hybrid system may be summarized as follows:

- o System Controls. Implementation of a control strategy which minimizes overall fuel consumption requires the development of a microprocessor based controller with considerably higher program and data storage requirements than existing automotive μP systems, along with a large amount of peripheral equipment (sensors, actuators, etc.). Integration of the control algorithms for the heat engine, motor, and transmission to obtain acceptable driveability is viewed as a major development task, particularly since on/off engine operation is involved.

- o Heat Engine. The development of a heat engine and related subsystems to provide adequate durability, acceptable driveability, and acceptable emissions under on/off engine operating conditions is critical. Without the successful implementation of a control strategy in which the heat engine is running only when required, the fuel economy figures given above will not be attainable, and the life cycle cost picture would be worse than it already is.

- Electric Propulsion Subsystem. The key development task here involves optimizing circuit designs to utilize lower cost componentry, and getting as much out of each component as possible. A start was made in the conceptual design generated in this study in the integration of battery charging and 12 V accessory supply functions with the basic motor power supply function.

- Propulsion Battery. Although the battery characteristics corresponding to ISOA lead-acid and nickel-zinc batteries were specified by LeRC for use in this program, the results indicate clearly that a battery designed specifically for a hybrid application should not have the same characteristics as an electric vehicle battery. Specific power and life need to be more heavily emphasized relative to specific energy than in an EV battery, and the discharge rates used in evaluating EV batteries are almost totally irrelevant to the hybrid application. For this reason, any hybrid propulsion system development effort should be paralleled by an effort to develop a battery with characteristics tailored to the hybrid system.

2. INTRODUCTION

Hybrid heat engine/battery electric vehicular propulsion systems offer the potential of reducing petroleum consumption by transferring vehicular energy consumption from on-board petroleum based fuel to wall plug electricity and, hence, to coal, nuclear, hydro, and other non-petroleum energy sources. This report presents the results of a study performed on an advanced version of such a system utilizing a rotary stratified charge engine and an AC motor/controller in a parallel hybrid configuration.

The study involved three major tasks:

- Parametric Studies, in which the applicability of this type of system to five different types of vehicles was studied, and a vehicle type and set of system parameters selected for further study.

- Design Tradeoff Studies, in which alternative design approaches were considered, the influences of various vehicle and propulsion system parameters on system performance, fuel economy and cost determined, and design directions for the major components established.

- Conceptual Design, in which the design directions were followed through in additional detail to establish feasibility of the selected approach.

Subsequent sections of this report will treat each of these areas of activity in detail, in terms of objectives, scope, technical approach, and results.

The study was performed by South Coast Technology, Inc., and two major subcontractors, Gould, Inc., and Curtiss-Wright Corporation. South Coast Technology performed all system level design and analysis, Gould was responsible for the electric propulsion subsystem, and Curtiss-Wright for the heat engine.

3. PARAMETRIC STUDIES

3.1 Objectives and Scope

There were two primary objectives of this task:

1. To isolate, from among a group of reference mission/vehicle combinations, that combination which is most suitable for application of a hybrid propulsion system.

2. To obtain a preliminary estimate of the system design parameters (power requirements, heat engine power fraction, battery weight fraction) appropriate to the selected mission/vehicle combination.

The scope of work undertaken to achieve these objectives is outlined below:

1. Construction of an analytical model of the energy consumption processes in a vehicle with a parallel hybrid propulsion system.

2. Development of a computer program based on this analytical model.

3. Initial trade-off of system options for five reference vehicles.

4. Evaluation of propulsion system performance in terms of:

   a. Energy Consumption
      - Spec. fuel consumption, l/km (gal/mi)
      - Spec. wall plug energy, mj/km (kw-h/mi)
      - Distance travelled, km (mi)
      - Fuel and electric energy usage on a yearly basis

   b. Energy Flow Distribution
      - Energy loss in each subsystem over five driving phases: Acceleration-cruise-coast-brake-idle
      - Subsystems: Heat engine; wall plug powered charger; primary storage; electric motor/generator; controller; transaxle
      - Mode: All heat engine, Hybrid 1 and 2, etc.

5. Life cycle cost estimates of each of the propulsion concept(s) for each of five reference vehicles.

6. Recommendation for single baseline mission/vehicle for more detailed study (1985 technology).

Design constraints and goals for the five reference mission/vehicle combinations were supplied by LeRC. These are summarized in Table 3-1. The usage patterns for the vehicles were also specified by LeRC; these are summarized in Table 3-2 and Figure 3-1. An analytical model for estimating vehicle mass was developed by LeRC and used in this study; this is defined in Table 3-3. Finally, the battery characteristics to be used in the study were defined by LeRC, based on the goals of the Argonne National Laboratory's Improved State-of-the-Art (ISOA) Battery Development Program. These characteristics are defined in Table 3-4 and Figures 3-2 and 3-3.

3.2 Technical Approach

Definition of Basic Parameters

The first step in these studies was to define a set of parameters which have a major influence on propulsion system manufacturing cost, weight, and fuel and energy consumption. The simplest set of such parameters is the following:

1. Battery type (lead-acid, nickel-zinc, etc.).

2. Battery weight fraction, $\overline{W}_B$, defined as the ratio of battery weight, W_B, to vehicle curb weight, W_V.

3. Heat engine power fraction, $\overline{P}_{HE}$, defined as the ratio of peak heat engine power, P_{HE}, to the maximum vehicle power requirement P_{TMAX}.

This parameter set intentionally leaves out a great deal of detail; it does not consider variations in the type of heat engine, traction motor, controller, and so forth. Essentially, the assumption was made that such variations would not affect significantly the range of 'basic' parameter values selected as containing an optimum. For example, if the characteristics of a turbocharged instead of a naturally aspirated engine were used in the various vehicle system

TABLE 3-1. REFERENCE MISSION/VEHICLE DESIGN CONSTRAINTS AND GOALS

A. Basic Design Constraints

Type of Use			Commuting	Family Use (Local)	Family Use (Intercity)	Van (Variable Rt.)	City Bus (Variable Rt.)
Mission/Vehicle Designation			A	B	C	D	E
Payload:	No. of Passengers	-------	2	4	6	8	50
	Cargo	kg (lb)	30 (66)	0 (0)	100 (220)	500 (1100)	225 (500)
	Total	kg (lb)	166 (366)	272 (600)	508 (1120)	1043 (2300)	3629 (8000)
Carriage Characteristics:	Weight (See Appendix A)						
	Aero. Coef., C_DA	m^2 (ft^2)	0.56 (6.0)	0.56 (6.0)	0.60 (6.5)	1.7 (18.3)	3.5 (37.7)
	Tire Roll. Res. Coef.	-------	$0.008 + 1 \times 10^{-5}V + 8 \times 10^{-8}V^1$ (V = km/h)				
	Tire Roll. Radius	m (ft)	0.27 (0.89)	0.29 (0.95)	0.31 (1.02)	0.34 (1.12)	0.518 (1.70)
Accessory Load (Maximum)		Watts	500	600	600	600	1200

B. Design Goals

Min. Top Speed on Level Road:	km/h (mph)	105 (65)	105 (65)	105 (65)	96 (60)	80 (50)
Max. Accel. Time:						
0-50 km/h (0-31 mph)	Seconds	6	5	5	6	12
0-90 km/h (0-56 mph)	Seconds	15	12	12	15	-
40-90 km/h (37-62 mph)	Seconds	12	10	10	12	-
Gradeability at Speed for Specified Distance:						
3% Grade, 90 km/h (56 mph)	km (mi)	1.0 (0.62)	1.5 (0.93)	1.5 (0.93)	1.5 (0.93)	-
8% Grade, 50 km/h (31 mph)	km (mi)	0.3 (0.19)	0.5 (0.31)	0.5 (0.31)	0.5 (0.31)	0.2 (0.12)
15% Grade, 25 km/h (16 mph)	km (mi)	0.2 (0.12)	0.3 (0.19)	0.3 (0.19)	0.3 (0.31)	15% Max. Grd.
Min. Ramp Speed Attainable from a Stop on Uphill 6% Grade in 300 m (984 ft):	km/h (mph)	80 (50)	80 (50)	90 (56)	80 (50)	65 (40)
Min. Sustained Speed up 4% Grade	km/h (mph)	90 (56)	90 (56)	90 (56)	90 (56)	70 (44)

TABLE 3-2. DAILY RANGE FREQUENCY FOR ONE YEAR

DAILY RANGE KM	(MI)	NO. DAY OF THE YEAR	TOTAL RANGE KM	(MI)
0	(0.0)	16	0	(0)
10	(6.2)	130	1300	(808)
30	(18.6)	85	2550	(1585)
50	(31.1)	57	2850	(1771)
80	(49.7)	54	4320	(2685)
130	(80.8)	12	1560	(970)
160	(99.4)	7	1120	(696)
500	(311.0)	3	1500	(932)
800	(497.0)	1	800	(497)
	TOTALS	365	16000	(9944)

NOTE: Use the above date to compute the yearly on-board fuel and wall plug energy consumption for all reference mission/vehicles except the city bus. For days with less than 80 km range, assume the "special test cycle" (STC) shown in Figure 3-1. For days with more than 80 km range, assume that 10% of the distance is driven over the STC and that 90% of the distance is driven at a steady speed of 90 km/h (56 mph).

For the city bus, assume that its daily range is constant and use SAE J227a, Schedule C. Yearly travel is 32000 km.

FIGURE 3-1. SPECIAL TEST CYCLE

(MODIFIED SAE J227a, D CYCLE)

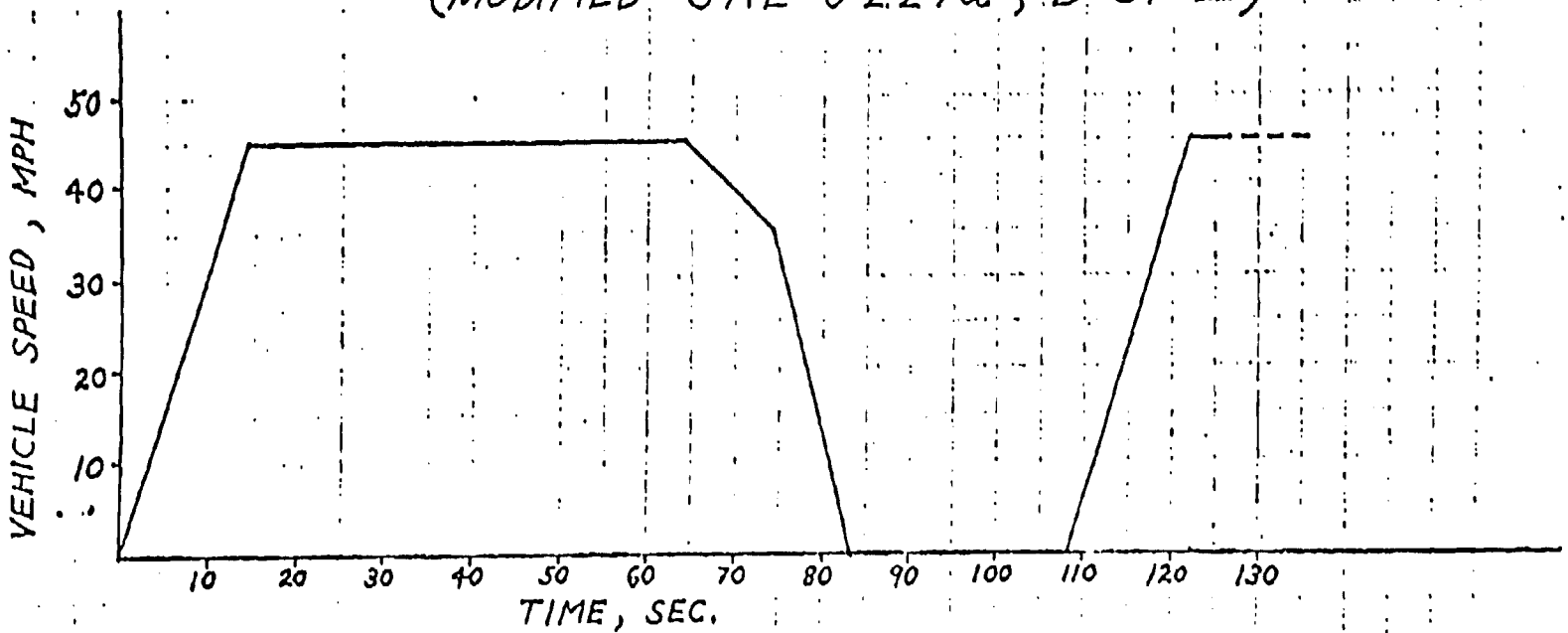

VEHICLE CRUISE SPEED, MPH (km/h)	45 (72)
ACCELERATION TIME, SEC.	14
CRUISE TIME, SEC.	50
COAST TIME, SEC.	10
BRAKING TIME, SEC.	9
IDLE TIME, SEC.	25

TABLE 3-3

PARAMETRIC REPRESENTATION OF WEIGHT

Symbol	Definition	Formula
$W_{PL,\ max.}$	Maximum design payload	-
W_{TL}	Test payload	-
W_F	Fixed weight	-
W_G	Gross vehicle weight	$W_G = W_S + W_{PL,max} + W_P + W_F$
W_C	Curb weight	$W_C = W_G - W_{PL,\ max.}$
W_T	Test weight	$W_T = W_C + W_{TL}$
W_S	Structure and chassis weight	$W_S = 0.23\ W_G$
W_P	Propulsion weight	Determined by contractor

MISSION/VEHICLE SPECIFIC WEIGHT CONSTANTS

Constant	Units	Mission/Vehicle A	B	C	D	E
$W_{PL,\ max.}$	kg (lb.)	166 (366)	272 (600)	508 (1120)	1043 (2300)	3629 (8000)
W_{TL}	kg (lb.)	83 (183)	136 (300)	254 (560)	522 (1150)	1815 (4000)
W_F	kg (lb.)	204 (450)	408 (900)	612 (1350)	816 (1800)	5200 (11464)

TABLE 3-4. ISOA BATTERY CHARACTERISTICS

	Lead-Acid	Nickel-Zinc
Specific Energy[a], Wh/kg	40	80
Specific Power[b], W/kg	100	150
Cycle Life[c]	800	500
Cost[d], $/kWh	50	75
Energy Efficiency	>.6	0.7

a. At a 3h discharge rate and an 8h charge rate.

b. Peak from battery - 15 second average

c. Number of discharges to 80% depth of discharge from rated capacity. Duty cycle is 4-8 hour charge, 2-4 hour discharge.

d. Price delivered to auto manufacturer with a production of 10,000 units per year.

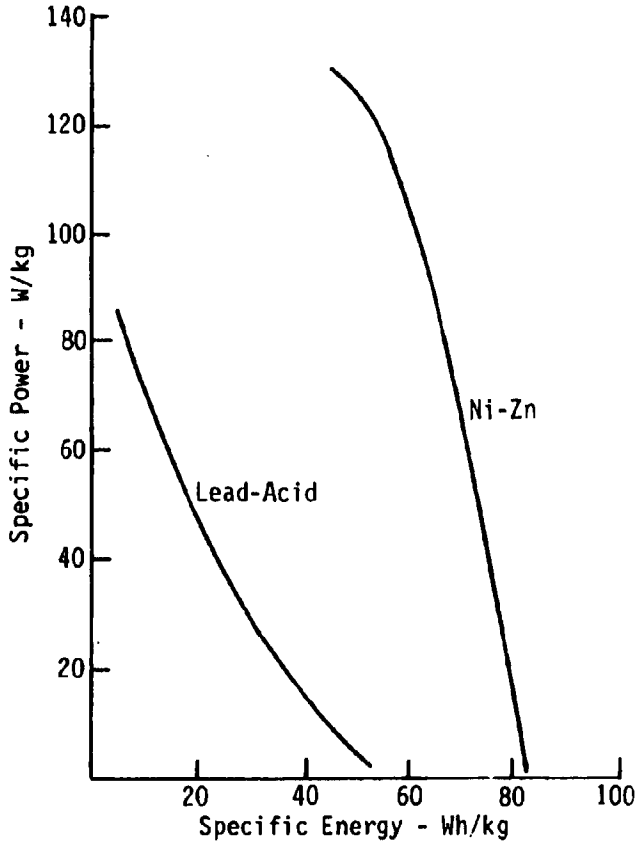

FIGURE 3-2. RAGONE PLOTS FOR ISOA BATTERIES

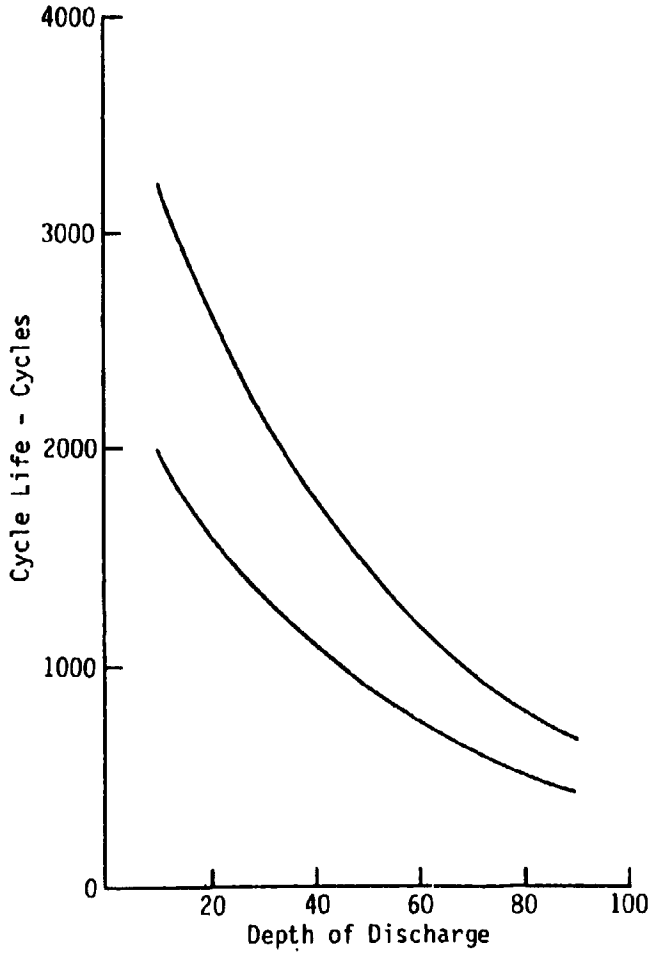

FIGURE 3-3. LIFE CHARACTERISTICS OF ISOA BATTERIES

models, this would not change the conclusion that the battery weight fraction should fall within a certain narrow range, and the heat engine power fraction within another narrow range, and so forth. This assumption was necessary to permit the universe of possibilities, which would be investigated in more detail in the design trade-off studies, to be kept down to a manageable size.

Vehicle and Propulsion System Design Parameters

The next step was to determined the variation in vehicle and propulsion system physical characteristics (power ratings, weights, etc.) with these basic parameters. This was done by first determining the power-to-mass ratios required to achieve the performance goals shown in Table 3-1. Because of the fact that an AC electric propulsion system has a power curve which is shaped differently than that of an internal combustion engine, the required power-to-mass ratio varies somewhat as a function of the heat engine power fraction. The following assumptions were made in determining the required power-to-mass ratio:

1. The heat engine has a maximum torque curve shape typified by that of a stratified charge rotary engine, as exemplified by the Curtiss-Wright RCI-60 engine (Figure 3-4).

2. The maximum torque curve for the electric propulsion system is defined by a constant torque output up to a certain speed, followed by a constant power output above that speed (Figure 3-5).

3. The transmission characteristics are typified by a 4-speed overdrive automatic transmission. The program which was used for simulating full throttle accelerations, VSPDUP, does not have the capability of modeling a torque converter. Consequently, the torque multiplication range of the torque converter was represented by the first gear in a 5-speed transmission; this gear was assigned a much lower efficiency than the other four gears.

A series of runs were made with the VSDUP program (see Section 3.3 for details) to determine the power-to-mass ratios needed to meet the acceleration performance goals with various heat engine power fractions, for the five dif-

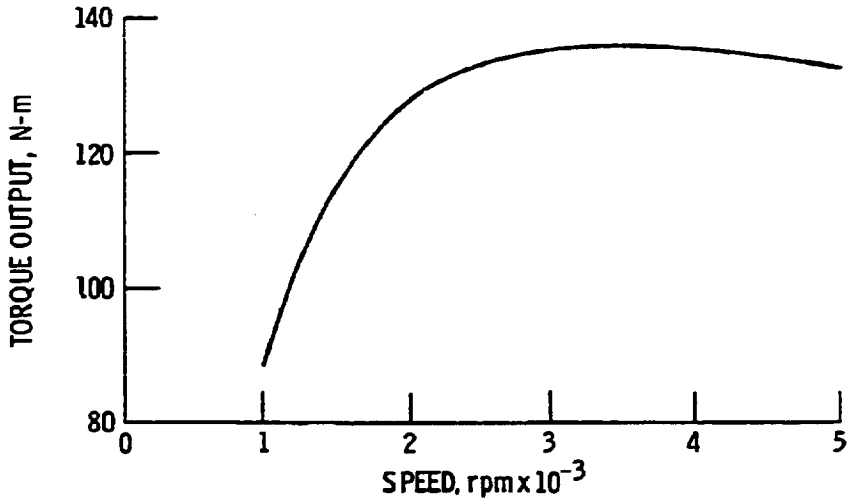

FIGURE 3-4. - TYPICAL MAXIMUM TORQUE CURVE FOR ROTARY STRATIFIED CHARGE ENGINE.

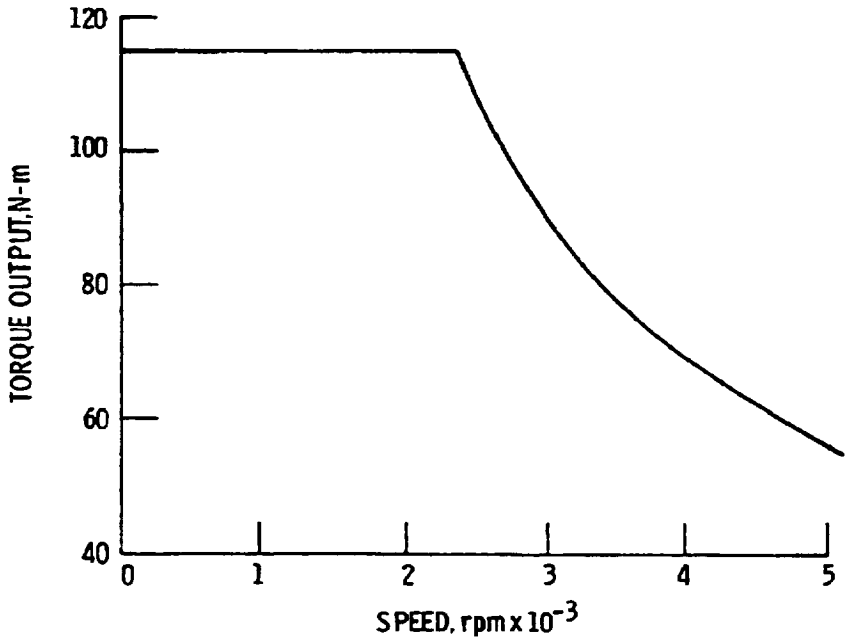

FIGURE 3-5. - TYPICAL MAX TORQUE CURVE FOR TRACTION MOTOR.

representation defined by LeRC (Table 3-3). The mass relationships shown in Table 3-3 reduce to the following:

Vehicle A	$W_T = 1.3\ W_p + 398$ (Kg)
Vehicle B	$W_T = 1.3\ W_p + 748$ (Kg)
Vehicle C	$W_T = 1.3\ W_p + 1202$ (Kg)
Vehicle D	$W_T = 1.3\ W_p + 1896$ (Kg)
Vehicle E	$W_T = 1.3\ W_p + 9664$ (Kg)

Thus, the test mass is a simple linear function of the propulsion system mass. Note that the above equations imply a mass propagation factor of .3; i.e., for ever Kg of propulsion system mass added, .3 Kg must be added in vehicle structure, brakes, etc.

The propulsion system masses were defined by a set of linear relationships, with the respective power levels, as summarized in Table 3-5. These relationships were based on information supplied by the heat engine and electrical propulsion subcontractors, Curtiss-Wright and Gould, and were subsequently updated in later phases of the program.

The procedure used to determine the power-to-mass ratios required to meet acceleration performance requirements was as follows:

1. Assume a value for the total power required and compute the heat engine and motor power ratings corresponding to the heat engine power fraction for the particular case under consideration.

2. Compute the propulsion system and test weights based on the relationships in Table 3-3 and 3-5.

3. Using the vehicle test weight and power ratings determined above, run VSPDUP to determine 0-50, 40-90, and 0-90 KPH acceleration times.

4. Adjust total power and heat engine and motor ratings in the direction indicated by the results of the VSPDUP runs and go back to step 2.

TABLE 3-5

Heat Engine: $W_h = 2.3 P_h + 95$

where W_h = heat engine weight, kg

P_h = heat engine power, kw

Electric Motor & Controller: $W_e = 3.3 P_e$

where W_e = electric motor weight, kg

P_e = electric motor input power, kw

ISOA Batteries: $W_b = 10 P_e$

where W_b = ISOA battery weight, kg

P_e = battery power, kw

NiZn Batteries: $W_b = 6.67 P_e$

where W_b = NiZn battery weight, kg

P_e = battery power, kw

Transmission Weight: $W_t = 1.12 P_t + 31$

where W_t = transmission weight, kg

P_t = transmission power, kw

Estimation of Fuel and Energy Consumption

Once the basic characteristics (weights and power ratings) of the five vehicle types were established, as functions of the heat engine power fraction, the next step was to estimate the fuel and energy consumption, again as functions of the heat engine power fraction. This estimation was done by the hybrid vehicle simulation program HYBRID, a detailed description of which is found in Section 3.3 of this report. This simulation computes fuel and energy consumption on specified driving cycles; for example, on the special test cycle and at constant speeds. Based on this information, it computes yearly average fuel and energy consumption using the daily range frequency provided by LeRC (Table 3-2).

In computing fuel and energy consumption on a driving cycle, it was necessary to provide the simulation with a means for determining how to allocate the total power demand between the heat engine and traction motor; i.e., a control strategy. This control strategy was designed to operate the heat engine as much as possible near its minimum bsfc, and to use stored energy for as much of the total driving as possible. As a result of earlier work on a near term hybrid vehicle program,[1] it was concluded that to minimize fuel consumption, it would be best to shut the heat engine off entirely unless the power demand was too high for the traction motor to handle, or the batteries were at too low a level of discharge. This approach presents some major development problems for heat engine, which are discussed later in this report. However, Curtiss-Wright felt that the problems are not insurmountable, and the fuel economy pay-off makes the approach worth pursuing.

Consequently, for a preliminary control strategy, a bi-modal strategy with the characteristics defined in Table 3-6 was assumed. The strategy is defined by two quantities: the maximum battery discharge level, D_{BMAX}, and a minimum heat engine operating power level, P_{EOMIN}. Until the battery reaches the discharge level D_{BMAX} (Mode 1), the system is operated on stored energy (Cases 1.1, 1.4) unless the system power demand P_{SO} exceeds the heat engine cut-in value P_{EOMIN}. For system demands above P_{EOMIN}, the heat engine is operated at P_{EOMIN} (Case 1.2) unless the system power demand is so great that the motor output exceeds the maximum available, P_{MMAX} (Case 1.3). Once the battery reaches the maximum discharge level, the second operating mode takes over. On this mode, the roles of the heat engine and traction motor are

TABLE 3-6

PRELIMINARY CONTROL STRATEGY

MODE	BATTERY DISCHARGE		COMBINED HEAT ENGINE & MOTOR OUTPUT POWER, P	HEAT ENGINE OUTPUT POWER,	MOTOR OUTPUT POWER,
1	$\leq D_{BMAX}$	1.1	$0 \leq P_{SO} \leq P_{EOMIN}$	0	P_{SO}
		1.2	$P_{EOMIN} < P_{SO} \leq P_{EOMIN} + P_{MMAX}$	P_{EOMIN}	$P_{SO} - P_{EOMIN}$
		1.3	$P_{EOMIN} + P_{MMAX} < P_{SO} < P_{HEMAX} + P_{MAX}$	$P_{SO} - P_{MMAX}$	P_{MMAX}
		1.4	$P_{SO} < 0$	0	MAX (P_{SO}, P_{MMIN})
2	$> D_{BMAX}$	2.1	$0 < P_{SO} \leq P_{HEMAX}$	P_{SO}	0
		2.2	$P_{HEMAX} < P_{SO} \leq P_{HEMAX} + P_{MAX}$	P_{HEMAX}	$P_{SO} - P_{HEMAX}$
		2.3	$P_{SO} \leq 0$	0	MAX (P_{SO}, P_{MMIN})

P_{EOMIN} = Minimum heat engine operating power level (Mode 1)

D_{BMAX} = Battery discharge level (0 = fully charged, 1 = fully discharged)

P_{HEMAX} = Maximum heat engine power output

P_{MMAX} = Maximum traction motor power output

essentially reversed; on Mode 1, the heat engine is used for peaking, whereas on Mode 2, the traction motor is used for peaking (and regenerative braking), and the heat engine supplies the average system requirements.

This control strategy is by no means optimum; however, it is plausible, and it accomplishes the two goals of running the heat engine as much as possible near its minimum bsfc and using as much stored energy as possible. Consequently, it is adequate for the purposes of comparing different values of the two basic parameters, and comparing the reference vehicle/mission combinations.

Component Characteristics

As discussed in Section 3-3, HYBRID models the heat engine fuel consumption characteristics by a curve of brake specific fuel consumption vs. power output. These curves were developed from engine fuel maps supplied by Curtiss-Wright by drawing a line which runs roughly normal to the lines of constant bsfc and passes through the region of minimum bsfc. An example of the resultant curve is shown in Figure 3-6, for Vehicle C.

The electric motor/controller were represented by a relationship of the form

$$P_{IN} = P_o + \frac{P_{OUT}}{\mu}$$

where P_o is a term representing fixed losses and μ is an efficiency factor. Typical values used were P_o = 1 kw and μ = .87 for a machine with 29 kw maximum power. At an average operating level of 10 kw, this gives an overall motor/controller efficiency of 80%, which is consistent with the preliminary estimates provided by Gould of 85-89% for the motor and 90-94% for the controller.

Transmission and differential were modeled simply as constant efficiency devices with efficiencies of .92 and .96, respectively.

Propulsion batteries were modeled by the curves shown in Figures 3-2 and 3-3; details on the structure of the battery model used will be found in Section 3.3.

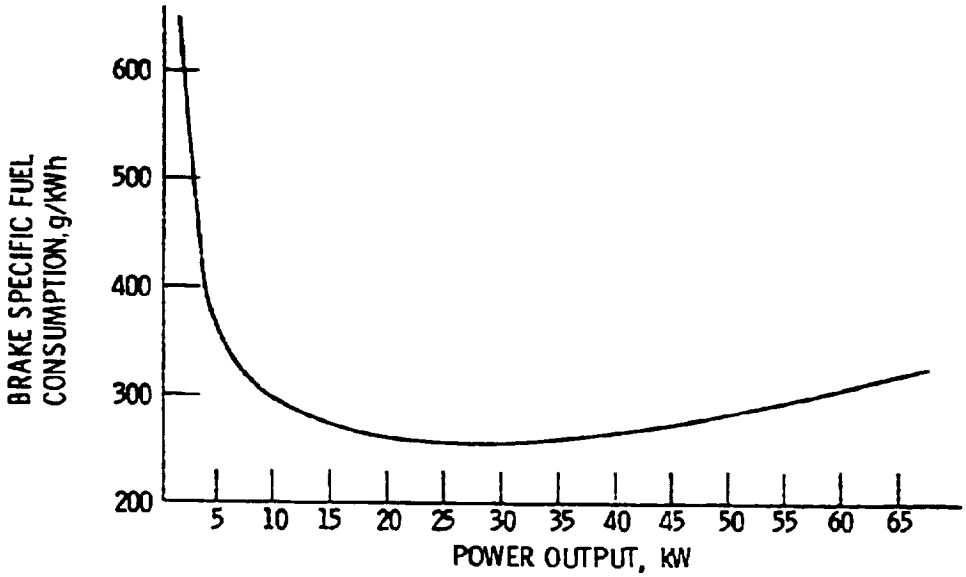

FIGURE 3-6. - TYPICAL CURVE OF BSFC vs POWER OUTPUT.

Life Cycle Cost

The final step in assembling the information required to select a reference vehicle/mission combination and a set of basic parameters for it was to determine the life cycle costs for various hybrid configurations for a life of 10 years and compare these costs to comparable heat engine powered vehicles. A computer program, LYFE2, described in Section 3.3, was used to determine these costs. This program computed costs only for the propulsion system, including batteries if used; other vehicle costs were not considered.

The cost factors included in the life cycle cost computation included the following:

- o Acquisition cost
- o Fuel and electrical energy cost (per gal., KWH)
- o Fuel and energy consumption
- o Battery replacement costs
- o Maintenance

Acquisition costs were based on the heat engine and electric drive system power ratings determined using the VSPDUP program. The following relationships were used in determining manufacturing cost:

Heat engine: $C_{HE} = \begin{cases} 110 + 4.4\ P_{HE} & \text{(1 rotor engine)} \\ 170 + 5.5\ P_{HE} & \text{(2 rotor engine)} \end{cases}$

where P_{HE} = heat engine power rating,

C_{HE} = heat engine manufacturing cost.

Electric drive system: $C_M = 350 + 16.6\ P_M$

where P_M = peak power rating of system,

C_M = system cost.

Transaxle: $C_T = 255 + .82\ (P_{HE} + P_M)$

Two cases were considered in deriving acquisition cost from manufacturing cost, which were considered to provide upper and lower bounds on this cost. In the first case, all manufacturing and OEM costs (including battery) were simply multiplied by a factor of two to obtain acquisition cost. The second corresponded to a situation in which the incremental cost of a hybrid over a conventional IC propulsion system is passed on at a minimum markup (i.e., no profit made on the increment). In this case, the cost was estimated as twice the manufacturing cost of the conventional system plus 1.25 times the increment between the conventional and hybrid systems.

Fuel and electrical energy costs were considered for two time periods, 1985 and 1990. Fuel costs were assumed to average $1.50/gal. for the time period starting in 1985 and $2.00/gal. for the period starting in 1990. Electrical (wall plug) energy costs were assumed to average $0.06/KWH for the period starting in 1985 and $0.07/KWH for the 1990 period.

Battery replacement costs were based on OEM prices of $2/kg for lead-acid batteries, and $6/kg for nickel-zinc batteries.

Vehicle/Mission Recommendation and Power Fraction Determination

The selection of the vehicle/mission combination for detailed study was made based on the fuel consumption and life cycle cost analyses. The criteria were the following:

- The selected vehicle/mission should have the highest potential fleetwide fuel savings when the mission is performed by hybrid vehicles.
- The life cycle cost of the hybrid propulsion system should be competitive with that of a conventional system.
- There should be substantial marketing as well as engineering reasons for using hybrid vehicles in the selected mission.

3.3 Analytical Models and Computer Programs

In this section, the general structure of the analytical models and corresponding computer programs used in the Parametric Studies task are discussed. Specific details including equations are found in Appendices A-C for those computer programs which were either developed or modified under this contract.

VSPDUP

This program was developed prior to this contract. It is used for estimating the acceleration and grade climbing ability of a vehicle, and is based on a straightforward analytical model which can be summarized as follows:

- Vehicle speed is obtained by the integration of vehicle acceleration, which is determined by the net accelerating force and the vehicle mass and wheel/tire and drive line inertias. Rotating speeds throughout the drive train are computed from the vehicle speed, tire rolling radius, and gear ratios. If the engine speed thus determined exceeds a specified value, the next higher transmission gear is selected.

- Engine and motor torques are computed from tables of maximum torques vs. speeds. Torques throughout the drive train are computed using from the sum of the engine and motor torques, gear ratios, and transmission and differential efficiencies. Transmission efficiency is a function of the gear selected.

- Tractive effort is computed from the differential output torque and tire rolling radius, and the net accelerating force is computed as the difference between the tractive effort and the sum of the forces required to overcome tire rolling resistance, aerodynamic drag, and gradient.

HYBRID

This program was originally developed by SCT under the DOE Near Term Hybrid Vehicle Program, and was improved and modified in the Advanced Hybrid

Propulsion System Program. The program is based on the simplest possible model which permits the effects of changes in the basic system parameters (heat engine power fraction, battery weight fraction, battery type) and control parameters (heat engine cut-in power, battery discharge limit) to be evaluated. The major components are modeled as follows:

- o Heat engine - Represented by a curve of brake specific fuel consumption vs. power output. In effect, this representation assumes the use of a continuously variable transmission which keeps the engine operating along an optimum line through its fuel map.

- o Electric drive system - Input power is represented by a constant plus the output power divided by a constant efficiency. The overall efficiency is thus forced to zero as the output goes to zero. When the motor acts as a generator, the input (actually the negative of the electrical output) is represented by a constant plus the output (negative of the mechanical input) multiplied by a constant efficiency.

- o Transmission - Assumed to be a constant efficiency device.

- o Differential - Likewise, constant efficiency.

- o Tires - Rolling resistance is considered to be linear with vehicle speed (generally, the speed sensitive term is small).

- o Aerodynamic drag - Proportional to the square of the vehicle speed.

- o Batteries - Battery depletion per kilometer on a specified composite driving cycle is assumed to be given by the expression

$$X = \frac{e_c}{\bar{E}_c \left(\frac{P_c}{M_B} \right) \cdot M_B} ,$$

where X is the battery depletion per kilometer

e_c is the battery energy output per kilometer on the composite driving cycle

P_c is the average battery power output over the composite driving cycle

M_B is the battery mass

$\bar{E}_c$ is the battery specific energy corresponding to the average specific power P_c/M_B (see Figure 3-2).

The distance d_1 travelled before the transition from Mode 1 to Mode 2 (see Table 3-6) is made is then given by

$$d_1 = \frac{D_{BMAX}}{X}$$

where D_{BMAX} is the battery discharge limit.

For the purpose of computing battery life, the program assumes that the battery discharge limit is reached on all travel days (which is very nearly true for any hybrid with a reasonably low battery weight fraction). Consequently, the battery life is computed as just the cycle life at a depth of discharge equal to the discharge limit (from Figure 3-3) times the average daily travel distance.

In computational terms, the program deals only with power rather than torques and speeds separately, which is one advantage of the simple component representations described above. A power demand at the drive wheels is computed from the vehicle mass and the acceleration demanded by the driving cycle being simulated, and from the rolling resistance and aerodynamic drag forces. The program then works its way from the drive wheels to the engine and motor output. Based on the control strategy defined in Table 3-6, the power split between the heat engine and electric drive system is computed for both Mode 1 and Mode 2 operations. From the heat engine and motor power levels, fuel rate and battery output power are computed, again, for both Mode 1 and Mode 2 operations. These variables are integrated with respect to time over the duration of the driving cycle to get fuel consumption and battery output energy.

With the fuel and energy consumption computed for Mode 1 and Mode 2 operation on the individual driving cycles, such as the 'special test cycle', the program then proceeds to compute the corresponding Mode 1 and Mode 2 quantities over the composite driving cycles (which vary as a function of the daily travel) by using the appropriate weighting factors. At this point, if the battery energy output on Mode 2 is not zero for any of the composite cycles, the corresponding fuel consumption on Mode 2 is adjusted appropriately to bring it to zero. This adjustment is based on the assumption that, if the battery output is negative (i.e., it is getting charged), then the operation will revert to Mode 1 after the state of charge has risen a small amount, then go back to Mode 2 when the discharge limit is reached again, and so forth. The same algebraic expression derived in the case of the battery energy output being negative

also works in case it is positive, although the physical significance is less clear. The program also computes the range on Mode 1, as previously explained.

Finally, the yearly average fuel and energy consumption are computed based on the distances travelled on Modes 1 and 2 for each of the composite driving cycles, the fuel and energy consumption in Modes 1 and 2 for each cycle, and the distribution of total travel relative to the various composite cycles. The wall plug output is then computed from the battery recharging efficiency.

Inputs to this program include vehicle information such as final drive ratio and efficiency, tire rolling radius, rolling resistance, gearbox efficiency, vehicle mass, driveline inertia, and aerodynamic drag; propulsion system data such as engine power vs. fuel consumption, minimum engine operating power, battery mass and discharge limit, battery data of depth of discharge vs. cycle life and specific power vs. specific energy, electric motor maximum power, motor efficiency, generator efficiency, and average battery regeneration efficiency; finally, usage data, including specifications for any number of driving cycles and their yearly distribution of use. Output includes time, speed, system power, aerodynamic drag energy, tire energy, final drive energy, transmission energy, motor power, engine power, generator power, braking power, motor output energy, engine output energy, generator input energy, brake energy, amount of fuel used and battery output energy. The output is printed at any time interval specified. Total fuel and electrical energy consumed for each driving cycle and the yearly combination of driving cycles are also printed as output.

LYFE2

This is a life cycle cost estimation program which is a simplified version of LYFECC, another program developed in the DOE Near Term Hybrid Vehicle Program. The simplifications made to this program involve deleting all costs which are not directly associated with operation of the propulsion system; e.g., insurance, parking and garaging, and so forth.

The program follows the guidelines set forth in the work statement for estimating life cycle costs. Input data to the program consists of:

- The manufacturing cost of the hybrid propulsion system
- The manufacturing cost of a reference conventional propulsion system
- Battery weight
- Heat engine and motor power ratings
- Percent down payment
- Fuel consumption
- Wall plug energy consumption
- Battery life
- Battery OEM cost
- Distance travelled as a function of vehicle age
- Repair factor as a function of vehicle age

The last item in the list is a factor which multiplies a constant baseline annual repair cost. The first year of the vehicle's life, it is zero and rises with cumulative distance travelled as shown in Figure 3-7. It then drops off in the last year or two of the vehicle's life. This approach to computing repair cost is the same as that used by JPL.[2]

The baseline repair cost, which is modified by the repair factor, is expressed as a linear function of the heat engine, motor, and transaxle power ratings. (See equations in Appendix B .) Maintenance costs are expressed similarly; these, however, are not modified by an age-dependent factor.

Program output consists of the annual operating costs for each year, average annual operating cost, discounted operating costs for each year, and gross and discounted life cycle costs. Discount factors of 2% for personal cars and 10% for commercial vehicles were assumed per work statement instructions.

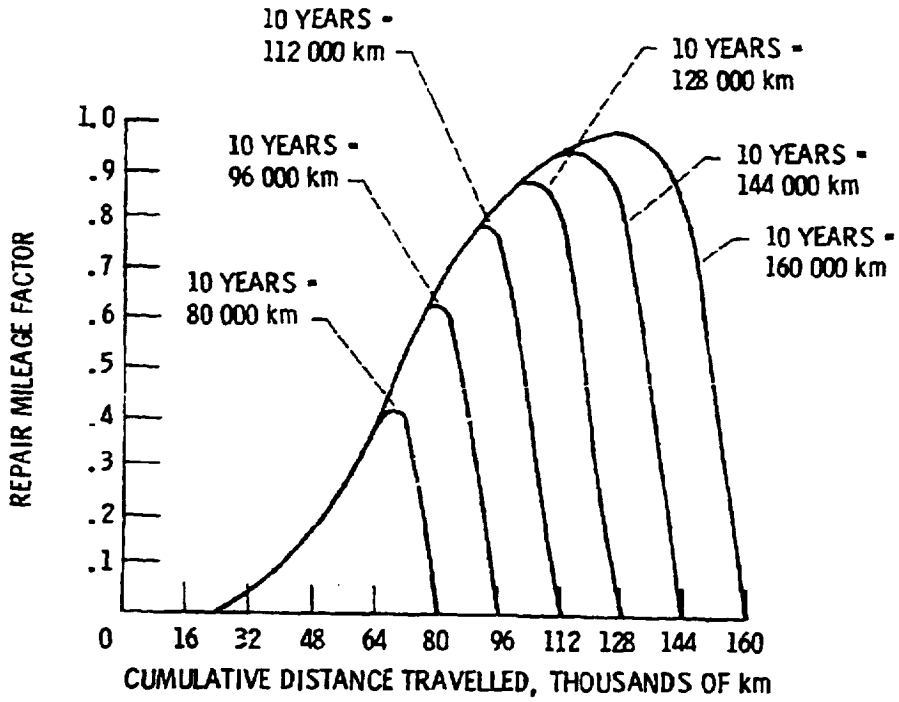

FIGURE 3-7. - REPAIR MILEAGE FACTOR.

3.4 Discussion of Results

3.4.1 Characteristics of Mission/Vehicle Combinations

Power Requirements and Performance Characteristics

A series of runs were made with the VSPDUP program to define the power requirements, vehicle masses, and other characteristics for hybrid vehicles with heat engine power fractions* ranging from 1.0 (all heat engine) to 0 (all electric). Both lead-acid and nickel-zinc battery types were considered for each of the five mission/vehicle combinations. In order to keep the number of combinations of parameter values investigated from becoming excessive, all the vehicles were 'constructed' so that the peak motor power corresponded to the peak battery specific power as defined in Table 3-4.

The results are summarized in Tables 3-7 through 3-11. The following observations are offered about these results:

- As the heat engine power fraction approaches 1, the low speed acceleration (0-50 km/hr) decreases relative to the high speed acceleration (0-90 km/hr and 40-90 km/hr). For heat engine power fractions of 0, .5, and .7, the maximum power requirements were generally defined by the 0-90 km/hr acceleration time. With sufficient power to meet the 0-90 goals, the 0-50 km/hr goals were also satisfied for these heat engine power fractions. However, in the pure heat engine case ($\overline{P}_{HE} = 1$), the amount of low speed torque relative to the torque at higher engine speeds is considerably less than for the other cases (i.e., the power curve is less 'fat'); and for these cases, the critical acceleration goal was generally the 0-50 kph goal. The change in shape of the torque available curve as the heat engine power fraction changes can be envisioned by comparing the typical heat engine and electric motor torque curves shown in Figures 3-4 and 3-5.

---

* The heat engine power fraction, $\overline{P}_{HE}$, was defined as the ratio of the maximum heat engine power to the sum of the maximum battery power output into the motor/controller electrical system and the maximum heat engine power. This definition was later changed (during the Design Tradeoff Studies task) to the ratio of the maximum heat engine power to maximum combined output of the heat engine and electric motor.

Table 3-7. Vehicle A - Commuting

Performance Calculations

		Heat Eng.	Hybrid Lead-Acid	Hybrid Lead-Acid	Electric Lead-Acid	Hybrid NiZn	Hybrid NiZn	Elec. NiZn
Heat Engine Fraction:		1.0	.7	.5	0	.7	.5	0
Power (kw)	- Total	35	36	38	39	34	36	31
	- Heat Eng.	35	25	19	--	24	18	--
	- Elec.	--	11	19	39	10	18	31
Power - Wt. Ratio p/wt.		.0488	.0410	.0378	.0333	.0418	.0400	.0330
Weight (kg)	- Test	718	878	1004	1170	813	900	938
	- Test Load	83	83	83	83	83	83	83
	- Curb	635	795	921	1087	730	817	855
	- Constant	398	398	398	398	398	398	398
	- Heat Eng.	176	152	139	--	150	136	--
	- Elec. Mot.	--	36	63	129	33	59	71
	- Battery	--	110	190	390	67	120	207
	- Trans.	70	71	74	75	69	71	66
Time: (sec)	0-50 km/hr	6.0	5.3	5.1	4.8	5.2	4.8	4.9
	0-90 km/hr	13.6	13.8	13.9	14.0	13.7	13.3	14.6
	40-90 km/hr	8.7	918	10.2	10.7	9.7	9.7	11.2

Table 3-8. Vehicle B - Family Use (Local)

Performance Calculations

		Heat Eng.	Hybrid Lead-Acid	Hybrid Lead-Acid	Electric Lead-Acid	Hybrid NiZn	Hybrid NiZn	Elec. NiZn
Heat Engine Fraction:		1.0	.7	.5	0	.7	.5	0
Power (kw)	- Total	64	69	74	84	64	66	66
	- Heat Eng.	64	48	37	--	45	33	--
	- Elec.		21	37	84	19	33	66
Power - Wt. Ratio p/wt.		.0535	.0455	.0418	.0355	.0462	.0430	.0379
Weight (kg)	- Test	1196	1518	1770	2363	1386	1534	1740
	- Test Load	136	136	136	136	136	136	136
	- Curb	1060	1382	1634	2227	1250	1398	1604
	- Constant	748	748	748	748	748	748	748
	- Heat Eng.	242	205	180	--	198	171	--
	- Elec. Mot.	--	69	122	277	63	109	218
	- Battery	--	210	370	840	127	220	440
	- Trans.	103	108	114	125	103	105	105
Time: (sec)	0-50 km/hr	5.2	4.6	4.4	4.3	4.5	4.4	4.1
	0-90 km/hr	11.4	11.5	11.7	12.2	11.4	11.5	11.6
		7.1	8.0	8.4	9.2	7.9	8.3	8.8

Table 3-9. Vehicle C - Family Use (Intercity)

Performance Calculations

		Heat Eng.	Hybrid Lead-Acid	Hybrid Lead-Acid	Electric Lead-Acid	Hybrid NiZn	Hybrid NiZn	Elec. NiZn
Heat Engine Fraction:		1.0	.7	.5	0	.7	.5	0
Power (kw)	- Total	92	96	104	125	88	90	92
	- Heat Eng.	92	67	52	--	62	45	--
	- Elec.	--	29	52	125	26	45	92
Power - Wt. Ratio p/wt.		.0517	.0435	.0404	.0349	.0436	.0407	.0358
Weight (kg)	- Test	1775	2208	2572	3585	2017	2213	2570
	- Test Load	254	254	254	254	254	254	254
	- Curb	1521	1954	2318	3331	1763	1959	2316
	- Constant	1202	1202	1202	1202	1202	1202	1202
	- Heat Eng.	307	249	215	---	238	198	---
	- Elec. Mot.	---	96	172	412	86	148	304
	- Battery	---	290	520	1250	173	300	614
	- Trans.	134	139	147	171	130	132	134
Time: (sec)	0-50 km/hr	5.3	4.7	4.5	4.4	4.7	4.5	4.3
	0-90 km/hr	11.4	11.8	11.8	12.2	11.9	11.9	12.1
	40-90 km/hr	7.1	8.2	8.5	9.2	8.3	8.5	9.1

Table 3-10. Vehicle D - Van

Performance Calculations

		Heat Eng.	Hybrid Lead-Acid	Hybrid Lead-Acid	Electric Lead-Acid	Hybrid NiZn	Hybrid NiZn	Elec. NiZn
Heat Engine Fraction:		1.0	.7	.5	0	.7	.5	0
Power (kw)	- Total	100	107	112	125	196	100	98
	- Heat Eng.	100	75	56	---	67	50	--
	- Elec.		32	56	125	29	50	98
Power - Wt. Ratio p/wt.		.0399	.0357	.0334	.0292	.0346	.0333	.0293
Weight (kg)	- Test	2504	2994	3358	4279	2776	3002	3349
	- Test Load	522	522	522	522	522	522	522
	- Curb	1982	2472	2836	3757	2254	2480	2827
	- Constant	1896	1896	1896	1896	1896	1896	1896
	- Heat Eng.	325	268	224	---	249	210	---
	- Elec. Mot.	---	106	185	412	96	165	323
	- Battery	---	320	560	1250	193	333	654
	- Trans.	143	151	156	171	139	143	141
Time: (sec)	0-50 km/hr	6.9	5.8	5.5	5.2	6.0	5.5	5.3
	0-90 km/hr	15.1	14.3	14.3	14.7	15.0	14.5	14.8
	40-90 km/hr	9.4	9.9	9.9	11.1	10.4	10.4	11.2

Table 3-11. Vehicle E - Bus

Performance Calculations

		Heat Eng.	Electric Lead-Acid	Hybrid Lead-Acid .7/.3	Electric NiZn	Hybrid NiZn .7/.3
Power (kw)	- Total	260	200	220	185	212
	- Heat Engine	260	-	154	-	148
	- Electric	-	200	66	185	64
Power p/wt.	- Wt. Ratio	.0237	.0149	.0187	.0150	
Weight (kg)	- Test	10,983	13,454	11,750	12,371	11,408
	- Test Load	1,815	1,815	1,815	1,815	1,815
	- Curb	9,168	11,639	9,935	10,556	9,593
	- Constant	9,664	9,664	9,664	9,664	9,664
	- Heat Eng.	693	--	449	--	435
	- Elec. Mot.	--	660	218	610	211
	- Battery	--	2,000	660	1,234	427
	- Trans.	322	255	277	238	268
Time: (sec)	0-50	11.9	10.8	11.4	10.8	11.5

- Due to the variation in the shape of the power curve with the heat engine power fraction, the power-to-mass ratio required to achieve the acceleration goals also varies with the parameter. This variation is summarized in Figure 3-8.

- The power requirements defined in the gradeability goals were, in general, considerably less than those determined by the acceleration goals. This is illustrated in Table 3-12 by the fact that in most cases, the power required to maintain the specified speed on the grade could be supplied by the heat engine alone, which indicates that vehicle could sustain that speed indefinitely. The only exception to this was the van (Vehicle D) with a .5 heat engine power fraction; in this case, the heat engine power determined by the acceleration requirements was insufficient to maintain 90 kph on a 4% grade. Note that the 3% / 90 kph gradeability requirements specified in Table 3-1 are not included in Table 3-12; this is because of the fact that the requirement to sustain 90 kph on a 4% grade, which applies to Vehicles A-D, obviously implies the ability to maintain 90 kph on a 3% grade for a limited distance (1.0 km for Vehicle A, 1.5 km for B-D).

At this point in the program, Vehicle E was dropped from further consideration. The very high power requirements for the traction motor, even for a heat engine power fraction of .7, put it outside the range in which the technology developed would be widely applicable.

Fuel and Energy Consumption

A series of runs with the HYBRID computer simulation was made for the four reference vehicle/mission combinations A-D with various heat engine power fractions and with the two battery types. These runs included the following hybrid configurations:

Heat Engine Fraction	Description
1.0	All heat engine power
.7	70% heat engine and 30% electric power
.5	50% heat engine and 50% electric power
.0	All electric power

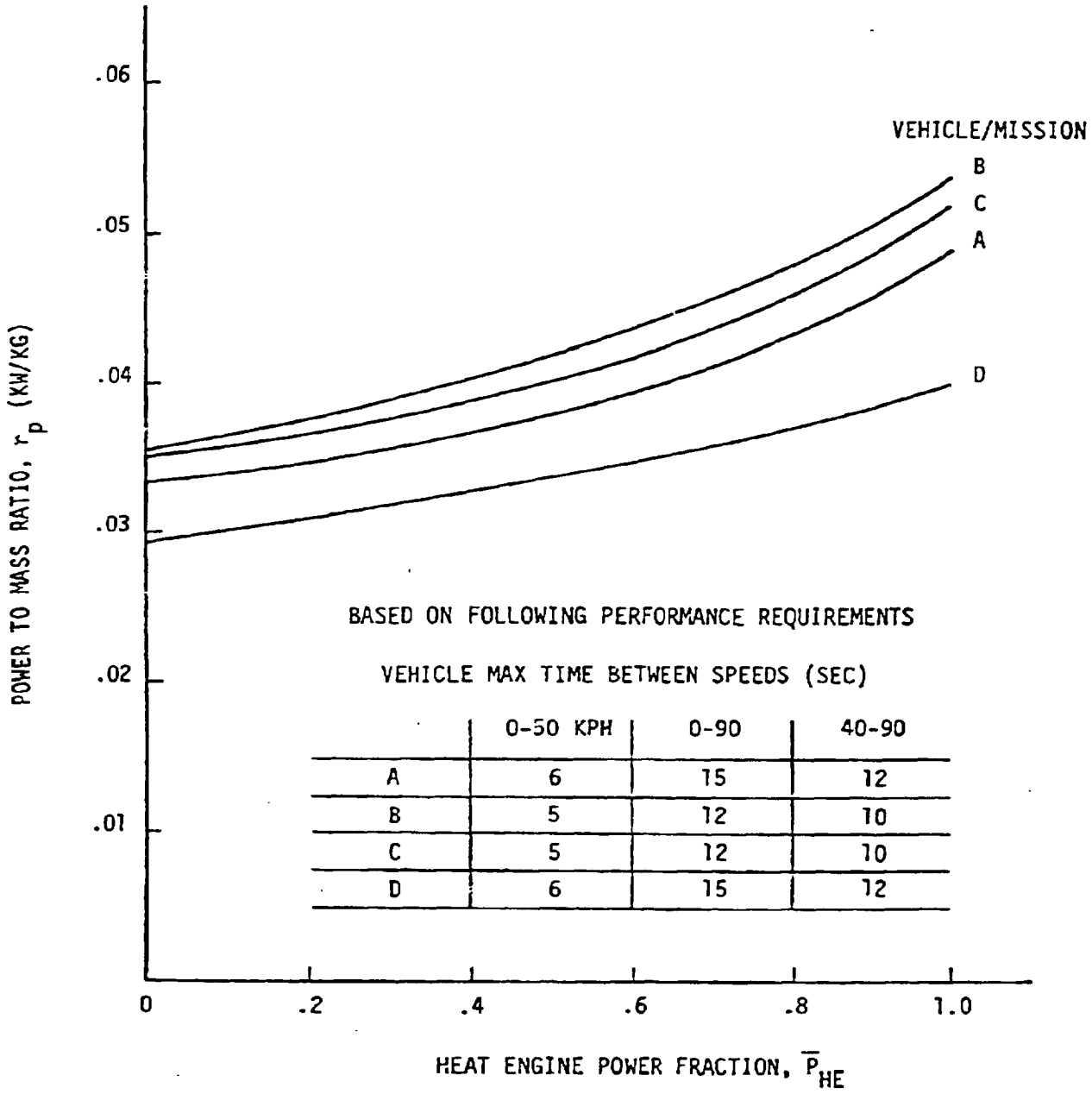

	0-50 KPH	0-90	40-90
A	6	15	12
B	5	12	10
C	5	12	10
D	6	15	12

Figure 3-8. VARIATION IN POWER-TO-MASS RATIO WITH HEAT ENGINE POWER FRACTION

TABLE 3-12

	Grade %	Distance Km	Velocity Km/Hr	Rear Wheel Power Required, Kw .5/.5	Rear Wheel Power Required, Kw .7/.3	Power Available From Heat Engine (at Rear Wheel) .5/.5	Power Available From Heat Engine (at Rear Wheel) .7/.3
Vehicle A	0	Sustained	105	10.8	10.5		
	4	Sustained	90	17.2	15.7	17	22
	8	.3	50	12.9	11.4		
	15	.2	25	10.8	9.5		
Vehicle B	0	Sustained	105	12.6	12.0		
	4	Sustained	90	26.2	23.2	33	43
	8	.5	50	22.1	19.1		
	15	.3	25	19.0	16.3		
Vehicle C	0	Sustained	105	15.0	14.2		
	4	Sustained	90	36.0	31.7	47	60
	8	.5	50	31.7	27.4		
	15	.3	25	27.5	23.6		
Vehicle D	0	Sustained	96	26.8	26.0		
	4	Sustained	90	55.8	51.5	50	67
	8	.5	50	42.9	38.6		
	15	.3	25	36.1	32.2		
Vehicle E	0	Sustained	80		60.8		
	4	Sustained	70		134.5		138.6
	8	.2	50		150.3		
	15	-	25		126.3		

All these vehicles were run on a modified SAE J227a(D) cycle driving cycle (STC) and a constant speed cruise, as defined in Table 3-1. The vehicle and propulsion system parameters were as defined in Tables 3-7 to 3-10. In all cases, the power demand P_{NOM} at which the heat engine was cut in during Mode 1 operation was set at 50% of the peak power available from the electric [illegible]. It was found that, overall, this gave better results than running the [illegible] the way to maximum before cutting in the heat engine, because of the severely diminished capacity of the battery at power levels close to its peak power capability.

The fuel and wall plug energy consumption values obtained from these simulations are summarized in Table 3-13. Vehicles C and D show, in general, the highest annual fuel savings for the hybrid configurations over the pure IC-engined vehicles (heat engine power fraction = 1.0). This is to be expected since these vehicles are larger than the other two. It also appears that the amount of the annual savings is less sensitive to the heat engine power fraction for Vehicle C (passenger car) than it is for Vehicle D (van). This, however, is somewhat exaggerated for the following reasons. In the case of the .7/.3 van, on the cruise section (72 kph) of the special test cycle, the power requirement was just in excess of the power level P_{NOM} at which the heat engine cuts in on Mode 1 operation. As a result, this portion of the driving cycle was done almost entirely on heat engine power. Similarly, on the constant speed (90 kph) cruise, the heat engine cut in and supplied about 60% of the power requirement on Mode 1 operation. The .7/.3 version of Vehicle C, on the other hand, because of its much lower cruise power requirement (due largely to lower aerodynamic drag), was able to handle the cruise portion of the special test cycle, as well as the 90 kph cruise, on motor power only, during Mode 1 operation. The .5/.5 versions of both Vehicles C and D drove both 72 and 90 kph cruise portions on motor power only during Mode 1 operation. As a result of this change in control behavior between the .5/.5 and .7/.3 versions of Vehicle D, this vehicle shows a much higher change in fuel consumption with the change in heat engine power fraction than does Vehicle C. A small change in the value used for P_{NOM} would allow the .7/.3 van to perform the 72 kph cruise under motor power alone; however, it would not be feasible to change P_{NOM} enough to perform the 90 kph cruise on motor power alone. This would take an unrealistically high sustained power from the propulsion battery. On this basis, it is still possible to conclude that Vehicle D's fuel consumption is more sensitive to battery weight fraction than Vehicle C's, although perhaps not to the extent indicated in Table 3-13.

TABLE 3-13

HYBRID VEHICLE SUMMARY

		HYBRID LEAD-ACID		HYBRID NiZn	
HEAT ENGINE FRACTION	1.0	0.7	0.5	0.7	0.5
VEHICLE A					
FUEL CONSUMPTION & ECONOMY - L/KM (MPG)	.0348 (67.6)	.0265 (88.8)	.0212 (110.7)	.0214 (110.1)	.0165 (142.6)
ELECTRICAL ENERGY - KWH/KM (KWH/MI)		.0614 (.0988)	.1033 (.1662)	.0834 (.1341)	.1180 (.1898)
DISTANCE TRAVELED*- KM (MILES)		23.4 (14.5)	44.1 (27.4)	35.3 (21.9)	64.5 (40.1)
YEARLY USAGE:					
FUEL - L (GAL)	556.8 (147.1)	395.2 (104.4)	339.2 (89.6)	342.4 (90.5)	264.0 (69.8)
ELECTRICAL ENERGY - KWH		982	1653	1334	1888
YEARLY FUEL SAVINGS - L (GAL)		161.6 (42.7)	217.6 (57.4)	214.4 (56.6)	292.8 (77.3)
VEHICLE B					
FUEL CONSUMPTION & ECONOMY - L/KM (MPG)	.04855 (48.5)	.03186 (73.8)	.0256 (91.8)	.0255 (91.8)	.02039 (115.3)
ELECTRICAL ENERGY - KWH/KM (KWH/MI)		.1199 (.1930)	.1772 (.2851)	.1449 (.2331)	.1814 (.2919)
DISTANCE TRAVELED*- KM (MILES)		32.1 (20.0)	70.5 (43.8)	47.1 (29.3)	87.5 (54.4)
YEARLY USAGE:					
FUEL - L (GAL)	776.8 (205.2)	509.8 (134.7)	409.6 (108.2)	408.0 (107.8)	326.2 (86.2)
ELECTRICAL ENERGY - KWH		1918	2835	2318	2902
YEARLY FUEL SAVINGS - L (GAL)		270 (70.5)	370.2 (97)	371.8 (97.4)	453.6 (119)
VEHICLE C					
FUEL CONSUMPTION & ECONOMY - L/KM (MPG)	.0660 (36.0)	.0400 (58.7)	.0318 (73.9)	.0313 (75.2)	.0253 (29.9)
ELECTRICAL ENERGY - KWH/KM (KWH/MI)		.1557 (.2505)	.2379 (.2732)	.1863 (.2998)	.2310 (.3717)
DISTANCE TRAVELED*- KM (MILES)		37.5 (23.3)	79.7 (50.8)	52.1 (32.4)	95.7 (59.5)
YEARLY USAGE:					
FUEL - L (GAL)	1056.0 (279.0)	640.0 (169.1)	508.6 (134.4)	500.8 (132.3)	404.8 (107.0)
ELECTRICAL ENERGY - KWH		2491	3710	2981	3696
YEARLY FUEL SAVINGS - L (GAL)		416 (109.9)	547.4 (144.6)	555.2 (1467)	651.2 (172)
VEHICLE D					
FUEL CONSUMPTION & ECONOMY - L/KM (MPG)	.1105 (21.3)	.0953 (24.7)	.0736 (31.9)	.0895 (26.3)	.0574 (41.0)
ELECTRICAL ENERGY - KWH/KM (KWH/MI)		.1221 (.1965)	.3235 (5205)	.1295 (.2084)	.3607 (.5804)
DISTANCE TRAVELED*- KM (MILES)		103.8 (64.5)	37.5 (23.3)	114.4 (71.1)	51.9 (32.3)
YEARLY USAGE:					
FUEL - L (GAL)	1768.0 (467.1)	1524.8 (402.9)	1177.6 (311.1)	1432.0 (378.3)	918.4 (242.6)
ELECTRICAL ENERGY - KWH		1954	5176	2072	5771
YEARLY FUEL SAVINGS - L (GAL)		243.2 (64.2)	590.4 (156)	336 (88.8)	849.6 (224.5)

*DISTANCE TRAVELED UNTIL BATTERY DEPLETION, RELATIVE TO THE DISCHARGE PATTERN ON THE RELEVANT DRIVING CYCLE, REACHES 60% (I.E., BATTERY DISCHARGE LIMIT = .6).

The change in control behavior of Vehicle D is illustrative of the fact that the driving cyclces used (special test cycle and 90 kph cruise) are too simple for effectively optimizing the system control strategy. That is, it would be possible to design a control strategy that works well on those cycles but which would not work well if the driving pattern changes by a small amount from the one defined in terms of these cycles. What is needed are driving cycles whose spectra of power requirements are much more widely distributed, and more representative of real-world driving patterns, than these two cycles. Consequently, in the subsequent tasks (design tradeoff studies and conceptual design), the special test cycle was replaced by the federal urban driving cycle (FUDC) and the 90 kph cruise by the highway cycle (FHDC).

When relative fuel economy, rather than absolute fuel savings, is considered, the situation is slightly different, as shown in Table 3-14. In these terms, Vehicle C shows the largest fuel economy gain relative to a comparable heat engine vehicle.

Life Cycle Costs

Life cycle costs were estimated with the program LYFE2, and the results are summarized in Table 3-19.

The approximate ratios of life cycle costs of the hybrid configurations to the corresponding pure heat engine propulsion system are summarized in Table 3-20.

Several facts are apparent upon inspection of these two tables:

- Life cycle costs for the hybrid propulsion system are considerably higher than for the pure heat engine system, even for cost case 1 in which the manufacturing cost is passed on at a minimum markup.

- Life cycle costs decrease with increasing heat engine power fraction, even at the 1990 period fuel pricing of $2.00/gal. This, of course, is the opposite of the trend of fuel consumption, which increases with increasing heat engine power fraction.

- Life cycle costs for the hybrids using nickel-zinc batteries are higher than those for the lead-acid systems. Even at a heat engine power fraction of .7, the nickel-zinc system costs are higher than

TABLE 3-14

FUEL ECONOMY OF HYBRID VEHICLES RELATIVE TO HEAT ENGINE POWERED VEHICLE

	Hybrid ISOA		Hybrid NiZn	
Heat Engine Fraction	0.5	0.7	0.5	0.7
Vehicle A	1.64	1.31	2.11	1.63
Vehicle B	1.89	1.52	2.37	1.90
Vehicle C	2.05	1.63	2.58	2.09
Vehicle D	1.50	1.15	1.92	1.23

TABLE 3-19

LIFE CYCLE COST SUMMARY

(DISCOUNTED $/KM)

	1985 Hybrid Propulsion					1990 Hybrid Propulsion				
	Heat Engine	Lead-Acid .5/.5	Lead-Acid .7/.3	NiZn .5/.5	NiZn .7/.3	Heat Engine	Lead-Acid .5/.5	Lead-Acid .7/.3	NiZn .5/.5	NiZn .7/.3
VEHICLE A										
Case 1	.02323	.03711	.03302	.05254	.04071	.02730	.04052	.03646	.05553	.04396
Case 2	.02323	.04481	.03884	.07019	.05126	.02730	.04821	.04228	.07317	.05450
VEHICLE B										
Case 1	.03247	.05660	.04452	.08303	.06261	.03814	.06118	.04933	.08704	.06689
Case 2	.03247	.07002	.05120	.11372	.08097	.03814	.07460	.05600	.11773	.08525
VEHICLE C										
Case 1	.04284	.07340	.05850	.10820	.08031	.05055	.07920	.06457	.11323	.08564
Case 2	.04284	.09143	.06833	.14924	.10452	.05055	.09723	.07440	.15427	.10985
VEHICLE D										
Case 1	.06001	.09570	.08084	.13515	.10358	.07292	.10720	.09306	.14509	.11519
Case 2	.06001	.11446	.09243	.18053	.13038	.07292	.12597	.10465	.19047	.14200

TABLE 3-16. RELATIVE LIFE CYCLE COSTS OF HYBRID CONFIGURATIONS

Configuration		1985 - Period Fuel & Electricity Pricing		1990 - Period Pricing	
		Cost Case 1	Cost Case 2	Cost Case 1	Cost Case 2
.5/.5	Lead-Acid	1.6-1.7	1.9-2.2	1.5-1.6	1.7-2.0
	Nickel-Zinc	2.3-2.6	3.0-3.5	2.0-2.3	2.6-3.1
.7/.3	Lead-Acid	1.4-1.6	1.6-1.9	1.3-1.4	1.4-1.6
		1.7-1.9	2.2-2.5	1.6-1.8	2.0-2.2

the lead-acid system costs at a power fraction of .5 (which provides fuel economy comparable to the .7/.3 nickel-zinc system) (see Table 3-13). The high nickel-zinc system life cycle costs are due to the high initial and replacement costs of the battery and its limited life; the slightly better fuel consumption of the nickel-zinc system (for a given power fraction) is not enough to pay for the increment in lifetime battery costs.

3.5 Conclusions

Applicability of Hybrid System to Mission/Vehicle Combinations

Vehicle A (2-passenger commuter) is a type of vehicle which does not exist in today's automobile market, although it will probably appear by the 1985 time frame with conventional IC propulsion, and possibly as an urban electric. The potential fuel economy of such a vehicle is so high (on the order of 60-70 mpg with an efficient engine such as the rotary stratified charge engine) that the magnitude of the potential fuel saving with a hybrid configuration is quite small, in the range of 42-77 gal/yr (depending on configuration) as indicated in Table 3-13. In view of the low fuel savings and uncertain market size for this class of vehicle, it does not appear to be a good candidate for a hybrid propulsion system. This conclusion is reinforced by the fact that, even in the .7/.3 configuration, the heat engine power rating is only 25 KW (33.5 HP), which puts it out of the mainstream of power plant sizes under development for automotive use.

Vehicle B (family use, local) corresponds roughly to a subcompact or slightly larger vehicle in today's marketplace. Quite high fuel economy was projected for the heat engine only version of this vehicle - in the vicinity of 45-50 mpg. Because this vehicle size represents a large fraction of the total market, replacement of these vehicles by hybrids would represent a significiant annual fuel savings. Four factors, however, tend to make this vehicle class less suitable for hybridization than the larger vehicles C (family use, intercity) and D (van): First, vehicles of type B are generally quite compact and efficient in their packaging, and not a great deal of room is available for packaging additional hardware (specifically, the propulsion battery). Second, the sensitivity of this market segment to price is higher; the added initial

cost of a hybrid is less likely to be accepted by a purchaser of this class of vehicle (particularly in view of its already high fuel economy) than by a purchaser of a larger vehicle. Third, the profitability of this type of vehicle to the manufacturer and dealer is generally less than that of the larger, usually more heavily optioned vehicle; consequently, the manufacturer has less discretion with the smaller vehicle in how the added cost of the hybrid is passed on. Finally, the larger vehicles are much more of a problem to manufacturers in terms of meeting fuel economy standards; and an increase in fuel economy by a factor of two in such vehicles would mean a good deal more to a manufacturer's CAFE (corporate average fuel economy) than a corresponding increase in the fuel economy of a smaller, more fuel efficient vehicle; consequently, there is more incentive for a manufacturer to produce such a vehicle than the smaller class of vehicle.

Vehicles C and D, then, appear to be the most suitable for hybrid application; however, Vehicle C represents a much larger market segment than D. Moreover, since Vehicle D is used predominantly in commercial applications in which life cycle cost is a paramount consideration, and since it appears likely that a hybrid system will suffer not only an initial cost penalty but also a life cycle cost penalty, Vehicle C is probably a better choice than D, at least until such time as hybrid costs become competitive with conventional heat engine systems. Consequently, the recommendation was made to LeRC (and accepted) that the remainder of the study concentrate on vehicle/mission combination C.

Preliminary Selection of Basic System Parameters

Because of the contravariant nature of life cycle costs and fuel consumption, there is not a clearly defined optimum heat engine power fraction. Economics drives one toward higher heat engine power fractions and, since quite substantial fuel savings with Vehicle C are attainable even at a power fraction of .7, it was felt that this was the region which should be investigated, rather than the region around .5. From a practical standpoint, a propulsion system designed around this heat engine power fraction could also be more easily packaged in the same vehicle as a conventional propulsion system than could one with the larger battery pack and motor/controller associated with a .5 power fraction. Since hybrid propulsion systems would undoubtedly be introduced as fuel efficient options in production vehicles which would also be available with conventional systems, it makes sense to design for

a situation in which both systems could be accommodated in one vehicle, with a minimum of modification.

With respect to battery weight fraction and battery type, it is clear that whatever can be done to minimize battery weight and replacement cost would be beneficial from a cost standpoint, as well as from the standpoint of ultimately integrating the system into a vehicle. Assuming that the projected battery characteristics supplied by LeRC are accurate, it was concluded that the lead-acid system is economically more viable in a hybrid application than the nickel-zinc system, and that the battery should be sized so that the peak power capability should not be much greater than the peak input to the motor/controller. Consequently, the emphasis in the subsequent tasks was placed on the lead-acid system; however, in recognition of the fact that projections of battery characteristics (particularly life and cost) are highly uncertain, the nickel-zinc system was carried along as an alternative; and, in fact, the nickel-iron system was introduced as a third possibility.

4. DESIGN TRADEOFF STUDIES

4.1 Objectives and Scope

The objective of this task was to develop, for the selected mission/vehicle application, a propulsion system design approach which would provide a balanced combination of performance and cost while meeting the design constraints and goals specified in Table 3-1. Development of this preferred design approach entailed performing design tradeoff studies at system and component levels. The scope of these tradeoff studies involved the following:

System Level

- o Variations in control strategy
- o Variations in system level parameters (heat engine power fraction, battery weight fraction, battery type)
- o Alternative system layouts (mechanical configuration)

Component Level

- o Heat engine design alternatives: single rotor stratified charge engine (RSC), multi-rotor variable displacement RSC engine, turbo-charged RSC engine
- o Motor/controller design alternatives: induction motor, brushless DC (electronically commutated) motor, controller power devices (SCR or transistor) and circuitry.
- o Transmission design alternatives: conventional automatic transmission with torque converter (possibly with lockup capability), automatically shifted gearbox with automatic clutch, various types of continuously variable transmission

These various design alternatives were to be investigated in terms of their effects on cost, fuel and energy consumption, and development requirements. Based on tradeoffs among these areas, a preferred design approach was characterized in terms of the alternatives investigated.

In addition to performing these tradeoff studies, the task also involved an investigation of the sensitivity of the system to changes in the basic assumptions made with respect to the following:

- o Vehicle weight
- o Vehicle performance requirements
- o Road load power requirements (rolling resistance and aerodynamic drag)
- o Battery performance characteristics

4.2 Technical Approach

The approach taken to the design tradeoff studies involved the following steps:

- o Construction of a baseline propulsion system with parameters within the range selected in the parametric studies task.
- o Development of a computer simulation of this system.
- o Preliminary optimization of a control strategy using this simulation.
- o Characterization of the baseline system in terms of fuel and energy consumption, cost factors.
- o Using the computer simulation and other analytical techniques, analysis of the effects of variations in parameters and design approach from the baseline system, and also of the effects of variations in performance requirements and other basic assumptions.
- o In parallel with the above steps, which involved primarily system level tradeoffs, design tradeoffs were conducted at the component level. An example of the work at this level would be the investigation of alternative controller circuit designs.

The basic tools used for these tradeoff studies were three computer simulations, which were somewhat more detailed than those used for the parametric studies task. The simulation programs were titled VSPDUP2 and HYBRID2. Descriptions of these programs and a discussion of the areas in which they differed from the earlier programs, VSPDUP and HYBRID, will be found in the following section of this report.

The basic guidelines, design constraints and goals, weight estimation methodology, and battery characteristics, which are summarized in Tables 3-1 through 3-4 and Figure 3-2, were used in this task as well as the earlier parametric studies task. The principal deviation from the assumptions and methodology used in the parametric studies task was the replacement of the 'special test cycle' defined by LeRC (Figure 3-1) by the Federal Urban Driving Cycle,

and the replacement of the 90 Km/h cruise by the Federal Highway Driving Cycle. The reason for these replacements was discussed in Section 3.4.1 of this report, under "Fuel and Energy Consumption."

4.3 Analytical Models and Computer Programs

The major computer simulations used in this task are modifications of the programs discussed in Section 3.3. Additional detail will be found in Appendices B and C.

VSPDUP2

This program, developed prior to this contract, is a modification of VSPDUP, with the principal difference being that VSPDUP2 incorporates a complete torque converter model. (With VSPDUP, it was necessary to model a torque converter by an additional transmission gear ratio, with low efficiency.) The torque converter is modelled by curves of torque ratio To/Ti (output torque/input torque) and speed ratio (No/Ni) (output speed/input speed) vs. an output speed-torque parameter $No/\sqrt{To}$ (output speed/$\sqrt{}$output torque). For each value of $No/\sqrt{To}$, the program also computes

$$\frac{No}{\sqrt{Ti}} = \frac{No}{\sqrt{To}} \cdot \sqrt{\frac{To}{Ti}}$$

The above set of parameters is adequate to define the input speed and torque for the torque converter given the output speed and torque, or input speed and output torque can be defined given output speed and input torque. However, in simulating a full throttle acceleration, all that is known at any given time is the output speed together with the fact that the power plant torque is a known function of speed. Consequently, a series of iterations is necessary at each step to match the power plant characteristics with the torque converter characteristics.

HYBRID2

This program is an expanded version of HYBRID. As in the case of HYBRID, it was originally developed by SCT under the DOE Near Term Hybrid Vehicle Program, and was improved and modified during this program. The major differences between HYBRID AND HYBRID2 lie in the modelling of the following components:

Heat Engine. HYBRID2 represents the heat engine by a map of bsfc (brake specific fuel consumption) as a function of bmep (brake mean effective pressure) and engine speed, together with a curve of maximum torque vs. engine speed. Because of this detailed engine modelling, it is necessary for the program to deal with torque and speed independently, rather than dealing only with power, as HYBRID does.

Electric Motor/Controls. HYBRID2 uses a representation in which input power is defined as a piecewise linear function of output power. The major difference between this model and the one used by HYBRID is that it models more accurately the drop-off in efficiency which occurs at high power levels.

Accessory Load. Torque required to drive motor driven accessories is modelled as a piecewise linear function of electric motor speed. These accessories include the transmission front pump and power steering pump. The air conditioning compressor, if operational, would also be included here; however, no simulations were actually run with an A/C load on the system. Other accessories, such as the engine cooling fan, are assumed to be electrically driven and do not represent a direct load on the motor.

Torque Converter. This is modelled as described in the last section describing the program VSPDUP2.

Gearbox. The losses in the transmission gears are represented by two components: losses which are proportional to the power being transmitted, and losses which are dependent only on speed (spin losses). The efficiency and spin loss coefficients are specified separately for each ratio in the transmission.

Final Drive. This is modelled like the gearbox, except, of course, there is only one gear ratio to consider.

Batteries. The battery model is similar both to a fractional utilization model and to that used in HYBRID; however, instead of averaging battery power over an entire driving cycle, power is averaged over a more

limited time. Thus, the time history of the battery output over a driving cycle is used to create, by taking a moving average over a specified time interval, a new output time history which is a smoothed version of the original. In mathematical terms,

$$\bar{P}_c(t) = \frac{1}{2\Delta t} \int_{t-\Delta t}^{t+\Delta t} P_c(\tau)\, d\tau$$

where the $P_c(t)$ is the actual battery power output as a function of time, $2\Delta t$ is the averaging interval, and $\bar{P}_c(t)$ is the smoothed output. From this point on, depletion is computed as in a fractional utilization model. At each time t, the available battery specific energy $\bar{E}_c(t)$ is computed from $\bar{P}_c(t)$, using a Ragone plot for the battery type under consideration (e.g., Fig. 3-2). The depletion per kilometer, X_K, is then computed as

$$X_K = \frac{1}{D_K} \int_0^t \frac{\bar{P}_c(t)/M_B}{\bar{E}_c\left(\bar{P}_c(t)/M_B\right)}\, dt$$

where D_K is the driving cycle distance.

This methodology for computing battery depletion is a generalized form of that used in HYBRID and of the fractional utilization model, which uses the same formula for computing depletion, but with actual power output time history used instead of a smoothed time history. SCT's experience with electric vehicles has indicated that the methodology used in HYBRID produces results which are optimistic, but the fractional utilization model is conservative. The approach of using a smoothed power time history with the fractional utilization model appears to produce realistic results provided the averaging interval is chosen properly. Test results with the "Electric by SCT" VW Rabbit conversion indicate that a suitable value for the averaging 1/2 interval is about 8 sec.

As in HYBRID, the program assumes that the battery discharge limit is reached on all but a negligible number of driving days. This assumption is very approximate, but in view of the other vagaries associated with estimating battery life, is an appropriate one to make. A change

from the life estimation methodology used in HYBRID resulted from recognition of the fact that the relatively high rates of discharge in Mode 1 result in the actual depth of discharge of battery not being numerically equal to the discharge limit when the discharge limit is reached, as assumed in HYBRID. Numerical equality of these two factors would be a reasonable assumption if the average Mode 1 discharge rate corresponded to the 3-hour rate; however, this rate is closer to the 1-hour rate than the 3-hour rate. With the recognition of this fact, the HYBRID2 battery modelling was changed from that used in HYBRID so that the depth of discharge at the discharge limit was computed as

$$DOD = \frac{E_B}{E_{BMAX}} ,$$

where E_B is the energy expended by the battery up to the discharge limit, and E_{BMAX} is the battery energy capacity at the 3-hour rate.

In all other aspects - vehicle modelling, computation of range, adjustment of Mode 2 fuel consumption to attain zero net discharge from the battery on Mode 2, computation of mode-averaged, cycle-averaged, and yearly-averaged fuel and energy consumptions, etc.. - HYBRID2 is identical to HYBRID.

LYFE2

The life cycle cost program described in Section 3.3 was modified slightly for the design tradeoff studies task. The modifications were based on a review of the life cycle cost methodology which revealed that, because of the fact that a higher capital investment is required to set up an engine line than to set up an electronic assembly line, the multiplier used in going from the base manufacturing cost level (exclusive of investment) to the retail price level should be higher for the heat engine and transmission than for the electric propulsion subsystem. A review of these capital investments together with typical factory and dealer markups, indicated that factors of 2.3 and 2.2 would be suitable for the heat engine and transmission, and the electric propulsion subsystem, respectively. The battery retail price was assumed to be a factor of 1.3 times the battery OEM price. Additional modifications were made based on more detailed analyses of the manufacturing cost of the subsystems. The following relationships were used:

Heat Engine Manufacturing Cost:

$$C_{HE} = 4.36\ P_{HE} + 121$$

Electric Propulsion Subsystem Manufacturing Cost:

$$C_M = 17.6\ P_M + 195$$

Transaxle Manufacturing Cost:

$$C_T = 1.31\ (P_{HE} + P_M) + 125$$

where P_{HE} and P_M are the peak power ratings of the heat engine and electric motor, respectively. All the above costs are expressed in 1976 dollars.

Battery replacement costs were based on OEM prices of $2/Kg for lead-acid batteries, $6/Kg for nickel-zinc batteries, and $3.75/Kg for nickel-iron batteries. Again, these numbers were based on ANL goals for battery cost per KWH of installed capacity and for battery specific energy in WH/Kg.

4.4 Discussion of Results

4.4.1 Baseline Propulsion System

Description

A schematic of the advanced hybrid propulsion system is shown in Figure 4-1. The heat engine drives through an electrically or hydraulically actuated clutch which, in conjunction with an ignition relay and the fuel injection pump, is the means for starting the heat engine and bringing it on line when it is required, and disengaging it and shutting it down when it is not required. The clutch output is coupled to one end of the motor shaft; the other end of the motor shaft drives the torque converter. The motor shaft, thus, serves as a summing junction for the heat engine and electric motor output torques.

With this configuration, the electric motor is always coupled to the torque converter input. The motor in this case idles at a low speed when the car is at rest, driving the transmission front pump and, if required, power steering pump.

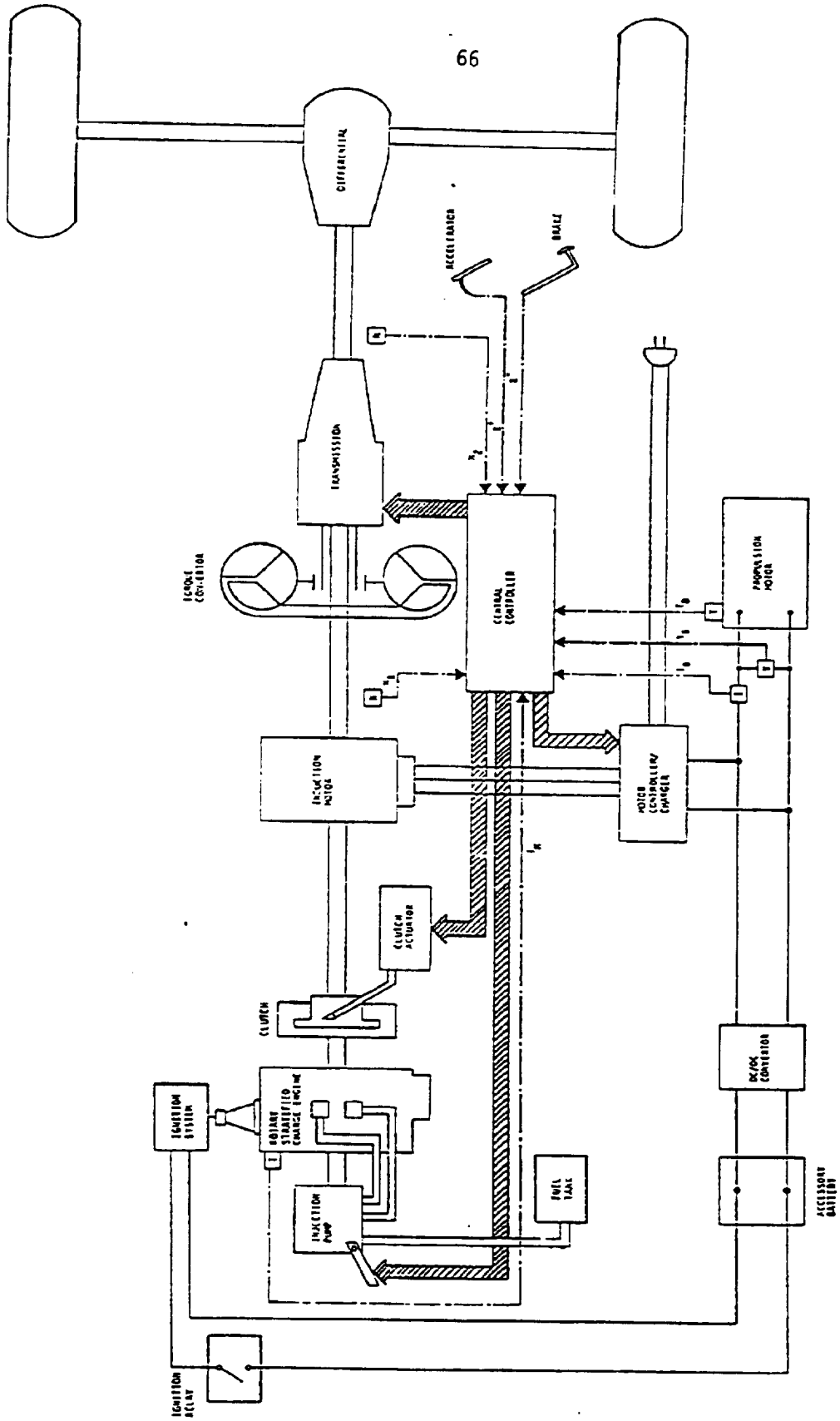

Figure 4-1. HYBRID PROPULSION SYSTEM BLOCK DIAGRAM

It should be noted that it is necessary to keep the hydraulic pressure in a conventional automatic transmission up to a minimum level at idle to prevent slippage and undue wear of the clutches and bands when accelerating from rest. Also, on a car of this class, power assisted brakes would be essential and, because of the lack of engine vacuum, either a separate vacuum pump or hydraulically assisted brakes (hydro-boost) would be required. Hydraulically assisted brakes can use the power steering pump as a supply, and since power steering would also likely be standard on a car of this class, the more economical approach would probably be to use hydro-boost rather than a separate vacuum pump. In either case, however, a power source would be needed for these components when the heat engine is shut down; and rather than incurring the not inconsiderable cost of a separate electric drive, it would be most economical to use the traction motor for this purpose. To accomplish this, it is necessary for the traction motor to drive through the torque converter, rather than coupling it to the drive train between the torque converter output and transmission input. In the latter case, it would, of necessity, be stationary when the vehicle is at rest and thus could not drive the transmission front pump and power steering pump. A discussion of the losses associated with this, as well as alternative mechanical configurations, will be found in Section 4.4.4 of this report.

Component Characteristics

Component design parameters for the baseline system are shown in Table 4-1. Peak power curves for the traction motor, heat engine and combined total are given in Figure 4-2, and the heat engine fuel map is shown in Figure 4-3. This figure also shows the shift logic which is used whenever the heat engine is operating; the transmission is shifted so that the heat engine operates, to the extent possible, within the region indicated by the heavy lines. It is, of course, possible to operate to the right of the upshift line if the transmission is in fourth gear (no upshift possible) or to the left of the downshift line if it is in first gear (no downshift possible). However, in general this shift strategy, in conjunction with the heat engine/motor control strategy, keeps the heat engine operating very close to its region of minimum bsfc; this will be discussed in a subsequent section.

The motor/controller characteristics used are summarized in Figure 4-4. These input vs. output power characteristics were based on an efficiency map

TABLE 4-1. BASELINE PROPULSION SYSTEM PARAMETERS

Component/Parameter	Type/Value
Heat Engine	
Type	Single rotor, direct-injected stratified charge
Peak Power	70 KW @ 6000 RPM
Heat Engine Power Fraction	.71
Electric Motor	
Type	Induction
Peak Power	28.5 KW @ 3600 RPM
Propulsion Battery	
Type	ISOA Lead-Acid
Weight	390 kg
Nominal Capacity	15.6 kwh
Peak Utilized Specific Power	96 w/kg
Battery Weight Fraction*	.2
Transmission/Final Drive	
Type	4-speed automatic with torque converter
Ratios	2.45, 1.45, 1.0, 0.75
Torque Converter Stall Ratio	2.1
Final Drive Ratio	4.12

* Relative to vehicle curb weight.

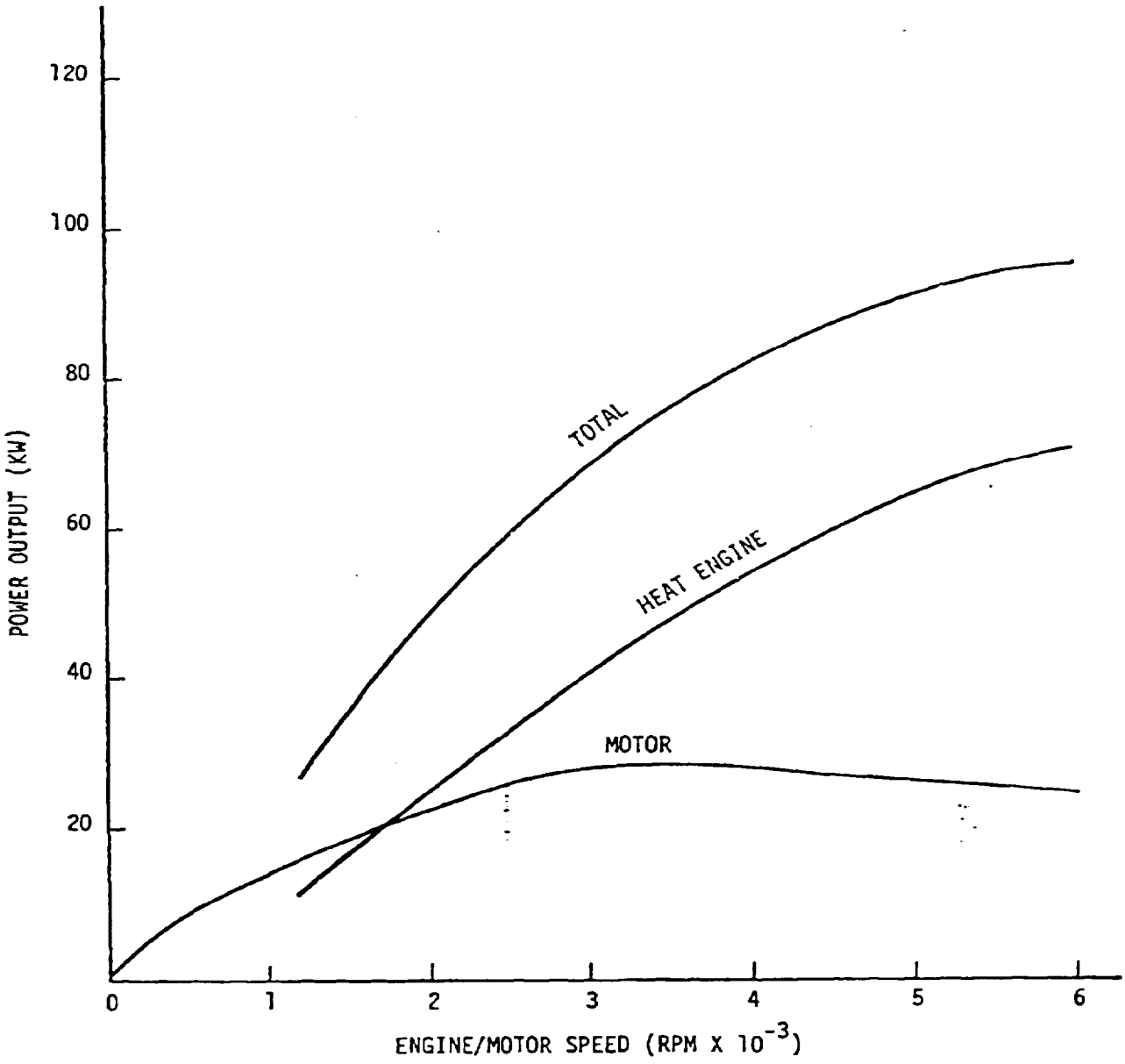

Figure 4-2. BASELINE PROPULSION SYSTEM POWER CURVES

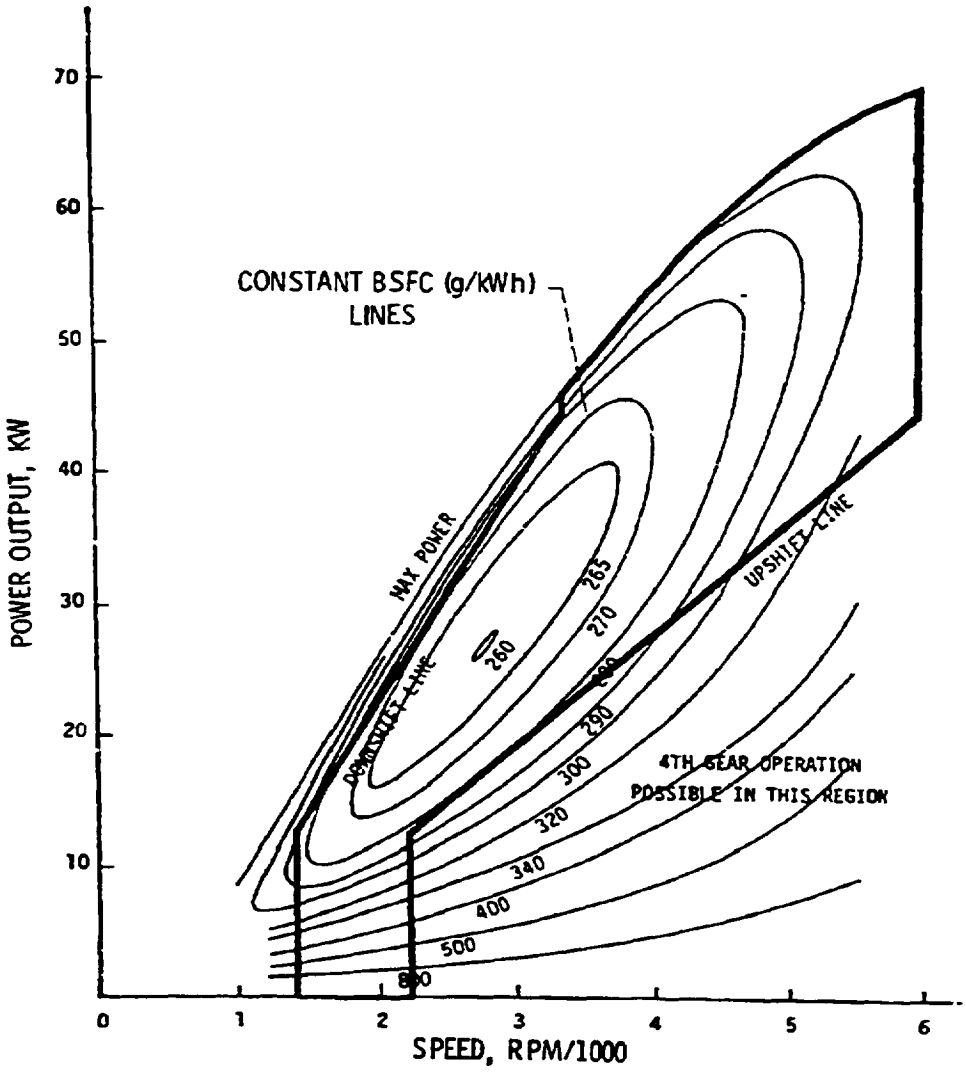

Figure 4-3. - Heat engine fuel map and shift logic for baseline hybrid.

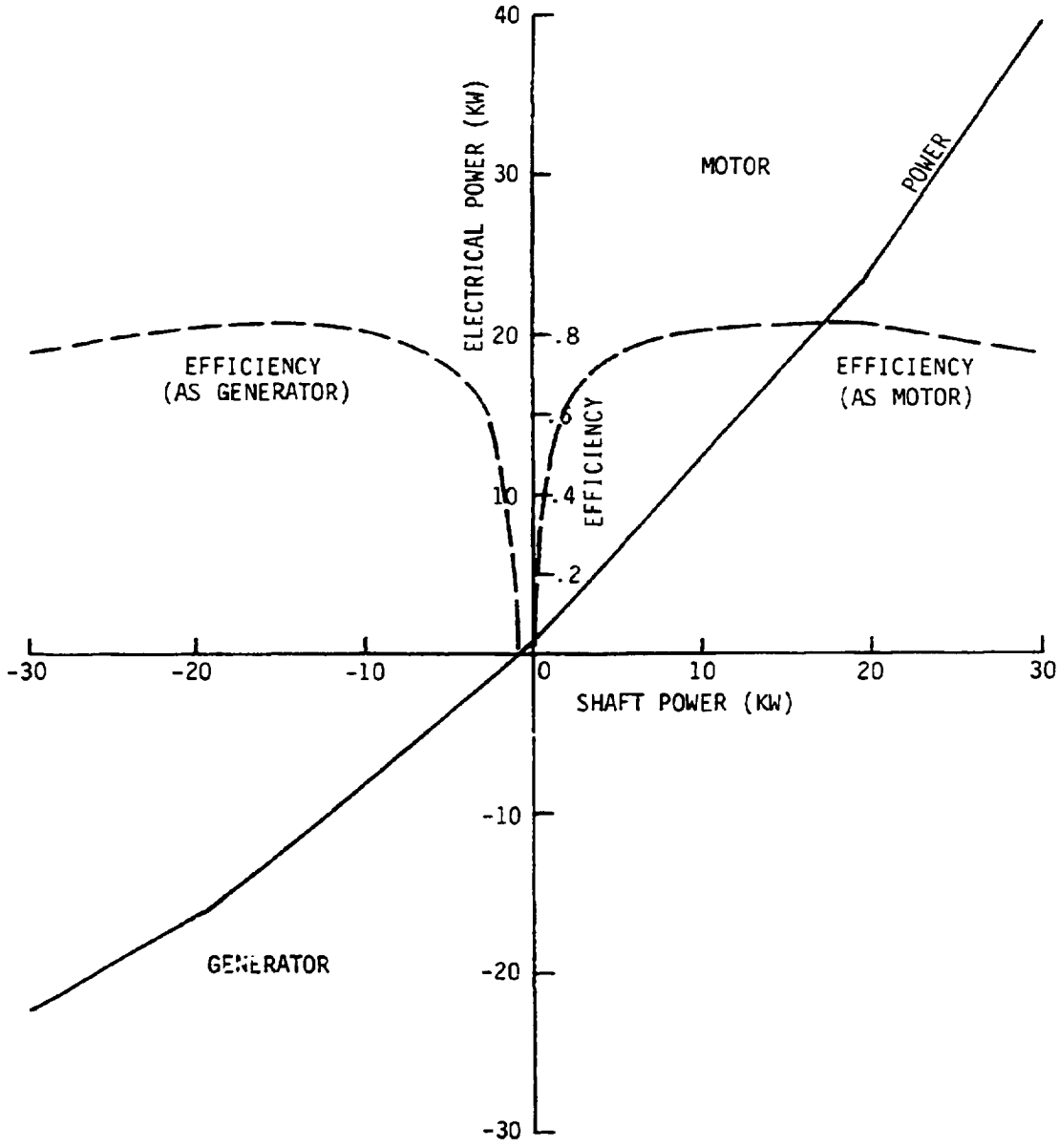

FIGURE 4-4. MOTOR/CONTROLLER INPUT/OUTPUT CHARACTERISTICS

by Gould (Fig. 4-5 in Section 4.4.5); when this data was replotted in terms of input power vs. output power, it was found that the points were grouped tightly along a curve which could be well approximated by the piecewise linear curve shown in Figure 4-4.

The torque converter was sized to give a stall speed of about 1700 RPM under full throttle acceleration. The torque converter characteristics, speed ratio and torque ratio as a function of the output capacity factor are shown in Figure 4-5.

Characteristics of the lead-acid propulsion battery were those defined in Figures 3-2 and 3-3; however, as discussed in Section 4.3, a procedure for estimating battery life was used which was somewhat different from that used in the parametric studies task.

Control Strategy Description

The control strategy used for the baseline is similar to that used in the parametric studies, in that the engine is operated in an on/off fashion and two operating modes are used, which depend on battery state of charge. The selection of the power split between the heat engine and motor, however, depends on both power and torque (equivalently, power and speed), rather than just power. A discussion of this strategy for Mode 1 and Mode 2 operation follows.

1. Mode 1 Operation

This mode applies, as before, when the battery has not been depleted beyond a discharge limit D_{BMAX}, and a net withdrawal of stored energy is made until that discharge limit is reached. In this mode, the decision to start the engine is made based on a power parameter, P_{NOM}, and a speed parameter, V_{MAX}. If the power demand does not exceed P_{NOM}, only the electric drive subsystem operates. P_{NOM} must be selected with two factors in mind: First, if it is too low, then the heat engine operates more than it has to and fuel consumption is high; and, second, if it is too high, the sustained power required from the battery is excessive, which results in poor utilization of stored energy.

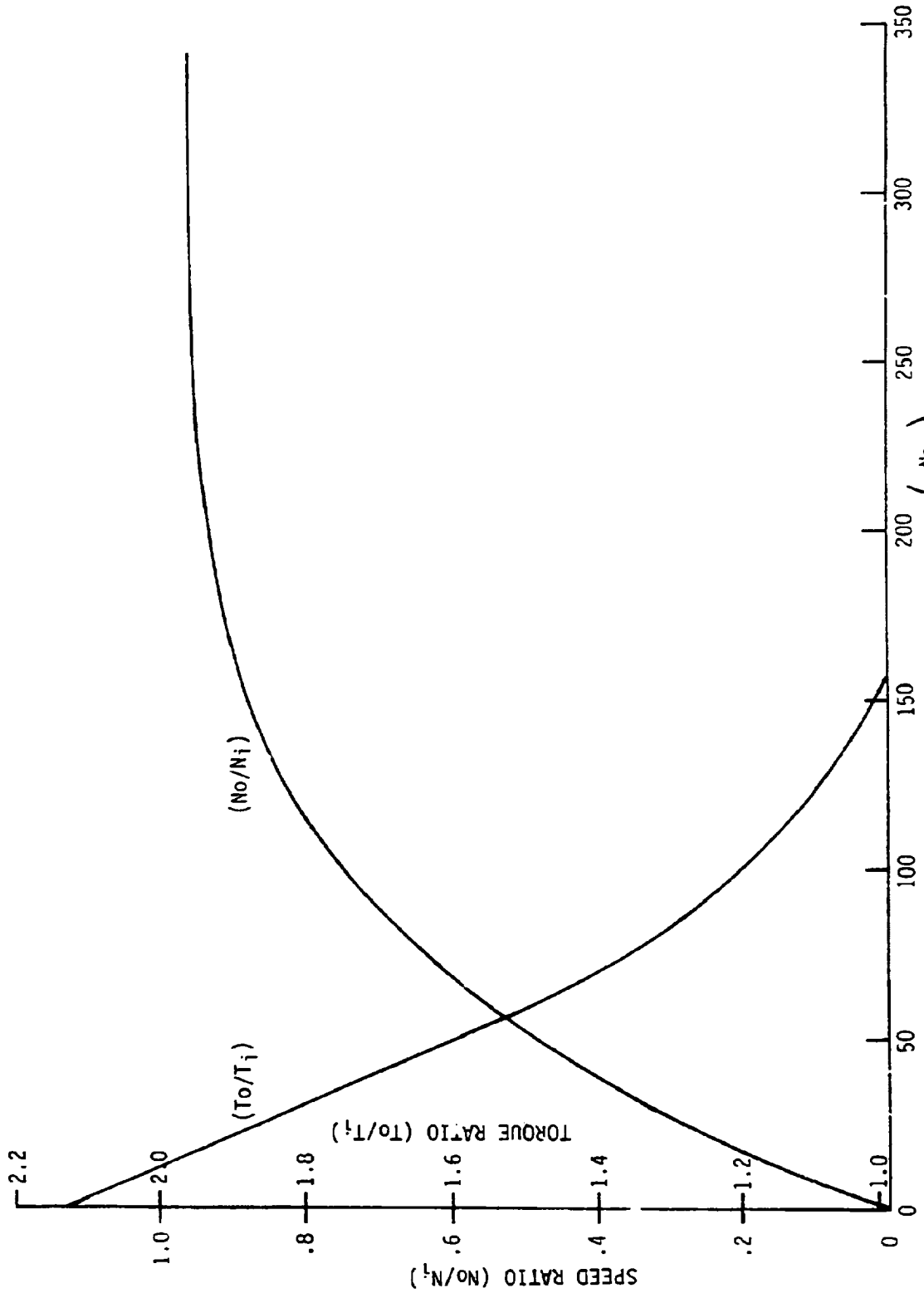

FIGURE 4-5. TORQUE CONVERTOR CHARACTERISTICS FOR HYBRID (BASELINE)

Regardless of the value of the power demand P_{COM} (as long as it is positive, i.e., the vehicle is not decelerating), the heat engine is started if the vehicle speed exceeds the value of the parameter V_{MAX}. This parameter was introduced primarily to insure that the sustained power capability of the battery is not exceeded in highway driving.

If the power demand exceeds P_{NOM} or speed exceeds V_{MAX}, then the power split between the heat engine and electric motor is determined primarily by the heat engine characteristics. A parameter P_{HEMIN}, which is a piecewise linear function of speed, defines a desirable operating line for the heat engine. This line is laid out on the fuel map so that it more or less parallels the long axis of the closed curves of constant brake specific fuel consumption. Note that it does not necessarily need to lie directly on these axes (i.e., pass directly through the minimum fuel consumption points at each power level); this point will be discussed further when control strategy optimization is discussed.

The position of the P_{HEMIN} and P_{NOM} lines on the engine fuel map is shown in Figure 4-6. The split between the heat engine and motor when the engine is running is determined as follows:

Case 1. $P_{NOM} < P_{COM} \leq P_{HEMIN}(N) + P_{MMAX}(N)$, where $P_{MMAX}(N)$ is the maximum motor power available at the speed in question, N. The heat engine is operated at $P_{HEMIN}(N)$, unless $P_{HEMIN}(N)$ exceeds P_{COM}, in which case the heat engine operates at P_{COM}. In any case, the motor provides the difference between P_{COM} and the heat engine output.

Case 2. $P_{HEMIN}(N) + P_{MMAX}(N) < P_{COM}$. In this case, the motor delivers its maximum power $P_{MMAX}(N)$, and the heat engine provides the difference between P_{COM} and the motor output; i.e., the heat engine power output is greater than $P_{HEMIN}(N)$.

The effect of $P_{HEMIN}(N)$ is thus to restrict the region of heat engine operation almost entirely to the shaded region in Figure 4-6, with most of its operation concentrated along the line P_{HEMIN}. As in the choice of the parameter P_{NOM}, there is an optimum positioning of the line P_{HEMIN}. If it is too low, too much of the engine operation is at lower values of bsfc, and fuel economy

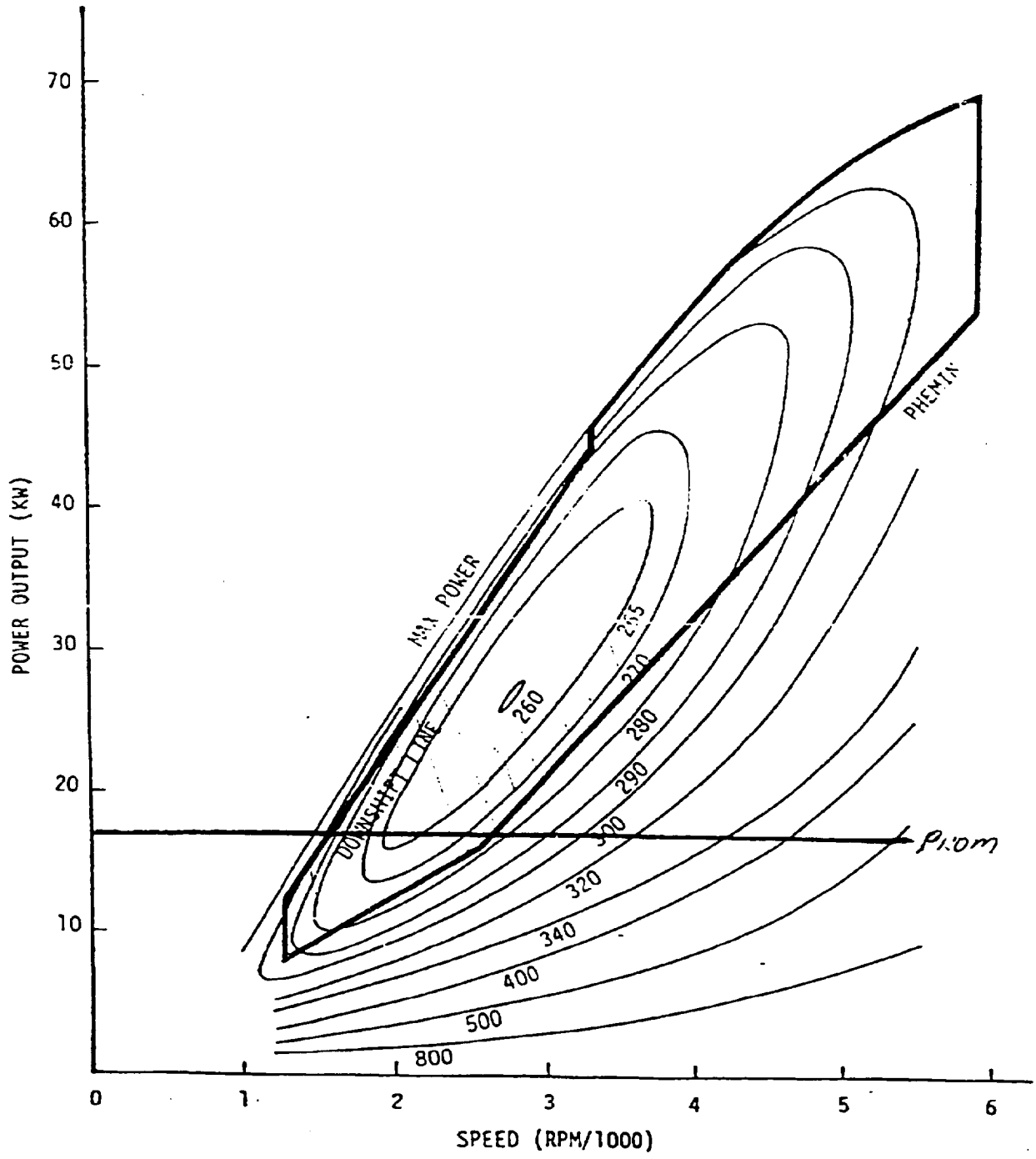

FIGURE 4-6. RESTRICTION OF REGION OF OPERATION OF HEAT ENGINE - MODE 1

suffers. If it is too high, although the average bsfc may be lower, the engine does more total work and the motor less; and, although the overall energy efficiency may be higher, so too is the fuel consumption.

2. Mode 2 Operation

In this mode, the heat engine must operate a large enough fraction of the total time, and at a high enough power level, to insure that the propulsion battery does not continue to discharge past the discharge limit. In this case, the heat engine is started if the power demand exceeds a level P_{HEMN2}, which corresponds to a constant torque line. Once the heat engine is started, it supplies the entire power demand unless the demand exceeds the maximum power capability of the heat engine at the speed in question, in which case the heat engine operates at maximum power and the electric motor makes up the difference. The restriction of the region of operation of the heat engine which results from this strategy is shown in Figure 4-7. It is evident that in Mode 2 operation, the heat engine can operate over a wider power range than in Mode 1.

The above scenario will not, in general, insure that the propulsion battery does not continue to discharge at a low rate, because the energy expended by the battery at power demands below P_{HEMN2} and when assisting the heat engine may exceed the amount returned to the battery during regenerative braking. Consequently, when the heat engine is operating, it may be necessary to adjust its power level so that it not only supplies the power required for propelling the vehicle, but also provides input power to the motor/generator for maintaining the battery state of charge.

Control Strategy Optimization

The program HYBRID2 was exercised with various values for the control parameters in an attempt to find a combination which would minimize fuel consumption. First, the line P_{HEMIN} was set up as shown in Figure 4-6 to restrict heat engine operation to a region over which the bsfc was within about 10% of the absolute minimum value of 260 g/kwh, except for very high power, high speed operation. Second, the parameters P_{NOM} and V_{MAX} were varied to minimize fuel consumption. Figure 4-8 shows the variation in annual average fuel consumption with these two parameters. A sharp drop in fuel consumption is evident between

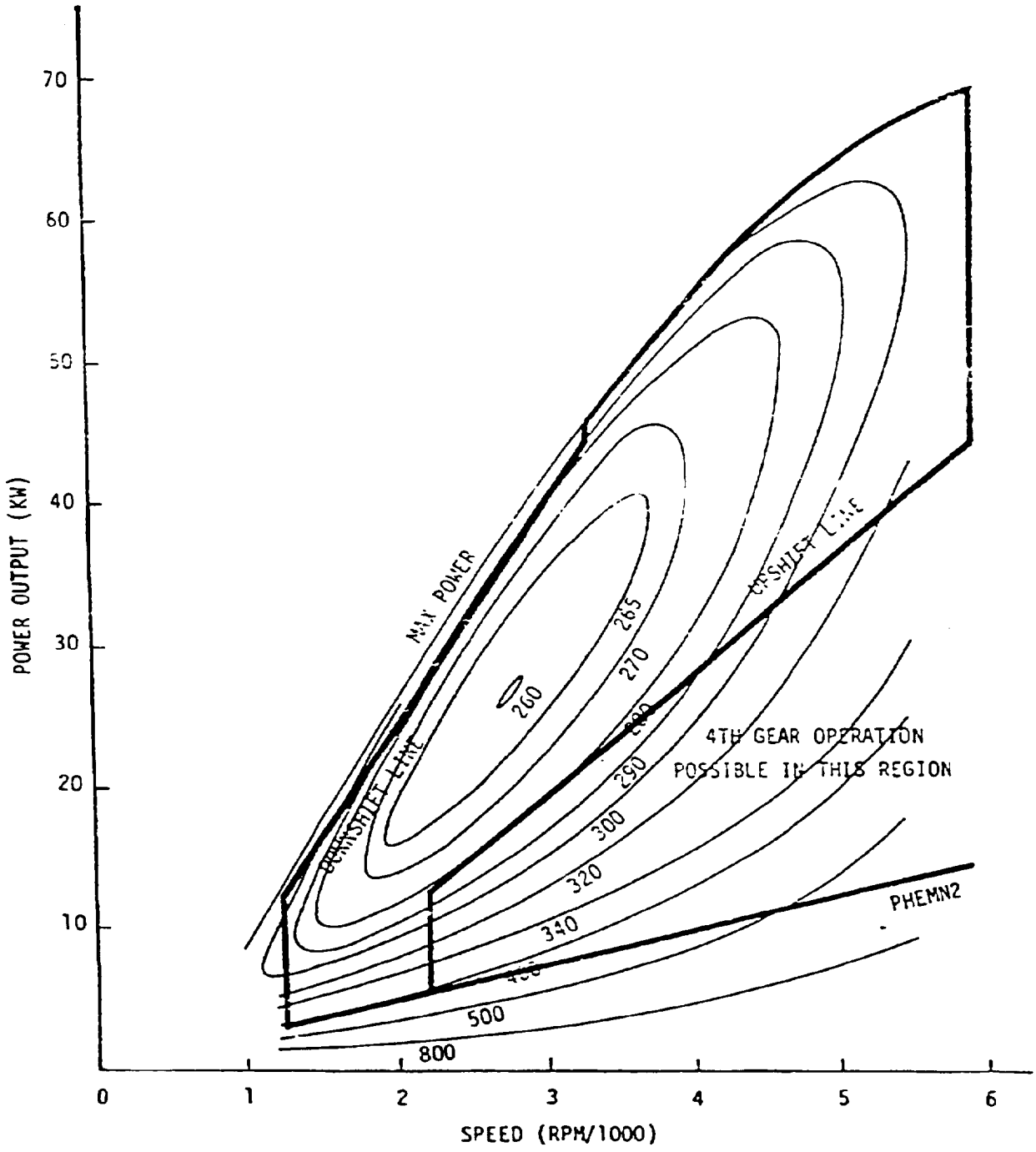

FIGURE 4-7. RESTRICTION OF REGION OF OPERATION OF HEAT ENGINE - MODE 2

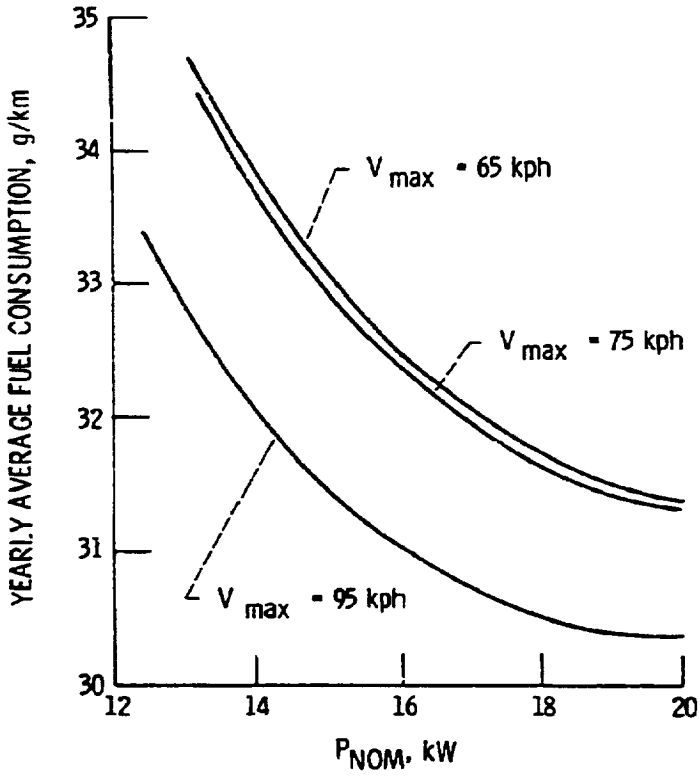

FIGURE 4-8. - VARIATION IN FUEL CONSUMPTION WITH CONTROL PARAMETERS P_{NOM} AND V_{max}.

V_{MAX} = 75 KPH and 95 KPH. With V_{MAX} = 95 KPH, this parameter does not significantly affect the system control on the federal urban or highway driving cycles, since, except for a few seconds on the highway cycle, the speeds on these driving cycles are all below 95 KPH. For V_{MAX} = 95 KPH, a minimum of fuel consumption appears to occur in the range for P_{NOM} of 19-20 KW. However, with a value of P_{NOM} of 20 Kw, the average battery output on the highway driving cycle on Mode 1 is about 10.5 KW; the corresponding specific power is 26.8 Kw/Kg, in excess of the ISOA goal for sustaining power of a lead-acid battery of 25 W/Kg. Because of this, the value of P_{NOM} was backed off to 17 Kw, which corresponds to a specific power of 23.1 W/Kg. The sensitivity of fuel consumption to P_{NOM} in the range from 17 to 20 Kw is small (about 1% change in fuel consumption over this range).

The question arises as to the significance of the V_{MAX} parameter if its best value is beyond the normal range of driving speeds. Obviously, it could be deleted from the control strategy if the only problem was to minimize the fuel consumption predicted by a computer simulation. Ultimately, however, other driving conditions must be considered, as well as overall vehicle driveability, which is a problem totally ignored by the computer simulation. It may be desirable to have V_{MAX} set lower than 95 MPH so that the heat engine operates continuously under highway cruise conditions in order to avoid the potential annoyance of having it start up and shut down in response to minor changes in grade and speed. Such questions cannot be resolved except with running hardware; and, until that point is reached, it was felt that it was better to keep the control strategy structured to include this parameter, even though it does not have much relevance to the computer simulation.

Attempts to improve the fuel economy by further restricting the operating region of the heat engine were not productive. For example, even when the P_{HEMIN} line approximated closely the locus of points defining the minimum fuel consumption vs. power level, fuel consumption was not improved. Although the average bsfc was improved slightly, the engine was also operated at a higher average power level, which more than compensated for the reduction in bsfc.

The control parameters which resulted from the optimization process are summarized below:

P_{NOM} = 17 KW

V_{MAX} = 95 KPH

$P_{HEMIN}(KW) = .10472\ [59.9\ \frac{N}{1000} + 47.1 MAX\ (0, \frac{N}{1000} - 2.6)]$

$P_{HEMN2}(KW) = .10472\ (23.8\ \frac{N}{1000}\ )$

This strategy's accomplishments in terms of minimizing the average brake specific fuel consumption are summarized in Table 4-2. Note that the minimum attainable bsfc with this engine is about 260 g/kwh.

Table 4-2. AVERAGE BSFC

	BSFC (g/kwh)	
	Urban Cycle	Highway Cycle
Mode 1	277 (6.5%)	277 (6.5%)
Mode 2	286 (10%)	279 (7.5%)

Table 4-2 also indicates the percent deviation of the average bsfc from the minimum attainable. Obviously, the control strategy is quite effective in keeping the engine operating close to its region of minimum bsfc.

Figures 4-9 and 4-10 show the distribution of engine operating points on the urban cycle, on Modes 1 and 2 respectively, with the shaded regions of Figures 4-6 and 4-7 shown superimposed. The numbers in the squares indicate the number of occurrences for which the engine operating point was within the boundaries of the cell within which the square is centered. For example, in Figure 4-9, the number 23 is in the square located in the cell which is contained between 2500 and 3000 RPM and between 15 and 20 KW. This indicates that, of the total number of sample occurrences, on 23 of these the engine was operating between 2500 and 3000 RPM with a power output between 15 and 20 KW. The areas of the squares have been drawn proportional to the number of occurrences. It should be noted that the number of occurrences within a cell is always shown at the center of the cell. Consequently, if a cell intersects the shaded region, but its center lies outside the cell, it is possible that an occurrence inside the shaded region could show up in the figure as apparently being outside that region. Taking this into account, Figure 4-9 shows that the majority of the operating points are clustered along the P_{HEMIN} line, and the remainder of the

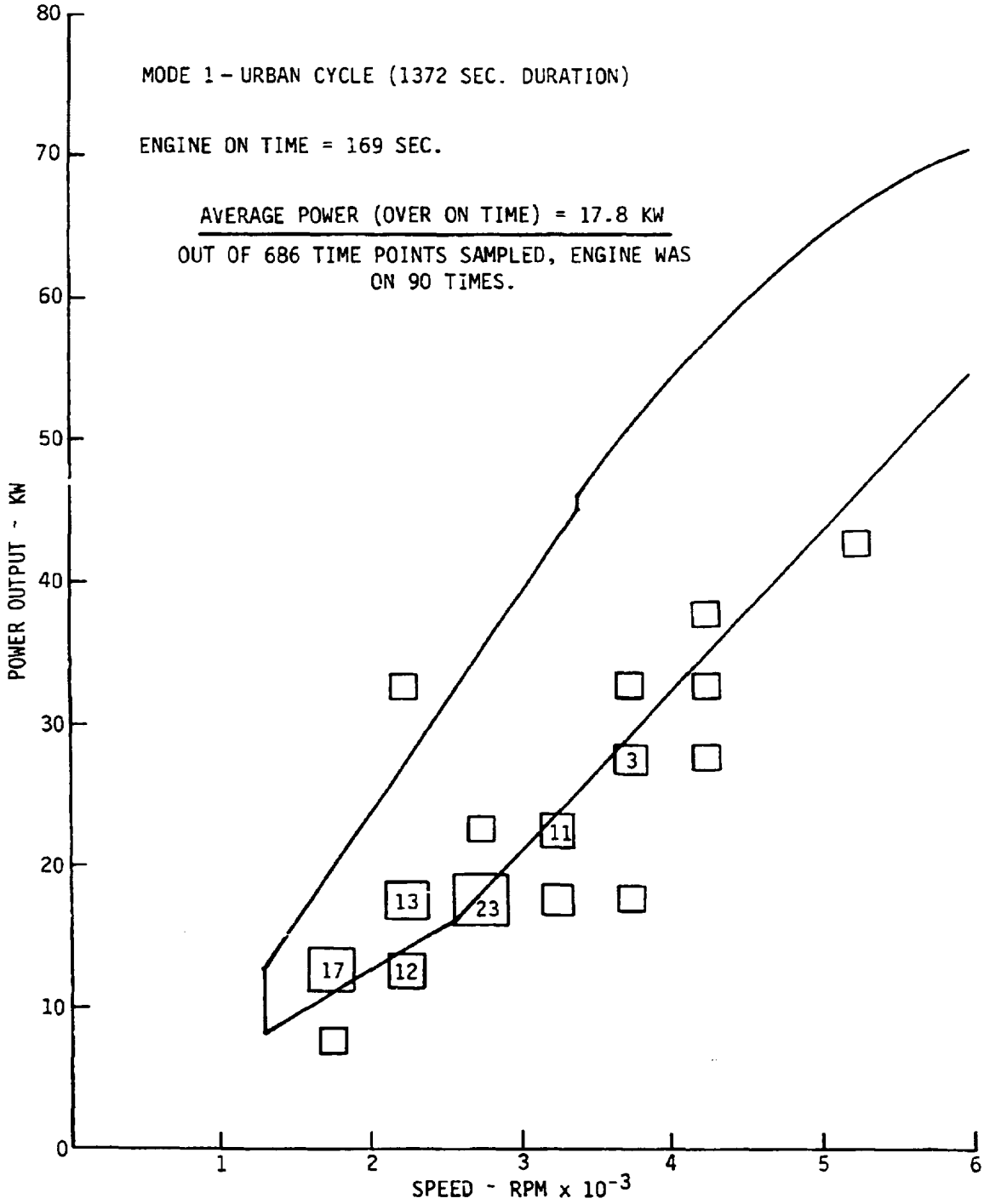

FIGURE 4-9. ENGINE SPEED VS. POWER DISTRIBUTION

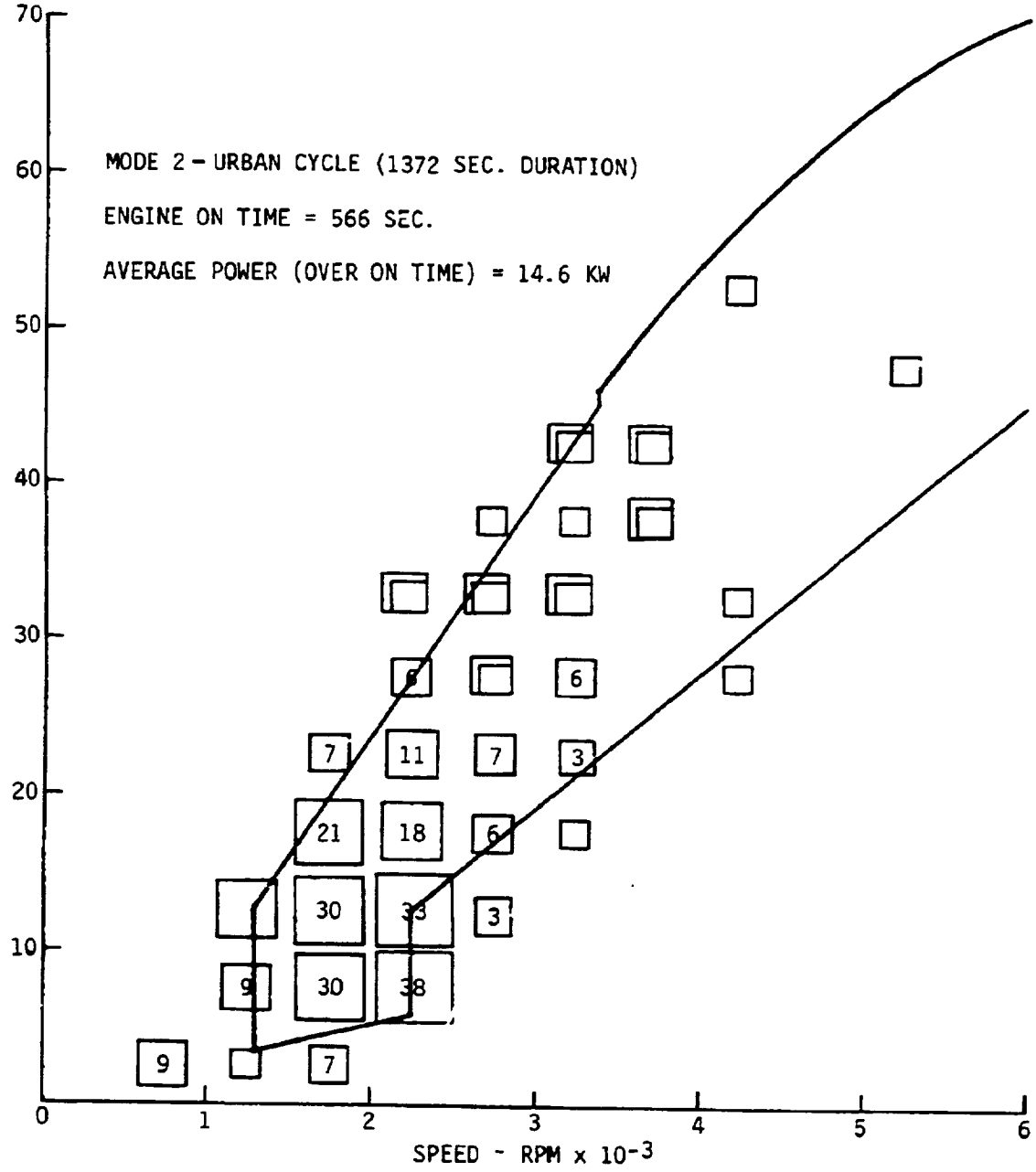

FIGURE 4-10. ENGINE SPEED VS. POWER DISTRIBUTION

of the points lie mostly within the shaded region; only a few isolated points are definitely outside the region.

As expected, the Mode 2 distribution shows a wider scatter than Mode 1, since the operating region of the engine is not as tightly controlled in this case. Most of the operating points here are clustered between 1500 and 2500 RPM, and 5 and 20 KW, with bsfc's ranging from about 265 to no more than 400 g/kwh.

Selection of the Battery Discharge Limit

All the above runs were made with D_{BMAX}, the battery discharge limit, equal to .6. Since this parameter defines the transition from Mode 1 to Mode 2 and does not affect how the system operates in the individual modes, its effects are independent of those of the other parameters. Consequently, investigation of its effects was postponed until the other parameters were optimized.

Increasing D_{BMAX} reduces fuel consumption and increases energy consumption since it increases the fraction of the total driving distance which is done on Mode 1 (low fuel consumption and high energy consumption) and decreases Mode 2 driving (high fuel consumption and zero energy consumption). The adverse effect of increasing D_{BMAX} is a reduction in battery life. The variation of these three quantities, fuel and energy consumption and battery life, are summarized in Figure 4-11. It should be noted that battery life is computed on the basis of the depth of discharge relative to the capacity at the 3-hour rate, as discussed in Section 4.3, whereas the battery depth of discharge in operation, which is compared with D_{BMAX} to determine when to switch from Mode 1 to Mode 2, is computed relative to the discharge pattern which the battery is undergoing in use. The average rate at which the battery is discharged in Mode 1 operation is considerably faster than the 3-hour rate; thus, it turns out that a value of D_{BMAX} of .6 corresponds to a depth of discharge relative to the 3-hour rate of only .31. This, then, explains the long battery life shown in Figure 4-11. It should also be noted that the variation in depth of discharge relative to the 3-hour rate is only from .25 to .35 as D_{BMAX} varies from .4 to .8, which explains the relatively small variation in battery life over this range for D_{BMAX}.

The effects of D_{BMAX} on life cycle cost will be discussed in a subsequent section. In addition to its effect on fuel and energy consumption and life cycle

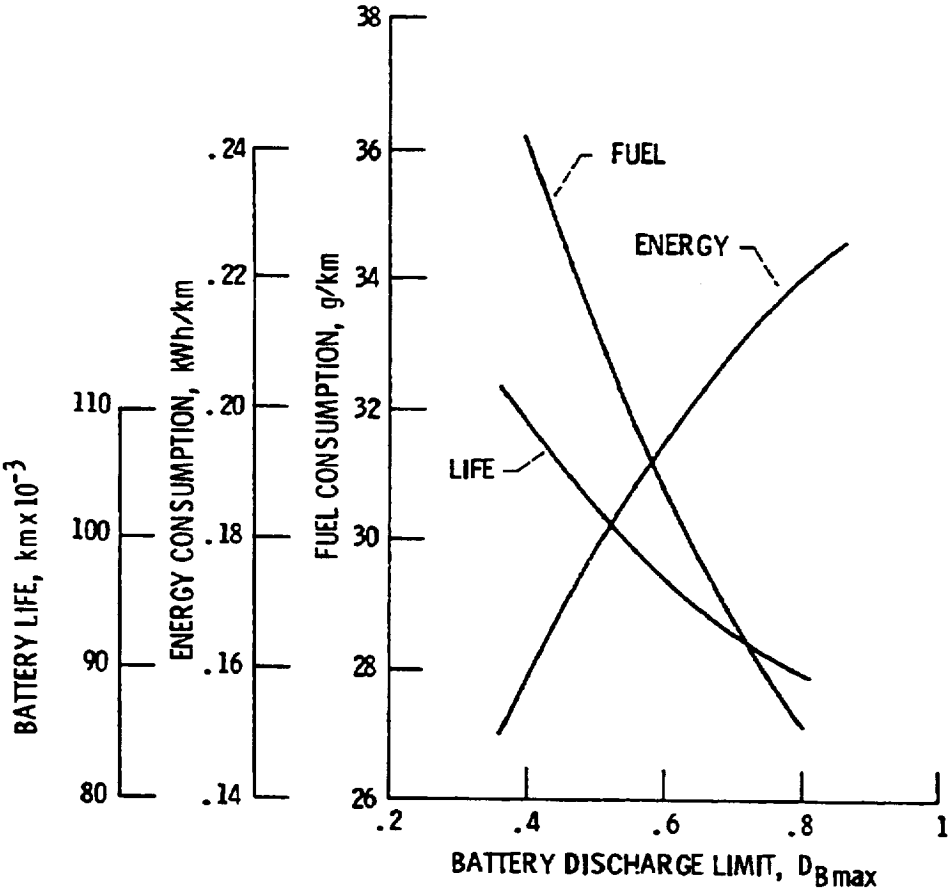

FIGURE 4-11. - EFFECTS OF BATTERY DISCHARGE LIMIT.

cost, one other factor could influence the selection of a value for this parameter, and that is gradeability. For a vehicle of this class, it is essential that it be able to maintain a reasonable speed on any grade likely to be encountered for whatever distance that grade may persist. In highway travel, the chances are that the batteries will already be at the discharge limit when a grade is encountered. If the power requirement on that grade at a reasonable operating speed exceeds that available from the heat engine, the electric motor will have to supply the difference, which means that the battery will suffer a net discharge, past the discharge limit, until the grade terminates. This means that there must be enough reserve beyond the discharge limit to permit the vehicle to continue to operate on the grade without significant loss of performance, for however long the grade is likely to last.

In addition to the design goal of maintaining 90 kph on a 4% grade for an indefinite period, the following gradeability conditions, developed during the Near Term Hybrid Vehicle design program, were considered.

8% grade, 85 kph, 5 km
8% grade, 65 kph, indefinitely
15% grade, 50 kph, 2 km

These are considerably more stringent conditions than those given as design goals in Table 3-1. However, they are more in line with the conditions which might be encountered in highway travel in mountainous sections of the country.

Even with these stringent requirements, however, the baseline hybrid system was able to handle the grade/speed combinations, in Mode 2, using only the heat engine. Table 4-3 summarizes the situation. In each case, the engine is capable of providing the required system output power, although rather marginally in two cases (8%, 85 kph, and 15%, 50 kph). Note that the gear listed in Table 4-3 is the one which would be called for by the shift strategy shown in Figure 4-3.

Thus, the high performance (0-90 kph in 12 sec.) and large heat engine power fraction (.71) of the baseline system make it unnecessary to consider Mode 2 gradeability in selecting a value for D_{BMAX}. This would not necessarily be the case for a vehicle with lesser acceleration performance, or a smaller heat engine power fraction, such as the SCT Near Term Hybrid Vehicle design.

Table 4-3. BASELINE HYBRID GRADEABILITY

		Mode 2 Operating Point					
Gradient (%)	Speed (kph)	Gear	Engine Speed (RPM)	System Output Power (kw)	Available Engine Power (kw)	Motor Output Power (kw)	Distance on Grade (km)
4	90	3	3320	37.9	44.9	0	Indef.
8	85	2	4520	59.1	59.8	0	"
8	65	2	3480	43.7	47.2	0	"
15	50	1	4490	57.9	59.5	0	"

Although gradeability does not enter into the selection of a value of D_{BMAX}, it is still necessary to leave some margin between the discharge limit and the value 1, which corresponds to the "discharged" state relative to the hybrid discharge pattern, in order to avoid a perceptible drop-off in performance when operating at the discharge limit. Consequently, throughout the Design Tradeoff Studies task, we continued to work with a value of .6 for D_{BMAX}. In retrospect, this may have been too conservative, and there appears to be no reason that a value as high as .8 could not be used.

Characterization of the Baseline System

1. Acceleration/Gradeability

The program VSPDUP2 was used to determine the acceleration and maximum gradeability of the baseline hybrid. The results are shown in Figure 4-12. A 0-90 km/h time of 11.6 sec. was obtained, slightly under the design goal of 12.0 sec. The 0-50 km/h time of 4.4 sec. and 40-90 km/h time of 8.4 sec. are both well within the design goals of 5 sec. and 10 sec., respectively.

The maximum gradeability (both heat engine and motor operating at maximum power) as a function of speed is shown in Figure 4-13. A usual requirement for an on-road vehicle is the ability to start up from rest on a 30% grade and climb the grade. It is evident from Figure 4-13 that the baseline hybrid would have no problem meeting such a requirement, since the maximum start-up torque corresponds to a grade of over 80%.

2. Fuel and Energy Consumption

Table 4-4 summarizes the fuel and energy consumption of the baseline hybrid system on both the urban and highway driving cycles, and for both Mode 1 and Mode 2 operation. For comparative purposes, Table 4-5 shows the same quantities for a reference conventional vehicle, also using a rotary stratified charge engine. Note that the hybrid dissipates more road load energy, due to its higher test weight (2216 kg vs. 1622 kg for the conventional vehicle). Energy dissipation in braking is much lower in the hybrid than in the conventional vehicle, particularly on the urban cycle, reflecting the fact that most of the braking is done regeneratively by the traction motor.

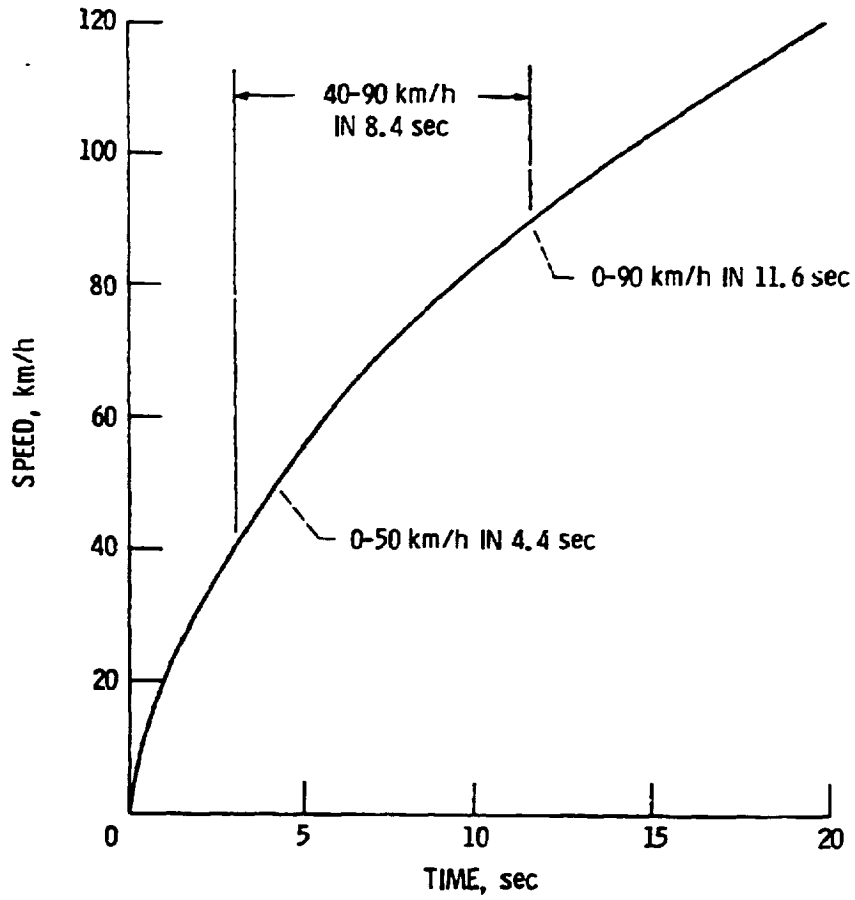

FIGURE 4-12. - BASELINE HYBRID - MAXIMUM EFFORT ACCEL-ERATION.

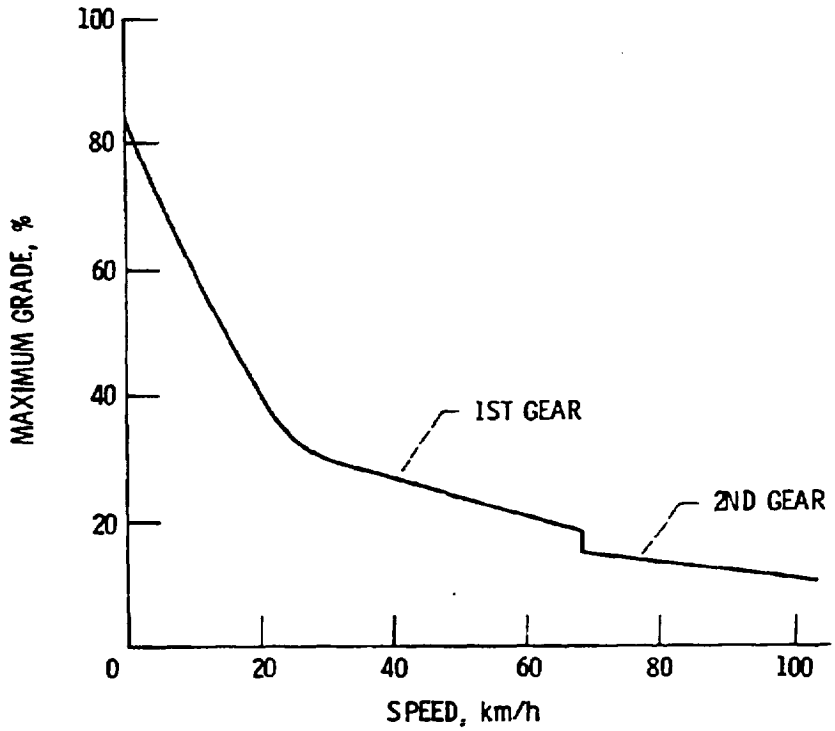

FIGURE 4-13. - BASELINE HYBRID - MAXIMUM GRADEABILITY.

TABLE 4-4. BASELINE HYBRID ENERGY CONSUMPTION

	Urban Cycle		Highway Cycle	
	Mode 1	Mode 2	Mode 1	Mode 2
Road Load Energy[1] (MJ/km)	.298	.298	.407	.407
Braking Energy (MJ/km)	.007	.007	.012	.012
Drive Train Energy[2] (MJ/km)	.321	.298	.136	.134
Engine Output Energy (MJ/km)	.251	.691	.241	.584
Motor Shaft Energy (MJ/km)				
Driving	.585	.122	.360	.015
Generating	-.210	-.210	-.046	-.046
Net Battery Output Energy (MJ/km)	.590	.058 (0)	.417	.020 (0)
Fuel Consumption (g/km)	19.4	54.9 (58.8)[3]	18.5	45.3 (46.6)[3]
Battery Depletion (km^{-1})	.0128	-	.0102	-
Operating Range to D_{BMAX} = .6 (km)	46.9	-	58.6	-

Yearly Averages:

Fuel Consumption (g/km)	30.72
Wall Plug Energy Consumption (kwh/km)	.196

1. Includes energy dissipated in aerodynamic drag and tire rolling resistance.
2. Includes loss in differential, gearbox, torque converter, and transmission and power steering hydraulic pumps.
3. Fuel consumption corrected for zero net battery output on Mode 2.

TABLE 4-5. REFERENCE CONVENTIONAL VEHICLE ENERGY CONSUMPTION

	Urban Cycle	Highway Cycle
Road Load Energy (MJ/km)	.240	.349
Braking Energy (MJ/km)	.089	.021
Drive Train Energy (MJ/km)	.235	.117
Engine Output Energy (MJ/km)	.564	.487
Fuel Consumption (g/km)	68.9	47.0
Yearly Average Fuel Consumption (g/km)	62.8	

The drive train losses in the urban cycle are slightly higher, in proportion to the road load energy, in the hybrid than they are in the conventional vehicle, particularly in Mode 1. This is apparently a result of the fact that the hybrid spends more time in the lower gears, with consequent lower overall efficiency, than the conventional car. Note that, although the hybrid heat engine does somewhat more work on Mode 2 than does the engine in the conventional system, the hybrid uses slightly less fuel (on the urban cycle), or an almost identical amount of fuel (highway cycle). This is due to the higher average loading and lower bsfc of the hybrid engine, combined with the fact that the hybrid engine is shut down at idle and when decelerating. The fuel savings for the hybrid comes on Mode 1 operation, of course; its fuel consumption is only 28% of that of the conventional vehicle on the urban cycle, and about 39% on the highway cycle. If a discharge limit of .6 is used, enough of the total annual driving is done on Mode 1 to bring the hybrid's annual fuel consumption down to 49% of that of the conventional vehicle. Stated in terms of miles per gallon, the hybrid achieves a fuel economy of 54.6 mpg vs. 26.7 mpg for the conventional vehicle. The hybrid's fuel economy goes up still further to 61.6 mpg if a discharge limit of .8 is used, which, as discussed previously, appears to be feasible.

If some assumptions are made with respect to refinery, distribution and power generating plant efficiencies, the preceding estimates of fuel and energy input to the vehicle can be converted into total energy consumption figures. This has been done in Table 4-6, under the assumptions indicated therein. The hybrid consumes more total energy than the conventional vehicle; however, since in the U.S. only about 15% of the total electric generation is in oil-fired plants, the hybrid's consumption of petroleum energy is 40-45% lower depending on the battery discharge limit. It is also noteworthy that the total energy consumption increases as the battery discharge limit increases; this is indicative of the fact that the on-board heat engine is more efficient than the battery charging and electric power generation/distribution processes.

3. Costs

As discussed in Section 4.2, the methodology used for estimating life cycle costs in the Design Tradeoff Studies task was modified somewhat from that

TABLE 4-6. TOTAL ENERGY CONSUMPTION COMPARISON FOR BASELINE HYBRID AND CONVENTIONAL VEHICLE

	Baseline Hybrid		Conventional Vehicle
	$D_{RMAX} = .6$	$D_{RMAX} = .8$	
Average Total Energy Consumption[1] (MJ/km)	3.89	4.00	3.21
Average Petroleum Energy Consumption[2] (MJ/km)	1.92	1.78	3.21

1. Computed as the energy equivalent of the total crude oil required at the refinery input, under the assumption that all the input energy comes from crude oil, and under the following assumptions:

   Refinery/distribution efficiency = .93 (fuel oil)
   .84 (gasoline)
   Electrical generation efficiency = .36
   Electrical distribution efficiency = .91

2. Same as 1, except the assumption is made that only 15% of the electrical energy generation comes from petroleum.

used in the parametric studies to reflect better estimates on the total markup from manufacturing or OEM cost to retail on the various propulsion system components. The retail (acquisition) cost breakdown for the system is as shown in Table 4-7.

Table 4-7. Baseline Hybrid Propulsion Acquisition Cost (1976 $)

	Acquisition Cost	% of Total
Heat Engine	$ 981	23.9
Electric Propulsion (Motor & Controls)	1,532	37.2
Transaxle	584	14.2
Propulsion Batteries	1,014	24.7
Totals	$4,111	100.0

As is evident from the above, the bulk of the acquisition cost (61.9%) lies in the electric propulsion subsystem and propulsion batteries. The corresponding acquisition costs for a conventional propulsion system using the rotary stratified charge engine are summarized in Table 4-8.

Table 4-8. Conventional Propulsion System Acquisition Costs (1976 $)

	Acquisition Cost	% of Total
Heat Engine	$1,207	68.1
Electric Propulsion	-	-
Transaxle	566	31.9
Propulsion Batteries	-	-
Totals	$1,773	100.0

The differential in acquisition cost between a conventional propulsion using the same IC engine technology and the hybrid system, both sized for a passenger car of the same accommodations, is thus about $2,338. For the hybrid to have competitive life cycle cost, it means that this $2,338, plus the cost of electricity used by the hybrid, plus the cost of replacing the propulsion battery, must be paid for by the fuel savings. It was found that a very high fuel price was required to do this.

The life cycle cost picture is summarized in Figure 4-14. It defines the life cycle cost of the baseline hybrid propulsion system as a function of the gasoline and electricity cost (all in 1976 $). Also plotted is the life cycle cost of a conventional propulsion system as a function of gasoline cost. The break-even points, in terms of equal life costs for the two systems, are indicated by the intersections of the lines in Figure 4-14. Thus, at an electricity cost of 5¢/KWH, it requires a gasoline price of about $2.70/gal. for the life cycle cost of the hybrid to equal that of the conventional system. At 7¢/KWH, the number is $3.00/gal., and so forth.

In subsequent investigations carried out in the design tradeoff studies task, life cycle costs were computed at the combination of $2.00/gal. for gasoline, and 7¢/KWH for electricity. No clear justification could be found for assuming gasoline prices any higher than this (again, bear in mind that these figures are in 1976 $), or electricity prices much lower. With this combination, the life cycle cost for the baseline hybrid system is 7.17¢/KM, vs. 6.11¢/KM for the conventional system. These costs break down as shown in Table 4-9 for the hybrid system. The major cost items constitute the following percentages of the total discounted life cycle cost:

Heat Engine & Transaxle Acquisition	13.65%
Electric Propulsion Subsystem Acquisition	13.36%
Battery Acquisition & Replacement	16.55%
Fuel	28.61%
Electricity	17.20%
Maintenance & Repair	12.49%
Salvage	-1.86%
	100.00%

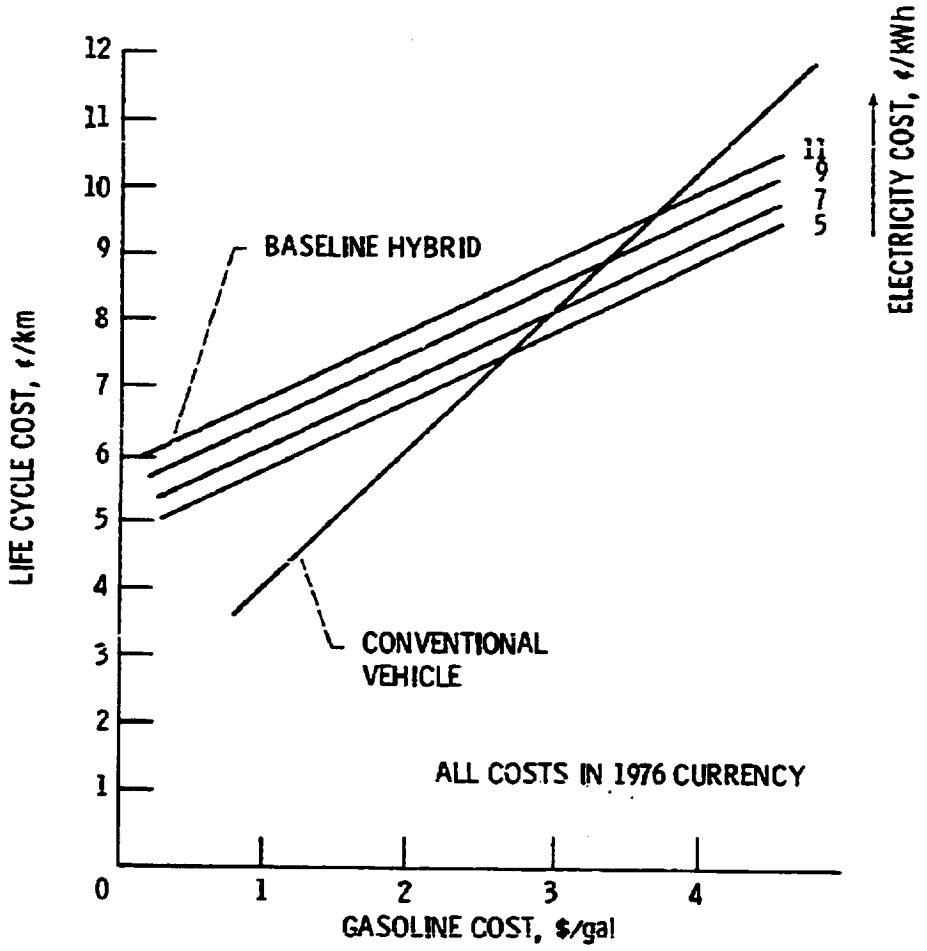

FIGURE 4-14. - BASELINE HYBRID LIFE CYCLE COST.

Table 4-9. HYBRID SYSTEM LIFE CYCLE COST BREAKDOWN

	YEAR												
	0	1	2	3	4	5	6	7	8	9	10	Total	¢/KM
1. Propulsion System Acquisition Cost	3097	-	-	-	-	-	-	-	-	-	-	3097	-
Discounted	3097	-	-	-	-	-	-	-	-	-	-	3097	1.936
2. Propulsion Battery	1014	-	-	-	-	-	-	1014	-	-	-	2028	-
Discounted	1014	-	-	-	-	-	-	882.75	-	-	-	1897	1.186
3. Fuel	0	365.32	365.32	365.32	365.32	365.32	365.32	365.32	365.32	365.32	365.32	3653	-
Discounted	0	358.16	351.14	344.25	337.50	330.88	324.39	318.03	311.79	305.69	299.69	3281	2.051
4. Electricity	0	219.63	219.63	219.63	219.63	219.63	219.63	219.63	219.63	219.63	219.63	2196	-
Discounted	0	215.32	211.10	206.96	202.90	198.93	195.03	191.20	187.46	183.78	180.17	1973	1.233
5. Maintenance & Repair	0	93.55	99.19	117.53	147.14	188.03	212.00	226.10	231.74	200.72	93.55	1610	-
Discounted	0	91.72	95.34	110.75	135.94	170.30	188.25	196.83	197.79	167.96	76.74	1431	.895
6. Salvage	-	-	-	-	-	-	-	-	-	-	-277.11	-277	-
Discounted	-	-	-	-	-	-	-	-	-	-	-213	-213	-.133
7. Total	4111	678.50	684.14	702.48	732.09	772.98	796.95	1825.05	816.70	785.67	678.50	12324	-
Discounted	4111	665.20	657.58	661.96	676.34	700.11	707.67	1588.82	697.04	657.42	556.61	11468	7.17

It should be noted that the discounted (present) value of the fuel consumed by the reference conventional propulsion system was $6,708, or $3,426 more than the present value of the fuel consumed by the hybrid. However, the hybrid also consumes $1,973 worth of electricity, which brings the net fuel/energy cost savings down to $1,453. This is not enough to pay for propulsion battery acquisition and replacement and the differential in propulsion system acquisition ($3,221 total). Thus, the baseline hybrid is about $1,768 in the hole, disregarding minor differences in maintenance, repairs, and salvage value. Cost is, consequently, an item which required rigorous attention during the system design and subsequent development phases.

4.4.2 Effects of Propulsion System Parameter Variations from Baseline

Heat Engine Power Fraction

It was concluded during the parametric studies task that a heat engine power fraction of about .7 was a suitable value to design the baseline system around. One of the first orders of business in the design tradeoff studies task was to determine whether any modifications to this conclusion were warranted, based on running the more detailed simulation program HYBRID2. These cases were run at a constant performance level, and with the peak battery specific power held constant at 96 w/kg. The results are summarized in Figure 4-15. As noted in the discussion in Section 3, fuel consumption decreases, and cost decreases with the increasing heat engine power fraction. Consequently, there is no clearly defined optimum value (at least at the cost levels of $2.00/gal. and 7¢/kwh) for the heat engine power fraction. What is evident is an increase in the slope of the fuel consumption curve beyond a heat engine power fraction of .7. Because of this, and because of the importance placed on achieving low fuel consumption, it was concluded that it would not be desirable to push the heat engine power fraction much beyond .7 in the interests of reducing life cycle cost. In view of this, the value of .71 used for the baseline appeared to be a good point to design around.

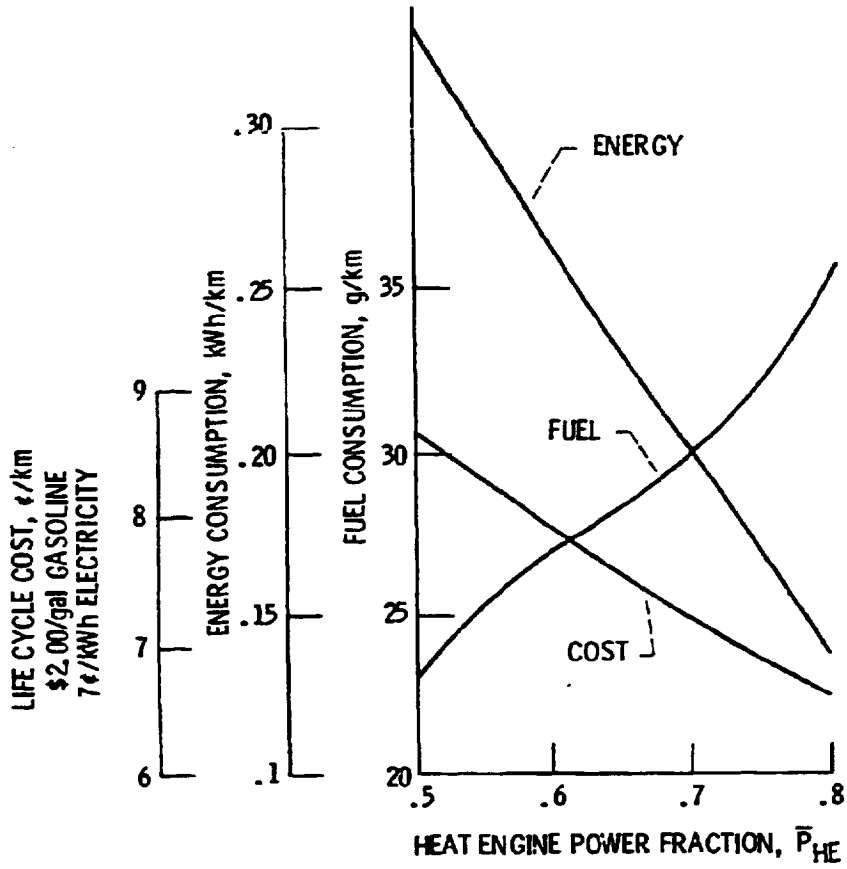

FIGURE 4-15. - EFFECTS OF HEAT ENGINE POWER FRACTION.

Variations in Battery Characteristics

1. Battery Weight

Since the cost (particularly replacement cost) of the propulsion battery is a significant factor in the overall life cycle cost of the hybrid propulsion system, it is of obvious interest to explore ways of reducing that cost. One approach to this is to reduce the battery weight, pushing the peak specific power of the battery higher. Since this peak specific power for the baseline system was 96 w/kg, which is very close to the nominal peak of 100 w/kg specified for ISOA lead-acid batteries in the assumptions and guidelines for the program, it was not possible to push this power level much higher and still hold to these guidelines. However, as an exercise to determine what the effects might be, the battery weight was reduced from 390 kg to 325 kg, a reduction of 65 kg, or 16.7%. Using a weight propagation factor of .3, the vehicle test mass dropped from 2216 kg to 2132 kg, or a 3.8% reduction. The power ratings of the heat engine and electric motor were dropped correspondingly. The overall effect on the peak battery specific power was to raise it from 96 w/kg to 111 w/kg, an increase of 15.6%.

The effects on the system characteristics which determine life cycle costs were as follows:

- Increase of 7% in fuel consumption (and cost).
- Decrease of 10% in energy consumption (and cost).
- Increase of 1% in the total of fuel and energy cost.
- Decrease of 16.7% battery acquisition and replacement cost.
- Decrease of 2.6% in propulsion system (non-battery acquisition cost), due to slight downsizing of components.
- Decrease of 3.1% in life cycle cost.

Note that in the baseline case, battery acquisition and replacement accounts for 16.55% of the total life cycle cost. If only this portion of the life cycle cost is considered, the 16.7% reduction in battery weight accounts for a reduction of 2.8% in life cycle cost. Thus, the remainder of the increases and decreases (fuel and energy costs, propulsion system acquisition) amount for an additional .3% savings. In other words, the cost savings due to using a

smaller battery are increased by a factor of about 10% when the effect on the overall system is considered, provided the weight reduction due to the smaller battery is fully taken advantage of, both in the vehicle and in the remainder of the propulsion system.

2. Battery Type

In addition to the two types of batteries (ISOA lead-acid and nickel-zinc) specified in the work statement, consideration was also given to the nickel-iron system. Assumed characteristics for this system are defined in Figures 4-16 and 4-17; the lead-acid and nickel-zinc characteristics are also shown for comparative purposes. The propulsion system parameters for the three systems considered are summarized in Table 4-10. Note that in each case, the batteries are sized for maximum specific powers in operation which are very close to the peak specific powers defined by the X-intercepts of the curves in Figure 4-16.

The results of simulations using HYBRID2 and life cycle cost are summarized in Table 4-11. The nickel-zinc system clearly has the potential for significantly lower (approx. 20%) fuel consumption than the other two battery systems, as a result of this battery's high specific energy. However, as concluded in the parametric studies task, it appears that the combination of short cycle life and high replacement cost makes this system rather uncompetitive in terms of life cycle cost. The nickel-iron system, on the other hand, looks quite attractive, primarily as a result of its projected extended cycle life. Its life cycle cost figure of 6.56¢/km is only 7.4% higher than the value of 6.11¢/km for the reference conventional propulsion system.

These conclusions must be regarded as being highly tentative since they are based on assumptions with respect to battery life and cost which may or may not prove to be true when and if batteries of the three types considered reach commercial production. The best that can be said about these cost and life assumptions is that they were in line with the goals set by the Argonne National Laboratory for Improved State of the Art batteries, at the time this study was being done.

In recognition of the uncertainty of these assumptions, and of the continual influx of new information on battery characteristics, the contribution

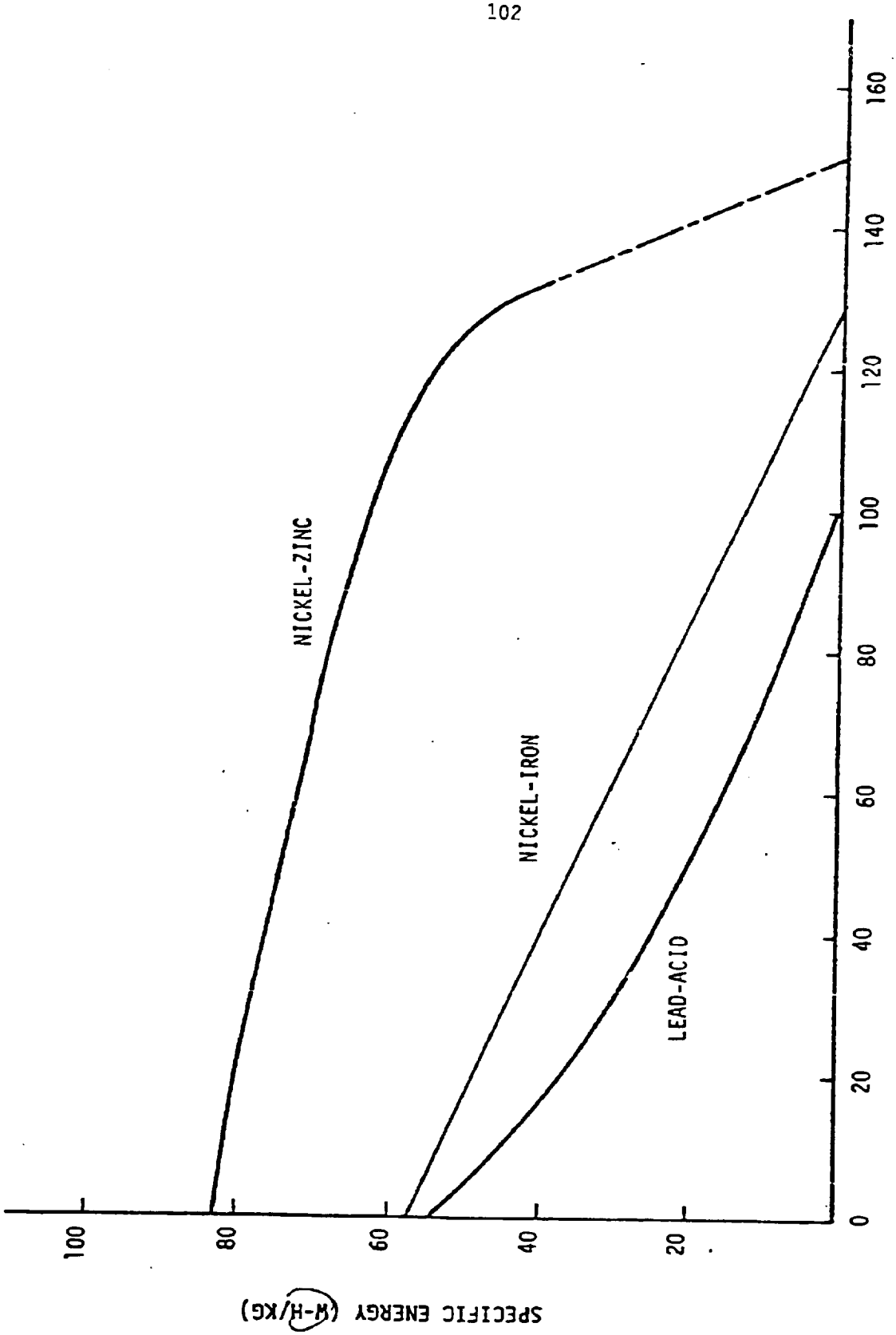

Figure 4-16. ISOA BATTERY CHARACTERISTICS

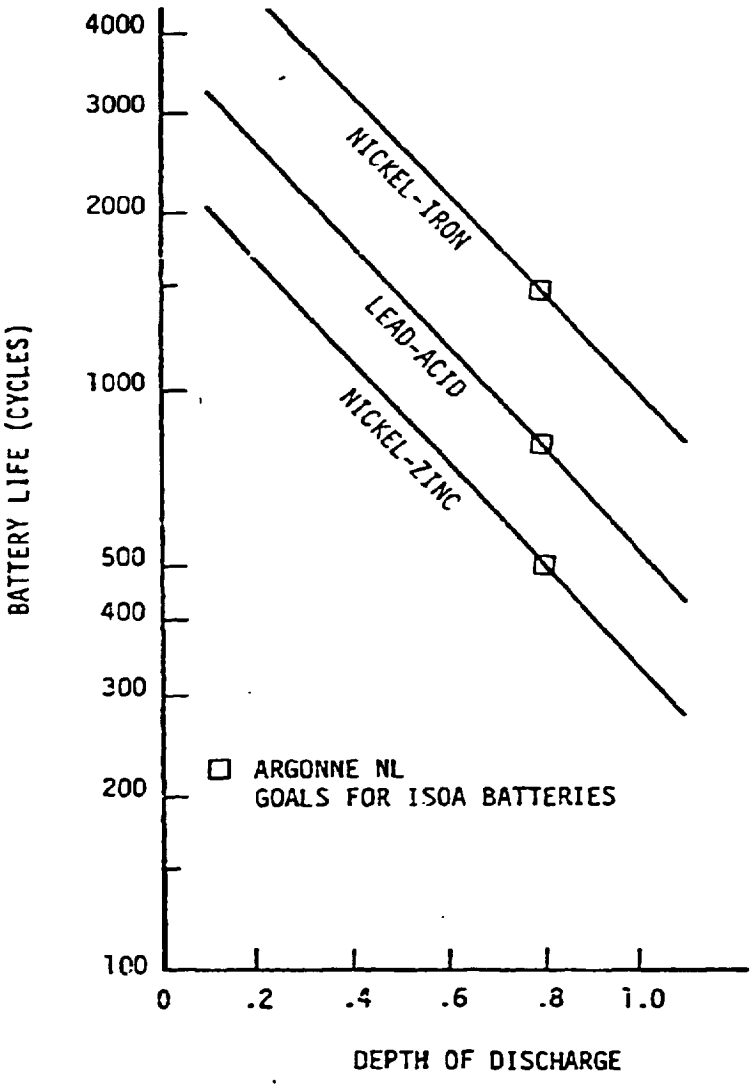

Figure 4-17. ASSUMED BATTERY LIFE CHARACTERISTICS

Table 4-10. PROPULSION SYSTEM PARAMETERS FOR THREE BATTERY TYPES

	Lead-Acid (Baseline)	Nickel-Zinc	Nickel-Iron
Heat Engine Max. Power (Kw)	70	72.1	64.3
Electric Drive Subsystem Max. Power (Kw)	28.5	25.4	26.3
Battery Weight (Kg)	390	229	274
Vehicle Test Weight (Kg)	2216	1968	2039
Peak Battery Specific Power	96	146	126

Table 4-11. EFFECTS OF BATTERY TYPE ON SYSTEM CHARACTERISTICS

	Lead-Acid (Baseline)	Nickel-Zinc	Nickel-Iron
Fuel Consumption (G/Km)	30.72	24.40	30.05
Wall Plug Energy Consumption (KWH/Km)	.196	.212	.181
Projected Battery Life (Km)	97000	62600	16000+ (life of vehicle)
Costs:			
Propulsion System Acquisition (exclusive of propulsion battery)($)	3097	2867	2931
Battery Acquisition ($)	1014	1786	1336
Life Cycle (¢/Km) (@ $2/gal. fuel, 7¢/KWH electricity)	7.17	8.40	6.56
Contribution of Battery Acquisition and Replacement to Life Cycle Cost (¢/Km)	1.19	3.10	.84

of battery costs (initial acquisition and replacement) to the life cycle cost is broken out separately in Table 4-11. If the reader wishes to make a different set of assumptions with respect to life and cost, he can correct these figures appropriately and estimate new values for life cycle cost. For example, if the assumed life characteristics for nickel-iron batteries are high by a factor of 1.5 and the cost low by a factor of 0.8, its contribution to the life cycle cost can be corrected to .84(1.5)/.8 = 1.58¢/km. The total life cycle cost can then be estimated as 6.56 - .84 + 1.58 = 7.30¢/km.

3. Battery Performance Characteristics

Apart from the uncertainties involving the cost and life of commercialized ISOA batteries, there are also uncertainties involving the specific energy characteristics. Consequently, some runs were made with the lead-acid and nickel-zinc systems to determine the effects if the specific energy at a given specific power is 20% lower than the values shown in Figure 4-16. The peak specific power and battery mass were left unchanged. For both these systems, this lowering of specific energy resulted in an increase in fuel consumption of about 10% and a decrease in wall plug energy consumption of about 9%. The relative increase in fuel consumption was more than the decrease in energy consumption because of the fact that the amount of operation on Mode 2 increased and Mode 1 operation decreased, and the overall efficiency of the heat engine on Mode 2 is somewhat less than its efficiency on Mode 1. It should also be noted that the decrease in wall plug consumption does not match, in percentage terms, the decrease in battery specific energy. This is a result of the fact that some driving takes place on days on which the battery discharge limit is not reached; this occurs both for the nominal case and the cases for which the specific energy was reduced 20%. On the short distance days, reducing the available energy from the battery has no effect on the relative consumption of fuel and wall plug electricity.

The net effect of this change on overall life cycle cost is still less: for the baseline lead-acid case, an increase in life cycle cost from 7.17¢/km to 7.26¢/km, or an increase of 2.1%.

4. Battery Figures of Merit for Hybrid Application

The life cycle cost of a hybrid propulsion system can be divided into three basic components:

LC_1 A component associated with the acquisition and replacement cost and life of the propulsion battery.

LC_2 A component associated with the cost of fuel and energy consumed.

LC_3 A component associated with the acquisition cost of the propulsion system, along with maintenance and repair costs.

Table 4-12 shows these different cost components for the hybrid system with the three different battery types considered. It is noteworthy that LC_2 and LC_3 are considerably less sensitive to battery type than is LC_1 .

Table 4-12. Life Cycle Cost Components for Three Battery Types

Cost Component	Lead-Acid	Nickel-Zinc	Nickel-Iron
LC_1 (Battery Acquisition & Replacement)	1.19¢/km	3.10	0.84
LC_2 (Fuel & Energy)	3.28	2.96	3.14
LC_3 (Propulsion System Acquisition)	2.70	2.34	2.58

Now, each of these cost components is affected by a different battery parameter. Consider LC_1 . Obviously, this is directly proportional to the ratio of battery acquisition cost to battery life. In turn, battery acquisition cost is proportional to the product of battery cost/mass by the battery mass. Since, to minimize battery weight and costs, the batteries have been sized so that the maximum specific power in operation is close to the peak usable specific power, battery mass is inversely proportional to peak usable specific power. We are, thus, led to the following definition of a battery cost parameter for the hybrid application:

$$P_{CB} = \frac{\bar{C}_B}{\bar{P}_{MAX}} \cdot L \qquad \left(\frac{¢}{W - CYCLE} \right)$$

where $\bar{C}_B$ = battery cost/mass (¢/kg)

$\bar{P}_{MAX}$ = peak usable power (w/kg)

L = cycle life (cycles at 80% DOD)

Note that this is quite a bit different than the cost parameters normally used for eavluating a battery for an electric vehicle application.

LC_2 is related primarily to the total energy stored in the battery. As this number increases, the amount of Mode 1 operation increases, the amount of fuel used decreases, and the amount of wall plug energy increases, which results in a net reduction in the total cost of fuel and energy. A suitable definition for this parameter is:

$$P_{EB} = \frac{\bar{E}}{\bar{P}_{MAX}} \text{ (hr.)}$$

where $\bar{E}$ = specific energy (w hr/kg)
and $\bar{P}_{MAX}$ is defined previously. Note that $\bar{E}$ should be defined at a rate which makes sense for the hybrid application; in particular, the one hour rate is more meaningful than the three hour rating commonly used for electric vehicles.

LC_3 is affected by the battery primarily as a result of its mass, since a reduction in battery mass results in a downsizing of the propulsion system, and a reduction in vehicle mass. As discussed previously, the battery mass is determined primarily by peak usable battery specific power, $\bar{P}_{MAX}$; consequently, LC_3 can be regarded as being dependent primarily on the parameter

$$P_{PB} = \bar{P}_{MAX}$$

These three parameters, $P_{CB} = \frac{\bar{C}_B}{\bar{P}_{MAX} L}$, $P_{EB} = \frac{\bar{E}}{\bar{P}_{MAX}}$, and $P_{PB} = \bar{P}_{MAX}$, can be regarded as economic figures of merit for use in evaluating a battery type for hybrid application. The next question is, what weights should be given these parameters? To answer this, the data generated on the life cycle costs of the hybrid system with the three battery types were used to generate an approximate linear relation between total life cycle cost and these three parameters. This relation is as follows:

$$L\ C\ C = 7.47 + 357.5\ P_{CB} - 1.74\ P_{EB} - .0072\ P_{PB} .$$

Table 4-13 compares the results provided by this expression with those discussed in previous paragraphs. Agreement is within 1.8%. Thus, this expression provides a useful means for estimating the effects of changes in battery parameters on life cycle costs. In using it, however, it must be recognized that its range of applicability is limited by the following:

Battery Type	$\bar{E}$ (1 hr rate), w-hr/kg	$\bar{P}_{MAX} = P_{PB}$, $\frac{W}{kg}$	L, Cycles	C_B, \$/kg	P_{CB}, ¢/w-cycle	P_{EB}, Hr.	LCC ¢/km (linear relation)	LCC ¢/km (simulation
1. Lead-Acid								
Nominal	30	100	800	200	.0025	.3	7.12	7.17
Higher Specific Power	30	115.6	800	200	.00216	.260	6.96	6.95
Lower Specific Energy	24	100	800	200	.0025	.24	7.22	7.26
2. Nickel-Zinc	70	150	500	600	.008	.467	8.44	8.40
3. Nickel-Iron	40	130	1500	375	.00192	.308	6.68	6.56

Table 4-13. BATTERY FIGURES OF MERIT AND THEIR USE IN ESTIMATING LIFE CYCLE COST

- The hybrid propulsion system must be similar to the baseline system in terms of size and general design.

- Fuel and electricity costs are $2/gal. and 7¢/kwh, respectively.

The expression may also be normalized to the baseline case (lead-acid batteries). The results are:

$$\tilde{LCC} = 1.049 + .1255\,\tilde{P}_{CB} - .0733\,\tilde{P}_{EB} - .1011\,\tilde{P}_{PB}$$

where $$\tilde{LCC} = \frac{LCC}{L_{CC}(\text{baseline})} ,$$

and so forth. The coefficients in this expression effectively define the relative weights of the three battery figures of merit. The battery cost parameter $\tilde{P}_{CB}$ is most significant, followed by the peak power parameter $\tilde{P}_{PB}$ and the total energy parameter $\tilde{P}_{EB}$, in that order.

This expression can also be linearized in terms of the more conventional parameters $\bar{P}_{MAX}$, $\bar{C}_{B/L}$, and $\bar{E}$. The results are

$$LCC = .1255\Delta\,(C_B/L) - .1533\Delta P_{MAX} - .0733\Delta E$$

What this expression says, for example, is that an increase of 10% in P_{MAX} from the baseline is worth about 1.5% decrease in life cycle cost, whereas a 10% increase in $\bar{E}$ is only worth about .7% on life cycle cost; that is, specific power is more than twice as important as specific energy in determining the life cycle cost of a hybrid. The ratio of cost per mass to battery life is of comparable weight to specific power, with a 10% decrease in this parameter being worth about a 1.3% decrease in life cycle cost.

Motor/Controller Efficiency

To assess the effects of motor/controller efficiency on the system performance, a simulation run was made with the average motor/controller efficiency 5% higher than the baseline case. The result was a reduction in fuel consumption of 3.2%, resulting from an extension of the average operating range on Mode 1 and a consequent greater fraction of the yearly operation on Mode 1. A minor reduction in energy consumption of 1.3% occurred, as a result of lower energy

consumption on those days for which the driving distance does not exceed the Mode 1 range. The impact on discounted lifetime fuel and energy costs was a savings of $130.70, or .08¢/km. This computation was made without any reduction in battery size to take advantage of the slightly lower peak power requirements of the motor/controller. With 5% lower battery weight, based on the results in Section 4.4.2 relating to the effects of a battery weight, a further reduction of $106.40 in life cycle cost could be achieved as a result of reduced propulsion system and battery acquisition and replacement costs. This would be accompanied by an increase in fuel consumption of 2.1%, and a decrease in energy consumption of 3%, for a net fuel economy improvement of about 1% and a reduction in energy consumption of about 4%. The resultant net decrease in discounted life cycle cost is $237, or .15¢/km. Consequently, if it costs more than $237 to achieve a 5% increase in motor/controller efficiency, that increase in efficiency is not economically justifiable.

Control Strategy Variations

1. Parameter Variations

The effects of the control parameters P_{HEMIN}, P_{HEMN2}, P_{MMAX}, V_{MAX}, and D_{BMAX} on fuel and energy consumption have been discussed in Section 4.4.1, Baseline Propulsion System. Since P_{HEMIN}, P_{HEMN2}, P_{MMAX}, and V_{MAX} were selected to minimize fuel and energy consumption on the two operating modes, variations in these parameters from the baseline values generally result in increased operating costs, so no further discussion of them is required. The effect of variations in the battery discharge limit, D_{BMAX}, on fuel and energy consumption were also discussed in Section 4.4.1; in this section, this discussion will be expanded to include the effect on life cycle cost.

These effects are summarized in Figure 4-18. Note that the reduction in life cycle cost associated with a given increase in D_{BMAX} decreases as D_{BMAX} increases; it appears that there may be an absolute minimum slightly above $D_{BMAX} = .8$. The change in life cycle cost between values of D_{BMAX} of .6 and .8 is only .04¢/km, or 0.6%; between .4 and .6, the change is .07¢/km, or 1%. Clearly, there is no point in dropping below D_{BMAX} of .6; and, as indicated in the discussion in Section 4.1.1, all factors indicate the desirability of operating near $D_{BMAX} = .8$ rather than the value of .6 used for the baseline.

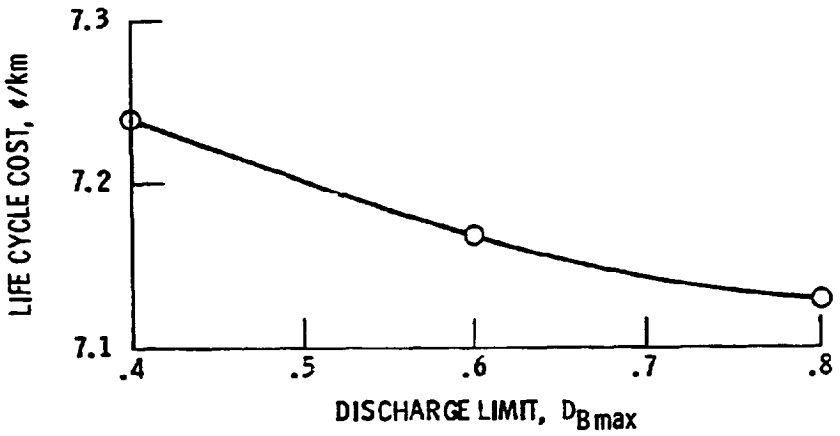

FIGURE 4-18. - VARIATION IN LIFE CYCLE COST WITH BATTERY DISCHARGE LIMIT.

2. Variations in Control Strategy Structure

The major variations considered in the structure of the control strategy involved elimination of on-off operation of the heat engine. These variations were considered, not as alternatives to the baseline strategy which might provide lower fuel consumption or life cycle cost, but as backup strategies which might be employed in the unlikely event that the on-off engine operation called for in the baseline strategy proves to be unworkable from a practical standpoint.

The variations included the following:

A. Strategy is the same as the baseline, except the engine is allowed to idle during the periods in which the vehicle is not stationary and in which the engine would normally be off if the baseline strategy were used. A clutch is still required to decouple the engine from the driveline during the idle periods.

B. The engine is never decoupled from the drivetrain, and the fuel is shut off during the periods in which the vehicle is not stationary and in which the engine would normally be off if the baseline strategy were used. During these periods, the electric motor supplies the torque required to motor the heat engine at the system speed.

C. Same as B, except enough fuel is supplied to keep the engine running at the system speed without putting additional load on the motor; i.e., the output torque of the heat engine is zero during the 'off' periods.

In all the above three variations, the engine was utilized, whenever the vehicle was stationary, to supply accessory, torque converter, and transmission front pump loads. Thus, in variation A, the engine clutch was always engaged when the vehicle was stationary.

The effects on fuel consumption, energy consumption, and lifetime fuel and energy costs are summarized in Table 4-14.

Table 4-14. Effects of Continuous Engine Operation on Fuel and Energy Consumption

	On-Off Operation (Baseline)	Continuous Operation		
		A	B	C
Fuel Consumption (g/km)	30.72	37.39	50.91	54.69
Wall Plug Energy Consumption (kwh/km)	.196	.173	.203	.173
Discounted Fuel/Energy Costs ($)	$5255	5736	7482	7584

Clearly, from standpoints of both fuel consumption and life cycle costs, variation A is the best of the three continuous operation variations considered. The difference in fuel and energy costs between A and the other two variations is far more than enough to pay for the additional clutch and controls which are required by A. Even variation A is not a very good alternative to the baseline strategy, however, since it uses about 22% more fuel. The net fuel and energy cost penalty of about $500 represents an increment in life cycle cost of about 0.3¢/km. It is clear that the pay-offs associated with on-off operation make it the place to start in a hybrid propulsion system development program.

4.4.3 Sensitivity to Assumptions About Vehicle Characteristics and Performance

The principal assumptions concerning vehicle performance and characteristics were supplied by LeRC and were summarized in Tables 3-1 and 3-3. These involve factors which directly affect road load power requirements, such as drag coefficient and rolling resistance coefficients, as well as factors which affect the computation of vehicle weight and, thus, indirectly affect the estimation of road load requirements. Changes in these assumptions affect the results of this study; the objective of this section is to quantify these effects.

Effects of Changes in Performance Requirements

Modifications of the baseline propulsion system parameters to accommodate changes in the acceleration performance requirements can be handled in a number of different ways.

The best way is probably to go back to the beginning of the design process and re-optimize the entire system around the new performance requirements. In lieu of this extremely time consuming process, the following scenarios may be considered:

A. Leave the electric propulsion system alone and adjust the heat engine size to meet the new requirements.

B. Leave the heat engine alone and adjust the electric propulsion subsystem.

C. Keep the heat engine power fraction and battery mass fraction constant; adjust both heat engine and electric propulsion subsystems.

D. Keep the heat engine power fraction and battery maximum specific power constant; adjust both subsystems.

Let us consider these alternative scenarios in light of some of the preceding discussions. First, in view of the large contribution of the electric propulsion system subsystem to life cycle cost, alternative B does not make much sense if the performance requirements are being adjusted upward. It is much cheaper to get additional performance by putting in more heat engine than by putting more electric motor and battery.

Conversely, alternative A does not make much sense if performance requirements are being adjusted downward, since it does not take advantage of potential cost reductions associated with reducing the size of the electric propulsion subsystem. For relatively small changes in performance requirements, either upward or downward, from the baseline values, it appears likely that keeping the heat engine power fraction constant more nearly approximates the optimum situation than either of alternatives A or B.

Scenarios C and D represent two alternative approaches in which the heat engine power fraction is held constant. In scenario C, the maximum specific power required of the battery increases with increasing vehicle performance requirements. Since the baseline system already operates very near the peak specific power capability of the battery (96 w/kg vs. 100 w/kh), scenario C

cannot be used if performance significantly above the baseline is required. There is, however, no problem in using it for lesser performance requirements. With scenario D, the battery weight fraction increases with increasing performance requirements. The result is that vehicle weight and, consequently, battery weight and propulsion system power requirements increase more rapidly under scenario D than under scenario C. Conversely, a relaxation in performance requirements results in a smaller change in vehicle and propulsion system size under scenario C than under D.

Vehicle and propulsion system parameters were computed for a range of values of power-to-mass ratio under both scenarios C and D, and simulations were run using the programs HYBRID2 and VSPDUP2 for these systems. The results are summarized in Figures 4-19 through Figure 4-21. Figure 4-19 shows the variation in acceleration performance with power-to-mass ratio for a fixed heat engine power fraction. A span of .035 to .05 kw/kg in power-to-mass ratio produces a range of 0-90 kph acceleration times from about 14 sec. down to about 10 sec. Most current production sedans fall within this range.

Figure 4-20 shows the variation in vehicle test mass with power-to-mass ratio. As indicated previously, the mass increases more rapidly with increasing performance (power-to-weight ratio) with the peak specific power held constant than with the battery weight fraction held constant. At a weight fraction of .176, the limiting peak specific power of 100 w/kg for lead-acid batteries is reached at a power-to-mass ratio of .046 kw/kg, close to the baseline value of .0429 kw/kg.

In Figure 4-21, fuel economy, energy consumption, and life cycle cost are plotted as functions of power-to-mass ratio for the two scenarios C and D. Surprisingly, for scenario D (constant battery specific power) fuel economy actually improves with increasing power-to-mass ratio and performance. The reason for this is that the battery mass fraction increases with increasing power-to-mass ratio under this scenario; consequently, the amount of energy storage relative to the vehicle mass also increases, and the relative amount of Mode 1 operation increases. This improves fuel economy. Under scenario C, fuel economy is a much weaker function of power-to-mass ratio, reaching a maximum at a power-to-mass ratio of .04 kw/kg, which is close to the baseline value.

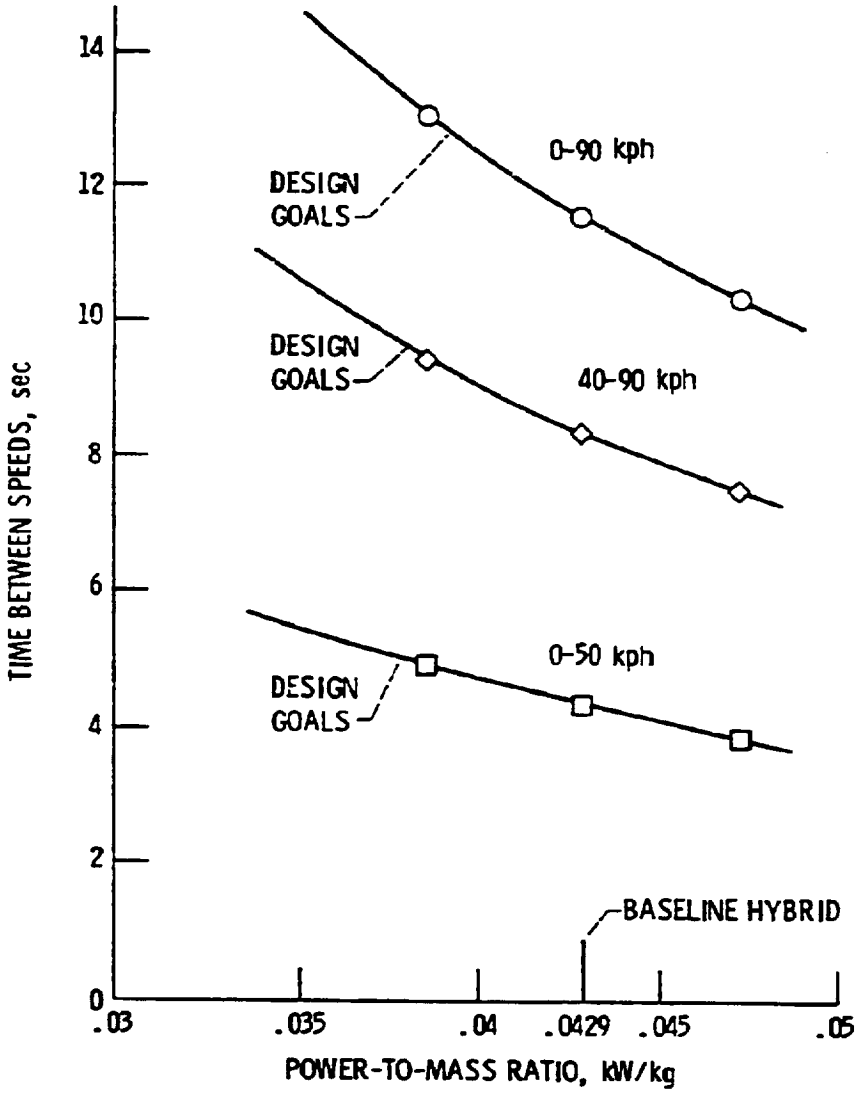

FIGURE 4-19. - VARIATION IN ACCELERATION PERFORMANCE WITH POWER-TO-WEIGHT RATIO, HEAT ENGINE POWER FRACTION = .71.

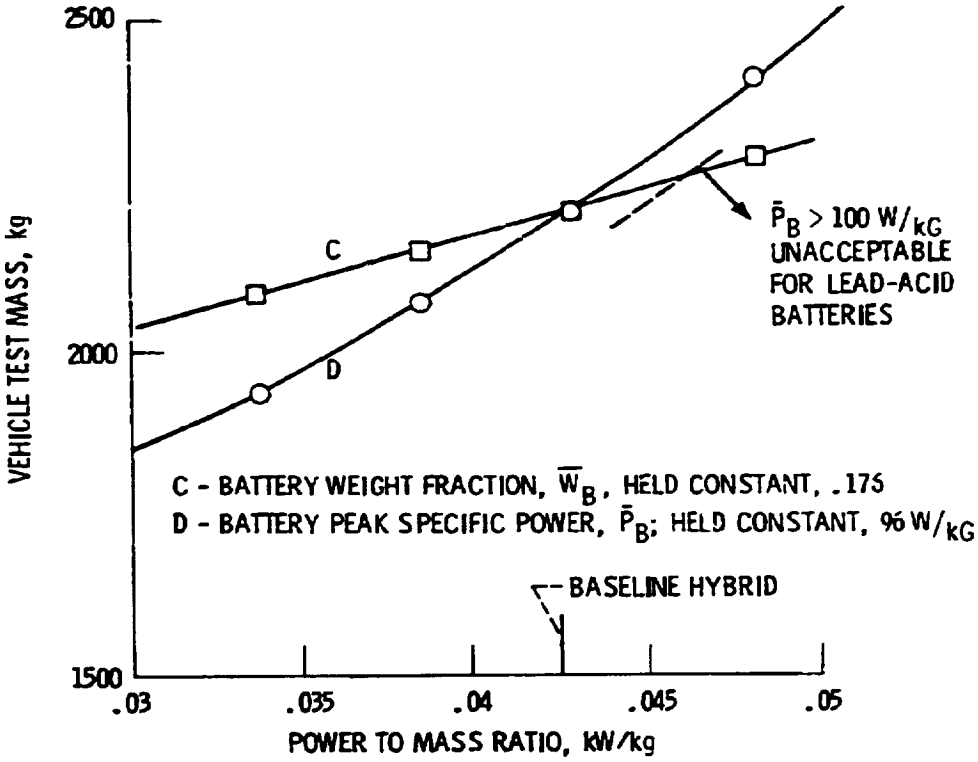

FIGURE 4-20. - VARIATION IN VEHICLE TEST MASS WITH POWER TO MASS RATIO, HEAT ENGINE POWER FRACTION = .71.

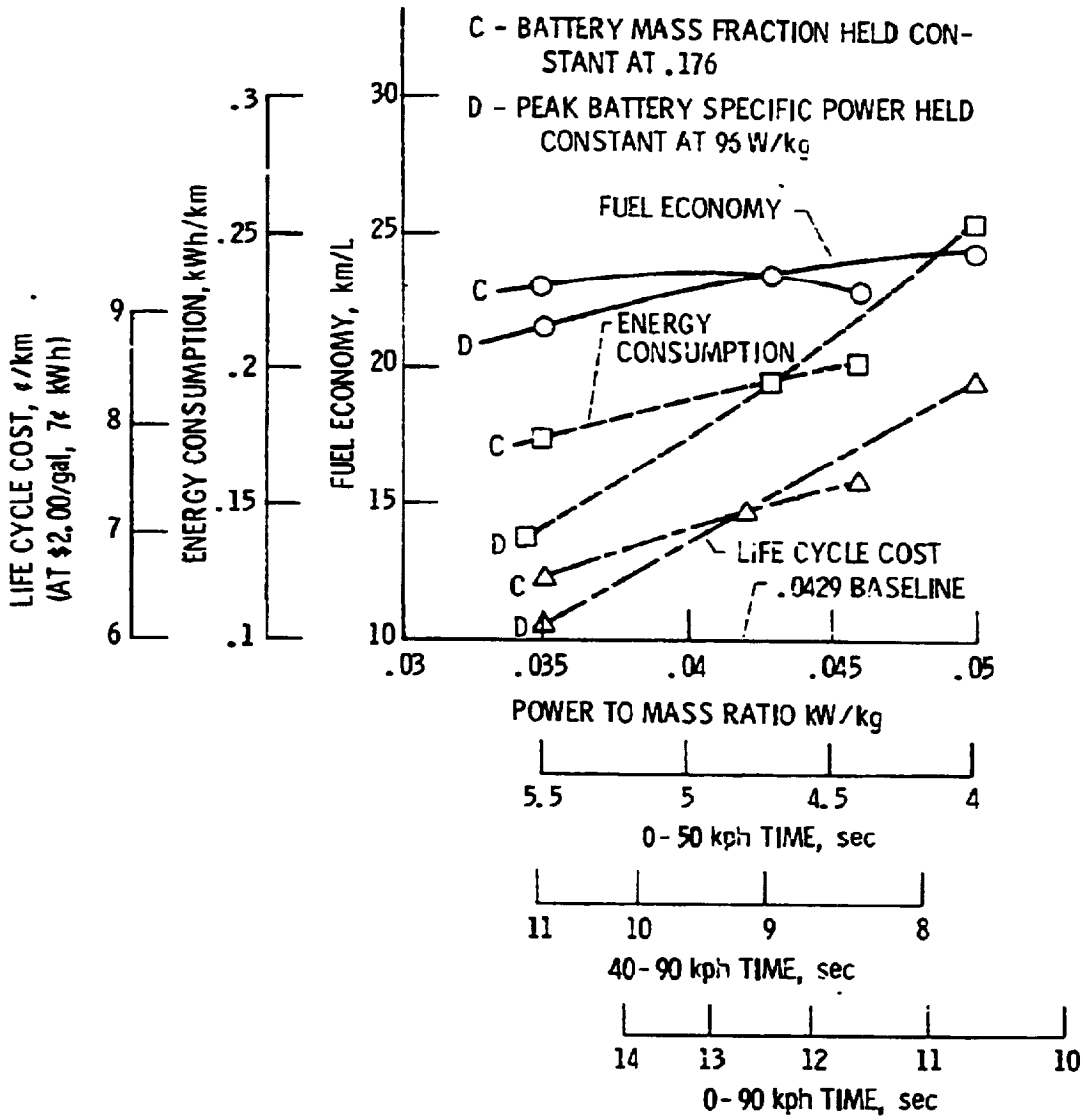

FIGURE 4-21 - EFFECTS OF CHANGES IN PERFORMANCE GOALS. HEAT ENGINE POWER FRACTION .71.

Note that in both cases, life cycle cost increases monotonically with increasing performance and power-to-weight ratio, so performance still extracts its toll.

To get a more concrete idea of what these results mean, consider a reduction in power-to-mass ratio from .0429 to .04, corresponding to an increase in 0-90 kph acceleration time from 11.6 to 12.5 sec., a decrease in performance of 7.8%. If the battery mass fraction is held constant, fuel economy increases only slightly, from 23.4 to 23.6 km/l, an improvement of only 0.85%, or about 1/10 of the relative decrease in performance. The reduction in life cycle cost is more significant, dropping from 7.17¢/km to 7.02¢/km, a decrease of 2.1%, or about 1/4 of the relative decrease in performance. On the other hand, if the battery peak specific power is held constant for the same performance reduction, the life cycle cost decreases to 6.88¢/km, a decrease of 4%, or about 1/2 of the relative decrease in performance. However, in this case, the fuel economy also decreases to 22.8 km/l, about 2.6%, or 1/3 of the relative performance decrease.

It appears, then, that fuel economy is a relatively weak function of the performance level. In fact, if the hybrid system design is aimed at low life cycle cost (scenario D), a reduction in the performance requirements results in a decrease, rather than an increase, in fuel economy. The life cycle cost can, however, be reduced significantly by backing off on the performance requirements.

Effects of Changes in Vehicle Characteristics Affecting Road Load Power Requirements

These characteristics include vehicle mass, aerodynamic drag coefficient, and tire rolling resistance. The vehicle mass is affected by assumptions regarding chassis and body mass and mass propagation factors.

The relation used for computing vehicle test mass, as derived from the mass relationships provided by LeRC (Table 3-3) is:

$$W_T = 1.3\ W_p + 1202\ (kg) \qquad (1)$$

where W_T is the test mass, and W_p is the propulsion system weight. Included in the fixed mass of 1202 kg is a test payload of 254 kg, so the vehicle curb mass is given by

$$W_C = 1.3\ W_p + 948\ (kg) \qquad (2)$$

The component mass vs. power relationships given in Table 3-5 were updated to the following:

Heat Engine:	$W_h = 1.5\ P_h + 80$
Electric Motor/Controller:	$W_e = 3.98\ P_m$ (P_m = peak motor output power)
Transaxle:	$W_t = .9\ (P_h + P_m) + 25$

These relationships, together with those defining the vehicle mass, gave a test mass of 2216 Kg (4875 lbs.) for the baseline hybrid, and a curb mass of 1962 Kg (4316 lbs.). The corresponding values for the reference conventional vehicle were 1622 Kg (3568 lbs.) for the test mass, and 1368 Kg (3010 lbs.) for the curb mass.

In view of the fact that the present Chrysler "K" cars are six passenger cars weighing under 3000 lbs., the masses which relationships (1) and (2) above give for a ca. 1990 conventional six passenger vehicle may be somewhat high. This may be a result of the fixed masses, or the mass propagation factor (0.3), being somewhat high, or a combination of the two. In particular, the mass propagation factor may vary over a fairly wide range, depending on where the mass added or removed from the vehicle is located. For example, a mass added directly over an axle requires less additional body structure to support it than a centrally located mass. Generally, a reasonable range for the weight propagation factor is from .2 to .5 depending on the mass location, so the value of .3 used is by no means unreasonable, only uncertain.

As a result of these considerations, it appears that there is a total uncertainty on the vehicle test mass of $\pm$ 10%, with the probability being that, if it is off in any direction, it is too high.

With this conclusion in mind, simulations were run with the HYBRID2 program at values of test mass 10% over and 10% under the nominal value of 2216 Kg. Propulsion system component sizes were adjusted to maintain a constant power-to-weight ratio and constant battery maximum specific power. The results are summarized in Table 4-15.

Table 4-15. EFFECTS OF CHANGES IN VEHICLE TEST MASS

Variable	Relative Mass Change +10%	-10%
1. Energy Expended in Brakes, Air Drag, and Tire Rolling Resistance:		
Urban Cycle	+7.4%	-7.4%
Highway Cycle	+5.5%	-5.6%
2. Fuel Consumption	+3.6%	-2.8%
3. Wall Plug Energy Consumption	+9.7%	-8.6%
4. Life Cycle Cost	+6.2%	-5.8%

Note that the increment in wall plug energy consumption closely approximates the change in vehicle mass. This is simply because the battery mass, and hence, the energy storage capacity, was adjusted up or down with the vehicle mass. Table 4-15 indicates that a relative error in the estimation of vehicle mass results in a relative error which is about 1/3 as large in the estimation of fuel economy, and one which is about 60% as large in the estimation of life cycle cost.

2. Tire Rolling Resistance

It is estimated that the assumption with regard to tire rolling resistance is subject to an uncertainty of about ± 20%. The effects of changes of this magnitude are summarized in Table 4-16. (Wall plug energy was not tabulated since the changes were not significant.) It should be noted that no adjustments were made in the sizes of propulsion system components for these runs, because of the very minor effect of rolling resistance on acceleration performance.

Table 4-16. Effects of Changes in Tire Rolling Resistance Coefficient

Variable	Relative Change in Rolling Resistance +20%	-20%
1. Energy expended in brakes, air drag, and tire rolling resistance		
Urban Cycle	+14.1%	-14.0%
Highway Cycle	+10.1%	-10.2%
2. Fuel consumption	+10.1%	- 9.2%
3. Life cycle cost	+ 2.9%	- 2.6%

Table 4-16 indicates that a relative error in estimation or tire rolling resistance results in an error of about 1/2 that magnitude in the estimation of fuel economy, and about 14% as large a relative error in the estimation of life cycle cost.

3. Aerodynamic Drag Coefficient

As in the case of tire rolling resistance, the assumption on the product of aerodynamic drag coefficient and frontal area are felt to have an uncertainty of about 20%. The effects of changes of this magnitude are summarized in Table 4-17.

Table 4-17. Effects of Changes in the Product of Drag Coefficient and Frontal Area (C_DA)

Variable	Relative Change in C_DA +20%	-20%
1. Energy expended in brakes, air drag, and tire rolling resistance		
Urban Cycle	+5.2%	-5.2%
Highway Cycle	+8.9%	-9.0%
2. Fuel consumption	+6.7%	-5.3%
3. Life cycle cost	+1.9%	-1.5%

The table indicates that a relative error in the estimation of drag coefficient results in a relative error in fuel consumption which is about 30% as large, and one in life cycle cost which is about 8% as large.

4.4.4 Effects of Alternative Design Approaches

Alternative System Layouts

In the baseline hybrid propulsion system, the heat engine and traction motor both drive through a torque converter and four-speed automatic transmission. In this section, we address the question of whether alternative mechanical layouts would offer superior overall performance.

As discussed in Section 4.4.1, the reason for allowing the traction motor to drive through the torque converter is to permit it to keep running while the vehicle is at rest in order to supply accessory power and to keep adequate hydraulic pressure available for the transmission and torque converter. Power must be supplied to meet these requirements when the vehicle is at rest, and if the heat engine is shut down (the most fuel efficient strategy), the only power source available is the propulsion battery. The only question is whether it is more economical to use the traction motor to drive these accessories or to use a separate drive motor. The major problem with the latter scheme is that the separate drive motor would also have to be large enough to drive accessories under all vehicle operating conditions, not just when it is at rest. Even with

constant speed operation, the peak accessory power requirement (air conditioning compressor, power steering pump, transmission front pump) would be in excess of 4 kw. This relatively large motor would have to be paid for by the fuel savings associated with the extension of the Mode 1 operating range obtained by eliminating the portion of the torque converter losses supplied in the baseline system by the traction motor. Analysis of the losses involved indicate that the average torque converter power loss which can be assigned to the electric motor (i.e., the fraction of the total torque converter loss which corresponds to the ratio of motor power to total power delivered) is about 1 kw. Now, the average motor output on Mode 1 over the urban driving cycle is about 5.1 kw, and 7.8 kw on the highway cycle. Most Mode 1 driving is done on the urban cycle, so an average of about 6 kw is reasonable. As a rough estimate, the range extension on Mode 1 can be estimated to be about 1/6, or approximately 17%. The resultant fuel savings amount to about 6.5%, with a present value (at the $2/gal level) of $214 over the vehicle lifetime. The acquisition cost, however, of a DC accessory drive system with a power rating of at least 4 kw can be expected to be considerably higher than this value. Whether a DC shunt motor with minimal controls, or an AC motor with an inverter is used, the OEM cost of a drive system with 5 kw peak output, 2.5 kw continuous output, would be in excess of $200.

Consequently, it does not appear that a separate electric drive for the accessory systems is economically justifiable; and the baseline system has much to recommend it in terms of simplicity and minimizing the development requirements for those subsystems which are not critical to overall system performance.

If, however, it is ultimately determined in the course of development that on-off engine operation presents insurmountable problems, then a configuration in which the traction motor does not drive through torque converter makes sense. Under those conditions, the heat engine is available at all times to supply accessory power, making a separate accessory drive unnecessary. A system of this type was simulated, and it is of interest to compare the results of this simulation with those obtained with the baseline system with continuous operation of the heat engine, as described in Section 4.2.2, "Control Strategy Variations."

The mechanical configuration of the system simulated is shown schematically in Figure 4-22. The component descriptions were identical to those used for the

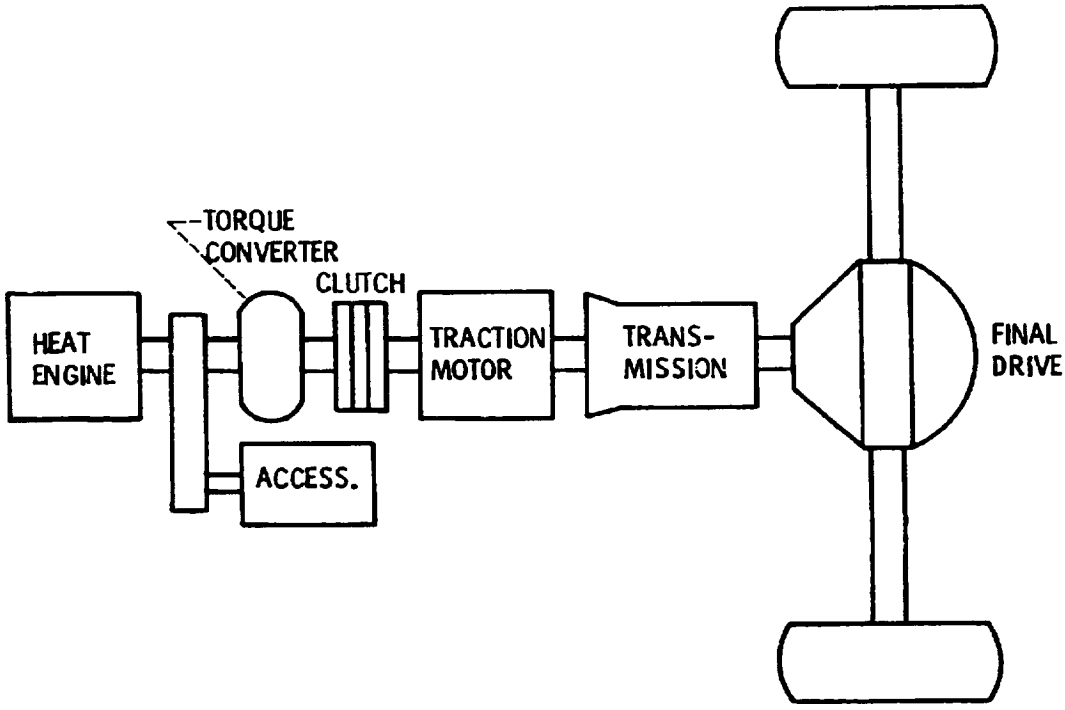

FIGURE 4-22. - ALTERNATIVE MECHANICAL CONFIGURATION.

baseline system, except that a smaller diameter torque converter (242 mm instead of 276 mm) was used. A higher stall torque ratio (2.4 rather than 2.0) was also used in order to compensate for the loss of low speed torque resulting from the fact that the electric motor's torque is not multiplied by the torque converter.

Compared with the best of the three continuous operation strategies (variation 'A') which were considered for the baseline layout, the revised mechanical layout left the fuel consumption virtually unchanges (37.44 g/km vs. 37.39 g/km). The wall plug energy consumption was reduced about 18% from .173 to .142 g/km. The reduction of wall plug energy consumption was due to a significant increase in Mode 1 range which was due not only to the elimination of a portion of the torque converter losses from the electric motor load, but also from the transfer of the accessory load from the motor to the heat engine under all operating conditions, not just at idle. The range extension was such that, even at a value of .6 for the battery discharge limit D_{BMAX}, the discharge limit was not reached on most driving days. If the control strategy were to be re-optimized for the different configuration (perhaps by using a larger value of P_{NOM}) some of the fuel energy usage could be shifted back to wall plug energy. Time did not permit going through this exercise; however, the results in hand do indicate that the configuration shown in Figure 4-22 is superior to the baseline if the heat engine is operated continuously. As discussed previously, however, this type of operation should be considered only if some serious development work indicates that on-off operation, with its high fuel economy payoff, is not feasible.

Alternative Transmissions

In the last section, the effects of relocating the torque converter relative to the heat engine and motor were discussed. The next obvious question to ask is, can the torque converter be completely eliminated using either an automatically shifted gearbox or a continuously variable transmission? Before attempting to answer this question, it is necessary to understand the function of the torque converter in the baseline system. That function is comprised of the following elements, the first two of which are common to both conventional and hybrid applications:

1. It provides additional torque multiplication at low speeds, increasing the effective ratio range of the transmission.

2. It provides a 'shock absorber' in the system, which reduces the severity of the shift transient as felt by the driver, and alleviates the problem of designing and developing a transmission which shifts smoothly without having the driver in the loop controlling throttle and clutch engagement.

3. It permits the traction motor to keep running, when the vehicle is at rest, to supply accessory power, including the requirements of the transmission front pump.

4. It smoothes out the transient (as felt by the vehicle occupants) which occurs when the heat engine clutch is engaged to start the heat engine.

The last point is one which must not be overlooked when considering the practical aspects of a hybrid system. The highest fuel economy payoff comes from the ability of the hybrid to utilize the heat engine in an on-off mode; in practical terms, this must be accomplished in a system which still provides smoothness and driveability which is acceptable to the average driver. Analyses performed in the previous Near Term Hybrid Vehicle Program[1] have shown that the magnitude of the transient experienced by the vehicle when the heat engine is started are on the order of 1/10 as severe when a torque converter is in the system as when it is locked up. This transient can be measured by either the maximum deceleration, or the total velocity change, experienced by the vehicle during the engine start up process. In that case, the peak vehicle deceleration was on the order of .1 G when no torque converter was used, vs. about .01 G with the torque converter in the system. This factor, coupled with item 3 on the list of torque converter functional elements, must be carefully considered when investigating the use of either an automatically shifted gearbox or a CVT in a hybrid application involving on-off engine operation.

Figure 4-23 shows schematically a mechanical layout for a hybrid system utilizing either an automatically shifted gearbox or a continuously variable transmission. In the case of an automatically shifted gearbox, the clutch between the induction motor and gearbox would have to be servo-controlled to disengage during the shifting process to provide smooth shifts. This would have to be synchronized properly with control of the heat engine and motor to prevent excessive speed excursions of these components while they are unloaded

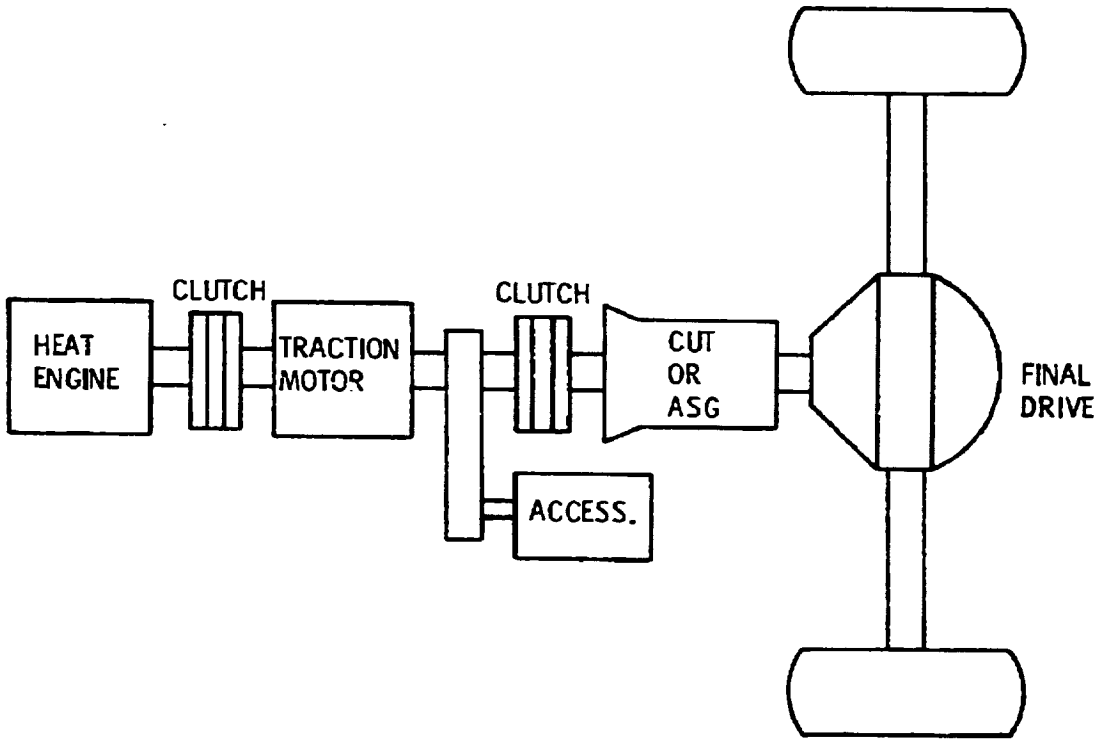

FIGURE 4-23. - HYBRID SYSTEM LAYOUT WITH CONTINUOUSLY VARIABLE TRANSMISSION (CVT) OR AUTOMATICALLY-SHIFTED GEARBOX (ASG).

during the shifting process. Because of the variables introduced by clutch wear, variations in clutch temperature, and speed and load at which the shift takes place, it is a difficult problem to get such a purely mecahnical system to shift smoothly under all conditions, without having an extremely sophisticated adaptive controller (i.e., a human driver) in the loop. It is conceivable that such a system could be made to work successfully when there is a precise measure of, and control over, speed and torque of the driving unit. For example, in a pure electric vehicle driven by a DC motor in which the controller limits armature current, setting this armature current limit to zero during the shifting process provides a precise means of insuring that the shift takes place under essentially zero torque. This can be combined with a phase-lock controller operating on the motor field, which synchronizes the motor input speed, while it is unloaded, with the transmission input speed in the gear to which gearbox is being shifted.

In the hybrid application, this picture is considerably complicated by the presence of the heat engine and the need for precise control over its output torque also, during the shift process. Such control would be particularly difficult if the shift was accompanied by a transition from engine-off to engine-on operation, which is likely to be the case in the event of a sudden increase in power demand. These considerations, coupled with the overall problem of trying to achieve a smooth transition from engine-off to engine-on operation without a hydrodynamic torque converter, led to the conclusion that the development of such a transmission, as an integral part of a hybrid system, should be given low priority relative to the more fundamental development problems of the hybrid system such as on-off control of the heat engine optimization of the overall control strategy, and reduction of life cycle cost.

The same conclusion was drawn with respect to the use of a continuously variable transmission, on the basis of slightly different considerations. The usual objective of a CVT is to obtain improved fuel economy, relative to that obtainable with a conventional automatic transmission, by keeping the engine operating closer to the minimum bsfc attainable at any given power demand, and by achieving a higher overall efficiency. In the case of the hybrid, heat engine operation is kept near the region of minimum bsfc by the system control strategy. As indicated in the discussion of the baseline hybrid in Section 4.4.1,

the average bsfc in any operating mode is never more than 10% greater than the absolute minimum attainable with this engine. Consequently, it cannot be expected that a CVT will provide much improvement in this regard. Consequently, there remains only the question of the average efficiency of a CVT vs. that of a conventional automatic.

Efficiency claims for CVT's vary widely; however, if attention is restricted to those which show serious promise of being available as well developed prototypes in the near future, and of achieving production staus in passenger cars by the year 1990, the problem of sorting these claims out becomes somewhat simplified. It is the judgment of the writers that the only CVT which warrants serious consideration within this time frame is the metallic belt drive being developed by Van Doorne's Transmissie B.V. in Holland, and Borg Warner in the U.S. (This judgment is admittedly colored by the feeling that a hybrid propulsion system development program should address primarily the fundamental development problems discussed previously; transmission development per se should be involved only secondarily.) This transmission transmits torque on the compression side of the belt, consisting of a set of endless maraging steel bands which support and guide a set of wedge shaped elements. These wedge shaped elements ride on the pulley surfaces and transmit torque from one pulley to the other by thrust forces between the elements. Tensioning of the bands must be greater than the thrust forces between the elements. This tensioning, together with the positioning of the pulleys to vary the transmission ratio, is accomplished hydraulically. As indicated in Figure 4-23 , a separate clutch is required for start up since slippage of the belt relative to the pulleys is not permissible.

Comparing this transmission with a conventional automatic, it appears that any major difference in efficiency lies primarily in the automatic's torque converter. Both transmissions require oil pumps to supply pressure for actuating clutches and bands (conventional automatic) or the variable ratio pulleys (CVT) The power requirements of these pumps are probably similar. As far as the efficiency of the basic 'gearing' is concerned, we would expect the average efficiency of the automatic to be, if anything, slightly higher than that of the CVT, since one gear is direct drive.

Based on these considerations, it was not expected that use of a CVT would make a great deal of difference on fuel or energy consumption. This was confirmed by a simulation, the essential characteristics of which were the following:

- o On-off operation of the heat engine was retained, using the same criteria for starting and stopping the heat engine as used in the baseline system.

- o The traction motor was de-clutched from the transmission at 500 RPM and allowed to idle when the vehicle was at rest in order to supply accessory loads (power steering and transmission hydraulic supply).

- o A 4:1 ratio range was assumed for the CVT, and the ratio was chosen as follows: If the heat engine was on, the ratio was selected to operate the heat engine at the minimum bsfc for the power level demanded. If the heat engine was off, the ratio was chosen to keep the traction motor operating as close as possible to its region of best efficiency.

Time did not permit the optimization of a control strategy for the CVT, and the simulation actually gave a slightly higher fuel consumption than the baseline, with considerably lower wall plug energy consumption. This would indicate that an optimized strategy could trade off fuel for energy consumption. Since the heat engine is kept close to its minimum bsfc point with both the baseline system and the CVT, it is very informative to just look at the differences in total energy consumption between the two systems. These may be summarized as follows:

(1) On the urban cycle, the CVT system had a 10.6% reduction in total drive train losses compared to the baseline system, and a reduction of 5.6% in total energy consumption.

(2) On the highway cycle, the corresponding reductions were 6.3% and 1.7%.

(3) The corresponding yearly average reductions were 9.9% and 4.6%.

Assuming that the reduction in total energy consumption was all taken from the fuel side of the picture, rather than from the wall plug, a CVT would be expected to yield about a 7% reduction in fuel consumption relative to the baseline system (about 63% of the total energy used to drive the vehicle, on a yearly average basis, comes from the heat engine in the baseline system).

The conclusion was that the gain in going to a CVT was small, relative to the disadvantages of giving up the shock absorbing characteristics of the torque converter, and having to incorporate an additional clutch in the system for the traction motor.

Alternative Heat Engine Configurations

Within the context of the work statement, which restricted attention to stratified charge rotary engines, turbocharged and multi-rotor, variable displacement variations in this basic engine type were considered. Both these variations represent approaches to a single problem, namely, to obtain the fuel economy advantages of a small displacement engine when the engine is lightly loaded, together with the performance advantages of a larger engine when the power demand is high. To put this subject in perspective, however, it should be noted that this problem is relevant to the hybrid propulsion system only if the type of control strategy used for the baseline hybrid, involving on-off operation of the heat engine, proves to be unworkable. First of all, the hybrid inherently allows for the use of a small displacement heat engine because the traction motor's output is available for peaking. Thus, at least part of the objective of turbocharging or variable displacement is achieved simply by the nature of the hybrid concept, independent of the control strategy. Second, the on-off aspect of the control strategy used for the baseline hybrid effectively removes light load operation from the province of the heat engine and gives it to the electric drive system. Both these factors result in a very low average bsfc for the heat engine, as discussed previously, and remove the need or desirability of turbocharging or variable displacement.

This is illustrated by the following analysis: The attached curve (Figure 4-24) is a fuel consumption comparison when operating a two rotor carbureted engine on one or two rotors. The curve for single rotor operation was determined analytically using data measured during two-rotor operation. By comparing output

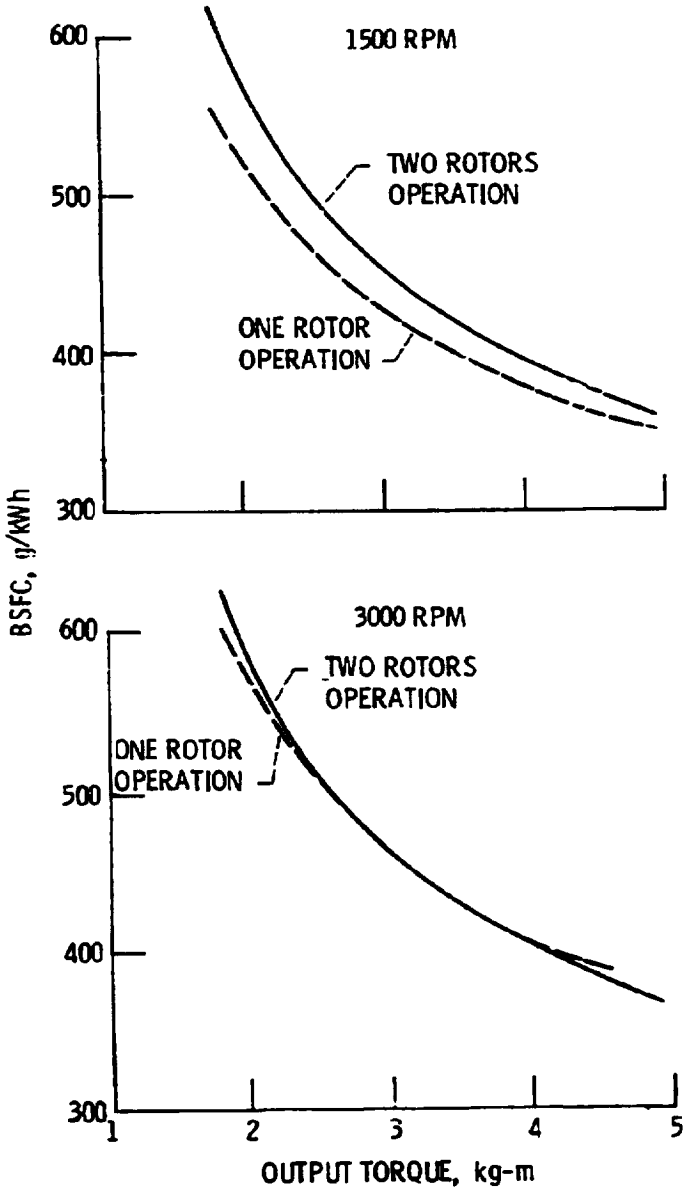

FIGURE 4-24. - EFFECT OF ONE ROTOR OPERATION IN AN ENGINE WITH TWO ROTORS ON BSFC, BSFC vs TORQUE. ENGINE DISPLACEMENT, 573 cc (35 cu. in.) x 2.

torque to bsfc at given engine speeds, a simpler comparison is possible than when using bmep and calculating to find the same horsepower points.

It can be seen that at 3000 RPM, the fuel economy was the same. At 1500 RPM, using 2.50 kg/m output torque as an operating point, a 7% bsfc improvement resulted with one rotor operation.

Referring back to Figure 4-9, it will be noted that the hybrid control strategy concentrates operation on the 1500-3000 RPM range during Mode 1 operation. Also, most of the operating points are grouped near the PHEMIN line, which corresponds to a bsfc between 275 and 280 g/kwn over the RPM range of 1500 to 3000 RPM. From this line to the minimum bsfc point, there is a variation of about 7% in bsfc. Therefore, if the range of variation could be cut to 3.5% by having two volumes to inject to attempt to further confine the operations to low sfc regions, the cumulative benefit might be about 2% at this region. The heavy cost penalty to have a multi-rotor engine vs. the planned single rotor engine, in addition to the added fuel control arrangements nullifies the slight potential gain possible. It should be noted that no potential gain was indicated in Figure 4-24 at 3000 RPM.

Additional data on this subject is shown in Figures 4-25 and 4-26. An NSU 871 gasoline homogeneous charge engine which can separately supply fuel to each bank was run on both two banks and with one bank firing. In Figure 4-25, horizontal lines have been added where vertical bmep lines of 15, 30, and 60 bmep intersect the curves shown. By projecting the horizontal lines to the sfc scale at the left, it can be seen that for the same horsepower, the sfc changes at 2000 RPM were not significant. Figure 4-26 indicates the same information in a plot of bhp vs. fuel flow.

In this effort, the conclusion has been made that in the hybrid engine application, the operating regime of the engine has been focused toward the better sfc areas as an inherent part of the system design, sufficiently to make the slight additional gains possible from variable displacement not worth the costs involved.

The same conclusion applies to turbocharging. Referring back to Figures 4-3, 4-6, and 4-7, the effect of turbocharging (maintaining constant power

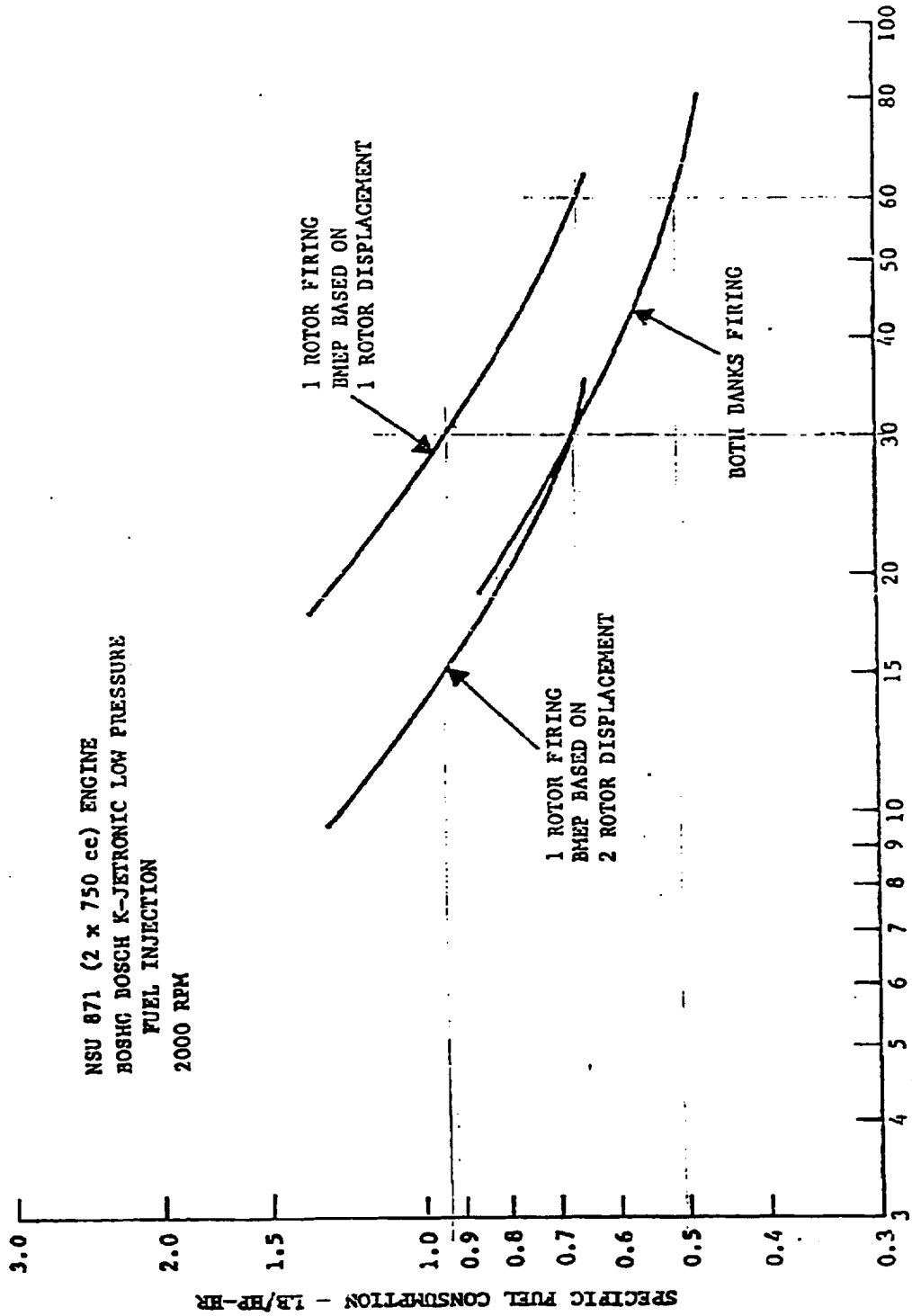

Figure 4-25. CURTISS-WRIGHT ROTARY COMBUSTION ENGINES - PART LOAD FUEL CONSUMPTION

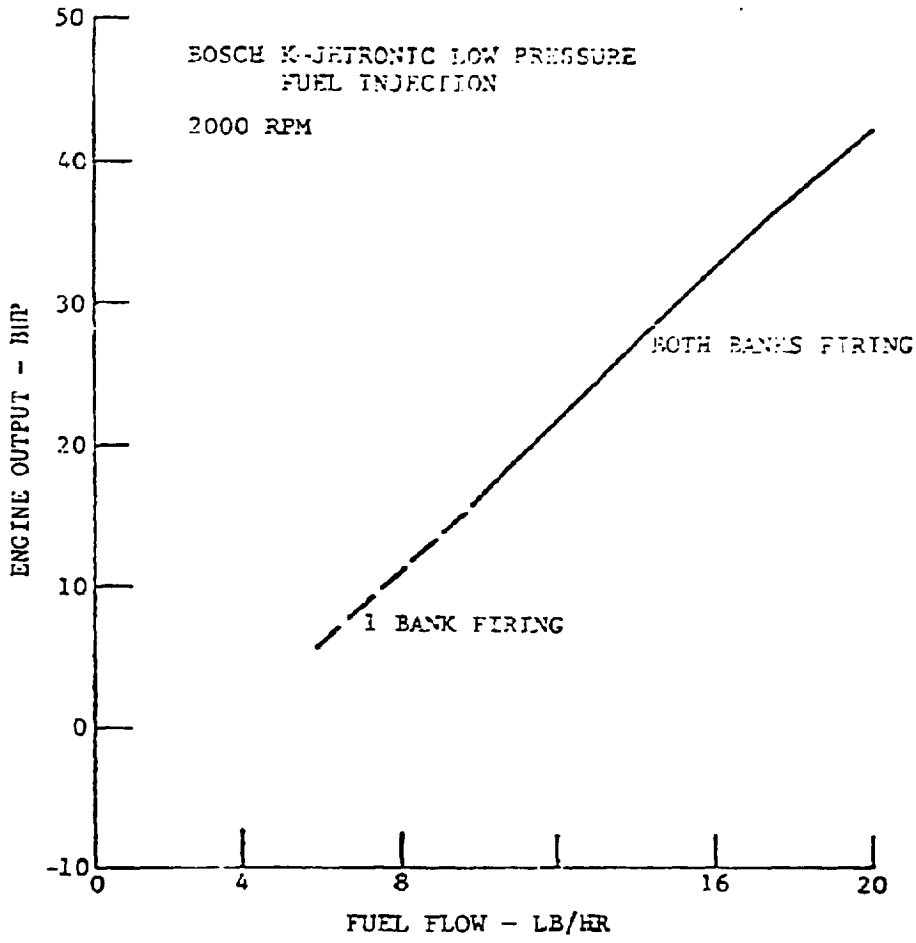

Figure 4-26. NSU 871 (2 x 759 cc) ENGINE - PART LOAD FUEL CONSUMPTION

output) would be to squeeze the lines of constant bsfc downward in the lower portion of the power range and increase the height of the basfc islands. Thus, the bsfc along the PHEMIN line (Figure 4-6), where most of the Mode 1 operation is concentrated, would move closer to the 260 g/kwh minimum. Again, the peak variation involved is only about 7%, which could be cut to about 3-4% by turbocharging. The small gain in fuel economy does not appear to be worth the cost penalty.

4.4.5 Electric Propulsion Subsystem Design Tradeoff Studies

The purpose of these studies was to evaluate various AC propulsion system technologies, with potential for reducing the life cycle cost of a hybrid electric vehicle, and then recommend one approach for further investigation. The overall goal is to demonstrate the technology selected in an engineering model by 1983 and in a test vehicle by 1985. As a result of the parametric study performed by South Coast Technology, the vehicle selected for further analysis was a six-passenger vehicle capable of inter-city travel. The electric motor output power requirements were established by South Coast Technology as being approximately 25 kw peak and 10 kw steady-state over a speed range of 2000 to 6000 RPM.

The major components used in an advanced AC propulsion system, and which are expected to have the greatest impact on system cost, efficiency, weight and volume are the:

1. AC motor
2. Power semiconductors
3. On-board charger
4. Accessory power supply

The low power control circuitry, although potentially a significant percentage of the AC propulsion system cost, is considered to be a secondary factor in terms of its influence on propulsion system performance, weight and volume.

Design Alternatives

The semiconductor devices considered as alternatives for the AC controller power stage are the bipolar power transistor and thyristor (SCR). Technologies such as gate turn-off SCR's (GTO), transcalent SCR's and power mosfet transistors

were considered to be either not cost competitive for this application or to be unavailable at the power level needed by 1933. Parametric studies of the power mosfet transistor[3] indicate, however, that it has the potential to control very high power levels and should not be dismissed for long range (1990) electric vehicle applications.

Valid comparisons between the bipolar transistor and the SCR must include the cost of the commutation circuitry used to turn off the SCR. The commutation circuit alternatives considered are individual pole and DC side commutation since they represent two entirely different approaches. The AC motor alternatives include the AC induction and permanent magnet synchronous motor. The use of a conventional DC motor was not proposed as an alternative for this program.

Methodology for Comparing Semiconductors

To compare the transistor and SCR, a correlation between device current rating and motor output power was developed assuming the use of a three-phase AC motor. Approximate expressions which relate motor output power to the transistor and SCR current rating were developed for a wye connected motor with the motor RMS line-line voltage denoted by VLL, motor RMS phase current by IPHASE, motor efficiency by EFF, motor power factor by PF, and the propulsion battery voltage by EBAT.

$$PMAX = \sqrt{3} \times VLL \times IPHASE \times EFF \times PF \quad (1)$$

For a six step waveform, the RMS value of the fundamental component can be expressed as:

$$VLL = \sqrt{6}/\pi \times EBAT \quad (2)$$

For a six step waveform, the relationship between the motor RMS phase current and the main device RMS current ID(RMS) can be approximated by equation 3 assuming the main devices are conducting the total phase current:

$$ID(RMS) = IPHASE/\sqrt{2} \quad (3)$$

Combining equations 1, 2, and 3 provides us with the following expression for motor output power as a function of device current and propulsion battery voltage:

$$PMAX = 6/\pi \times EBAT \times ID(RMS) \times EFF \times PF \quad (4)$$

Equation 4 was used in estimating the required power handling capability and cost of the main inverter SCR's, given a specified motor output power. Equation 5, shown below, was used in estimating the required power handling capability and cost of the main inverter power transistors. Transistors are rated on the basis of maximum collector current (IC) and not RMS current as are SCR's. For equation 5, the transistor peak current is approximated as being twice the device RMS current. An exact relationship between RMS and peak transistor current would require defining a specific pulse-width-modulation approach.

$$PMAX(TRANS) = 6/\pi \times EBAT \times IC/2 \times EFF \times PF \quad (5)$$

Controller Design Considerations

1. Bipolar Transistor Capability

Cost reductions and improvements in the power handling capability of bipolar power transistors during the past five years has significantly increased the feasibility of developing a vehicle propulsion system which utilizes an AC motor.

Several questions concerning the use of bipolar power transistors in an advanced hybrid electric vehicle are:

1. What transistor voltage, current and frequency capability is realistic to assume for an advanced AC propulsion system? What effect will the above transistor capability have on controller efficiency?

2. What will high power transistors, produced in large quantities, cost? How will their cost compare to thyristors?

3. Will low voltage, high current bipolar power transistors have a higher cost than high voltage, low current transistors assuming both are designed to control the same motor output power?

4. What percentage of the total AC propulsion system component cost is due to the cost of the power transistors? Is it a significant percentage of the total propulsion system cost?

Several authors (4, 5, 6) have explored the tradeoffs between transistor collector characteristics, switching and storage time and safe operating area. One analysis of the capabilities of the power transistor, proposed by Johnson[4], is based on the ultimate performance limits of the transistor as being established by the product $(E \times VS)/2\pi$, where E is the semiconductor dielectric breakdown voltage and VS is the minority carrier saturated drift velocity. This product, which has a value of about 2×10^{11} volts/second for silicon, emphasizes the fact that a semiconductor material has a maximum capability for imparting energy to a charge carrier. If the operating frequency is high, the time period is

short; and only a small amount of energy can be given to a charge carrier. At low frequencies, the inverse is true. In other words, device physics demands an inverse relationship between frequency and the transistor power capability.

The relationship developed by Johnson between the transistor volt-ampere product, impedance level (XC) and gain-bandwidth frequency (FT) is shown as equation 6:

$$(VCEO \times IC \times XC)^{1/2} \times FT = 2 \times 10^{11} \quad (6)$$

For the above equation, VCEO is the maximum collector-emitter voltage rating (VCEO-SUS), IC is the maximum collector current with a minimum current gain of 10 (VCE-SAT = 2 volts), XC is the device impedance, and FT is the device current gain-bandwidth frequency. For reference, the transistor impedance is defined by equation 7 where COB is the device output capacitance:

$$XC = 1/(2 \times \pi \times FT \times COB) \quad (7)$$

One conclusion established by Johnson from equation 6 is that as the volt-ampere product ability of a transistor is increased, the transistor current gain-bandwidth frequency (FT) must decrease. As will be discussed below, decreases in the current gain-bandwidth frequency (FT), as the transistor power rating is increased, can be translated into increased transistor switching times. This implies that transistor switching losses become a larger percentage of the total controller losses as the maximum motor output power is increased. This assumes that the motor operating frequency is held constant as motor output power is varied.

To verify that Johnson's analysis is still valid, we examined the capabilities of present (1980) power transistors and compared them with transistors which existed in 1965. This comparison is shown in Figure 4-27 where the dashed line represents transistor technology in 1965 and the solid line represents transistor technology today (1980). The line corresponding to the technology available in 1965 was obtained from Reference 1. The numbers shown in Figure correspond to power transistors commercially available today and which are listed in Table 4-18 for reference.

Figure 4-27 indicates that the major contribution of the last 15 years is the availability of higher

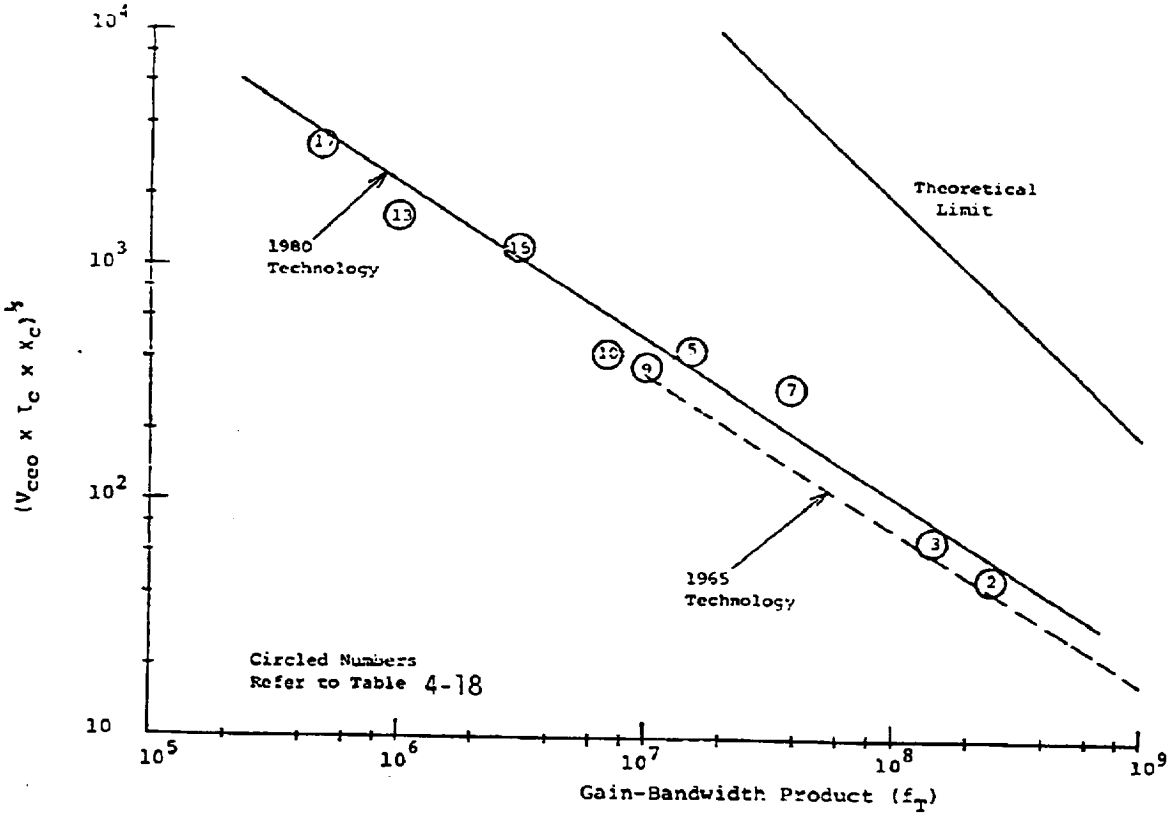

Figure 4-27. POWER-FREQUENCY RELATIONSHIP FOR TRANSISTORS

Table 4-18. CHARACTERISTICS OF COMMERCIAL POWER TRANSISTORS (1980)

ITEM NO.	DEVICE P/N	VCEO (VOLTS)	IC (AMPS)	TR+TF (USEC)	FT (MHZ)	COB (PF)
1	2N5583 (M)	30	0.5	.035	1300	4.0
2	2N4401 (M)	40	0.6	.05	250	6.5
3	2N3500 (M)	150	0.3	.12	150	8.0
4*	MJ10009 (M)	500	20	3.0	8	325
5*	MJ10021 (M)	250	50	1.5	15	700
6	BUR51 (SGS)	250	50	1.6	15	600
7	GSDS50020 (GS)	200	50	0.4	40	350
8*	SVT804C (TRW)	400	40	2.0	---	750
9	HPT545 (IR)	450	40	1.3	10	2000
10	D60T450 (W)	450	40	1.6	7	2500
11	PT-3523 (PT)	450	50	1.0	10	400
12	WTS504 (WCODE)	450	50	1.5	---	---
13*	D67D (GE)	400	100(1)	8.5	1.0	2500
14	MT-6002 (PT)	400	100	---	---	---
15	WTS704 (WCODE)	450	200	6.0	3.0	3000
16*	2SD647 (TOSH)	600	100(1)	8.0	---	---
17*	2SD648 (TOSH)	300	400(1)	12.0	0.5	3500
18*	MT-6006 (PT)	400	300(2)	---	---	---
19*	2SD698 (TOSH)	200	600(2)	---	---	---

* DARLINGTON

(1) CURRENT GAIN OF 50 AT IC

(2) CURRENT GAIN OF 100 AT IC

power transistors. It also indicates that very high power, fast switching power transistors appear to be difficult to obtain as a single device (i.e., a 400 V, 300 A transistor with a switching time of less than 1 μSEC). The possibility that two or more devices can be paralleled to obtain this power/speed capability is being investigated;[7] and in certain instances, parallel transistors are manufactured for commercial use.

2. Transistor Controller Efficiency

Based on the information presented in Figure 4-27, we estimated what transistor capability is realistic to assume for a 1985 system and what effect increasing motor output power will have on controller efficiency. For our analysis, transistor inductive switching time (TC) was approximated as the sum of the current rise and fall time obtained with a resistive load. This method of estimating transistor inductive switching time is considered optimistic (provides a low estimate) based on the procedure proposed by Westinghouse.[8] The reason for estimating inductive switching time is that not all power transistor manufacturers provide this information in their device literature. Using Table 4-18, we plotted the sum of transistor rise (TR) and fall (TF) time as function of device KVA rating [(VCEO x IC)/1000]. This information is shown in Figure 4-28 and was used to estimate transistor switching loss when controlling a three-phase AC motor.

The assumptions made with respect to transistor switching loss are: (1) the major percentage of transistor switching loss occurs at turn-off (since the motor load is inductive, turn-on losses are assumed to be negligible); (2) the turn-off waveform is based on switching an inductive load; and (3) the energy dissipated in the transistor is based on a triangular power waveform. The maximum power dissipated in the transistor was assumed to occur when the transistor current has dropped to 90% of its initial value and the voltage has risen to 90% of its final value. With these assumptions identified, the energy dissipated in the transistor at turn-off is:

$$\text{WATT-SEC/PULSE} = 1/2 \times 0.9 \times \text{VCE} \times 0.9 \times \text{IC} \times \text{TC}, \qquad (8)$$

where VCE is the voltage across the transistor, IC is the peak collector current prior to turn-off and TC is the crossover time as illustrated in Figure 4-29. Based on the information presented in Figure 4-28, an empirical relationship for

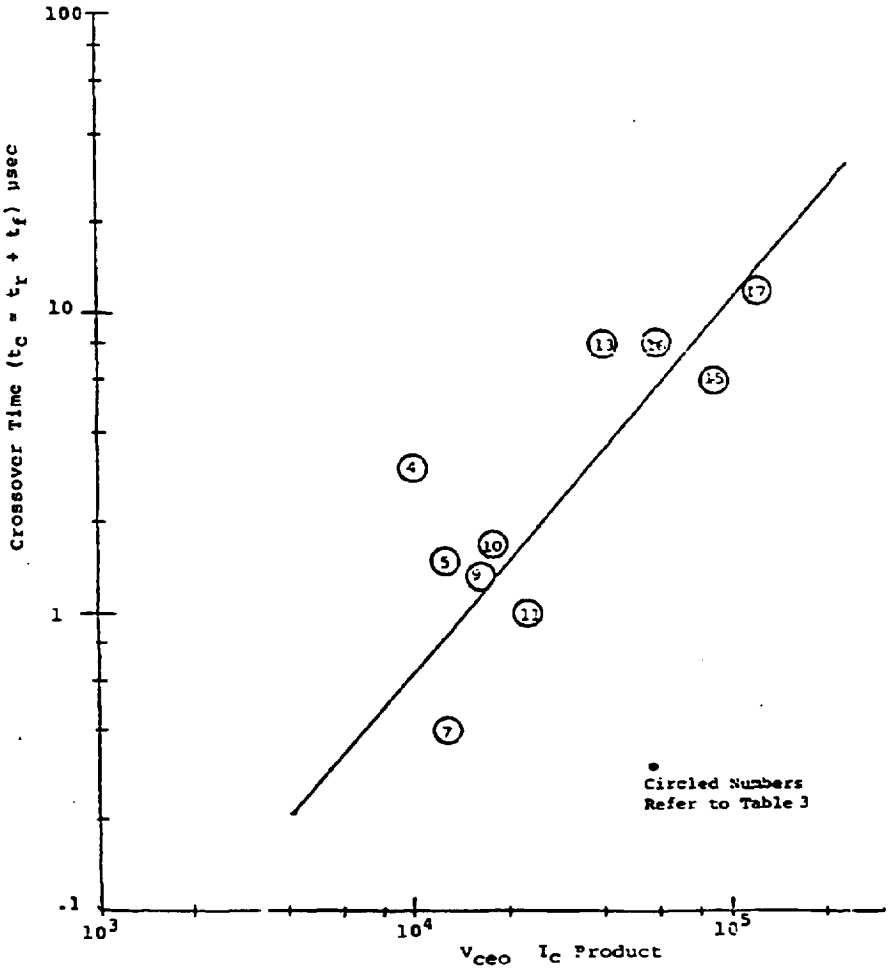

Figure 4-28. CROSSOVER TIME (t_c) VERSUS V_{ceo} x I_c PRODUCT

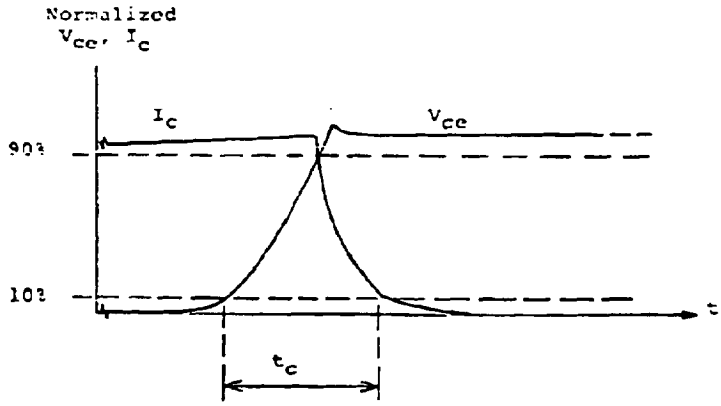

FIGURE 4-29. TRANSISTOR VOLTAGE AT CURRENT TURN-OFF

the crossover time as a function of transistor KVA rating can be developed,

$$TC = 3.4 \times 10^{-8} [KVA]^{1.24} \quad , \tag{9}$$

where KVA is the transistor power handling capability and is related to the maximum motor power as presented in equation 12. Our loss analysis assumed that the transistor voltage rating (VCEO-SUS) is three times the minimum battery voltage (EBAT) which occurs when the battery is providing maximum motor power. This takes into account the decrease in battery voltage under load, the increase in battery voltage during regeneration, and the use of a safety margin in the transistor voltage rating.

$$PMAX = (6/\pi) \times (VCEO/3) \times (IC/2) \times EFF \times PF \tag{10}$$

$$KVA = (VCEO \times IC)/1000 \tag{11}$$

Combining equations 10 and 11 to eliminate VCEO and IC establishes the transistor KVA rating to be used in equation 8.

$$KVA = [PMAX \times 3 \times 2 \times \pi]/[6000 \times EFF \times PF] \tag{12}$$

The VCE and IC values used in equation 8 are the actual transistor voltage and current when the transistor is being turned off. As stated previously, the transistor voltage at turn-off, when switching maximum motor power, is one-third the actual transistor voltage rating.

$$VCE \times IC = [PMAX \times 2 \times \pi]/[6 \times EFF \times PF] \tag{13}$$

Inserting equations 9 and 13 into equation 8 establishes an empirical relationship for the watt-seconds dissipated in the transistor at turn-off as a function of the motor output power.

$$WATT\text{-}SEC/PULSE = [(PMAX \times 2 \times \pi)/(6 \times EFF \times PF)]^{2.24} \times 10^{-11} \tag{14}$$

Using equation 14, controller efficiency as a function of transistor switching frequency can be determined for a motor output power of 25 kw. The result is shown in Figure 4-30 where the line represented as one pulse/cycle corresponds to six step operation; and the lines represented as 5, 8, and 14 pulses/cycle correspond to operation under pulse-width-modulation conditions. Transistor conduction losses were approximated using equation 15, assuming a saturation voltage drop of 1.5 volts per device.

$$P(COND) = (PMAX \times 3 \times \pi)/(6 \times EFF \times PF \times EBAT) \tag{15}$$

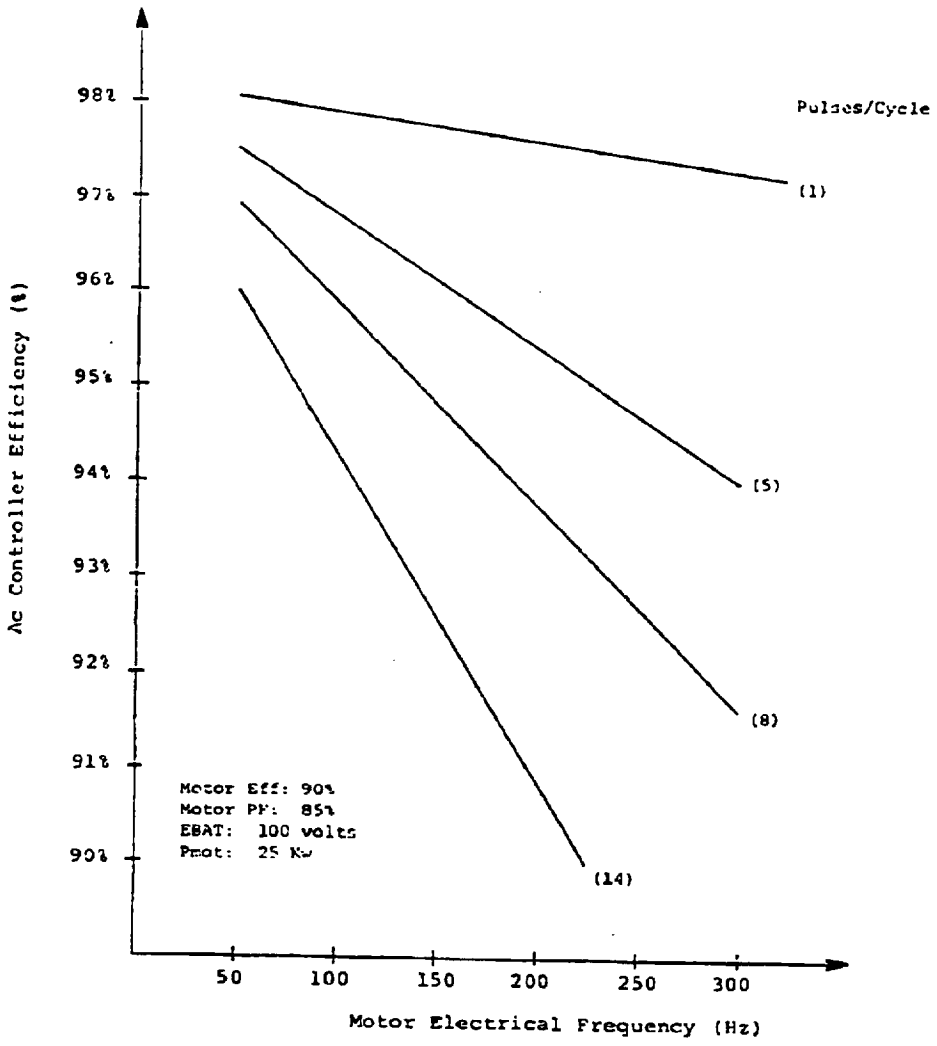

Figure 4-30. TRANSISTOR CONTROLLER EFFICIENCY VS. MOTOR FREQUENCY

As is evident from Figure 4-30, the efficiency of a transistor controller is dependent on the pulse-width-modulation approach used and the motor electrical frequency. The effect of variations in maximum motor output power on controller efficiency is shown in Figure 4-31 and indicates the significant improvement in controller efficiency as the maximum motor power requirement is reduced. The information shown in Figure 4-31 assumes that the transistor switching frequency is held constant as motor power is varied and that the motor operating frequency is 150 HZ.

3. Thyristor (SCR) Capabilities

To obtain a measure of the capabilities of the thyristor, we used an approach developed by Newell,[9] in which he derived a general relationship between SCR turn-off time (TREV), blocking voltage (VDRM), and current rating (ID(RMS)). In examining the capabilities of the SCR, our goals were, first, to identify what variations from commercially available devices are feasible, and second, to identify those variations with potential for reducing the cost of an advanced AC propulsion system.

The relationship, developed by Newell, for the power controlling capability of an SCR as a function of its blocking voltage, turn-off time, and SCR cathode area is shown in Figure 4-32. The accuracy of Figure 4-32 has been verified by comparing it with SCR's commercially available today.

Based on the information shown in Figure 4-32, it appears feasible to consider the use of SCR's having turn-off times less than 10 μSEC (10 μSEC is commercially available today) provided we can operate with the resulting lower blocking voltage. This appears feasible since the SCR voltage rating required for an electric vehicle AC controller will probably be lower than that used in industrial applications. From Figure 4-32, an SCR with a turn-off time of 1 μSEC would have a blocking voltage capability of 400 to 500 volts when designed for maximum power handling capability. This low voltage rating, although not usable for certain industrial applications (i.e., 480 VAC), may be suitable for

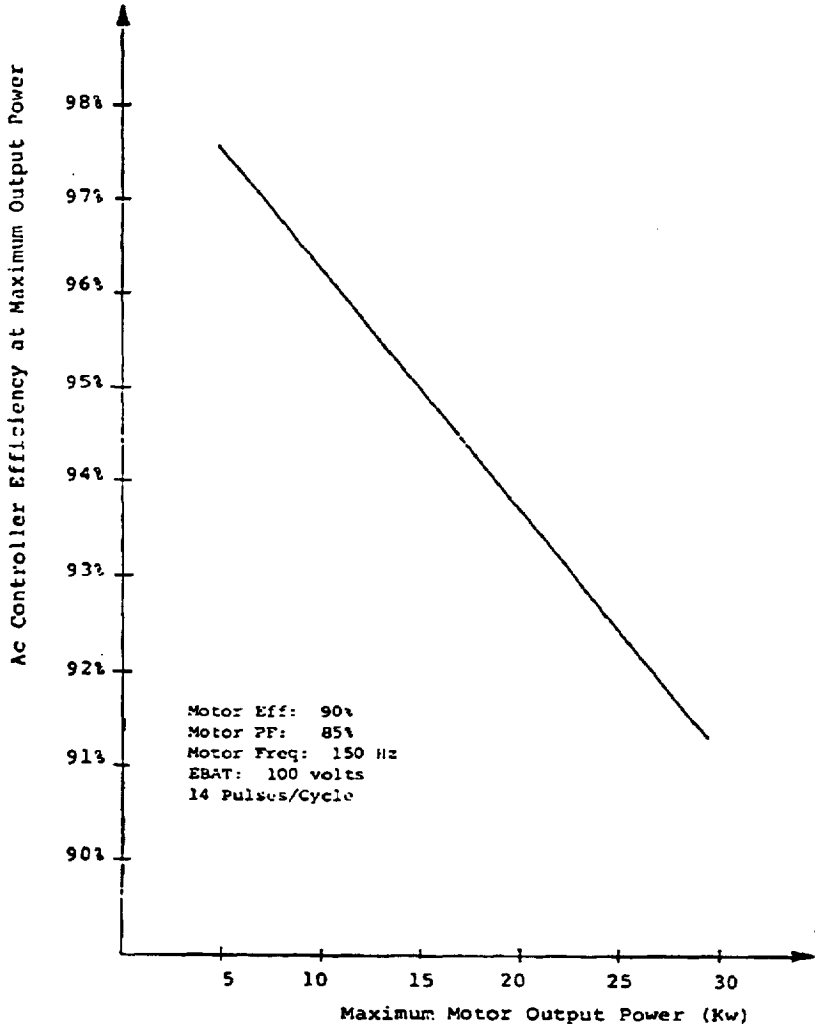

Figure 4-31. TRANSISTOR CONTROLLER EFFICIENCY VS. MOTOR POWER

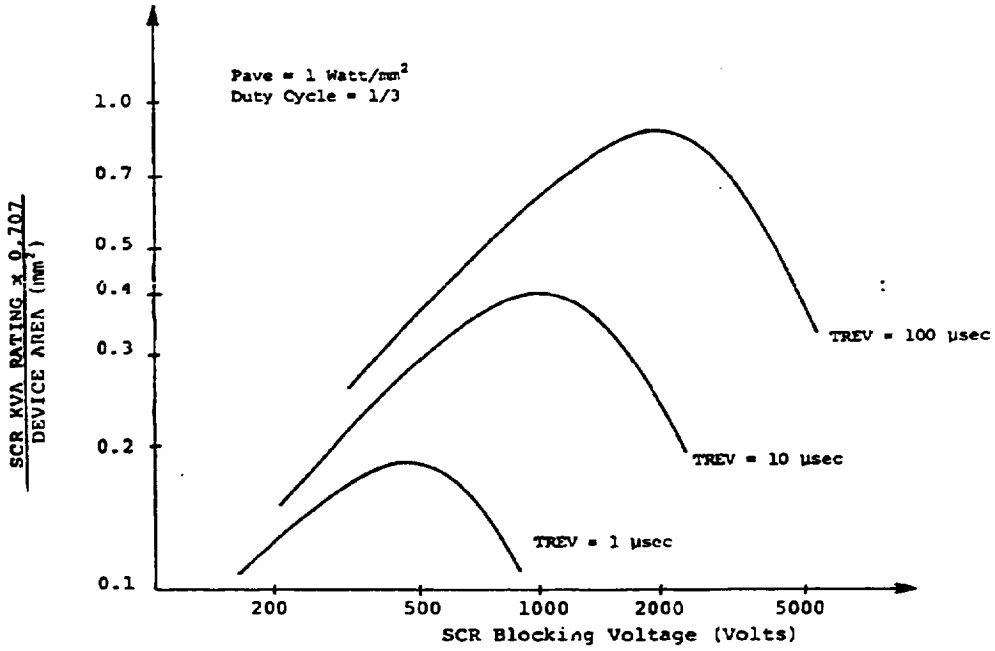

Figure 4-32. SCR POWER HANDLING CAPABILITY VS. BLOCKING VOLTAGE AND TURN-OFF TIME

an AC controller operating from a propulsion battery voltage of 100 volts. Using Figure 4-32, an SCR with a diameter of 23 mm (i.e., an area comparable to a Westinghouse T627 or a GE C384 SCR) would have a maximum RMS current rating of 200-250 amps. This is approximately the current rating required by a 25 kw AC controller operating from a battery voltage of 70 volts (at maximum power).

The reason for minimizing SCR turn-off time is to reduce controller commutation losses, which are a significant percentage of the total SCR controller losses. Discussions with Westinghouse and Brown-Boveri concerning the feasibility of developing SCR's having turn-off times of 5 μsec or less have been very positive. As turn-off time is reduced below 5 μsec, the conduction voltage drop increases and may become a limiting factor.

4. SCR Commutation Circuitry

Comparisons made between AC controllers that use either transistors or thyristors (SCR's) must include the cost of the SCR commutation circuitry. The process of commutation is a power function and, as such, is a major factor in the economic design of an inverter. Also important is the influence of the commutation process on controller efficiency, since efficiency affects not only controller cost (i.e., package design) but also propulsion system cost (i.e., propulsion battery size) and fuel consumption.

An SCR can be switched on by applying a suitable voltage and current to its gate. The power required for this is almost insignificant when compared to the power controlled by the device. To turn off an SCR requires that its anode to cathode voltage be reversed for a period of time sufficient to enable the SCR junction to regain its blocking state. This requires that the load current flowing through the SCR be decreased to zero, a process which involves power levels substantially higher than those used to turn the SCR on. The process of turning off an SCR, defined as commutation, is a major factor in the design of an SCR inverter.

During the past 15 to 20 years, numerous SCR commutation approaches have been developed and comparisons made to determine if one approach is truly

superior. The conclusion reached by Abbondanti and Wood[10] with respect to the idea of a truly superior commutation circuit seems most realistic. Their conclusion was that the peculiarities of the application enhance the desirability of certain features and increase the penalties attached to others, thereby affecting the selection of the commutation circuit. This dependence on the application is one reason for re-examining the commutation circuit used in an electric vehicle AC controller.

Our approach was to examine two fundamentally different commutation circuits with the goals being, first, to obtain an estimate of commutation circuit cost, and second, to identify areas for potentially improving commutation circuit performance.

The two commutation circuits selected are individual pole commutation and DC-side commutation. For each approach, there are many different variations which can be developed. However, our goal was to examine basic capabilities and not dwell on the many possible design variations. Individual pole commutation is probably best represented by the McMurray inverter illustrated in Figure 4-33. A review of the comparisons[11,12] made between this circuit and others tends to support the selection of the McMurray inverter as being representative of individual pole commutation.

The second approach is DC-side commutation, also known as input or buss commutation. The major difference between these two approaches is that with buss commutation, more than one main inverter SCR is turned off during each commutation cycle, whereas with individual pole commutation, only one inverter SCR is turned off.

As was the case for individual pole commutation, there are various approaches to DC-side commutation. However, the use of DC-side commutation is not as widespread as individual pole commutation; and, therefore, few comparisons exist in the literature to assist us in selecting the most representative approach. The circuit arrangement shown in Figure 4-34 is considered representative of those approaches proposed by several authors[13-17] and will, therefore, be used in our comparison.

The cost of an SCR inverter circuit is greatly influenced by two items, the cost of essential passive components, i.e., the commutation inductors and

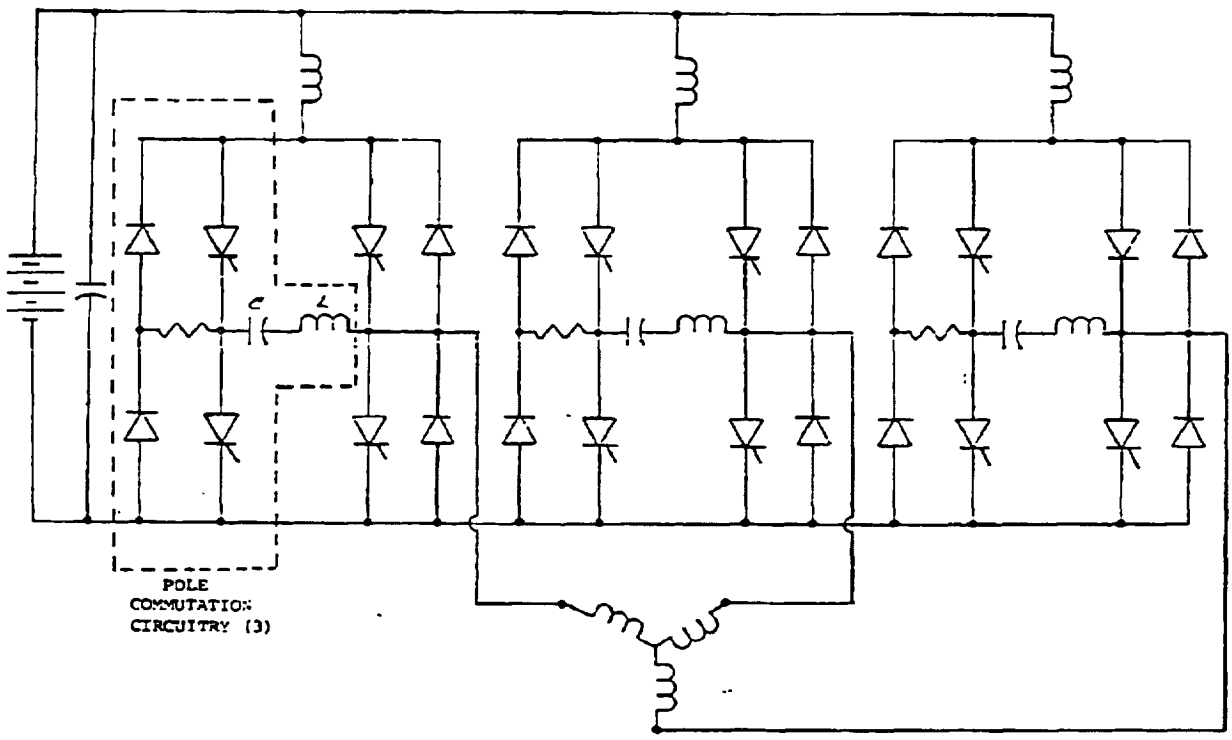

Figure 4-33. McMURRAY FORCED COMMUTATED INVERTER (3-PHASE)

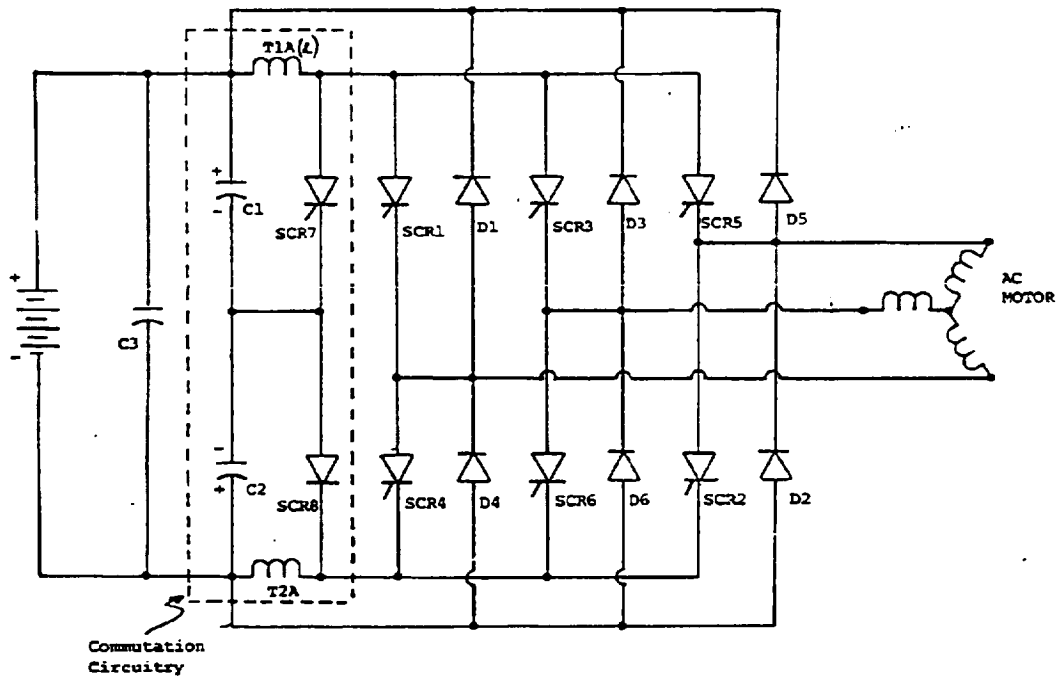

Figure 4-34. BUSS COMMUTATED INVERTER (3-PHASE)

capacitors, and the cost of the semiconductor devices. The cost of ancillary items such as snubber networks, gate drive modules, fuses, etc., also contribute but are not considered the dominant items for the motor power level being considered (25 kw).

To a first approximation, the task of appraising and then selecting an SCR commutation approach can be made simpler if we can evaluate the size of the passive components and use this information as a means of assessing circuit suitability. Equations for sizing the commutation inductors and capacitors have been previously developed for both the McMurray[18] and buss commutation circuits[13] based on minimizing the amount of stored energy required to commutate a specific power level. These relationships are given by equations 17 and 18 for the McMurray inverter, and equations 19 and 20 for the buss commutated inverter. The values of L and C given below for the McMurray inverter correspond to the components identified as L and C in Figure 4-33. The values of L and C for the Buss commutated inverter correspond to the components identified in Figure 4-34 as L, C1 and C2, where the value of C given by equation 19 is the sum of C1 and C2.

$$C(\text{McMurray}) = (.893 \times IL \times TREV)/EBAT \quad (17)$$

$$L(\text{McMurray}) = (.397 \times EBAT \times TREV)/IL \quad (18)$$

$$C(\text{Buss}) = (1.47 \times IL \times TREV)/EBAT \quad (19)$$

$$L(\text{Buss}) = (1.82 \times EBAT \times TREV)/IL \quad (20)$$

EBAT is the minimum battery voltage in volts, IL is the peak load current to be commutated in amps, and TREV is the circuit turn-off time in μsec. Circuit turn-off time is the sum of the required SCR turn-off time and the additional margin provided to take into account circuit tolerances. The peak load current (IL) for six-step operation is approximated as being 2.3 times the SCR RMS current ID(RMS). IL is given below as a function of motor output power.

$$IL = (PMAX \times \pi \times 2.3)/(6 \times EFF \times PF \times EBAT) \quad (21)$$

Commutation Inductor Parameters

Our approach to estimating the value and cost of the commutation inductor was based on the premise that the product of inductor core cross sectional

area (AC) and window area (AW) is proportional to the amount of energy to be commutated. This approach is frequently used[19] in the design of power transformers and inductors, and most manufacturers rate the power handling capability of their cores in terms of the core and window area product. This relationship is developed below for the McMurray inverter:

$$L = (3.2 \times N^2 \times AC \times 10^{-8})/LG \quad (22)$$

where L is the commutation inductance in μH, N is the number of turns, AC is the core area in square inches, and LG is the gap length in inches. The expression for the commutation inductance used in the McMurray inverter is based on the peak current in the commutation circuit being 1.5 times the peak load current IL. With this established, the peak flux density in the commutation inductor is:

$$B = (0.495 \times N \times IL \times 1.5)/LG \quad (23)$$

The inductor window area (AW) can be expressed as shown below, where IW(RMS) is the RMS current in the inductor winding, J is the current density in amps/sq.in., and KC is the percentage of the window area occupied by the winding.

$$AW = (N \times IW(RMS))/(J \times KC) \quad (24)$$

Combining equations 22, 23, and 24, we obtain the following expression for the window area and core area product:

$$AW \times AC = (L \times IL \times 1.5 \times IW(RMS) \times 10^8)/(6.46 \times B \times J \times KC) \quad (25)$$

To establish the value of the RMS current in the commutation inductor, we will assume a sinusoidal current waveform (half sine-wave) where the current pulse width (TP) is a function of the commutation inductance and capacitance as shown below. The commutation inductor operating frequency (FC) is twice the motor frequency for the McMurray inverter and three times the motor frequency for the buss commutated inverter.

$$IW(RMS) = IL \times 1.5 \times [(TP \times FC)/2]^{1/2} \quad (26)$$

$$TP = 3.412 \times (L \times C)^{1/2} \quad (27)$$

$$FC = 2 \times FM \text{ (McMurray inverter)} \quad (28)$$

$$FC = 3 \times FM \text{ (Buss Commutated inverter)} \quad (29)$$

Substituting equations 26 and 27 into 25, we obtain the following expression for the window area and core area product:

$$AW \times AC = [(LxIL^2x2.25x10^8)/(6.46xBxJxKC)]x[(\pi x(LxC)^{1/2}xFC)/2]^{1/2} \quad (30)$$

Inserting the expressions for the commutation inductance and capacitance into equation 30 and assuming a peak flux density of 12,000 Gauss, a current density of 2000 amps/in^2, a window utilization of 50% and a cost in high volume of \$20/in^4 (2 mil silicon-iron C cores), we obtain the following expressions for the total cost of the commutation inductors. Inductor cost for the Buss commutation circuit is based on a peak current in the commutation circuit of 1.8 times the peak load current. Equations 31 and 32 are for the total cost of the inductors in the Buss inverter and McMurray inverter.

$$SL(Buss) = 864 \times IL \times EBAT \times TREV^{3/2} \times FM^{1/2} \quad (31)$$

$$SL(McMurray) = 129 \times IL \times EBAT \times TREV^{3/2} \times FM^{1/2} \quad (32)$$

One conclusion which is evident from examining equations 31 and 32 is that the cost of the commutation inductors is significantly higher for the Buss inverter than for the McMurray inverter. The reasons for this are:

1. The operating frequency of the commutation inductors in the Buss inverter is 50% higher than in the McMurray inverter for the same motor frequency.

2. The inductance required with the Buss commutated inverter, as given by equation 20, is almost 5 times the value required with the McMurray inverter.

One difference between the McMurray and Buss commutation inverters, not evident from equations 31 and 32, is the difference in the main SCR turn-off time due to the method of commutation. The diode connected in inverse parallel across the main SCR of the McMurray inverter increases the SCR turn-off time on the order of 1.5 to 2 times that which can be obtained with a reverse voltage of 50 volts. In estimating the cost of the commutation inductance and capacitance, main SCR turn-off times of 10 and 20 μsec. have been assumed for the Buss and McMurray inverters, respectively. An additional 5 μsec. has been added to account for circuit tolerances.

Commutation Capacitor Parameters

To a first approximation, the cost of the commutation capacitors is proportional to the product of capacitance and capacitor peak voltage rating. To estimate the capacitor cost in high volume, we assumed a cost of $0.0007 times the CV product where C is in uF and V is the capacitor peak DC voltage rating in volts. The capacitor voltage rating for both methods of commutation is assumed to be three times the battery voltage (EBAT) when the battery is supplying maximum power (25 kw). This takes into account the higher propulsion battery voltage during regeneration and the overshoot in the capacitor voltage due to the operation of the energy recovery circuit of the McMurray inverter. Maximum motor power is assumed to be the same for motoring and regeneration (25 kw). Based on these relationships, the cost of the commutation capacitors is:

$$SC(Buss) = 3087 \times IL \times TREV \quad (33)$$

$$SC(McMurray) = 5626 \times IL \times TREV \quad (34)$$

Commutation SCR Parameters

To estimate the cost of the auxiliary SCR's used in the commutation circuit, an empirical relationship (EQ 35), for the RMS current rating of commercially available fast switching SCR's was developed. This relationship is a function of SCR peak current and switching frequency (FAUX) and is based on an SCR current pulse width of 50 µsec. and an SCR case temperature of 90 C.

$$IAUX(RMS) = [IPK \times (FAUX)^{1/2}]/110 \quad (35)$$

The operating frequency of the commutation SCR for the Buss and McMurray inverters is:

$$FAUX(Buss) = 3 \times FM \quad (36)$$

$$FAUX(McMurray) = FM \quad (37)$$

where FM is the motor electrical frequency. For the ratio between the peak current in the commutation SCR to the load current being 1.8 for the Buss inverter and 1.5 for the McMurray inverter, the RMS current rating of the auxiliary SCR's is:

$$IAUX(Buss) = (IL \times FM^{1/2})/35.3 \quad (38)$$

$$IAUX(McMurray) = (IL \times FM^{1/2})/73.3 \quad (39)$$

The voltage rating of the auxiliary SCR's is based on the maximum SCR voltage being four times the battery voltage (EBAT) when the battery is supplying maximum output power. This includes regeneration conditions and a safety factor of 33%.

$$VAUX = 4 \times EBAT \tag{40}$$

Combining equations 38 and 40, the total cost of the commutation SCR's in the Buss inverter and the commutation SCR's in the McMurray inverter is:

$$SAUX\ SCRS(Buss) = [EBAT \times IL \times FM^{1/2} \times \$/KVA]/4410 \tag{41}$$

$$SAUX\ SCRS(McM) = [EBAT \times IL \times FM^{1/2} \times \$/KVA]/3055 \tag{42}$$

Shown in Figure 4-35 is the total commutation circuit component cost, as a function of battery voltage, for both the McMurray and Buss commutated inverters (3-phase). Included in the component cost, in addition to the commutation capacitors, inductors and auxiliary SCR's, are estimates for the cost of the snubber and gate drive circuits ($3/SCR) and the energy recovery circuits for the McMurray inverter ($1.0/kw). As is evident, the fewer commutation components required with the Buss commutation circuit significantly reduces its cost compared to the McMurray inverter. As indicated in Figure 4-35 , the cost difference between the two approaches also becomes less as the battery voltage is increased. This is considered to be part of the reason for the popularity of the McMurray inverter in industrial applications. Another factor is the effect commutation circuit trapped energy has on inverter efficiency and component losses.

5. SCR Controller Efficiency

Five factors which influence the efficiency of an SCR controller are:

1. The commutation circuit quality factor
2. The turn-off time of the main SCR's
3. The regeneration power requirement
4. The circuit turn-off time tolerance
5. The method used to adjust the turn-off time as a function of motor output power

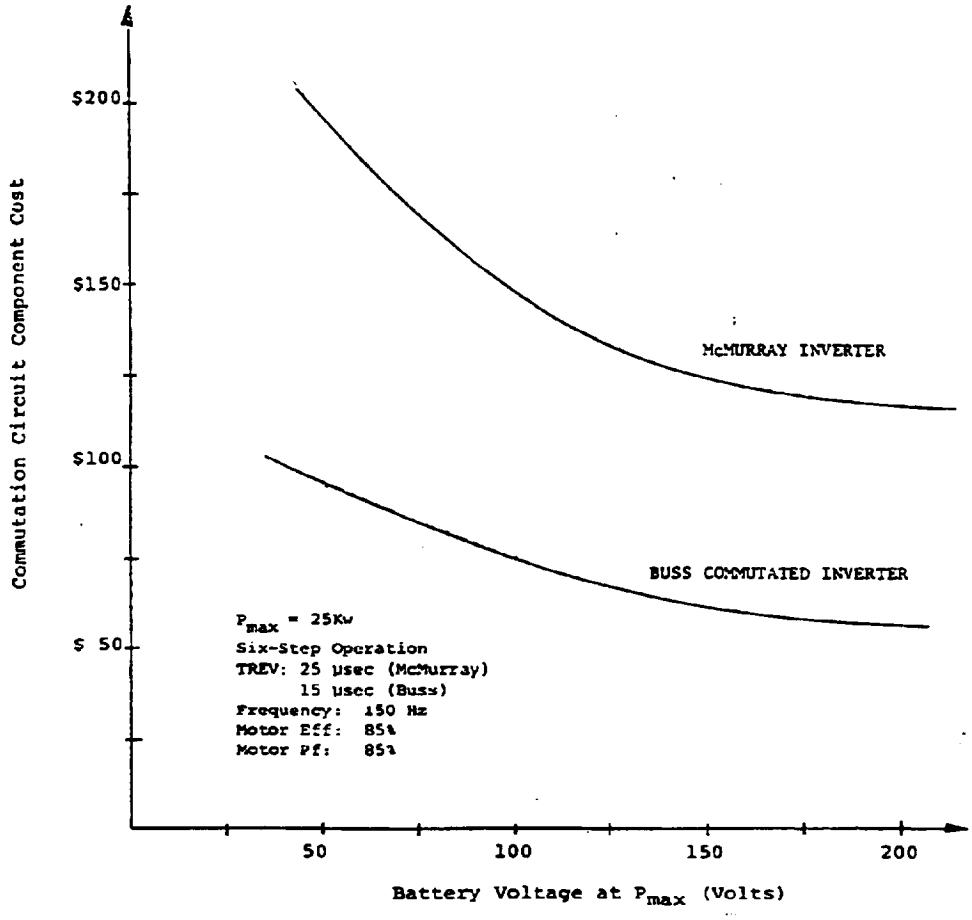

Figure 4-35. COMMUTATION CIRCUIT COMPONENT COST VS. V_{BAT}

To a first approximation, the commutation circuit quality factor can be represented as an energy loss which occurs at each commutation and is a fixed percentage of the total energy stored in the commutation circuit. The effect of variations in the commutation circuit quality factor on controller efficiency is illustrated in Figure 4-36 , based on loss percentages of 15%, 20%, and 25%, a motor output power of 25 kw, a main SCR turn-off time of 20 μsec., and a propulsion battery voltage of 100 volts. Equation 15 has been used to calculate SCR conduction losses assuming a voltage drop of 1.5 volts per SCR. The total energy stored in the commutation circuit of the Buss commutated inverter is given by the following expressions:

$$\text{ENERGY (WATT-SEC)} = 1/2[(C \times 2 \times EBAT^2) + (L \times IL^2)] \quad (43)$$

$$\text{ENERGY (WATT-SEC)} = (4.64 \times PMAX \times TREV)/(EFF \times PF) \quad (44)$$

Designing the commutation circuit for a regeneration power level of 50 kw and then operating at a maximum power during motoring of only 25 kw reduces controller efficiency as also shown in Figure 4-36. For the hybrid system under investigation, the maximum regeneration power has been limited to the maximum motoring power.

The effect of decreasing the main SCR turn-off time from 20 μsec. to 7 μsec. is shown in Figure 4-36 based on a fixed energy loss of 20% of the total energy stored in the commutation circuit at each commutation. The increase in controller efficiency if both fast turn-off SCR's are used (5 μsec.), and the design margin (circuit tolerance) minimized, is evident.

The effect of adjusting the energy stored in the commutation circuit, as a function of motor output power, is illustrated in Figure 4-37 and shows that a significant improvement in efficiency can be obtained. Various techniques[20] to accomplish this are possible. For example, by adjusting the firing sequence between the main inverter SCR's and the commutation SCR's in the McMurray inverter, the energy stored in the commutation circuit can be adjusted as a function of load. The advantages of this are significant when it is realized that an electric or hybrid vehicle application is characterized by brief operating periods at high power levels (i.e., acceleration at 25 kw) followed by considerably longer operating periods at low power levels (i.e., cruise at 10 kw).

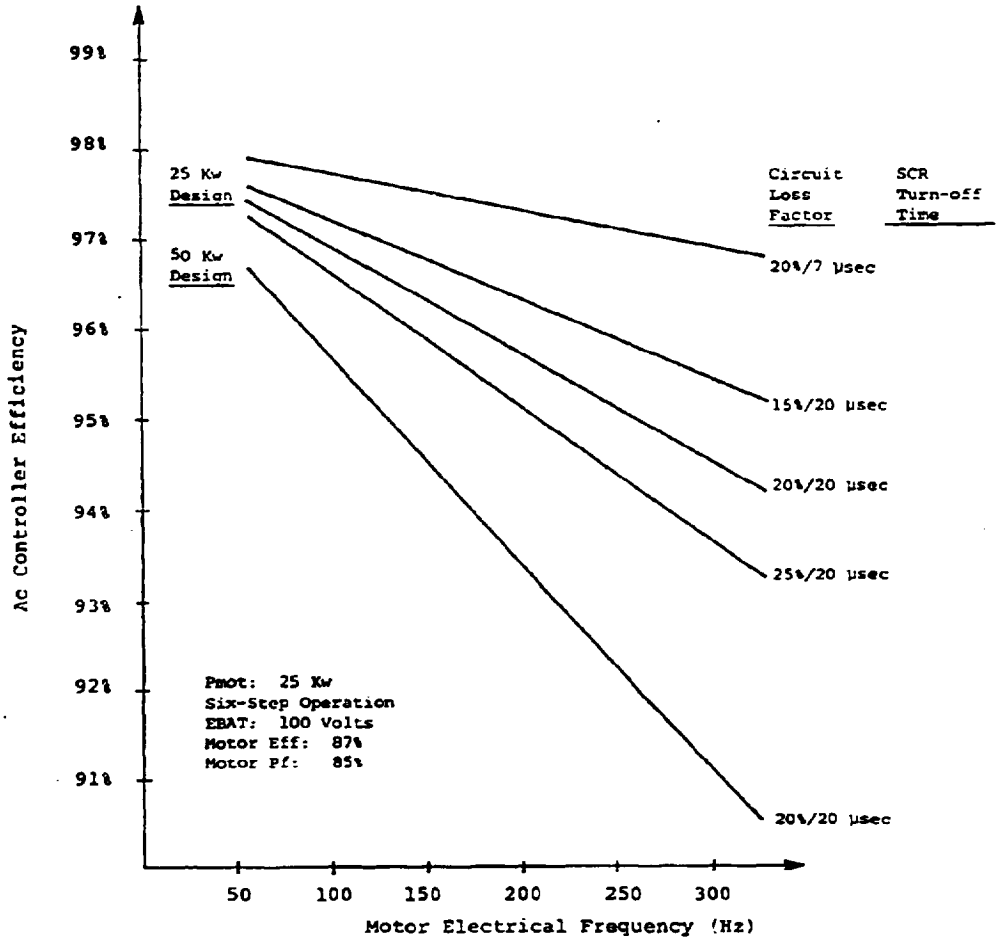

Figure 4-36. SCR CONTROLLER EFFICIENCY VERSUS MOTOR FREQUENCY

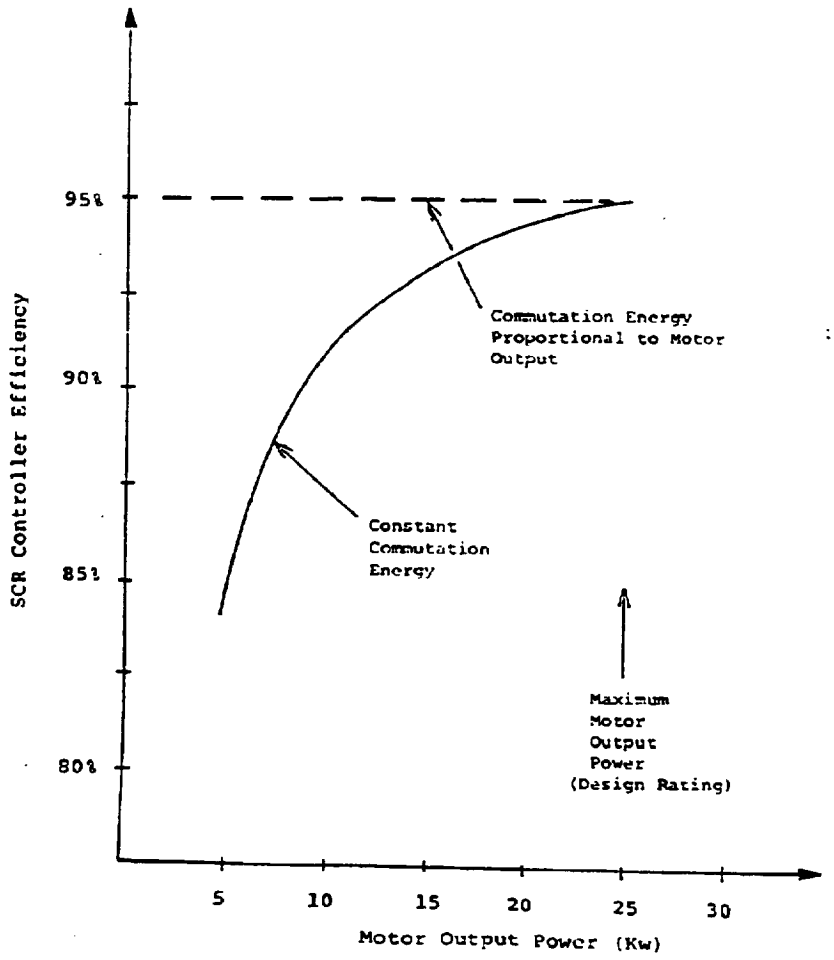

Figure 4-37. EFFECT OF PROPORTIONAL COM ENERGY ON CONTROLLER EFFICIENCY

Successful implementation of "programmed commutation" (adjusting the commutation energy as a function of load), regardless of the technique used, is considered critical to the design of an efficient SCR controller for an electric or hybrid vehicle application.

6. Transistor and Thyristor Cost Projections

Several factors which are relevant when discussing the cost of power semiconductors for electric vehicles are: First, present production capability is well below the level needed to manufacture 100,000 propulsion systems per year. Second, large quantities will probably be produced using special production lines tailored to the characteristics of the particular device used.[21] Third, high power transistors have only been commercially available during the past few years which implies that significant cost reductions can be expected to occur over the next five years as their use in energy conscious applications (i.e., industrial drives) increases.

The approach used in establishing semiconductor costs was to obtain information from the major semiconductor manufacturers on what cost goals for power transistors and SCR's could be established. Projected costs were discussed with several manufacturers and their estimates compared for consistency. The manufacturers contacted were Westinghouse, GE, Toshiba, Motorola, PTC, International Rectifier, TRW, Power Tech, General Semiconductor, and Westcode. Their projections and recommendations were very consistent.

The expected cost of Darlington transistors, in high volumes, is estimated to be in a range from \$0.5-\$1.0/KVA (per transistor) with the two extremes being optimistic and conservative. Cost for non-Darlington transistors are estimated to be \$1.0-\$2.0/KVA. In subsequent discussions, non-Darlington transistors are assumed to be operated either in a Darlington configuration or with a forced gain of less than 10 in order to maximize power handling capability and minimize cost. Information provided by Westinghouse for their D60T and D70T power transistors shows an expected cost reduction from \$200 in 1980 to \$80 in 1985 for the D70T, and from \$100 in 1980 to \$40 in 1984 for the D60T. These are based on a production level of 250,000 transistors per year. Cost projections for fast switching SCR's produced in high volume are \$0.2-\$0.3/KVA (KVA = [VDRM x ID(RMS)]/1000).

One interesting result is that semiconductor costs (SCR and transistor) are almost directly related to device power level (i.e., KVA rating) and that no significant penalty is encountered for either high voltage, low current devices or low voltage, high current devices. Extreme variations outside the voltage range normally considered for an electric vehicle application (a battery voltage of 60 to 200 volts) and at power levels much greater than 25 kw may, however, present conditions which affect cost more significantly.

Curves showing transistor and SCR costs as a function of maximum motor output power are shown in Figures 4-38 and 4-39 , respectively, with device cost, as a function of motor output power, given by equation 16 for both transistors and SCR's:

$$\text{SMAIN DEVICE} = [\text{PMAX} \times 2 \times 2 \times \pi]/[6000 \times \text{EFF} \times \text{PF}] \times 6 \times \text{S/KVA} \qquad (16)$$

The transistor VCEO rating used in developing equation 16 is twice the battery voltage under load (VCEO = 2 x EBAT). This assumes the transistor operating voltage range has been minimized to reduce device cost. The method used in estimating transistor switching losses (equation 10) assumed that VCEO = 3 x EBAT and is considered a more conservative estimate for the transistor voltage rating. The SCR voltage rating is assumed to be four times the battery voltage under load (VDRM = 4 x EBAT). The SCR voltage rating takes into account the effect of the commutation process on SCR voltage rating.

Motor Design Considerations

1. AC Induction Motor

One objective in selecting the AC induction motor power rating is to effectively utilize the maximum power capability of the propulsion battery over a wide motor speed range. In addition, it is desirable to accomplish this with the smallest motor possible in order to reduce motor cost and weight. The operating speed of the rotary heat engine is in the range of 2000 to 6000 RPM. Selecting the same operating speed range for the electric motor eliminates the need for a speed reducer between the heat engine and electric motor and opens up the possibility of using a coaxial mechanical configuration.

Specifying the maximum motor output power (PMAX) establishes the relationship between the controller current rating and the minimum battery voltage.

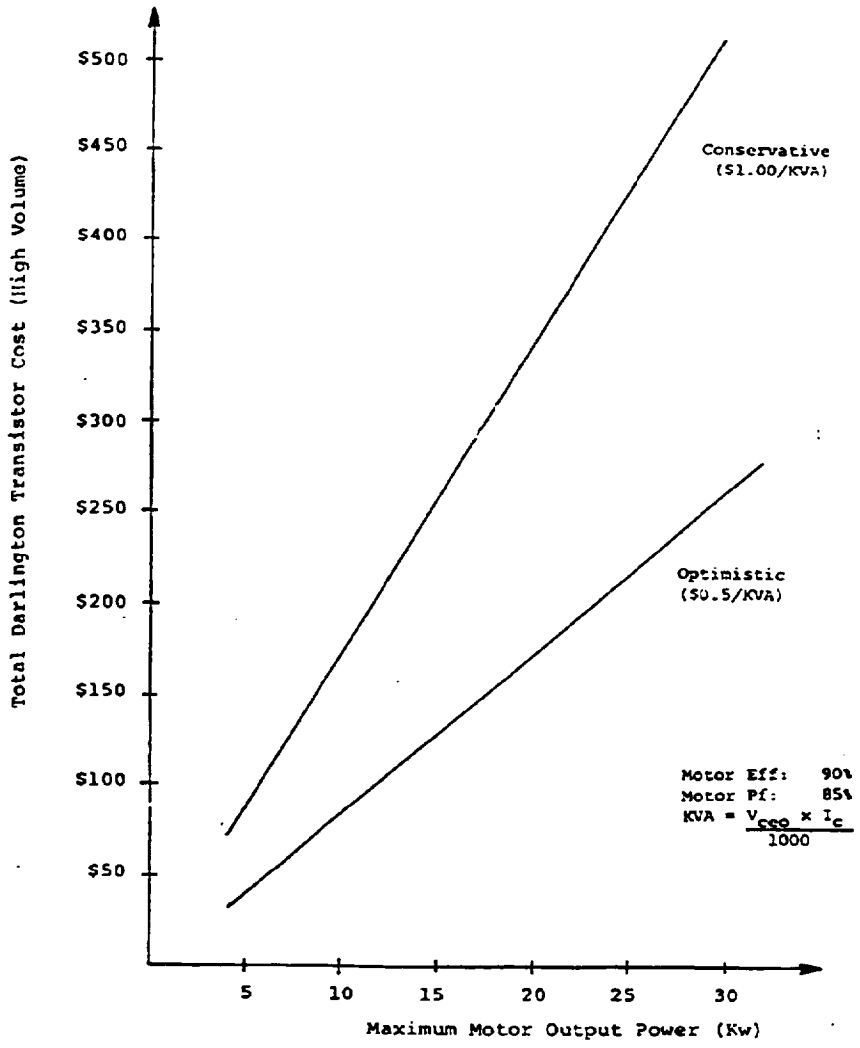

Figure 4-38. DARLINGTON TRANSISTOR COST VW. MOTOR OUTPUT POWER

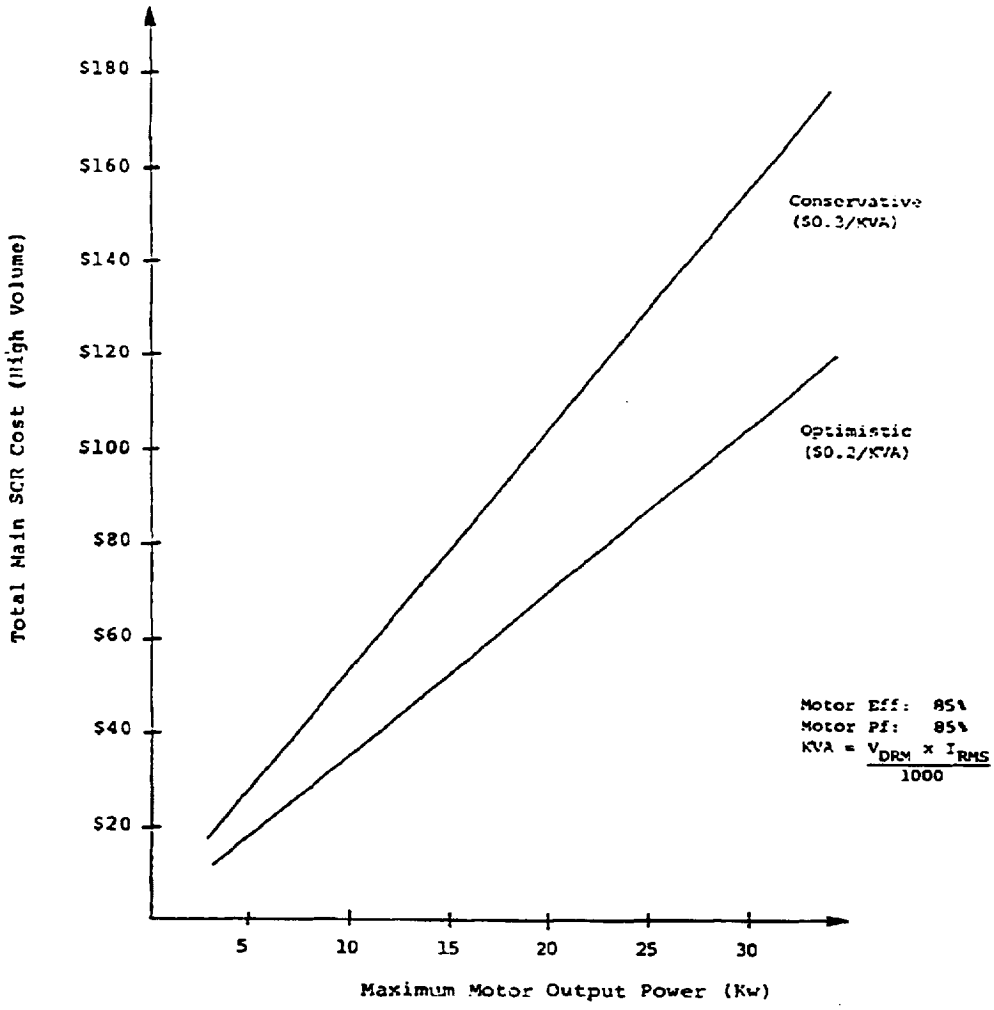

Figure 4-39. MAIN SCR COST VS. MOTOR OUTPUT POWER

This relationship was developed previously, based on a six-step waveform, and is shown below for reference:

$$PMAX = (6/\pi) \times EBAT \times ID(RMS) \times EFF \times PF \quad (45)$$

where motor efficiency is denoted by EFF, motor power factor by PF, main device current rating by ID(RMS), and the minimum battery voltage by EBAT.

Since the same motor output power can be obtained with different battery voltages, a tradeoff between battery voltage and device current rating must be made. Using semiconductors commercially available today (both bipolar transistors and SCR's) provides us with considerable flexibility in selecting the battery voltage as shown in Figure 4-40 for device RMS current ratings of 125, 250, and 375 amps. As discussed previously, device cost is based on semiconductor power handling capability (KVA rating) and is, therefore, not considered a dominant factor in selecting the propulsion battery voltage.

To obtain maximum motor power (PMAX) over as wide a motor speed range as possible requires tradeoffs in selecting the base speed at which the maximum motor power is reached. The reason for this will be identified with the aid of Figure 4-41 where base speed is defined as the motor speed at which the transition from constant torque to "constant power" occurs.

In the constant torque operating region, the motor terminal voltage is increased almost linearly with frequency in order to maintain a constant air gap flux. The method used to control the applied motor voltage in this region is referred to as pulse-width-modulation (PWM). The basic approach is to apply the battery voltage to the motor as a series of pulses during each half cycle with the width of each pulse being varied to control the motor voltage. In a preferred approach, illustrated in Figure 4-42 , the width of each pulse is varied throughout the half cycle in a sinusoidal manner in order to improve motor performance. As shown in Figure 4-41, motor output power in this region increases linearly from zero speed to the base speed.

Motor output power in the constant torque region could be increased for the same controller rating by shifting the motor base speed so that it occurs at a speed lower than the 3000 RPM point. This is accomplished by changing the motor voltage rating; but motor performance at high speeds will be degraded, as will be discussed.

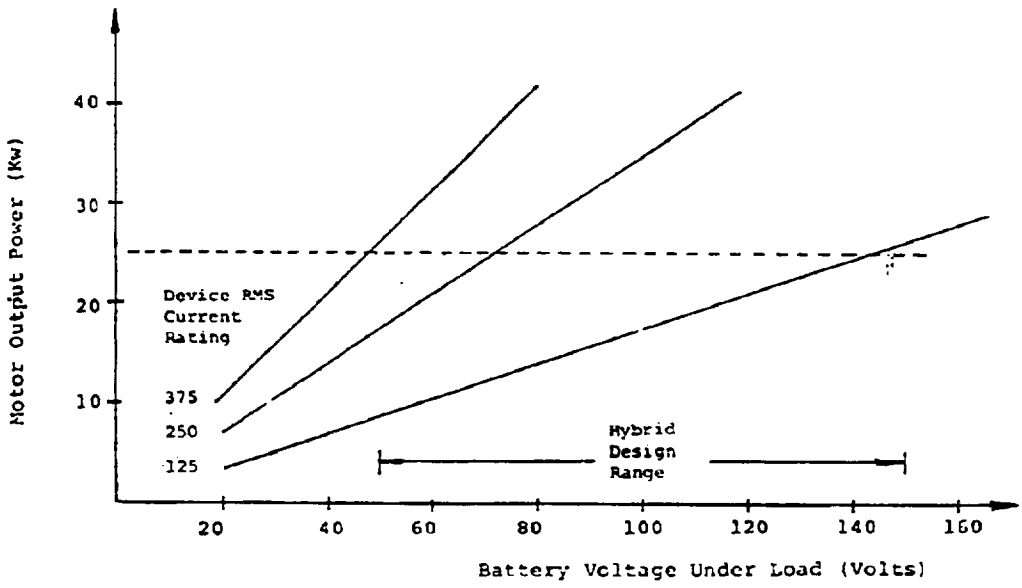

Figure 4-40. EFFECT OF DEVICE CURRENT RATING ON BATTERY VOLTAGE

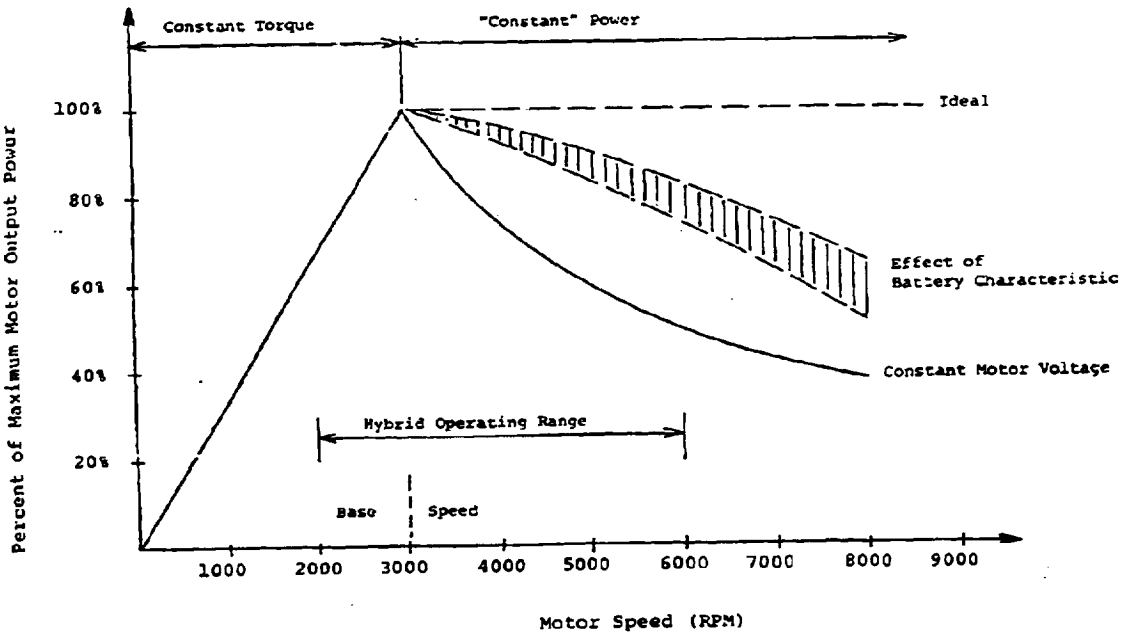

Figure 4-41. AC INDUCTION MOTOR OUTPUT POWER VERSUS SPEED

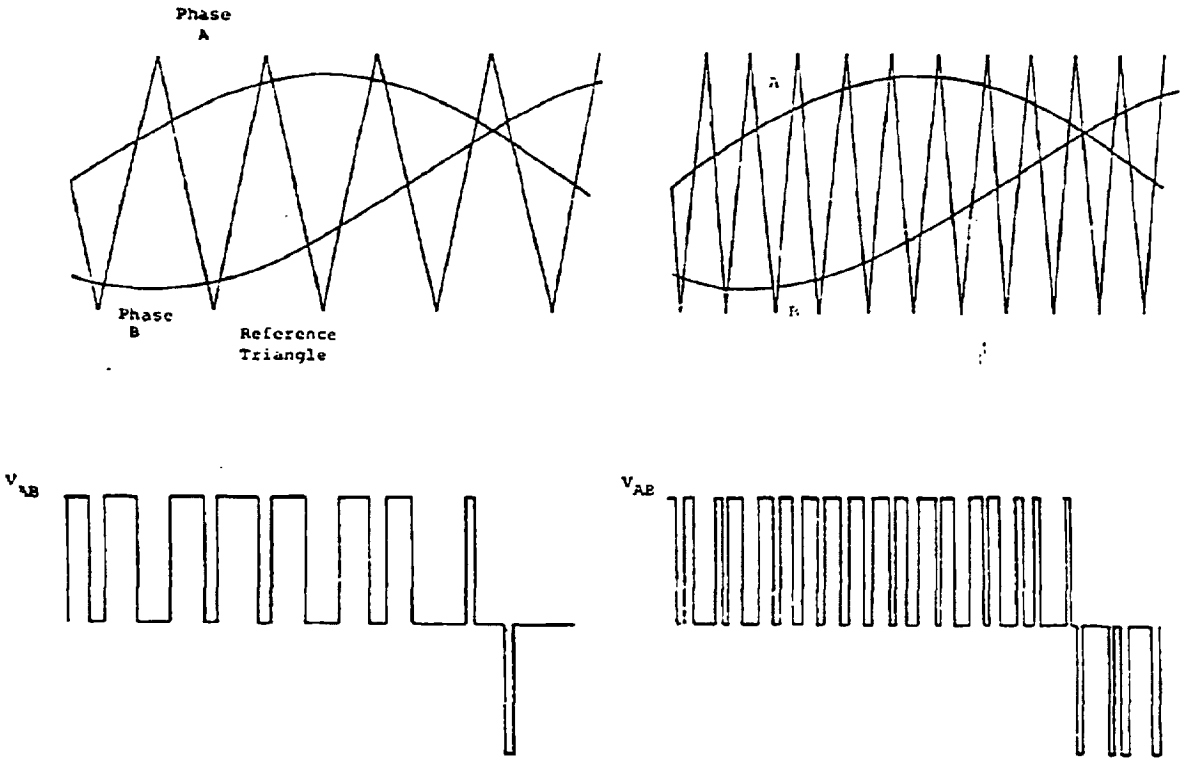

Figure 4-42. OUTPUT VOLTAGE WAVEFORM OF A PWM INVERTER WITH SINUSOIDAL MODULATION

When the motor voltage has been increased to the maximum output voltage of the controller, which is established by the propulsion battery voltage, the transition from the constant torque region to the "constant" power region is made. This is the maximum power point which occurs at 3000 RPM for the example shown in Figure 4-41. Operation above this speed with an SCR controller is accomplished with a six-step voltage waveform applied to the motor, i.e., PWM is no longer required and operation is at constant voltage. If the motor rating has been selected such that the motor is operating near its breakdown torque at base speed (3000 RPM), then increasing motor speed above base speed will decrease motor output power. For this example, operation at twice base speed will reduce the maximum motor output power by 50% based on constant applied motor voltage. This is illustrated as the constant voltage line in Figure 4-41 .

The decrease in maximum motor power above base speed is a departure from our goal of being able to utilize the maximum power capability of the propulsion battery over a wide speed range. Shifting the maximum power point to a lower base speed, as discussed previously, will further reduce the maximum motor output power at high speeds.

A beneficial factor affecting motor performance is the effect of the battery characteristic on maximum motor power. The output voltage of the controller is a function of the power drawn from the propulsion battery, and any decrease in the motor output power will increase the battery voltage. This will be reflected as an increase in the motor output power above that represented by the constant voltage line and is shown as the cross-hatched area in Figure 4-41.

The overall objective is shown as a dashed line and represents the ability to utilize the maximum power capability of the propulsion battery at any motor speed above base speed. This characteristic could be achieved with increased controller complexity by using a step-up chopper in front of the inverter to regulate the motor voltage as a function of speed. One possible circuit arrangement to accomplish this is shown in Figure 4-43. One advantage of this circuit arrangement is the ability to use a high voltage AC motor with a low voltage propulsion battery, thereby minimizing the safety hazards associated with high battery voltages. One disadvantage is that to supply power from the motor to the battery (regeneration) requires additional circuitry not shown in Figure 4-43.

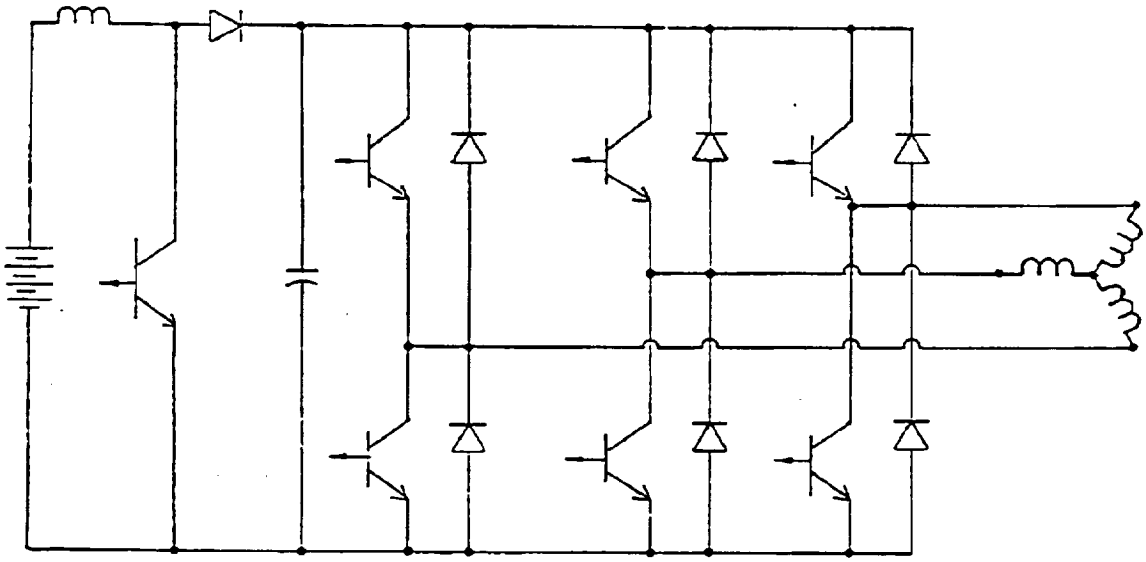

Figure 4-43. TRANSISTOR AC CONTROLLER WITH STEP-UP CHOPPER

For the design tradeoff study, a method of estimating the maximum battery power, given the maximum motor power, was required. To accomplish this, the information shown in Figures 4-44 and 4-45 was developed using a computer model of the AC propulsion system. Included in the model were equivalent circuits for the AC induction motor, AC controller, and propulsion battery. The parameters of the AC induction motor were provided by Gould's Electric Motor Division. AC controller semiconductor voltage drops, commutation losses and the characteristics of the propulsion battery are included. The maximum battery power [PBAT(MAX)], shown in Figure 4-44, was determined by multiplying the battery's specific power density in watts/kg by the battery weight in kg. In developing Figures and 4-45 , the battery's maximum power [PBAT(MAX)] was approximated as being 80% of the battery's peak power capability [PBAT(PEAK)], as shown below, where EOC is the nominal open circuit voltage of the propulsion battery.

$$PBAT(PEAK) = (EOC)^2/4RBAT) \quad (46)$$

$$PBAT(MAX) = (EOC^2/4RBAT) \times 0.8 \quad (47)$$

The relationship shown in Figure 4-44 is based on matching the battery and AC propulsion system in order to maximize power transfer from the propulsion battery to the AC motor while also minimizing the size and cost of the AC induction motor. Use of Figures 4-44 and 4-45 can be illustrated with the following example. Assume that the maximum motor output power required to meet the specified acceleration requirements has been previously determined to be 29 kw. Also assume that this power is required over a motor speed range of 2300-4600 RPM. From the efficiency map, shown in Figure 4-45, the ratio of maximum to rated motor/controller power is a factor of 2.6. For this example, the required motor/controller steady-state power rating is then 11.2 kw, or 15 HP. From Figure 4-44 the maximum battery power given a motor/controller power rating of 15 HP is estimated to be 43 kw. For a lead-acid battery with a specific power density of 100 watts/kg, the battery weight is 430 kg.

Cost for a totally enclosed AC induction motor (4 pole), as a function of motor 60 Hz power rating, is shown in Figure 4-46. Background data provided by Gould's electric motor division is also plotted in Figure 4-47. The motor/controller rated power, given in Figure 4-44, is assumed to be 50% higher than the standard 60 Hz rating.

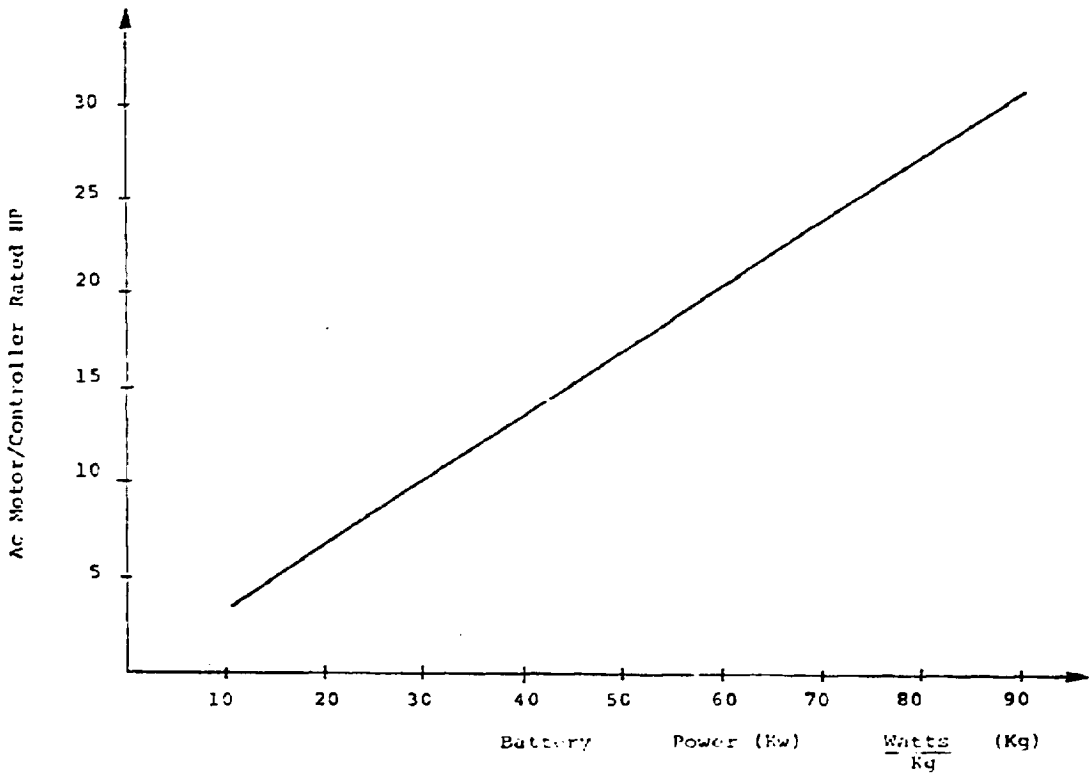

Figure 4-44. AC MOTOR/CONTROLLER RATED HP VERSUS BATTERY MAXIMUM POWER $P_{BAT}(MAX)$

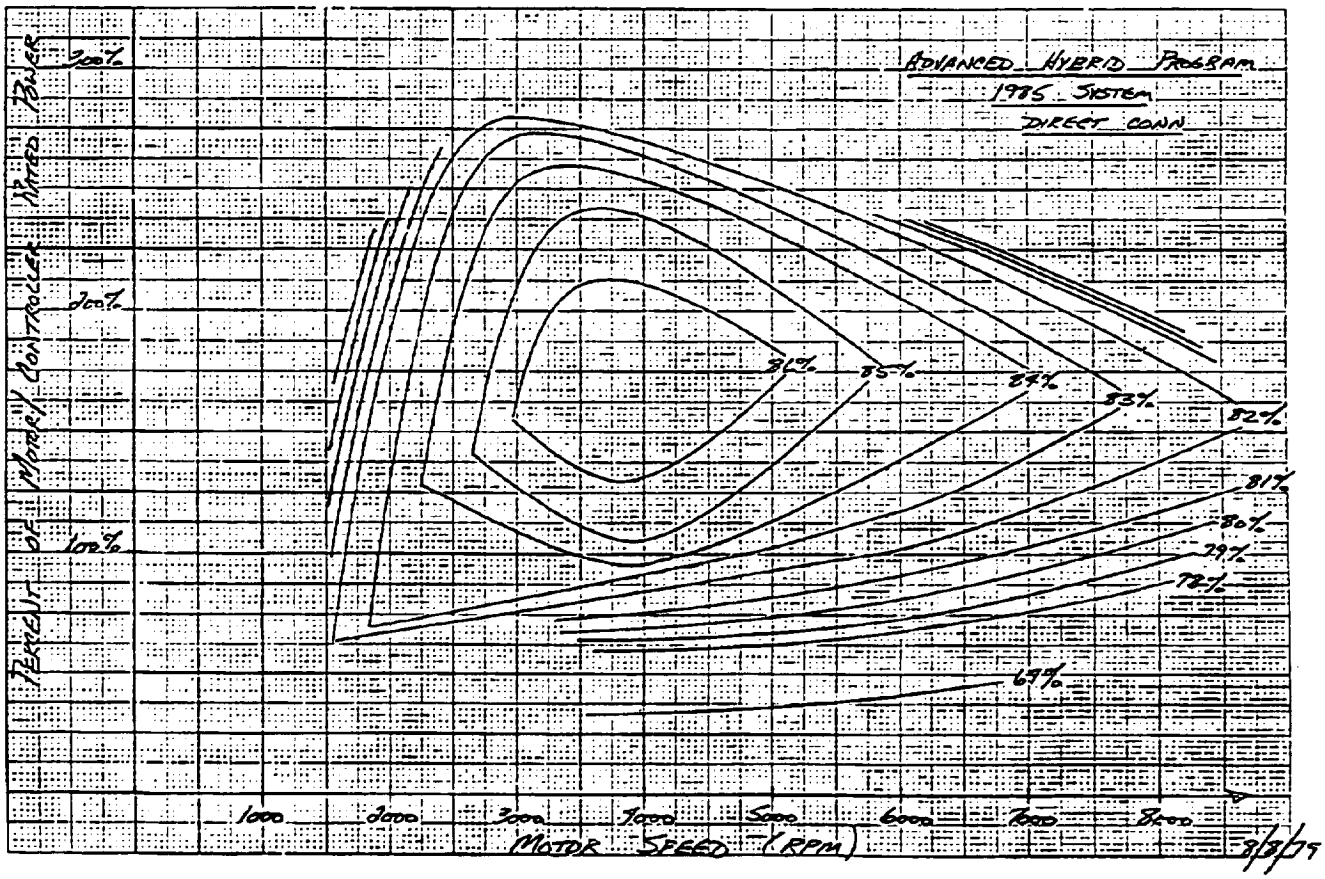

Figure 4-45. AC INDUCTION MOTOR/CONTROLLER EFFICIENCY MAP

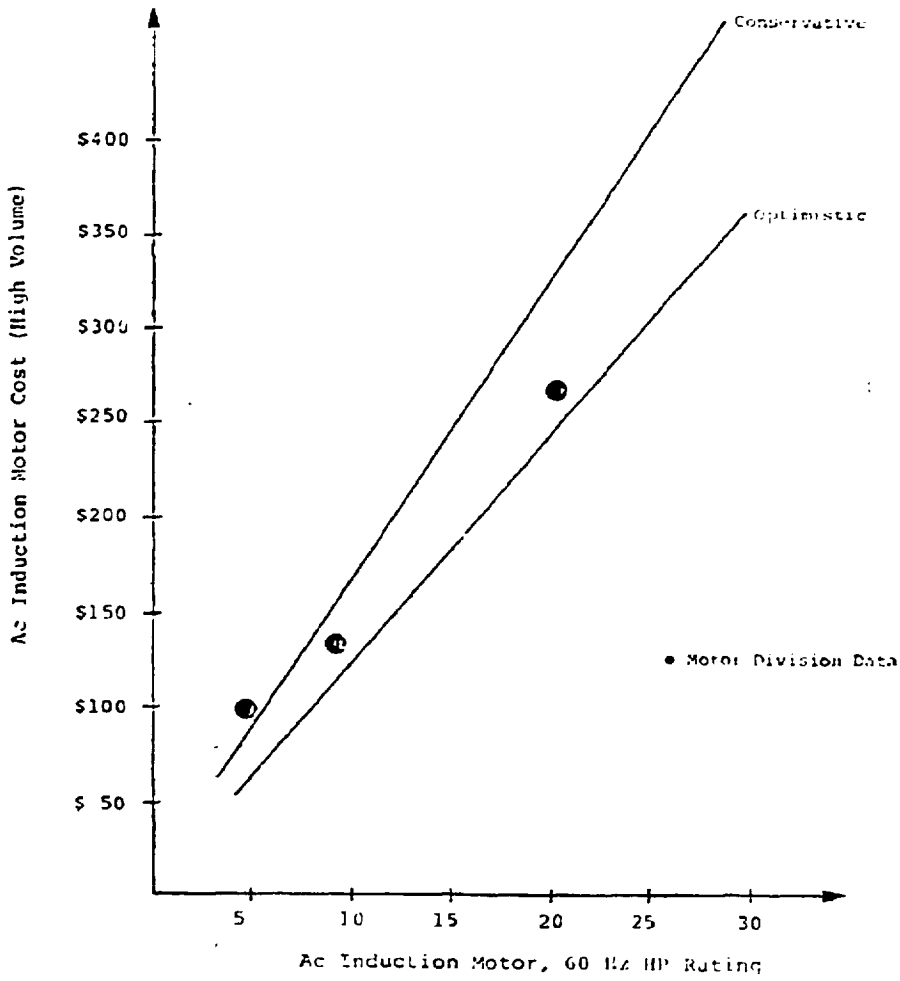

Figure 4-46. AC MOTOR COST VS. 60 HZ HP RATING

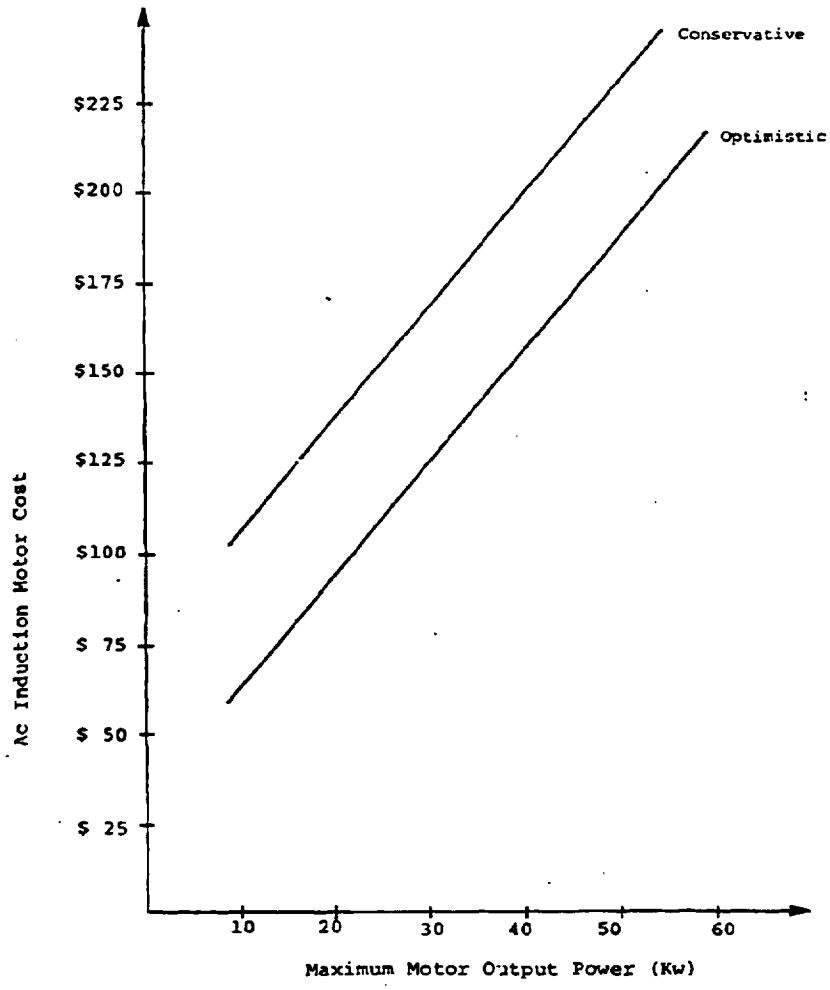

Figure 4-47. AC INDUCTION MOTOR COST VS. MAXIMUM MOTOR POWER

The final steady-state motor/controller power rating will, however, depend on the motor's location in the vehicle and the cooling provided by vehicle ram air. AC motor cost, as a function of maximum motor output power, is shown in Figure 4-47 and is based on the maximum motor power being 2.6 times the motor controller rating given in Figure 4-46.

2. AC Permanent Magnet Synchronous Motor

Recent advances in the development of magnetic materials has aroused interest in the use of permanent magnet synchronous motors for several applications including its use as a traction motor in an electric vehicle.[22] Its major advantages are high efficiency and power factor, and reduced controller complexity when compared to conventional AC induction motors and their associated SCR controllers. Its major disadvantage has been high cost, but recent effort[23] in this area indicates that the permanent magnet motor could be cost competitive with the induction motor depending on the results of ongoing development work.

Advantages of higher motor efficiency and power factor are the reduction in semiconductor cost, the more efficient utilization of the battery stored energy, and a reduction of life cycle cost. The performance stated[22,24-26] to be obtainable with the permanent magnet motor is an efficiency of 90-95% and a power factor of 94-99%.

A third and equally important advantage, when compared to the AC induction motor, is the ability of the motor to commutate the main inverter SCR's (six-step operation), and thereby reduce controller complexity and cost by eliminating the commutation circuitry. Obtaining low speed performance with a permanent magnet motor does require a limited amount of commutation circuitry.[27] However, once the motor has reached a speed where its back EMF is sufficient to turn off the main inverter SCR's, the commutation circuitry can be rendered inoperative. This eliminates commutation losses when operating above a specific motor speed, and is reflected in a higher controller efficiency. Compared to both the McMurray and Buss commutated inverters, use of a permanent magnet motor offers significant advantages in terms of reducing SCR controller cost. With a transistor controller, no commutating circuitry is required; and, therefore, the advantages of the permanent magnet motor over an AC induction motor are not considered to be as significant with this type of controller. The effect of the nigher efficiency

of the permanent magnet motor on main device cost, for both transistor and SCR AC controllers, is shown in Figures 4-48 and 4-49 , respectively.

The critical question concerning the future use of apermanent magnet motor is the motor's cost in high volume production. Brown-Boveri and Siemens, who manufacture rare earth (samarium-cobalt) and ferrite permanent magnet motors, respectively, indicated that a cost from 3 to 4 times that of a comparably rated AC induction motor was realistic with present technology. Obviously, the results of development work being done to reduce motor cost must be monitored closely and the results factored into a hybrid development program.

On-Board Charger

The assumptions made relative to the battery charger and accessory power supply used in an advanced hybrid vehicle are:

1. The vehicle will have an on-board battery charger and 600 watt accessory power supply. The charger power requirements are dependent on the size (stored energy) of the propulsion battery and the recharge time available. The advantages of each vehicle having its own on-board charger are well recognized. For example, charging can be accomplished at any location having a suitable AC power source (i.e., 120/208/240 VAC), and each charger can be individually programmed for the type of propulsion battery being used (i.e., lead-acid, nickel-zinc, nickel-iron, etc.).

2. Both the on-board charger and accessory power supply should be integrated into the AC controller to the greatest extent possible in order to reduce cost. This can be accomplished with the majority of electric vehicle propulsion systems (DC or AC) since the motoring and charging functions do not occur simultaneously.

3. The input AC line to the on-board battery charger and the accessory power supply output should be isolated from the propulsion battery. This is an assessment of what will be done in the future based on our experience with electric vehicle power systems.

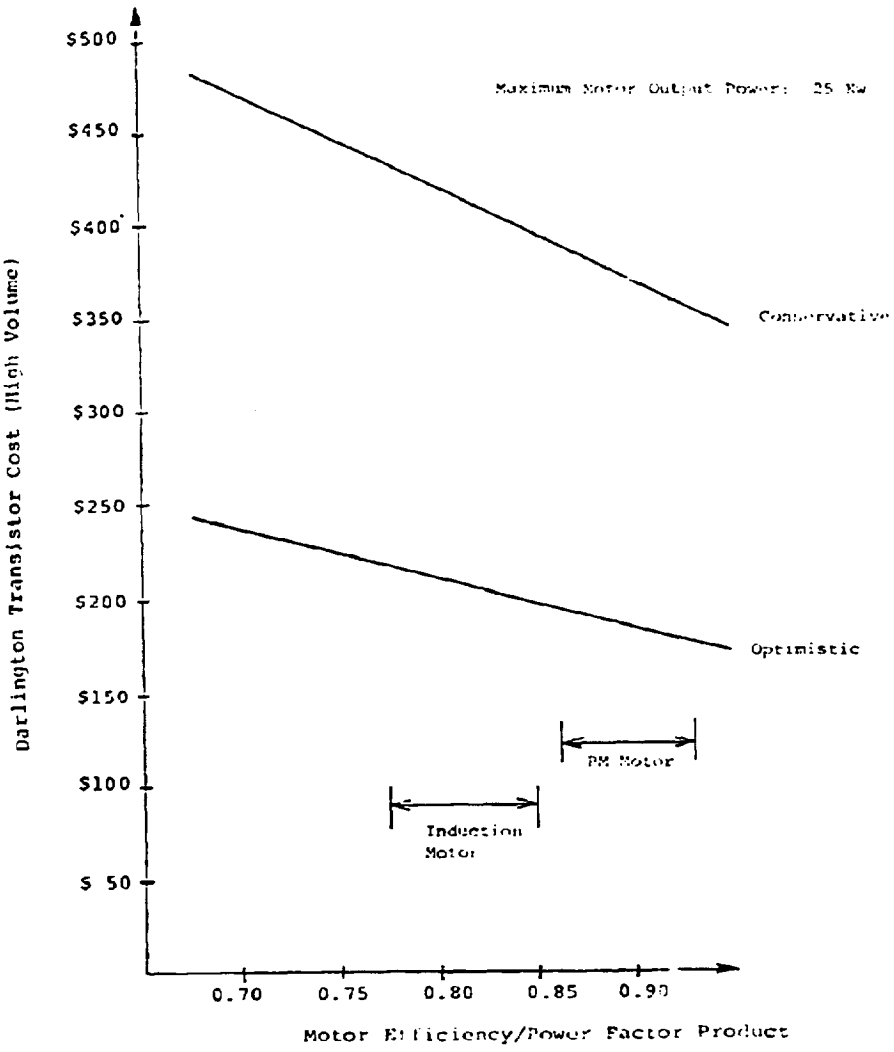

Figure 4-48. EFFECT OF MOTOR EFF/POWER FACTOR ON TRANSISTOR COST

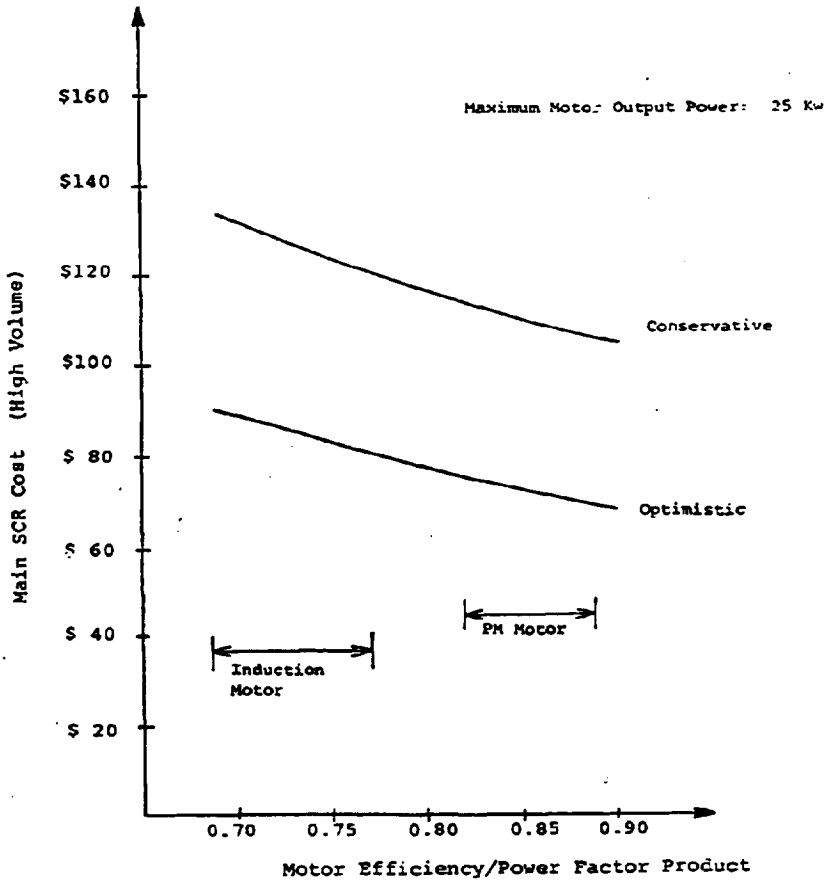

Figure 4-49. EFFECT OF MOTOR EFF/POWER FACTOR ON MAIN SCR COST

An evaluation of on-board charger and accessory power supply approaches is really an assessment of the circuit topologies of the transistor and SCR AC controllers. Of the many different techniques for accomplishing the charging function, only one topology for both the transistor and SCR approaches will be selected for discussion. The transistor and SCR circuit topologies for performing the motoring function are shown in Figures 4-50 and 4-51. Modifications to these two topologies to provide an on-board charger are illustrated in Figures 4-52 and 4-53, with the assumptions made relative to these two approaches being as follows:

1. Existing power semiconductors are used to control the battery charging current.

2. The charger input stage for both approaches is configured as a step-up chopper. This improves the input power factor and reduces the input harmonic current by proper shaping of the input current waveform. With the transistor approach, the semiconductors in one motor phase are used as a step-up chopper, whereas with the SCR approach, the commutation circuit is used in a step-up operating mode.

3. Transformer isolation is accomplished with the transistor topology by using an isolation transformer in combination with the two remaining motor phases. The transistors in these two motor phases are assumed to be connected in a bridge configuration. Transformer isolation with the SCR approach is obtained by adding a secondary winding to the commutation inductor to provide both isolation and power transfer from the commutation circuit to the propulsion battery. In this configuration, the commutation circuit is being used as a DC/DC converter and not for commutation.

4. A circuit breaker is used with both approaches in order to separate the battery and motor from the charger. If a circuit breaker were not utilized to separate the battery and charger, some form of positive disconnect is still required. Test results obtained using a Heinemann DC circuit breaker to protect an SCR inverter have been very favorable and indicate that with further refinements,

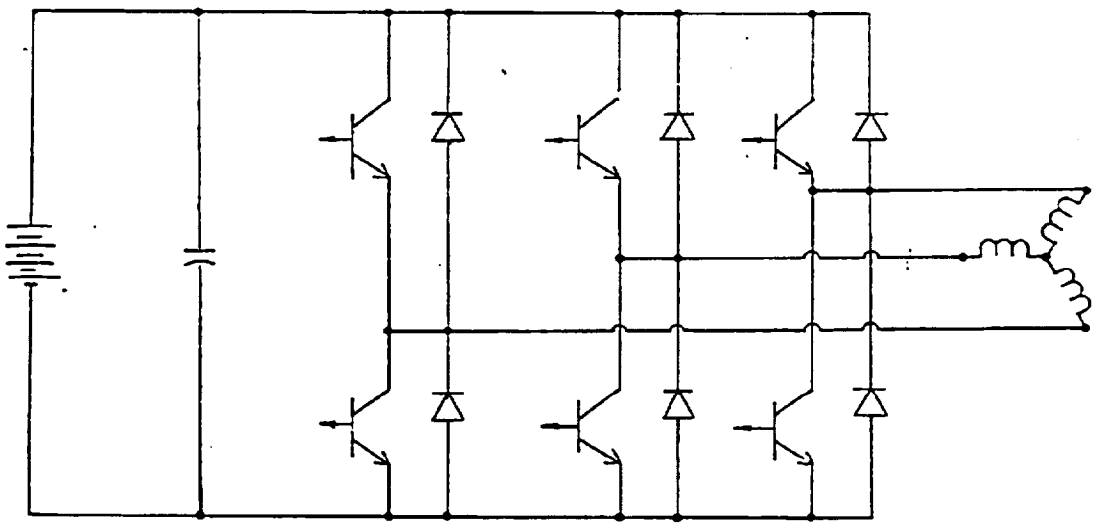

Figure 4-50. TRANSISTOR AC CONTROLLER (3-PHASE)

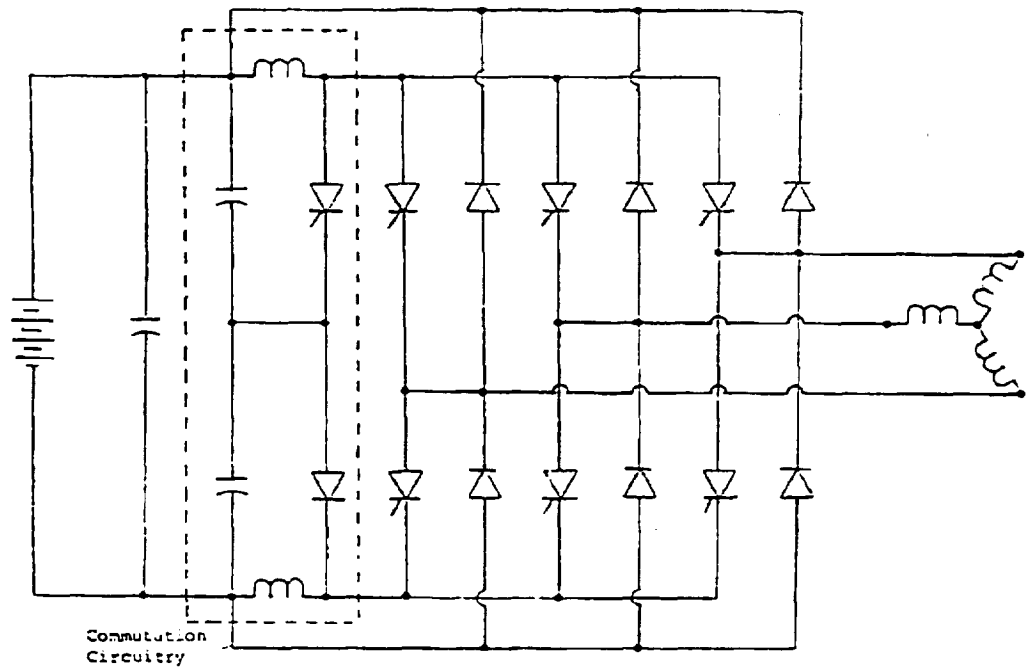

Figure 4-51. SCR AC CONTROLLER (3-PHASE)

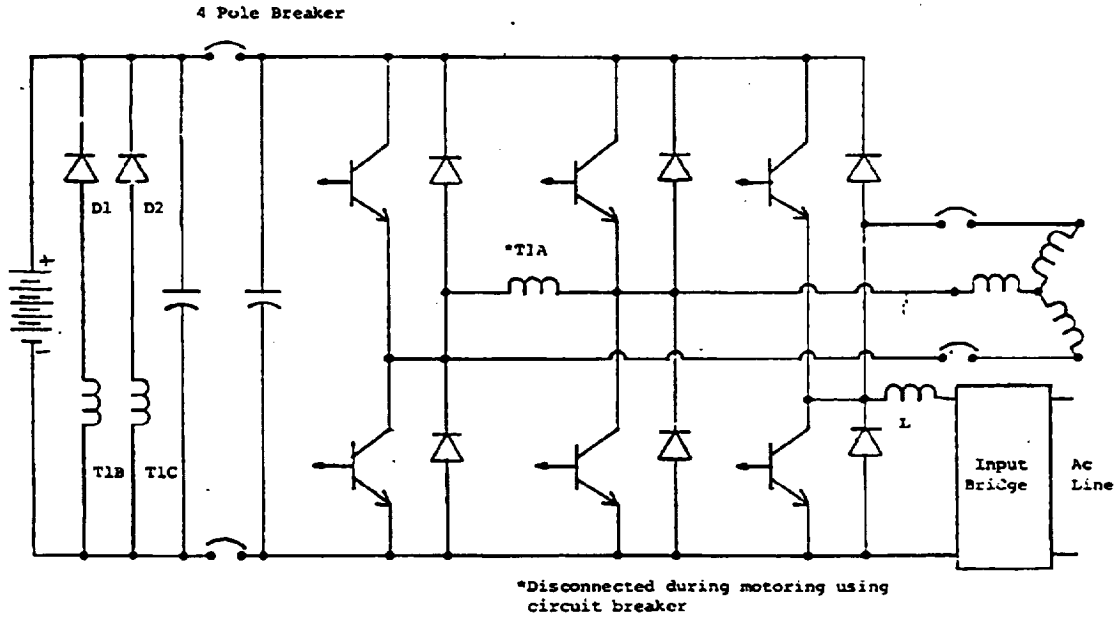

Figure 4-52. INTEGRATED TRANSISTOR AC CONTROLLER/CHARGER

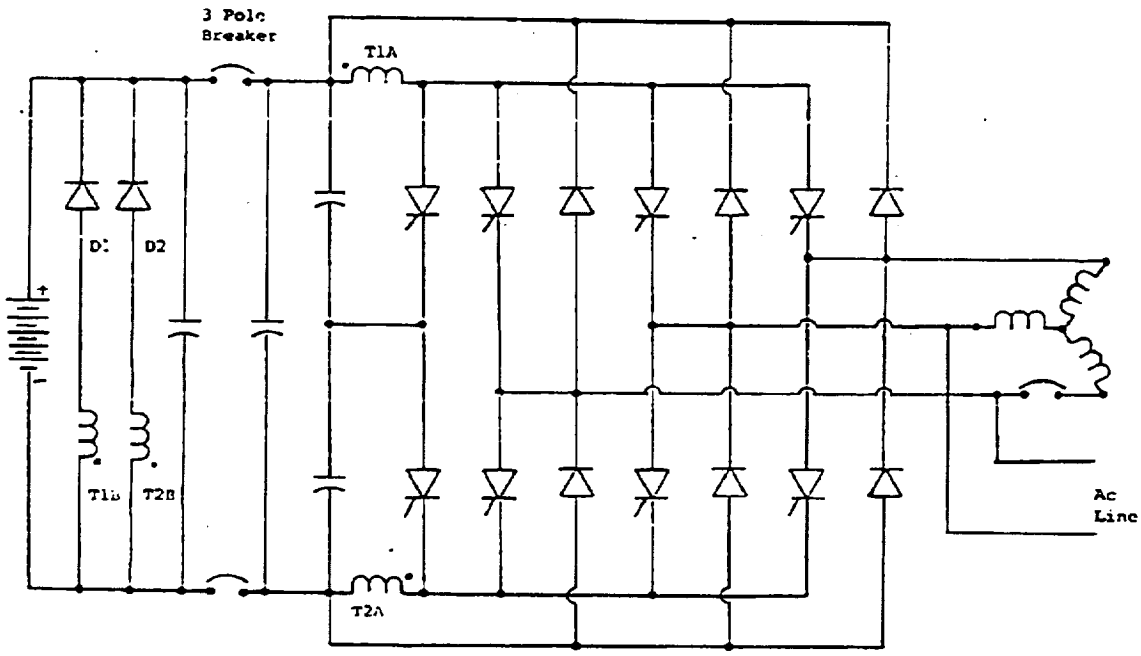

*Components labeled are added or modified for charging

Figure 4-53. INTEGRATED SCR AC CONTROLLER/CHARGER

a circuit breaker could replace the semiconductor fuse in an SCR controller.

5. The low power control used to control the motoring functions will also be used to control the charger and monitor the propulsion battery.

For these charging approaches, the cost of the components which must be added to perform the charging function have been estimated, as shown in Table 4-19. Costs are for a 2 kw charger.

Table 4-19. On-Board Charger Component Cost Estimate (2 kw)

	Transistor	SCR
Input Bridge	$ 10	$--
Input Inductor	10	--
Isolation Transformer	30	--
Power Devices	--	--
Circuit Breaker	30	30
Filter Capacitors	10	10
Output Inductor	10	--
Output Rectifier	10	10
Ground-Fault-Interrupter	10	10
Total Power Component Cost	$120	$60

With both approaches, the cost of the on-board charger has been significantly reduced by integrating it into the AC controller. The major advantages associated with integrating the charger into the controller are the reduction in semiconductor cost, gate/base drive circuitry, heatsink requirements and package complexity. The charger efficiency for both approaches is estimated to be in the range of 85-90%.

Accessory Power Supply

The accessory power supply is usually not considered a major component; however, a closer examination of the overall function indicates that using conventional techniques to provide an accessory power supply makes it a significant part of the cost. For example, a 600 watt switching power supply, produced in high volume, is estimated, based on discussions with Gould's power supply division, to have an OEM cost of $125-150. This is a cost comparable to that of the AC induction motor (25 kw maximum power) and assumes that cost reductions have been implemented to eliminate those components which are not required in an electric vehicle application (i.e., input rectifiers, hold-up capacitors, tight ripple and regulation specifications, and a separate package).

An examination of the transistor AC controller topology provides no immediately obvious method of incorporating the accessory power supply into the controller. Additional investigation may indicate an approach. The SCR controller topology can, in a manner similar to that used for the on-board charger, be modified to allow the accessory power supply to be integrated into the controller. One approach is to add an isolated winding to each commutation inductor and use the excess commutation energy normally returned to the propulsion battery during motoring to be used to charge the accessory battery. One circuit arrangement to accomplish this is shown in Figure 4-54.

Battery Voltage Selection

The selection of the "optimum" battery voltage for an electric or hybrid vehicle application has been and will continue to be a very complex and controversial subject. The criteria for selecting the "optimum" battery voltage for an advanced electric vehicle will most likely be influenced by the goal to minimize vehicle life cycle costs. To accomplish this requires that we be aware of those factors which influence life cycle cost.

To imply that presently available test data on electric vehicle batteries is sufficient to enable one to select the "optimum" battery voltage is unrealistic. One reason is that the development of batteries specifically for electric vehicles has yet to reach the point where sufficient test data is available to make a firm commitment to either high or low voltage systems. For example, work

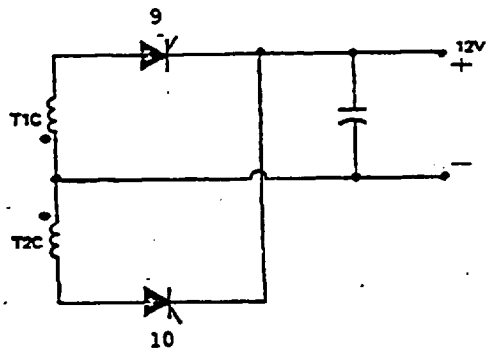

12 VOLT ACCESSORY POWER CIRCUIT

Figure 4-54. INTEGRATED ACCESSORY POWER APPROACH - SCR CONTROLLER

being done on low maintenance batteries and the improvements expected in battery design and manufacturing techniques may have a significant impact on battery reliability and, therefore, minimize the drawbacks of high voltage battery systems.

Increasing the propulsion battery voltage for the same motor output power increases controller efficiency. This reduces the controller initial cost and battery power and energy requirements for the same vehicle performance and range. For example, increasing the battery voltage decreases the semiconductor conduction losses and reduces the controller heat sink requirements and package size. As discussed previously, variations in the propulsion battery voltage do not influence the cost of the power semiconductors significantly since they are sized and priced according to the peak power to be controlled. Extreme variations outside the range of 60-200 volts, normally considered for electric vehicle propulsion systems, may, however, affect device cost due to the significant increase in device area or device voltage requirements.

The effect on life cycle cost of increasing the propulsion battery voltage can be examined using the results of the sensitivity studies performed by South Coast Technology. Their results indicated that increasing the combined motor/controller efficiency by one percentage point reduces vehicle life cycle cost by about $48, or .03¢/km. Increasing the battery voltage (at maximum power) from 50 volts to 150 volts was calculated to increase the controller efficiency from 93.5% to 95.5%, as shown in Figure 4-55. The efficiency curve is based on a peak motor output power of 25 kw and a motor frequency of 250 Hz. For a motor efficiency of 87-91%, the increase in the combined motor and controller efficiency is approximately two percentage points. This effect, by itself, results in a reduction in the vehicle life cycle cost of $96 based on a 10-year life, or .06¢/km.

This, however, does not constitute the total change in life cycle cost. For a fixed battery energy capacity, raising the battery voltage will increase the battery acquisition cost and increase the weight, both of which impact the life cycle cost. The magnitude of these effects for ISOA batteries are not known; however, if the behavior of existing batteries is any indication, the effect on acquisition cost is more significant than the effect on weight. In other words, the larger quantity of smaller hardware (cell interconnections,

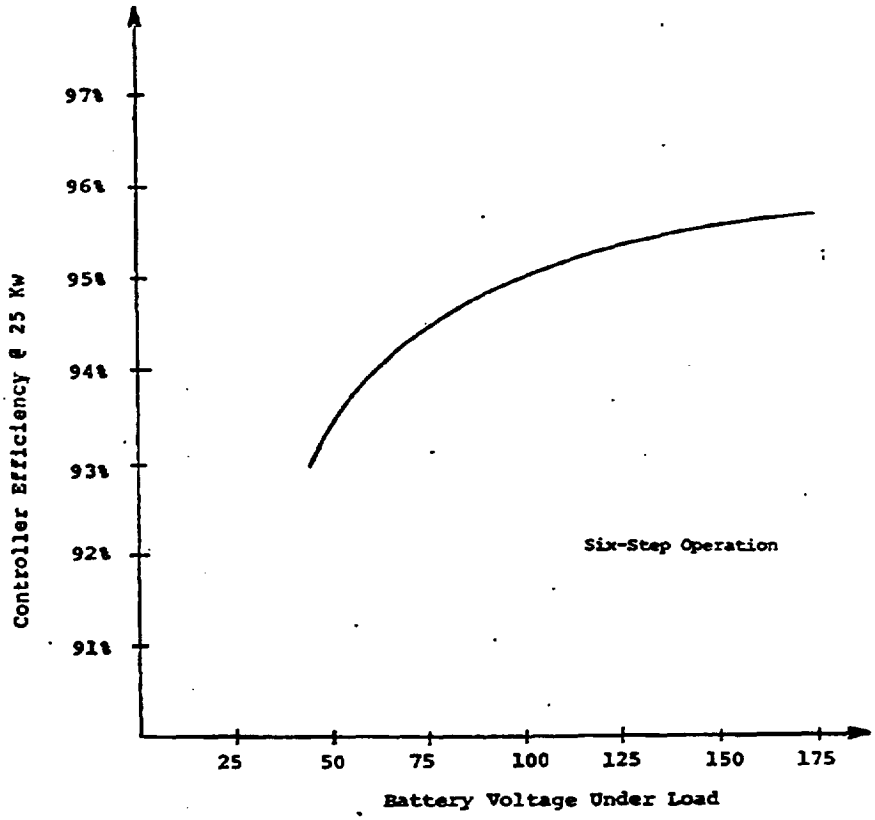

Figure 4-55. SCR CONTROLLER EFFICIENCY VS. BATTERY VOLTAGE

etc.) required for a higher voltage battery affects cost more than it does weight. Increasing the number of cells (voltage) also has an effect on battery reliability.

Reducing the propulsion battery voltage presents the possibility of reducing the cost of the propulsion system by minimizing the number of additional components which must be added to prevent accidental contact with the battery. The contact resistance of the human body between different points and the effect of different current levels on life functions is well documented. For reference, the effect of various current levels on a 150 lb. man are listed in Table 4-20. The resistance for different skin contact conditions is shown in Table 4-21. From the standpoint of safety, the lower the battery voltage, the lower the probability of reaching the paralysis limits shown in Table 4-20 . Translating this into equivalent system cost must still be accomplished with the cost factors being not only special enclosures and barriers, but also indirect costs such as insurance.

What can be concluded at this point, in view of the fact that the factors discussed above (battery cost, reliability, etc.) tend to offset the effects on life cycle cost of controller efficiency, is that battery voltage has only a minor influence on life cycle cost; and the ultimate selection of battery voltage will be based more on factors of technical convenience rather than cost.

4.5 General Conclusions

In order to focus the reader's attention on the salient elements of the design approach, before discussing the conceptual design task, it would be well to restate and generalize on some of the major conclusions of the design trade-off studies task. The intent of this section is not to recap all the detailed conclusions discussed previously but only to highlight them in terms of their impact on the overall design philosophy. Since the major objective of a hybrid propulsion system is to conserve petroleum based energy at a life cycle cost competitive with a conventional propulsion system, we shall discuss these conclusions in light of these two factors: fuel consumption and life cycle cost.

The hybrid system is at a cost disadvantage, relative to a conventional system, because of the high acquisition cost of the electric propulsion subsystem,

Table 4-20

CURRENT RANGE AND EFFECT ON A 150 LB. MAN

CURRENT (60 HZ) *	PHYSIOLOGICAL PHENOMENONS	FEEL OR LETHAL INCIDENCE
(1 mA	None	Imperceptible
1 mA	Perception Threshold	
1-3 mA		Mild Sensation
3-10 mA		Painful Sensation
10 mA	Paralysis Threshold of Arms	Cannot release Hand Grip: If No Grip, Victim May Be Thrown Clear (May Progress To Higher Current & Be Fatal)
30 mA	Respiratory Paralysis	Stoppage Of Breathing (Frequently Fatal)
75 mA	Fibrillation Threshold 0.5 Percent (>5 Second Exposure)	Heart Action Discoordinated (Probably Fatal)
250 mA	Fibrillation Threshold 99.5 Percent (>5 Second Exposure)	
4A	Heart Paralysis Threshold (No Fibrillation)	Heart Stops For Duration Of Current Passage. For Short Shocks, May Restart On Interruption Of Current (Usually Not Fatal From Heart Dysfunction)
>5 A	Tissue Burning	Not Fatal Unless Vital Organs Are Burned

* Data for D.C. currents not located but according to Dalziel (ref.) U.L. tests conducted in 1930 indicated slightly higher values can be withstood for a short time until a hot spot occurs at the point of contact.

Table 4-21

HUMAN RESISTANCE FOR VARIOUS SKIN-CONTACT CONDITIONS

CONDITION (AREA TO SUIT)	RESISTANCE, OHMS DRY	WET
Finger Touch	40K-1M	4-15K
Hand Holding Wire	15-50K	3-6K
Finger-Thumb Grasp*	10-30K	2-5K
Hand Holding Pliers	5-10K	1-3K
Palm Touch	3-8K	1-2K
Hand Around 1-1/2-Inch Pipe (Or Drill Handle)	1-3K	0.5-1.5K
Two Hands Around 1-1/2-Inch Pipe	0.5-1.5K	250-750
Hand Immersed	——	200-500
Foot Immersed	——	100-300

Human Body, Internal, Excluding Skin = 200-1000 Ohms

* Data Interpolated

RESISTANCE VALUES FOR EQUAL AREAS (130 cm^2) VARIOUS MATERIALS

MATERIAL	RESISTANCE, OHMS
Rubber Gloves Or Soles	>20M
Dry Concrete Above Grade	1-5M
Dry Concrete On Grade	0.2-1M
Leather Sole, Dry, Including Foot	0.1-0.5M
Leather Sole, Damp, Including Foot	5K-20K
Wet Concrete On Grade	1K-5K

and replacement costs for batteries. This cost disadvantage can be minimized in three ways: first, by making the electric propulsion system small, thereby keeping its acquisition cost and battery replacement cost at reasonable levels, second, by achieving fuel savings which are large enough to pay, or nearly pay, for the acquisition cost discrepancy, and third, by avoiding high cost design approaches in areas which only marginally affect fuel consumption. It is necessary to keep the maximum output of the electric propulsion subsystem below 30% of the maximum system power requirement, and work the propulsion battery at or near its peak power when the electric motor output is at its maximum, in order to keep the propulsion system and battery economics reasonable. However, the rate of increase in fuel consumption becomes quite large as the electric propulsion system output gets below about 25% of the system output, so 25-30% (.7-.75 heat engine power fraction) appears to be the range for the electric propulsion system which gives the "best" combination of cost and fuel consumption. This corresponds roughly to a peak electric motor output of 25 to 30 kw.

The factors to consider in specifying, designing, or evaluating a propulsion battery for use in a hybrid vehicle are not necessarily weighted the same way they would be if the application is a pure electric vehicle. Specifically, the most important factors for a hybrid application are specific power (w/kg) and the ratio of specific cost to life ($/kg-cycle). Although specific energy is a factor to consider, its impact on life cycle cost is much lower than the previous two factors.

The most productive things that can be done to minimize fuel consumption, and thereby obtain fuel cost savings which are large enough to offset the costs associated with the electric propulsion subsystem and batteries, are to shut down the heat engine when the system power requirements do not dictate its use, and to load it enough (i.e., operate at a high enough bmep) to achieve a low bsfc when the power requirements dictate its use. This requires that the heat engine be capable of being shut down and decoupled from the system, and restarted and brought back on line, according to the power demand. These events occur quite frequently, and there are obvious development problems associated with such a strategy in the areas of driveability, emissions control, and engine thermal control; however, this appears to be the only route that offers the potential of achieving enough fuel savings to make the system economically viable.

In addition, by limiting the load range over which the engine must operate to relatively high bmep's, this approach attains the same basic objective at which turbocharging, variable displacement engines, and continuously variable transmissions are aimed. Consequently, applying such high cost approaches to the hybrid does not return much in the way of fuel savings, and only compounds the problem of acquisition cost.

The design approach dictated by these considerations involves doing everything possible to alleviate the development problems associated with on/off operation of the heat engine and to minimize overall system cost. An example of this approach is the use of a torque converter in the transmission for driveability and to soften the transients associated with turning the heat engine on and off. The losses associated with the torque converter are outweighed by the gains involved with on/off operation of the heat engine. Another example is the use of the traction motor to supply hydraulic power for the transmission and power steering when the heat engine is off, rather than using a separate electric auxiliary drive. This necessitates the traction motor driving through the torque converter; however, the costs involved in the associated torque converter losses are far outweighed by the cost of a separate auxiliary drive.

In summary, then, the Design Tradeoff Studies task resulted in the conclusion that the design parameters and system configuration used in the baseline design would provide a suitable starting point for a conceptual design, and that the areas in which subsequent design and development activity should be concentrated are:

- Heat engine on/off operation, especially thermal control during on/off cycling to minimize emission control problems.

- Cost reduction of the electric propulsion subsystem by optimizing circuit design and device selection for the required power level, and by integration of various functions (motoring, charging, accessory power supply) to minimize total hardware.

- Design and development of propulsion batteries specifically for the hybrid application (which is outside the scope of this particular program).

5. CONCEPTUAL DESIGN

5.1 Objectives and Scope

The primary objective of this task was to develop a conceptual design of a hybrid propulsion system following the design directions established in the Design Tradeoff Studies task. This design was to define design approaches for all the major components and subsystems, and would illustrate how the system might be packaged in a vehicle.

The scope of this effort involved carrying the design and analytical effort far enough along to, first of all, establish the feasibility of the approach (at least within the limits of what can be accomplished in a paper study), and second, to define principal areas where development would be required.

5.2 Technical Approach

One of the basic conclusions of the Design Tradeoff Studies task was that the baseline hybrid propulsion system constructed in that task constituted a suitable starting point for a more detailed design effort. Consequently, the approach taken to the Conceptual Design task was simply to expand on the detail of this baseline system, with particular emphasis on the following areas:

- Identification of hardware design approaches which appear to be promising in terms of cost reductions or efficiency gains.
- Integration and packaging of components.
- Conceptual design and integration of ancillary subsystems, such as cooling, lubrication, hydraulic supply, fuel injection, ignition, 12 V supply, and so forth.

5.3 System Description

The reader is referred to Section 4.4.1, Baseline System Description, for a discussion of the basic elements of the conceptual design. In the following subsections, we will elaborate on some of the design details of the system.

5.3.1 System Controller

The control strategy for the advanced hybrid propulsion system is as outlined in Section 4.4.1 under "Control Strategy Description." This basic strategy may require modifications during the warm up period for the heat engine, particularly in cold weather operation; for example, it may be necessary to permit the heat engine to operate continuously until a pre-determined coolant temperature is reached. With the addition of such modifications, then, it can be concluded that the basic input/output variables for the system controller are the following:

1. Inputs (from suitable sensors)

   - o Driver
     - Accelerator pedal position (power demand)
     - Braking effort (probably measured by brake fluid pressure)
   - o Vehicle
     - Speed
   - o Heat engine
     - Coolant temperature
   - o Electric motor/controller
     - Speed (also measures heat engine speed when heat engine is running)
   - o Battery pack
     - Current
     - Voltage
     - Temperature

2. Outputs (to suitable interface circuitry and electro-mechanical actuators)

   - o Heat engine
     - Injector pump rack position
     - Ignition on/off
   - o Motor controller
     - Power (or current) command
   - o Transmission
     - Upshift/downshift signal
   - o Heat engine clutch
     - Engage/disengage signal

In order to process these input signals and generate outputs based on the strategy described in Section 4.4.1, the controller must have the following basic computational capability:

- Computation of battery state of charge from the parameters of current, voltage and temperature. Based on this computation, the controller decides whether Mode 1 or Mode 2 operation is required.

- Computation of upshift and downshift speeds at the demanded power level (see Figure 4-3); comparison of these speeds with present motor speed to determine if an upshift or downshift is required.

- Computation of maximum available heat engine power and electric motor power at the measured speed, from stored tables of these values (see Figure 4-2) as well as the value of the control parameter PHEMIN or PHEMN2 at the measured speed.

- Determination of the power split between the heat engine and traction motor based on the algorithm defined in Section 4.4.1.

- Generation of command signals to the injector rack actuator and motor controller to bring the heat engine and motor to the desired power levels. This requires a table of rack position vs. heat engine power and speed, and a similar function for the motor and controller.

These computational requirements imply that the only feasible method for implementing the control strategy discussed above and in Section 4.4.1 is with a microprocessor based system. A very similar control strategy was developed in the Near Term Hybrid Vehicle Program conducted for the Jet Propulsion Laboratory, and a complete discussion of the hardware and software for the microprocessor based system implementing this strategy is presented in Appendix C of the final report on that program.[1] Because those results are directly applicable to the system controller for the advanced hybrid, only the major features will be outlined here; and the reader is referred to the cited report for more detail.

A suitable basic microprocessor would be an 8 bit unit, probably based on N channel MOS (NMOS) technology, although a complementary MOS (CMOS) device would also be a possibility. The software program must be executable at a rate of at least 20 times per second to provide adequate power response, and it is estimated that a program memory of between 2 and 4K bytes is required with a data memory of 256 x 8.

5.3.2 Heat Engine and Controls

General Characteristics

The engine designed for the hybrid propulsion system is a single rotor Wankel type rotary of 72 cubic inch displacement rated at 70 kw (93.8 HP) which employs the direct injected stratified charge process.

Application of the stratified charge combustion process allows the significant size and weight advantages of the homogenous charge rotary engine to be retained, while offering diesel competitive fuel economy, exhaust emissions at the best reciprocating engine level, and broad base liquid fuel capability. A comparison of a 60 kw single rotor rotary with a 56 kw 6 cylinder VW diesel is offered in Figure 5-1 .

When the stratified charge process is applied to the rotary, it, like the reciprocating engine, benefits from the higher enthalpy efficiency accompanying the use of high overall air fuel ratios, the reduced pumping losses resulting from elimination of the throttle; and because of its geometry and kinematics, it eliminates the need for the special devices added to the reciprocating engine to generate the air swirl essential to the direct injected stratified charge process.

The air movement, which is a byproduct of the rotary engine's kinematics, is conceptually depicted in Figure 5-2 and compared to the same event in a stratified charge combustion process as it occurs in a reciprocating stratified charge engine with a similar combustion process, the Texaco TCCS engine.

The combustion chamber configuration recommended for the hybrid rotary is an outgrowth of an extensive stratified charge engine development program.

COMPARISON OF SC RC1-60 WITH VOLKSWAGEN 6 CYLINDER DIESEL

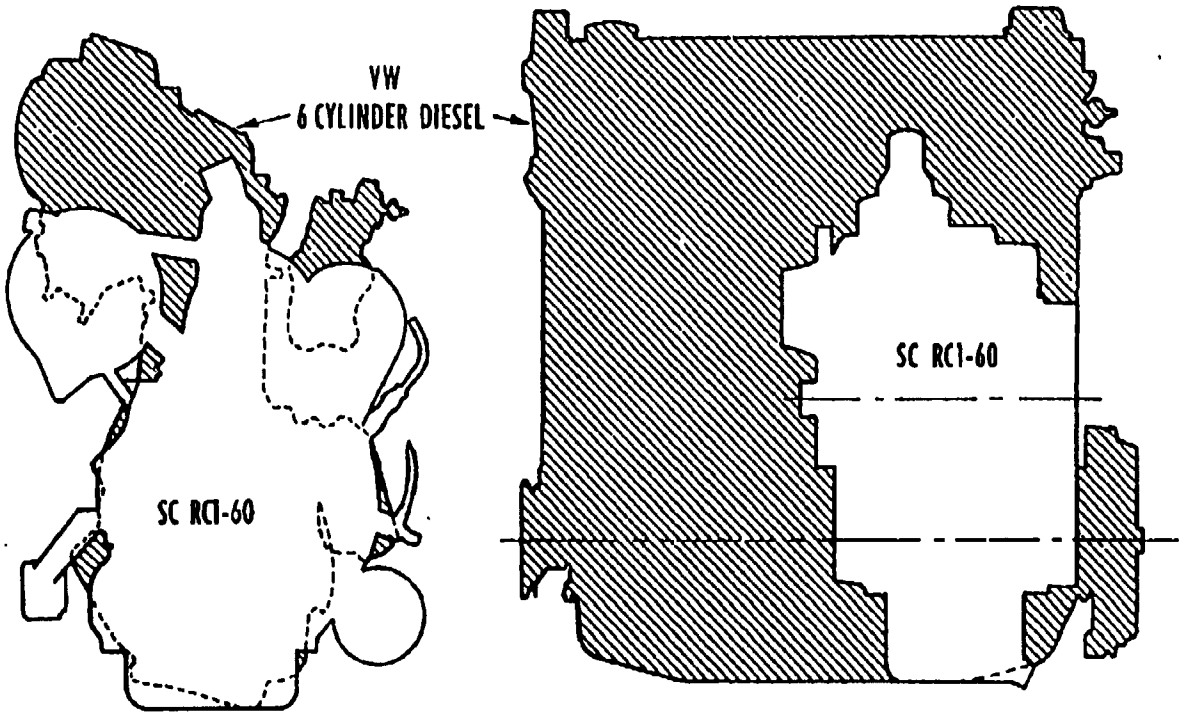

		SC RC1-60	VW 6 CYL DIESEL
kW (BHP)/RPM		60 (80)/5000	56 (75)/4500
kg (LB)		109 (240)	184 (405)
L x W x H	mm	368 x 559 x 635	780 x 490 x 780
	INCHES	14.5 x 22 x 25	30.7 x 19.3 x 30.7

Figure 5-1

STRATIFIED CHARGE PROCESSES

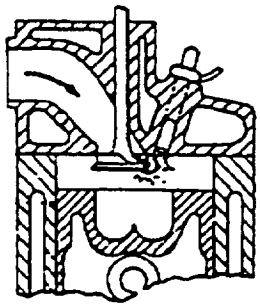

TEXACO TCCS

FORD PROCO

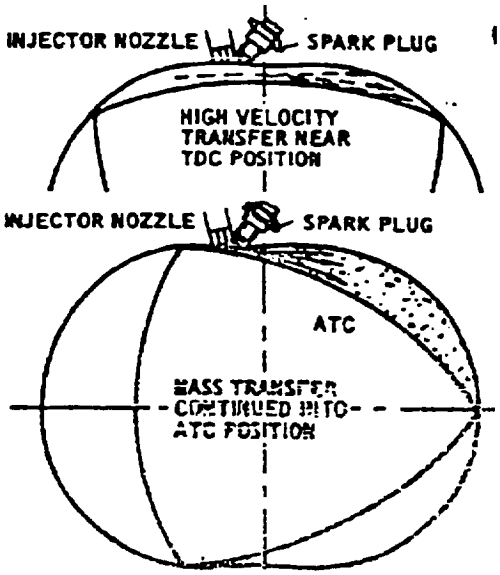

ROTARY

Figure 5-2

Two of the more significant features in the rotary combustion chamber configuration include the use of a pilot injector and maintenance of high rotor combustion chamber pocket temperature.

During this development activity, it was concluded that the considerable fuel distribution differences between light load to full load operation could best be satisfied by using a pilot nozzle to initiate combustion and a main injector to accommodate the varying load requirement. Oscilloscope traces of combustion pressures show that use of a pilot injector provides for firing regularity over the complete load/speed range, along with superior performance and fuel economy.

A major benefit of the stratified charge engine is improvement of fuel consumption, particularly in the part load range, over the homogenous charge engine. Accordingly, Curtiss-Wright's efforts were directed toward exploiting the fuel economy benefit for the rotary, not, however, at the expense of exhaust emissions. Throughout the development cycle, the various parameters affecting emissions, including the fuel delivery system and combustion chamber component shapes and operating temperature, were controlled to minimize exhaust emissions while improving fuel economy. Fuel economy and emission characteristics of the stratified charge RC1-60 are shown in Figures 5-3 and 5-4 .

The end effect is that the raw emission level of the stratified charge rotary is substantially lower than the homogenous charge version and representative of the lowest emitting reciprocating engines.

Testing revealed that a high rotor combustion chamber pocket temperature tended to reduce exhaust emissions; therefore, a design was introduced which uses an insulating air gap to maintain a high rotor pocket temperature. In the designs tested to date, an insert, which is in effect the combustion chamber pocket, is bolted to the rotor face. A favorable byproduct of this design is that heat rejection to the oil is reduced; and, therefore, oil cooler size and weight can be reduced. Particulates have not been measured for the stratified charge rotary, but tests of other stratified charge engines indicate emissions from this type engine are significantly lower than diesels.

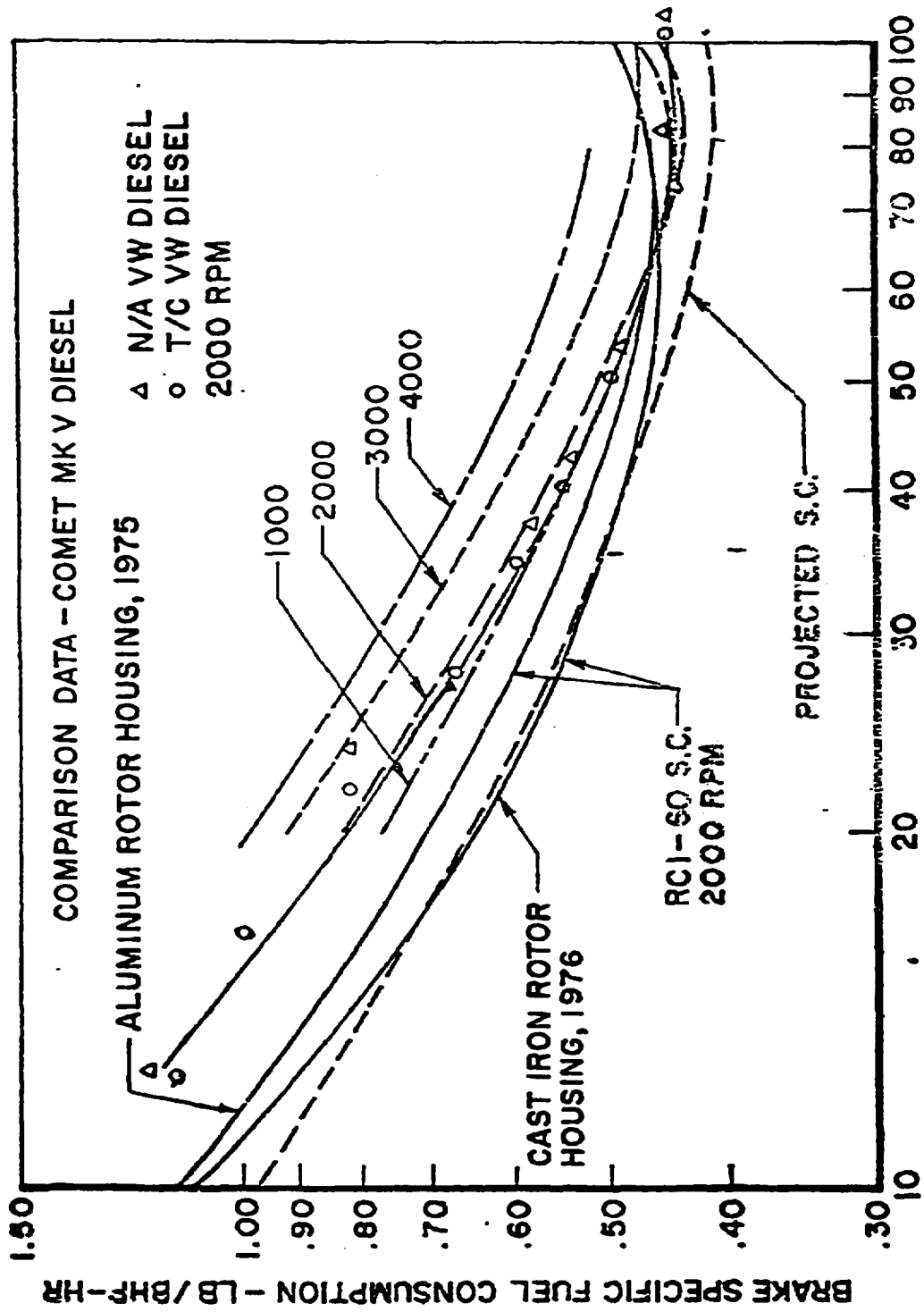
COMPARISON DATA – COMET MK V DIESEL
ALUMINUM ROTOR HOUSING, 1975
Δ N/A VW DIESEL
o T/C VW DIESEL
2000 RPM
1000
2000
3000
4000
CAST IRON ROTOR HOUSING, 1976
RCI-60 S.C. 2000 RPM
PROJECTED S.C.
BRAKE SPECIFIC FUEL CONSUMPTION – LB/BHP-HR
BRAKE MEAN EFFECTIVE PRESSURE-PSI
1.50
1.00
.90
.80
.70
.60
.50
.40
.30
10
20
30
40
50
60
70
80
90
100

Figure 5-3

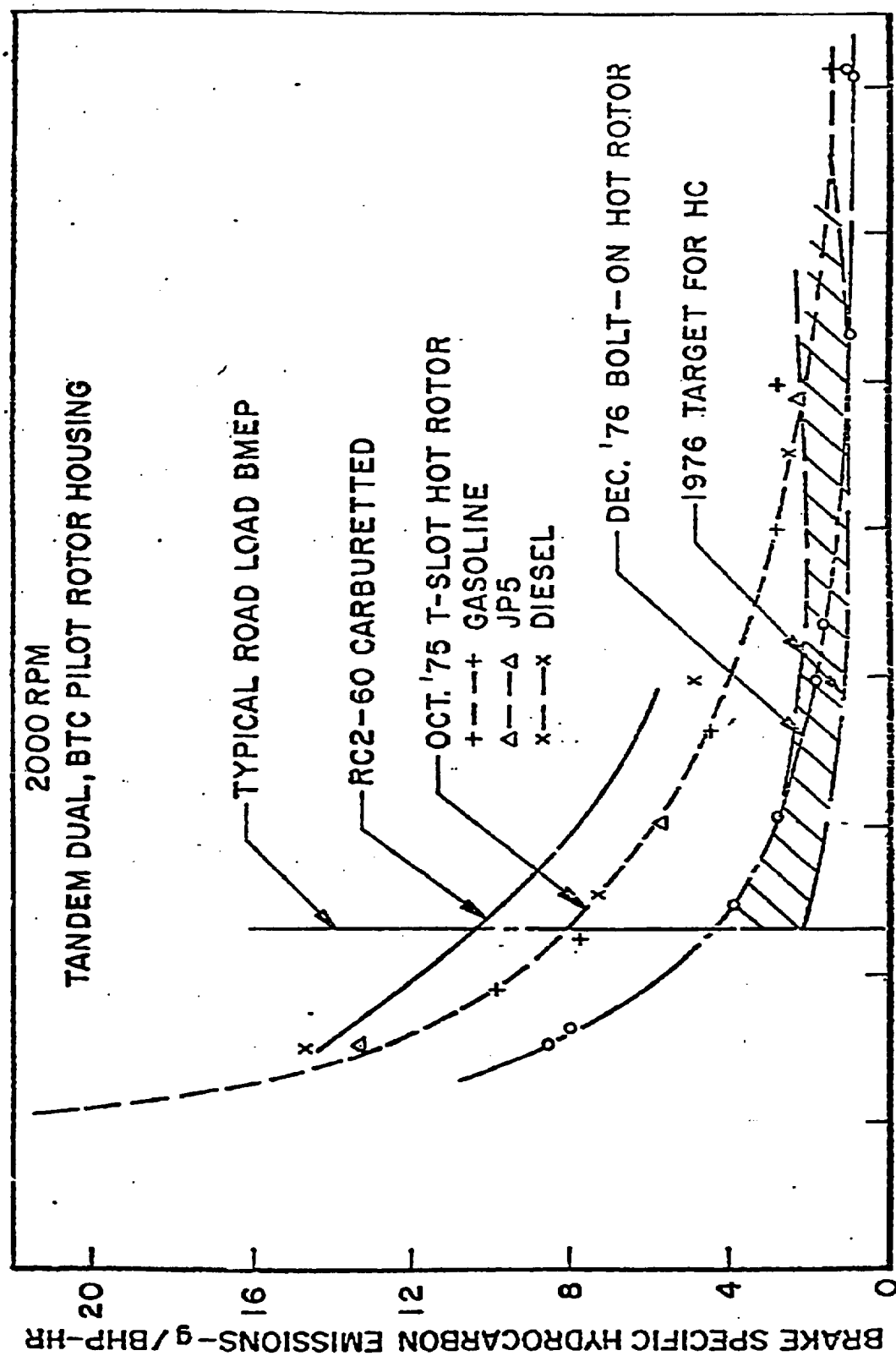
2000 RPM
TANDEM DUAL, BTC PILOT ROTOR HOUSING
TYPICAL ROAD LOAD BMEP
RC2-60 CARBURETTED
OCT. '75 T-SLOT HOT ROTOR
+—+ GASOLINE
Δ—Δ JP5
x—x DIESEL
DEC. '76 BOLT-ON HOT ROTOR
1976 TARGET FOR HC
BRAKE SPECIFIC HYDROCARBON EMISSIONS-g/BHP-HR
BMEP-PSI
0
4
8
12
16
20
10
20
30
40
50
60
70
80

Figure 5-4

The ability noted earlier to burn a broad base of fuels is another benefit derived from the use of the direct injected stratified charge combustion process employed by Texaco in their reciprocating engine design and by Curtiss-Wright in their rotary engine design. This multi-fuel capability is achieved by combining spark ignition with the fuel injection rate closely matched to the combustion rate, a process which obviates the need for a specific cetane or octane rating. The engine's insensitivity to octane or cetane requirements would, therefore, permit use of existing fuels ranging from gasoline to diesel; but, more importantly, refinery output could be optimized to produce a middle distillate fuel which obtained the maximum heat energy from a barrel of crude oil.

The heat engine in the hybrid system will be continuously subjected to brief periods of acceleration/deceleration cycles to supplement electric system power output as required to maintain performance requirements. The rotary's low rotating moment of inertia minimizes time delays and reduces power transmission shaft loading during the heat engine assisted portions of the acceleration/deceleration cycle.

Again, the unique characteristics of the rotary make possible the use of a single rotor system, namely, dynamic balance over the entire operating range with a torque output curve of comparable smoothness to a 4-cylinder reciprocating engine.

Heat engine costs are minimized by the use of a single rotor configuration, which means that costs are low for the basic engine as well as the fuel injection system, which required only two injectors instead of the four required by a four cylinder diesel. The cost increment of the injection system over a carbureted engine is minimized by this factor as well as by the use of state-of-the-art diesel fuel injection equipment.

Engine Description

1. Basic Engine

The heat engine for the hybrid vehicle is a one rotor stratified charge rotary combustion engine with a cell swept volume of 72 cubic inches. The arrangement of the rotor, housing, injectors and spark plug is shown on the sectional drawing, Figure 5-5.

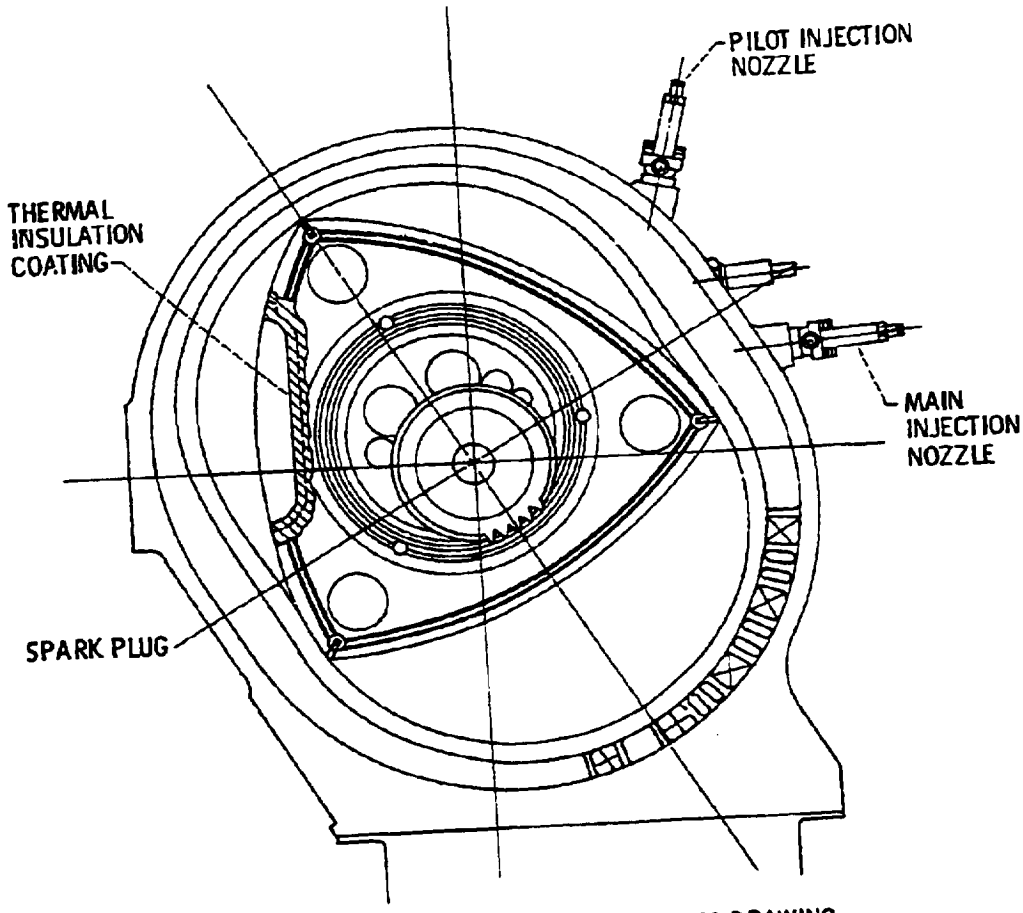

FIGURE 5-5. - HEAT ENGINE SECTIONAL DRAWING.

The single rotor is supported by a short crankshaft mounted on two bearings. Counterweights are provided at each end of the crankshaft to balance the rotating assembly. The drive end counterweight is incorporated in the flywheel by removing material at the appropriate location.

The rotor is case of nodular iron. It is equipped with various seals, a bearing, and internal ribbing to provide for strength and for oil cooling. The rotor flank surfaces, and combustion pockets are coated with insulating material. The consequent high surface temperatures are conducive to reduced emissions and reduced heat transfer to the lubrication system.

At the accessory end, drives are provided for the coolant, oil, and fuel injection pumps. The first two are toothed belt driven, and the fuel injection pump is driven directly from the counterweight by means of a slotted disc coupling and an automatic timing device. Injector fuel delivery is controlled by positioning a rack, discussed under "Auxiliaries".

Coolant circulation is provided with a centrifugal pump, and temperature is controlled with a full flow bypass type of thermostat. An air-to-coolant heat exchanger is required. An electrically operated fan controlled by a coolant temperature switch is used to augment air flow through the heat exchanger. Consequently, no engine driven fan has been provided. Curves of heat rejection to the coolant and oil are given in Figures 5-6 and 5-7. Oil circulation is produced with a gear pump from the three quart sump.

A tentative flywheel size has been chosen to limit instantaneous angular acceleration of the crankshaft to an acceptable level. The consequent coefficient of speed fluctuation is 2.8 percent at 5000 RPM and 90 horsepower. A final choice of flywheel size will require consideration of the vehicle drive system. Detailed analysis of the overall vehicle drive system include the inertia contributions of the AC motor and torque convertor driving element, which are directly coupled to the engine whenever it is running. These contributions may be quite important in minimizing the inertia of the engine and its flywheel in order to provide the shortest possible start up time within the basic limits on engine angular acceleration.

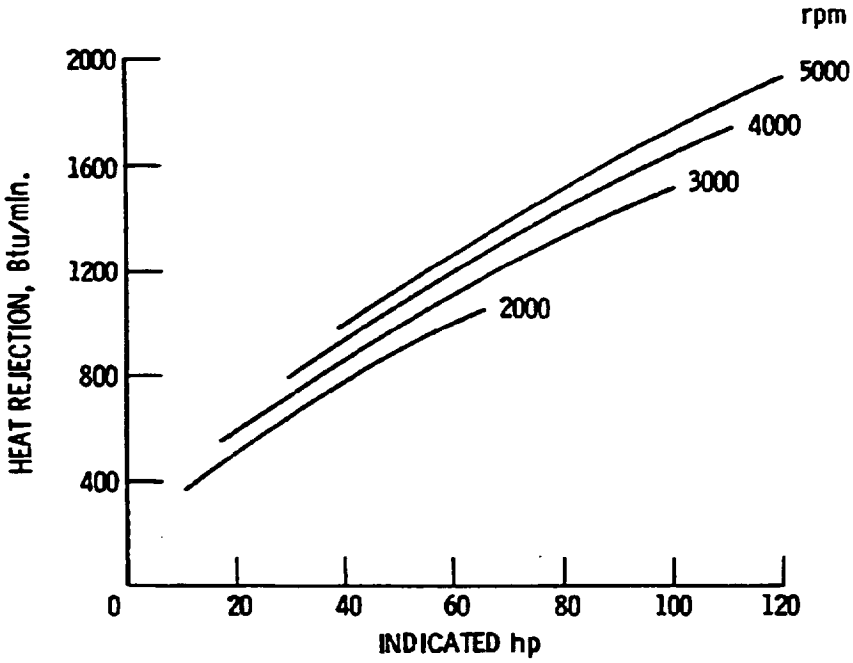

FIGURE 5-6. - RC1-72 COOLANT HEAT REJECTION; COOLANT - WATER + 44% ETHYLENE GLYCOL.

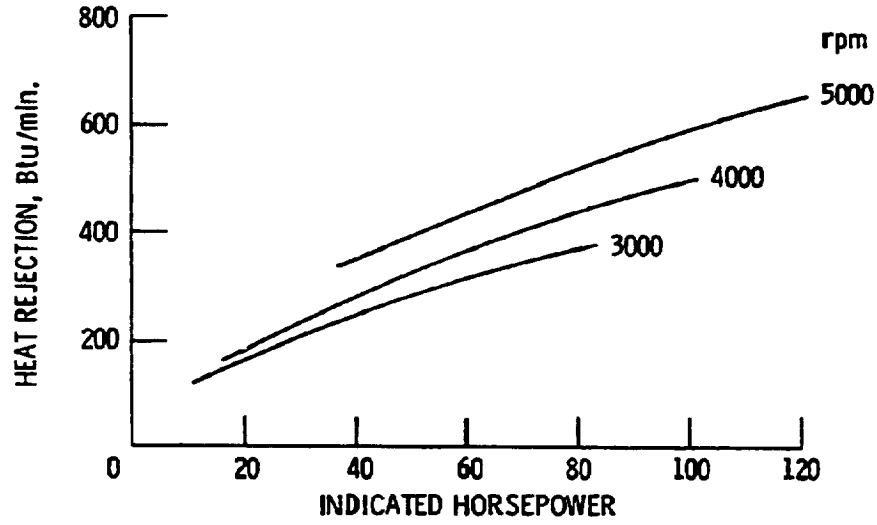

FIGURE 5-7. - RC1-72 OIL HEAT REJECTION; ROTOR COATED WITH STABILIZED ZIRCONIA .04 in. THICK.

2. Auxiliaries

The accessories required on the subject single rotor stratified charge rotary combustion engine are relatively few in number and consist of the following:

- o Oil pressure pump and pressure control
- o Oil metering pump and control
- o Coolant pump and thermostat
- o Ignition system
- o Fuel injection system

A normal (non-hybrid) installation would require the addition of an alternator, a starter motor, and engine speed governor. The following is a brief description of each of the auxiliaries to be used, with emphasis on maintainability, reliability, safety operational characteristics, and known problem areas.

Oil Pressure Pump and Pressure Control

The lubricating oil for this engine will be supplied by a positive displacement gear type pump belt driven from the engine crankshaft. A typical oil system schematic is shown in Figure 5-8 ; this system may ultimately be integrated with the transmission oil system and a cooling/heat recovery system for the AC motor/controller, as outlined in Section 5.3.5 . The system provides pressurized oil flow to lubricate the engine bearings. This flow is assured by having the proper sizing of flow components and controls such that a minimum oil pressure below a permissible maximum temperature is always maintained at the bearings. The system consists of a sump which is sized to provide adequate surface area and settling time for de-aereation to occur, thus eliminating oil foaming as a problem. A suction strainer and suction tube duct oil to the inlet of the belt driven positive displacement pump. The strainer is sized to protect the pump against foreign objects which can be accidentally dropped into the oil sump during oil level checks or refilling. The oil then is ducted to an oil cooler, bypass, and diverting type thermostatic valve arrangement which either allows full oil flow to the engine directly or diverts a portion of the vehicle mounted oil cooler as

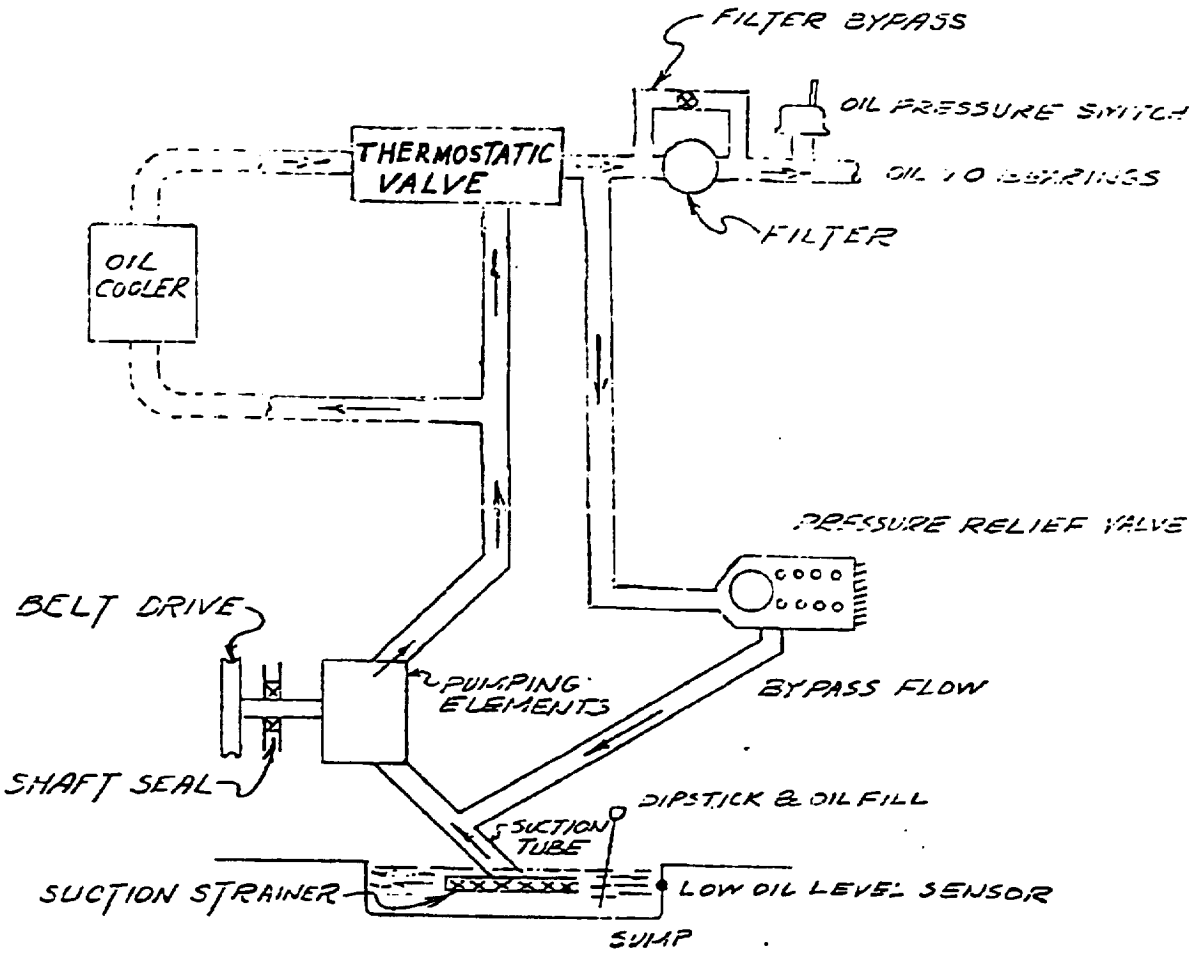

Figure 5-8

LUBRICATION - SYSTEM SCHEMATIC

necessary to limit the oil temperature to some maximum value. The oil from the cooler then rejoins the main oil flow before the pressure valve which controls the oil pressure by bypassing all excess oil flow back to the pump inlet. The oil then goes to an ordinary spin-on type full flow oil filter with integral bypass valve to prevent filter element rupture and subsequent engine contamination. The bypass would open only during operation with very cold oil or in case of gross filter plugging due to lack of proper maintenance.

Two safety systems are employed in the oil supply system. The first is the standard low oil pressure switch at the oil gallery which will illuminate a warning light on the panel if the oil pressure is below a preset minimum level; a logic signal will, of course, be needed to de-energize the warning when the heat engine is in the off mode. The second sensor is a low oil level switch to remind the operator to add oil.

The maintenance of this system requires that the oil filter be changed after a pre-set number of engine operating hours and that a certain minimum oil level be maintained. The latter will be taken care of by providing the oil level switch and dipstick for manual check and the provision of a normal type oil fill location and opening. The filter change presents a problem in that the operator will not know how many hours or miles the heat engine has operated; therefore, the vehicle control computer should be programmed to keep track of the heat engine accumulated operating time to permit periodic filter changes.

Oil Metering Pump and Control

The rotary engines require that a small quantity of lubricating oil be introduced into the combustion chamber to lubricate the apex seals. The approach used on this engine design is to meter the oil to a spray bar located in the intake manifold and mix the oil with the inducted air. This method is well proven and does an excellent job of lubricating. The system consists of a variable displacement pump (or shuttle valve which receives oil from the pressure pump) whose displacement is controlled by a linkage connected to the fuel injection pump rack such that on a per revolution basis, a given percentage of the fuel flow is metered

and provided to the spray bar in the intake. A simple flow switch is included in the line from the pump to provide an electrical means of monitoring whether the system is functioning.

Coolant Pump and Thermostat

The cooling system for this engine is of the same type as all other gasoline or diesel engine of rotary or piston type and should not present any problems or unique maintenance considerations. There is, of course, a possibility that a certain minimum coolant temperature will have to be maintained constantly either for vehicle space heating or to protect the engine so that the intermittent operation is not destructive to the engine. The need for preheating will have to be determined during the cyclic engine test program. A schematic is shown in Figure 5- 9.

Ignition System

The ignition system for this engine consists of a trigger or timing signal, an ignition module to generate the required voltage and current, and a spark plug. The system is kept as simple and reliable as possible while maintaining a very high performance level. The trigger signal is generated by a solid state device located in the fuel injection pump such that it can use the variable timing mechanism of the pump to time the spark to the engine and provide the proper relationship between pilot injection and ignition. This means that the ignition is timed integrally with the fuel pump and is pre-set at manufacturing and is not adjustable. The ignition module is a "black box" which receives power from the vehicle and the trigger signal, and produces an output which is proper to drive the spark plug and reliably fire the mixture. This output is of relatively long duration and has the capability of multiple re-lighting of the mixture if necessary to eliminate misfiring. The spark plug is of standard automotive type and cost, and will have to be replaced at a pre-set number of operating hours with an indication of the accumulated operating time provided by the vehicle computer as described above for the oil filter. The ignition system design, being similar to that in use on all automobiles today, is considered to be of proven safety and reliability. Repair of this type of system is not

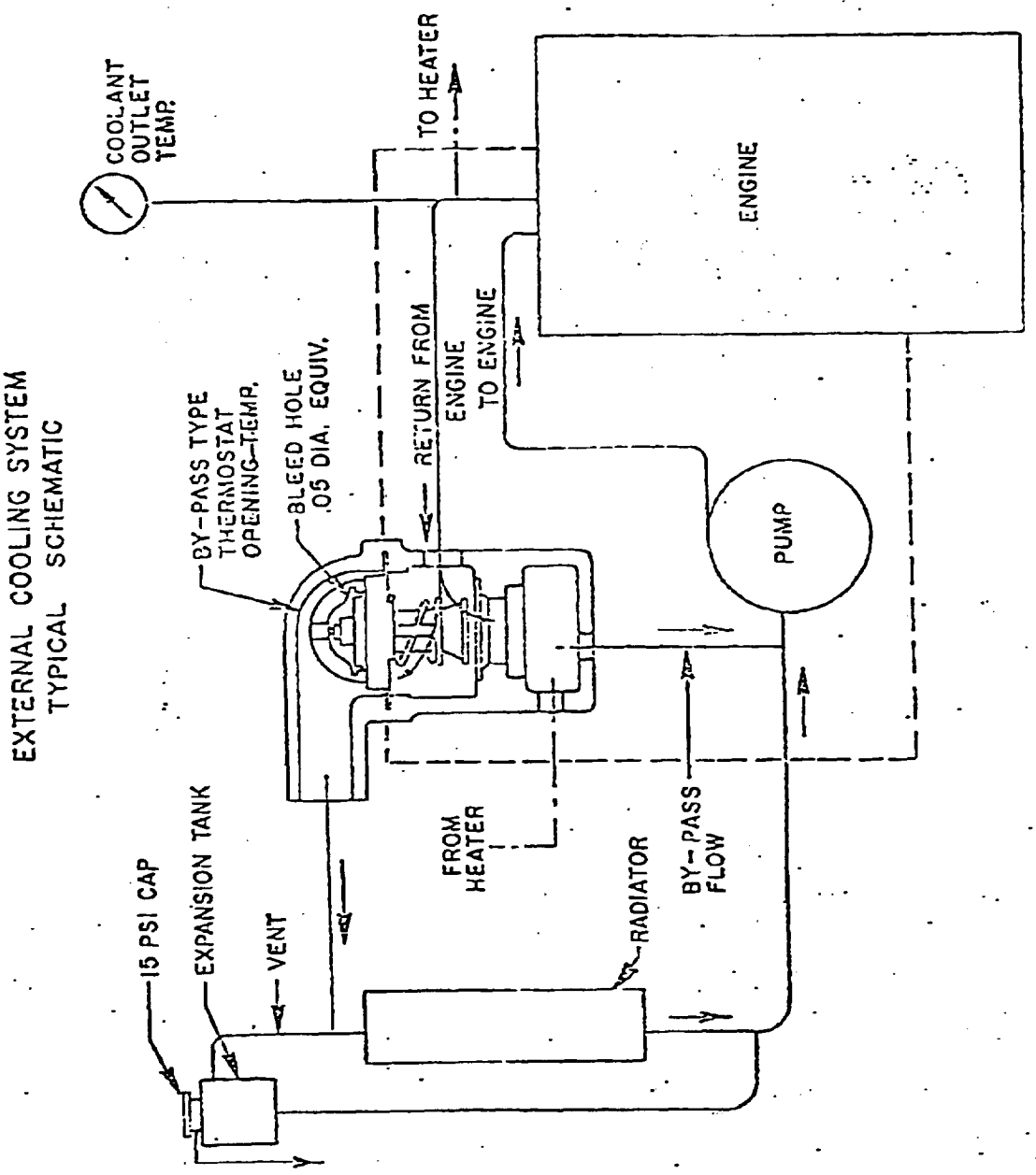
EXTERNAL COOLING SYSTEM
TYPICAL SCHEMATIC
COOLANT OUTLET TEMP.
TO HEATER
ENGINE
RETURN FROM ENGINE
TO ENGINE
BY-PASS TYPE THERMOSTAT OPENING-TEMP.
BLEED HOLE .05 DIA. EQUIV.
PUMP
FROM HEATER
RADIATOR
BY-PASS FLOW
15 PSI CAP
EXPANSION TANK
VENT

Figure 5-9

something that the average mechanic can do. Instead, he will have to have a single tester to determine whether the trigger module, ignition control module, high tension lead or spark plug is the problem, and simply replace the faulty item. It is, of course, possible to program the on-board computer to diagnose the system; and it is possible to build a fully redundant system. These items will have to be addressed in the final design of the vehicle once all inputs are fully analyzed.

Fuel Injection System and Controls

The fuel injection system consists of a two cylinder, in-line type Diesel fuel injection pump driven by the engine crankshaft through a centrifugal type variable timing device. Fuel is drawn from the tank by a piston type pump integral with the fuel pump and passed through a fuel filter before entering the injection pump gallery. This low pressure fuel is vented thru the pump by a relief valve set at about 55 psi and recirculated back to the tank as per standard diesel practice. The two fuel injection pump plungers are of different sizes with the smaller being for the pilot fuel. Preliminary analysis of the RCI-72 indicates that an injection system is required which will deliver 10 mm^3/stroke from the pilot plunger and 85 mm^3/stroke from the main plunger. The quantity of fuel injected is controlled by a rack in the pump which varies the displacement of the pumping elements. The motion of the rack has a different effect on the two pump elements in that it is basically only an on-off control for the pilot pump with the pilot flow reduced to zero when the rack is in the cut-off position. The control of the main flow is linearly increased as the rack is moved from the cut-off towards the maximum fuel position. It is presently planned that the rack will be controlled by the vehicle control computer thru a servo-actuator to control the instantaneous fuel flow to govern the speed of the engine/vehicle, to limit the maximum fuel flow at all engine speeds, to limit the maximum torque at all speeds, and to limit the exhaust smoke and emissions.

The only maintenance required will be for periodic fuel filter changes, probably tied in with oil filter changing. Troubleshooting will be done with ordinary Diesel diagnostics equipment including a set of clamp-on injection line pressure transducers and either a diagnostic computer or an oscilloscope and a set of pattern analysis pictures. The primary

mode of failure will be injector failure due to a variety of sources such as fuel contamination and will require injector replacement. The ease of operating this engine and its safety aspects will be governed by how well the control system is implemented as the engine will have no control of its own. It is recommended that a separate overspeed control capable of fully overriding the primary control of the fuel pump rack be implemented to provide for the safe control of an engine overspeed due to primary control failure.

Problem Areas

There are several potential problem areas associated with this application of the rotary engine. The success of the design will depend on their proper resolution.

1. Emissions - The stratified charge rotary engine is normally an unthrottled engine and, consequently, provides an excess of air in the exhaust at part load. Therefore, exhaust temperatures are low. Although this should be beneficial for exhaust system durability, it complicates the task of reducing emissions. Exhaust treatment devices such as a catalytic converter require high temperature exhaust to be effective. It may be necessary to incorporate an inlet throttle to raise exhaust temperatures for the sake of emission control. The problem may be complicated on Mode 1 operation by the converter cool-down during engine off periods.

2. Rotor Insulation - Thermal insulation of the rotor flanks is used to reduce emissions, fuel consumption, combustion deposits and heat rejection to the oil. These highly desirable results require the use of an insulating coating on the rotor or, alternatively, a metal heat shield or both.

   Experience with ceramic coating has shown benefits but indicates that coating durability will need improvement. A metal heat shield will require extensive development to insure mechanical reliability.

3. Torsional Excitation - The torque curve for the engine is shown on Figure 5-10. It is important to note that high positive peak torques

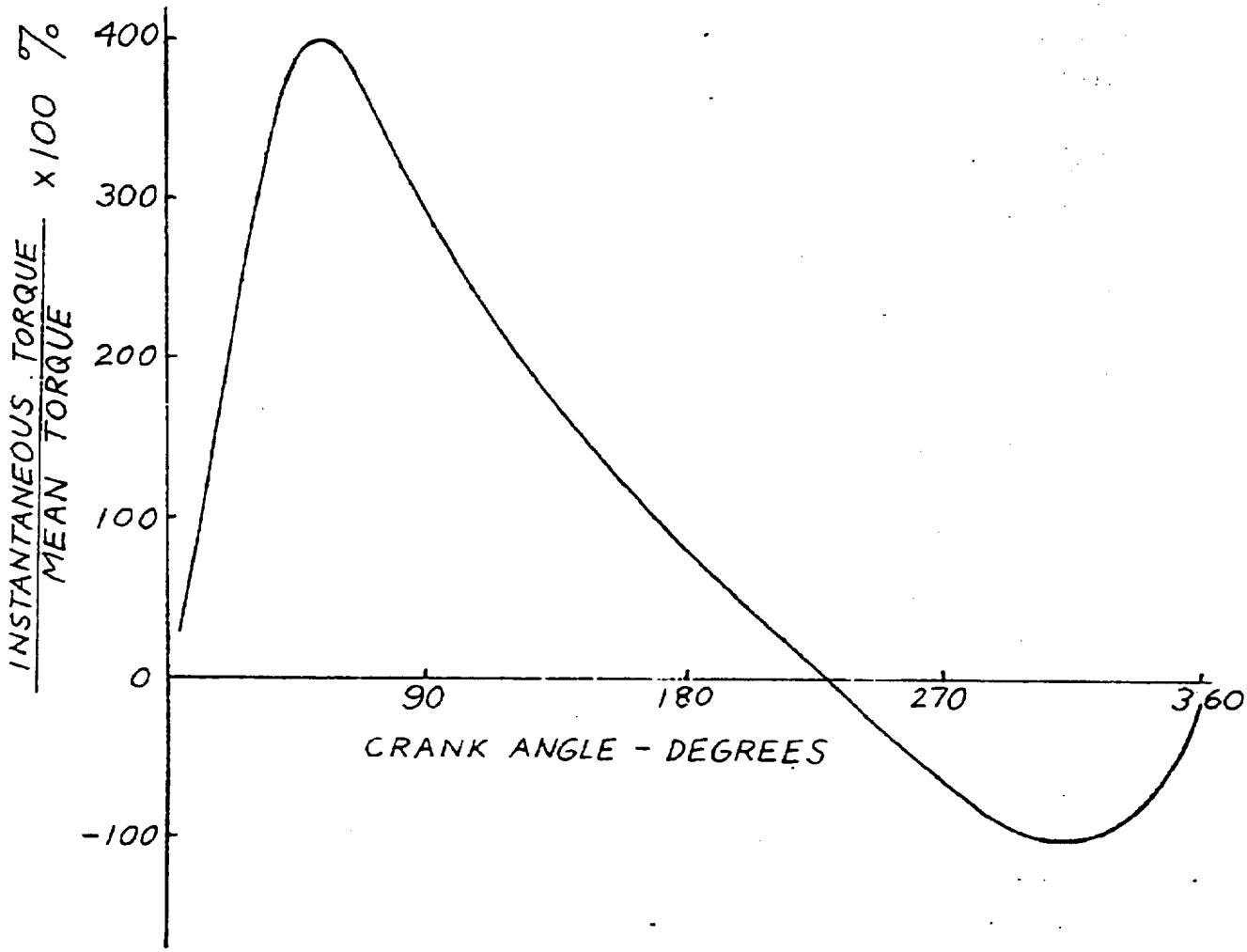

Figure 5-10 INSTANTANEOUS TORQUE AS PERCENT OF MEAN TORQUE.

and significant negative torques are produced during each revolution of the engine. Some form of torsional isolation will be required to protect the engine and the vehicle's drive train, and to insure attainment of a smooth power flow. Thorough analysis of the complete system will be necessary.

Startup Transient Analysis

In order to assess the effects of the variables involved in the engine startup process on the transient acceleration experienced by the vehicle, a dynamic analysis was performed utilizing a computer simulation developed during the Near Term Hybrid Vehicle Design Program.[1] This simulation contained the following elements:

- The vehicle was assumed to be travelling initially at a steady speed, being driven by the traction motor only, with the engine off.

- At time zero, the command is given to engage the engine clutch. The engagement of the clutch was modelled by a constant engagement rate; i.e., torque transmitted was assumed to increase linearly with time until full engagement was reached. Full engagement was defined by the engine speed becoming equal to the motor speed.

- The engine was modelled by its rotating inertia, together with a torque characteristic. This torque characteristic started at time zero at a value corresponding to the engine motoring torque. The torque was then assumed to rise to a fixed positive value, corresponding to the power command. The rise was assumed to take one engine revolution and was to begin a certain number of revolutions after time zero.

- The traction motor was modelled by a torque/speed characteristic; specifically, the torque was assumed to increase linearly with a drop off in speed.

- Torque converter, transmission, and vehicle were modelled as in the HYBRID2 program.

The effects of the following parameters were investigated in this analysis:

- o Clutch engagement rate
- o Motor torque/speed characteristic
- o Vehicle speed
- o Engine torque rise delay

Engine rotating inertia (including clutch driving plate) and motor rotating inertia (including torque converter driving element and clutch driven plate) were kept constant at .08 kg-m^2 and .19 kg-m^2 throughout the analysis. All other drive line and vehicle characteristics were as defined for the baseline hybrid system.

The results of the analysis are shown in Figures 5-11 through 5-14. Figure 5-11 shows the peak vehicle acceleration, peak clutch torque, and clutch engagement time plotted as functions of clutch engagement rate for two motor speed/torque characteristics, at a vehicle speed of 20 kph. The engine torque rise is assumed to start after one engine revolution. In one case, the motor torque was assumed to be independent of speed; and in the second case, a fairly "stiff" speed/torque characteristic with an increase of .4 N-M of torque for every RPM drop off in speed was assumed. As is evident, the results were quite insensitive to the motor speed/torque characteristic, and this variable was removed from further investigation.

Figures 5-12 and 5-13 are similar plots, but at vehicle speeds of 50 kph and 80 kph. These figures show peak vehicle accelerations very similar to those in Figure 5-11 , but with somewhat longer clutch engagement times and higher peak clutch torques.

Figure 5-14 shows the variation in clutch engagement time with the delay in engine torque rise, for a vehicle speed of 50 kph. As is evident, this time is relatively insensitive to the torque rise delay. This, in conjunction with the lack of sensitivity to the motor torque/speed characteristic, indicates that most of the impetus to bring the engine speed up to match the motor speed comes from motor, drive train, and vehicle inertia. Having the engine and motor torque increase during startup helps but does not provide the major starting impetus.

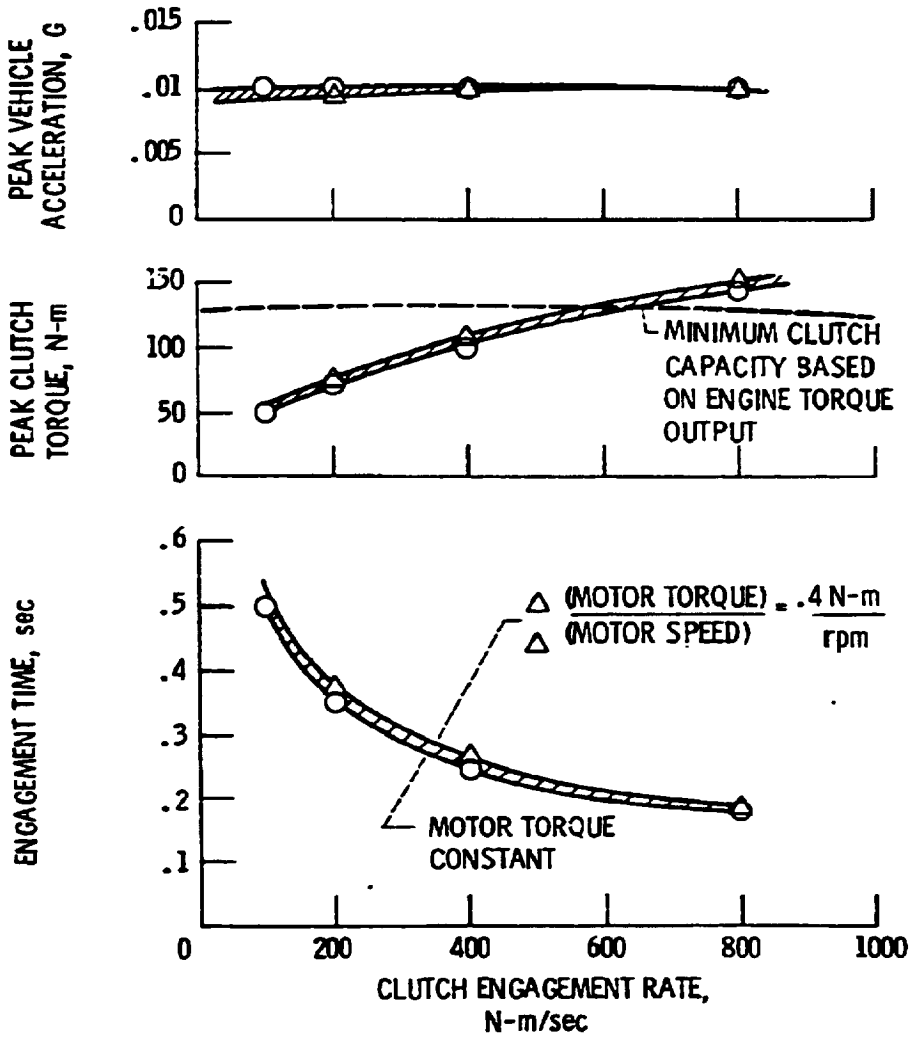

FIGURE 5-11. - STARTUP CHARACTERISTICS AT 20 kph AS A FUNCTION OF CLUTCH ENGAGEMENT RATE. ENGINE TORQUE BUILDUP STARTS AFTER ONE REVOLUTION.

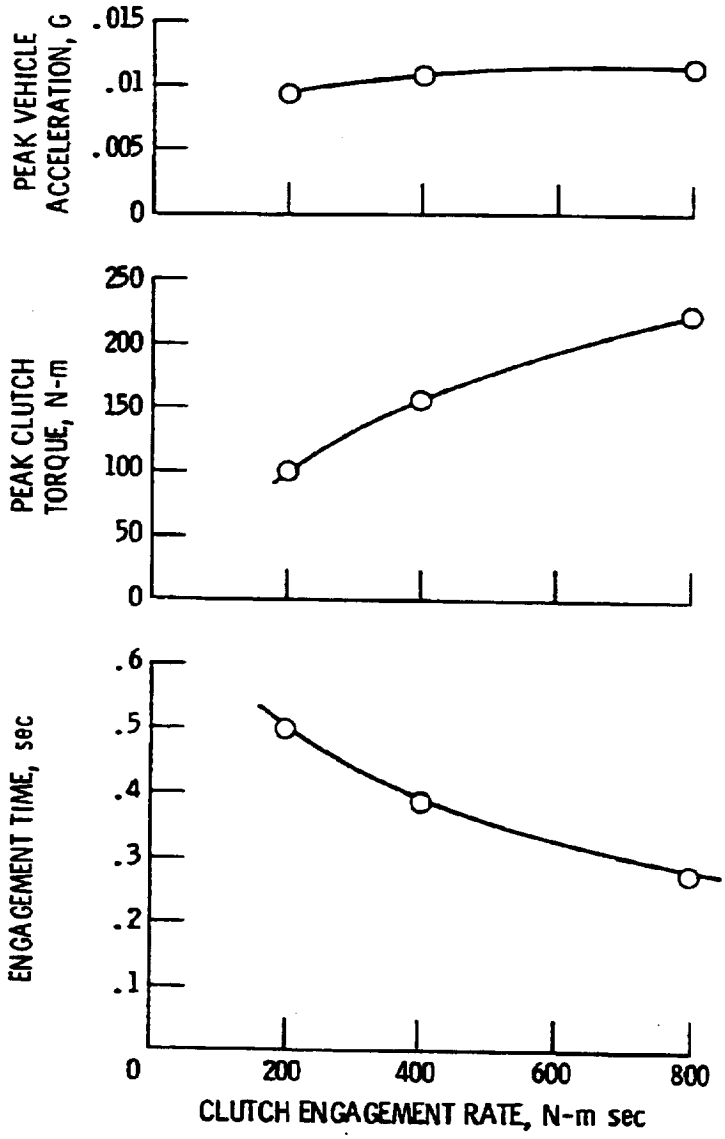

FIGURE 5-12. - STARTUP CHARACTERISTICS AT 50 kph AS A FUNCTION OF CLUTCH ENGAGEMENT RATE. ENGINE TORQUE BUILD-UP STARTS AFTER ONE REVOLUTION.

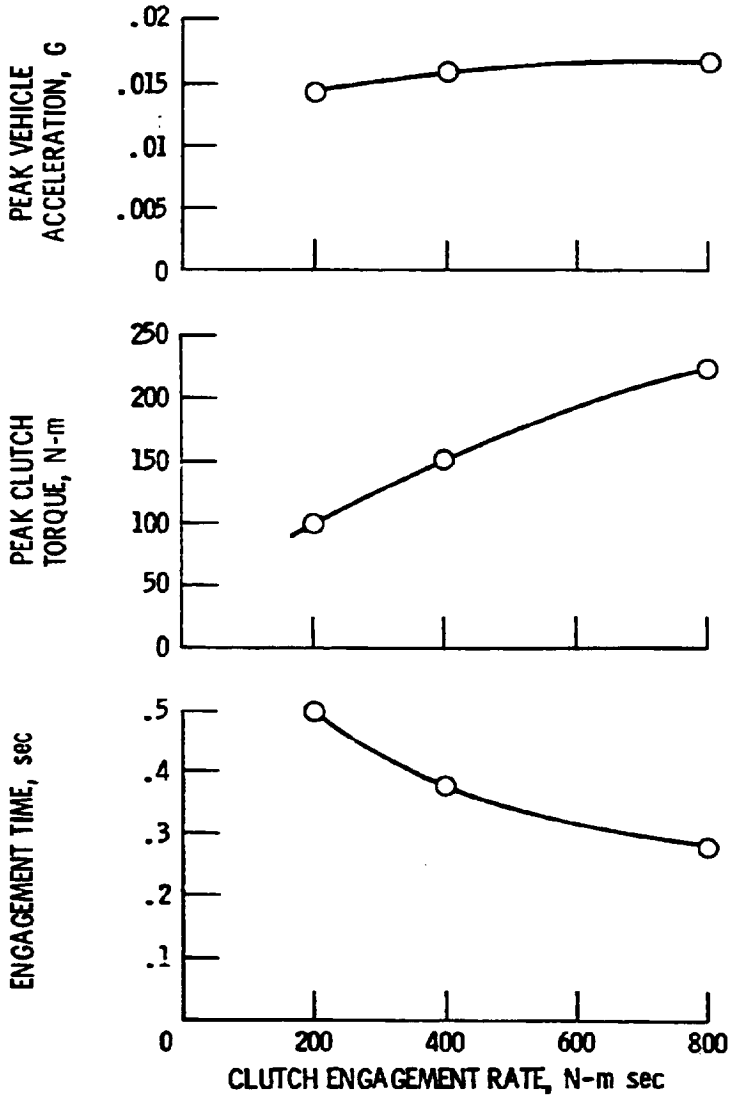

FIGURE 5-13. - STARTUP CHARACTERISTICS AT 80 kph AS A FUNCTION OF CLUTCH ENGAGEMENT RATE. ENGINE TORQUE BUILDUP STARTS AFTER ONE REVOLUTION.

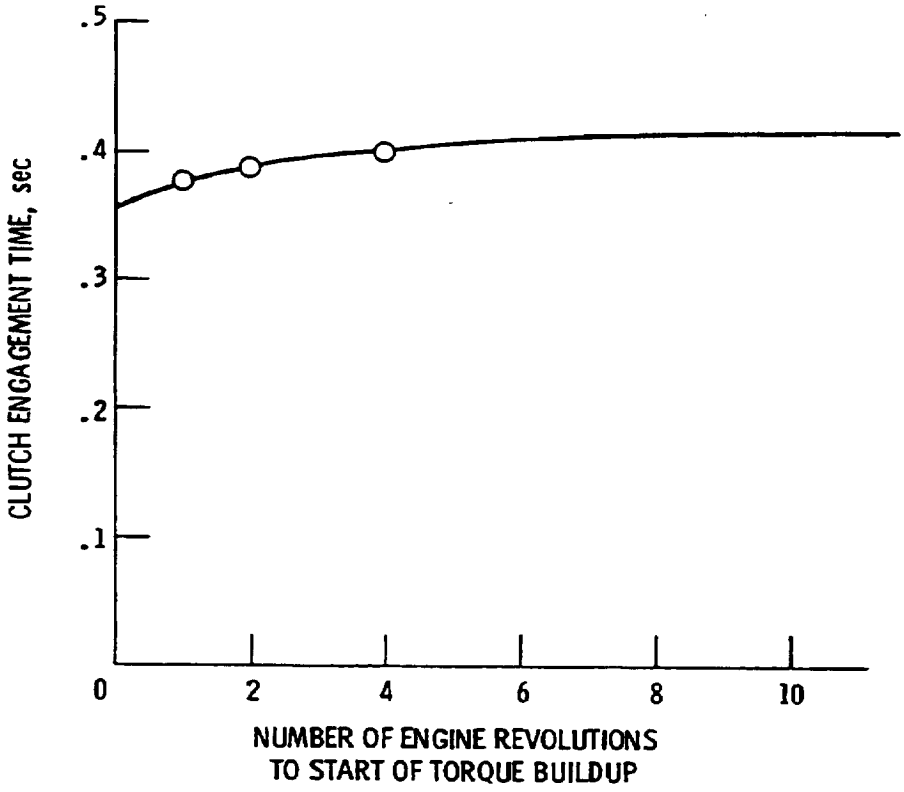

FIGURE 5-14. - VARIATION IN CLUTCH ENGAGEMENT TIME WITH ENGINE STARTUP DELAY.

Additional conclusions drawn from this study include the following:

- Pushing the clutch engagement rate beyond about 600 N-M/sec does not result in a substantial reduction in engagement time and requires clutch capacities which are considerably higher than that required to handle the peak engine output torque.

- At 600 N-M/sec, the engagement time does not exceed 1/3 second, and a clutch capacity of about 200 N-M would be required. With a small amount of flywheel on the engine, this would probably also be enough to handle the nominal peak engine output of 130 N-M. In the detail design phase, a more detailed dynamic analysis of the engine and flywheel, using the actual engine torque variation over each revolution, would, of course, be required to more accurately define the clutch and flywheel requirements.

- At higher vehicle speeds, it is probably not feasible to achieve startup times less than 1/4 second without improving unreasonably heavy requirements on the engine clutch. At low speeds, 1/5 second looks like a reasonable lower limit.

5.3.3 Motor/Controller

In this section, a description of the major AC propulsion system components is presented and those areas where detailed design effort is required are identified.

Power Semiconductor Selection

Based on the results of the design tradeoff study, transistors and thyristors (SCR's) must both be considered as candidates for the main power semiconductors in an advanced electric vehicle propulsion system. This is based on an AC controller designed to supply a maximum motor output power in the 25-30 kw range.

Selection of only one type of power semiconductor for further development is difficult since, at this power level, neither a transistor or SCR approach

has such a significant advantage over the other that the selection is obvious. In a different application, i.e., an industrial drive, the selection process may, however, be easier.

From the standpoint of commercialization, the major question is when power transistors, capable of controlling a maximum motor output power in this range, will be cost competitive with SCR's. A cost comparison between SCR and transistor AC propulsion systems is shown in Table 5-1 for the 25 kw level and indicates that transistor costs must approach the optimistic estimate given for the transistor inverter to be cost competitive with an SCR Buss commutated inverter on a first cost basis.

Controller Circuit Operation

For the conceptual design, an SCR has been selected as the main power semiconductor with the inverter configuration being a voltage source, force-commutated inverter. The approach selected uses DC-side commutation to turn off the main inverter SCR's. As discussed previously, one of the major advantages of the Buss or DC-side commutated inverter is the minimum number of power components required to control a three-phase AC motor.

Based on the information presented in the design tradeoff study, it is possible to identify approximate values for the controller components. In addition, it is possible to obtain an indication of where development effort is required.

For our example, a nominal open circuit battery voltage (EOC) of 72 volts will be used. This does not imply that this is the optimum battery voltage but is used only as an example of a controller designed to operate from a low voltage propulsion battery. If we assume that the maximum motor output power (PMAX) has been previously established as 25 kw, then using Figures 4-44 and 4-45 , we can estimate the battery power rating [PBAT(MAX)] as 37 kw. For a lead-acid battery having a specific power density of 100 w/kg, the battery parameters are shown below:

$$EOC = 72 \text{ volts} \quad (1)$$

$$RBAT = 0.028 \text{ ohms} \quad (2)$$

Table 5-1. **ADVANCED AC PROPULSION SYSTEM - COMPONENT COST COMPARISON**

(25KW PEAK/10KW STEADY-STATE)

	TRANSISTOR		SCR	
	OPTIMISTIC	CONSERVATIVE	OPTIMISTIC	CONSERVATIVE
INDUCTION MOTOR	$100	$150	$100	$150
LOW POWER CONTROL	$100	$150	$100	$150
MISC	$100	$100	$100	$100
COMMUTATION	——	——	$ 80	$100
CHARGER/ACC. PWR	$150	$200	$ 80	$100
MAIN DEVICES	$250	$500	$120	$200
TOTAL	$700	$1100	$580	$800
SYSTEM EFFICIENCY		86%		82%

The battery output power when supplying a maximum motor power of 25 kw is determined using equation 3 below, where EFF(M) is the motor efficiency and EFF(C) is the controller efficiency.

$$PBAT = PMAX/[EFF(M) \times EFF(C)] \quad (3)$$

For an average motor efficiency at this power level of 83% (over the motor speed range of 2300-4600 RPM) and a controller efficiency of 94%, the battery output power is:

$$PBAT = 32 \text{ kw} \quad (4)$$

At this power level, the minimum battery voltage (EBAT) is

$$EBAT = 56 \text{ volts} \quad (5)$$

Using equation 4, given in Section 4.4.5 of the design tradeoff study, the main inverter SCR RMS current rating is estimated to be 330 amps. A Westinghouse T627 SCR, designed to have a turn off time of five μsec. and packaged in a power module having appropriate thermal characteristics may be used.

The commutation circuit parameters are estimated based on the information presented in the design tradeoff study and are given below:

$$TREV = 7 \text{ μsec.} \quad (6)$$

$$C = 140 \text{ μF} \quad (7)$$

$$L = 1 \text{ μH}$$

The value given above for the commutation inductor may be suitable for motoring; however, it is too low to accomplish the charging function as discussed in the on-board charger section below. As discussed, the inductance must be increased from 1 μH to 5 μH; and, therefore, the inductor cost is also increased by the same factor.

The cost of the power stage components, for a maximum motor power of 25 kw and a nominal battery voltage of 72 volts is shown below:

SAux(SCRs)	$24
$Commutation capacitors	$16
$Commutation inductor	$40
Gate Drive/snubbers	$ 6
	$86

The cost of the main devices is:

$Main SCR cost (6 SCR's)	$89
$Main diode cost (6 diodes)	$44
	$133

Operation of the Buss commutated inverter, shown in Figure 4-34 in Section 4.4.5, can be described as follows. Assume that C1 is charged to 2E volts with the polarity shown and that C2 is charged to E volts with the polarity shown. Also assume that inverter SCR's numbered SCR1, SCR2 and SCR3 are conducting current. To commutate SCR1 requires that SCR7 be gated on which will place 2E volts across the commutation transformer winding T1A. This will reverse bias SCR1 and also SCR3 and allow them to regain their blocking state. The effective path to turn off SCR1 is through D4, SCR1, T1A, and the filter capacitor C3. Once SCR1 has regained its blocking capability, rectifiers D4, D6, and SCR2 provide a path for inductive load current.

Since the circuit formed by SCR7, T1A, C1 and C2 is a resonant circuit, the voltage on C1 will reverse. When the voltage on C1 reaches E volts with a polarity opposite that shown in Figure 4-34 , the voltage across winding T1B will also be E volts and in such a direction that D1 will now conduct current and return energy to the propulsion battery. This will clamp the voltage on C1 at E volts and the voltage on C2 at 2E volts with a polarity opposite that shown. The commutation circuit formed by C1, C2, T2A, and SCR8 is now ready to commutate SCR2.

As indicated in the design tradeoff study, there are various approaches to implementing a DC-side commutated inverter. The approaches described in the literature generally refer to one area as presenting special difficulty: recovery of the trapped energy circulating in the commutation circuit after a main SCR is turned off.

Trapped energy in the commutation circuit is considered to be one of the primary reasons for the limited use of DC-side commutation in industrial applications, due to the following factors:

1. Trapped energy decreases controller efficiency.
2. Commutation circuit losses are dissipated by fewer components in a DC-side commutated inverter than in a McMurray inverter. This implies that individual component temperatures will be higher.

As discussed previously, controller efficiency can be increased and, therefore, component temperatures reduced by adjusting the commutation energy as a function of load. This is particularly applicable to an electric vehicle where motor output power varies over a very wide range.

One approach to accomplishing this is illustrated in Figure 5-15. For discussion, assume a turns ratio between T1A and T1B of 1:1. This turns ratio establishes the maximum commutation capacitor voltage (2E) and the maximum stored energy in the commutation circuit. This energy must be sufficient to commutate the main SCR's when the motor is supplying the peak output power of 25 kw. Efficient operation at a motor power less than 25 kw is expected to require some form of programmed commutation energy in order to decrease the stored energy in the commutation circuit. One approach is to control the gating of the main SCR's in such a manner as to transfer energy from the commutation transformer to the motor instead of returning the energy to the propulsion battery.

The Buss commutated inverter shown in Figure 5-15 requires that commutation of the main inverter SCR's occur alternately between the top SCR's (SCR1, SCR3, and SCR5) and the bottom SCR's (SCR2, SCR4 and SCR6). The commutation interval can be considered as consisting of two phases. The first phase is the forced commutation of either the top or bottom SCR's. The second phase is the recharging of the commutation capacitors to store energy for the next commutation. The time duration of Phase I is a function of the energy stored in the commutation capacitors and the load current. The duration of Phase II is a function of the commutation inductance and capacitance. For a successful recharge of the commutation capacitors to occur, gating of the main SCR's in the Buss being commutated must be inhibited for a minimum period of time. This time interval starts with the gating of the appropriate commutation SCR and ends when the commutation capacitors have been charged to their desired value. When the commutation capacitors have been charged to their desired value, the main SCR's, in the Buss which has been commutated, can be gated which places the load across

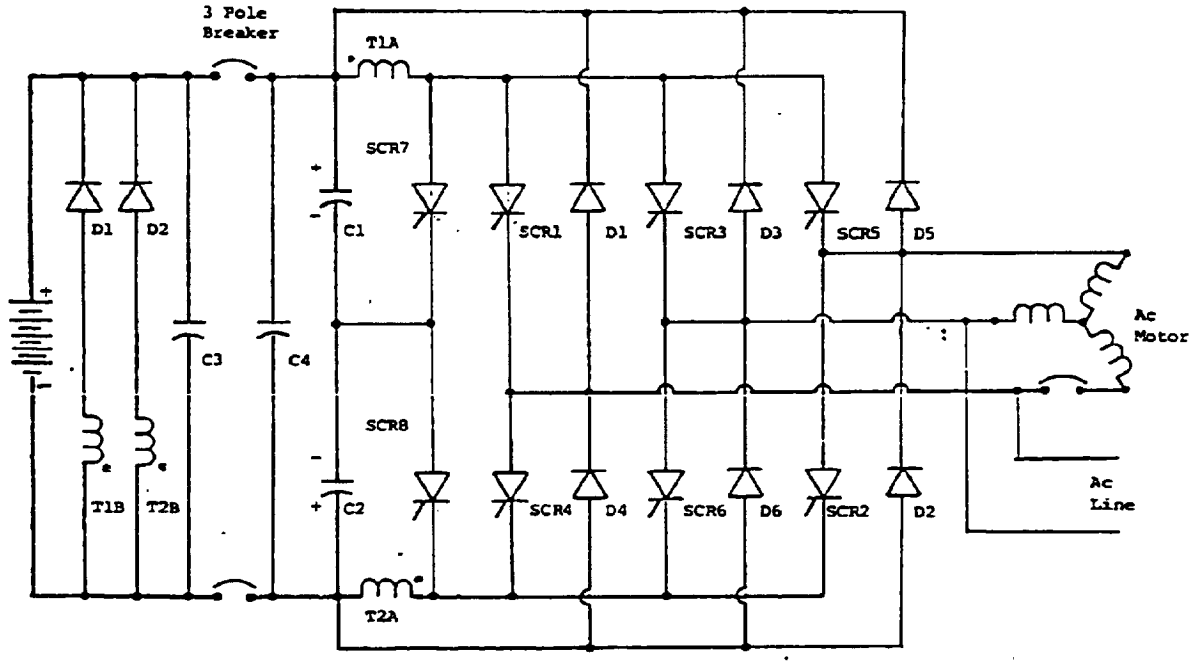

Figure 5-15. INTEGRATED SCR CONTROLLER/CHARGER

the resonating LC commutation circuit via the main SCR devices and, thus, diverts the energy in the commutation transformer to the load.

Integrated Controller/Charger/Accessory Power Supply

In an advanced AC propulsion system, integration of the on-board charger and accessory power supply with the controller is expected to provide significant advantages in terms of reducing cost, weight and volume. Integration is also expected to present conflicting requirements which must be addressed during the actual hardware design. For example, if motoring was the only function to be accomplished with the power circuit shown in Figure 5-15, then the commutation inductors could potentially be constructed in an air-core configuration. However, if we also want to use these inductors as transformers during charging, by the addition of windings T1B and T2B, then to obtain good coupling, a magnetic core material such as powdered iron or a metallic glass may be required. Identifying the tradeoffs to be made between these different functions is considered one of the major development areas to be addressed during the hardware design.

As one example, assume that the capacitor C1 is charged to 260 volts based on a peak AC line voltage of 170 volts and a battery voltage of 90 volts (2.50 volts/cell and 36 lead-acid cells). At this capacitor voltage, the peak current in winding T1A, based on an inductance of 1 μH, will be approximately 3000 amps and would exceed the current rating of SCR7. To reduce the peak current in the commutation SCR, the inductance of winding T1A must be increased to approximately 5 μH.

Each time SCR7 (and SCR8) is gated on, a percentage of the energy stored in capacitors C1 and C2 is transferred to the propulsion battery. This percentage is approximated as:

$$\text{Energy (Charge)} = 0.5 \times C \times V^2 \times 0.5 \qquad (9)$$

where C is the total capacitance (C1 + C2) given by equation 19 of Section 4.4.5, and V is the initial capacitor voltage. For a capacitor value of 140 μF and an initial capacitor voltage of 260 volts, the energy transferred to the propulsion battery is 2.37 watt-seconds each time SCR7 or SCR8 is gated on. If SCR7 and SCR8 are cycled at a combined frequency of 1000 Hz, then the total power transferred to the propulsion battery is 2370 watts. For a commutation circuit loss factor of

10%, the total commutation losses are 473 watts and the charger efficiency is approximately 83%.

On-Board Charger Operation

One approach to providing an on-board charger can be illustrated using Figure 5-15. For single phase operation AC line power is applied to two phases of the inverter. Rectifiers D1, D3, D4, and D6 are used in a full bridge configuration to convert the AC line voltage to a rectified DC which appears across the filter capacitor C4. Capacitor C4 is considered to be part of the main capacitor bank used during motoring, and which has been separated into two separate units (C3 and C4) by the P/LI excircuit breaker. By cycling the commutation circuit, consisting of T1, T2, C1, C2, SCR7 and SCR8, in a manner similar to that used during motoring, energy can be transferred from the commutation circuit to the propulsion battery via transformer windings T1B, T2B, and rectifiers D7 and D8.

The major development areas considered important to the success of this charging approach are:

1. Optimizing transformer efficiency by exploring new methods of using conventional and/or new magnetic materials (i.e., metallic glass).

2. Identifying techniques to minimize line harmonics and maximize the AC line power factor.

3. Development of a circuit breaker capable of protecting the main SCR's during motoring.

Although not critical to operation of the charger, a circuit breaker does provide a positive means of disconnecting the propulsion battery and eliminates the inconvenience and potential safety hazards encountered in replacing a semiconductor fuse.

Accessory Power Supply Operation

One possible approach to an integrated 12 volt accessory power supply is illustrated in Figures 4-54 and 4-55 in Section 4.4.5. When SCR7 in the commutation circuit is gated on, the voltage across the transformer winding T1A is in

such a direction that the voltage at the dot is positive. In the accessory power circuit, this means that SCR9 is reversed biased and cannot conduct. When the voltage across winding T1A reverses, the voltage across winding T1C in the accessory power circuit will also reverse. If SCR9 is gated on after the commutation process has been completed and the commutation capacitor has been charged to the desired value, then the energy stored in the transformer T1, which would normally be returned to either the load or the propulsion battery, can now be used to supply the 12 volt accessories.

In a similar manner, T2C can also supply energy to the 12 volt accessories when SCR8 is gated on. This does not interfere with the commutation process since the commutation capacitors C1 and C2 can still be charged to the desired level since only the excess energy which is trapped in the commutation circuit is used. The advantages of this approach are the relatively few components needed to provide the 12 volt accessory supply, the size of the accessory battery can be reduced and isolation between the propulsion battery and the accessory battery is provided by the transformer.

AC Induction Motor

AC motor development for an advanced hybrid electric vehicle is envisioned as addressing three major areas: First, improvement of motor efficiency; second, elimination or simplification of the shaft mounted tachometer; third, development of an integral motor/controller package.

1. Efficiency Improvement

Improvements in motor efficiency must address both the overall motor design and its interaction with the controller. This includes not only the use of better core materials, the use of copper rotor bars and improvements in the stator copper utilization, but also an evaluation of how to optimize the stator winding configuration for operation on the particular excitation waveform supplied by the controller. With regard to this last area for improving motor efficiency, the idea is to improve the motor air-gap flux waveform by careful design of the stator winding arrangement in order to improve system efficiency. This could potentially allow a 6-step waveform to provide a motor efficiency comparable to that developed from a PWM inverter.

Conventional AC induction motors are designed to operate from a sinusoidal three-phase AC source. An AC induction motor, designed specifically for an advanced hybrid electric vehicle, need not, however, be restricted to three phases. Based on the limited amount of work described in the literature,[28-30] it has been shown that increasing the number of motor phases can increase motor efficiency, reduce the amplitude of the torque pulsations and potentially increase the overall system reliability. The division of the total inverter rating into a greater number of phases reduces the required current rating of the individual semiconductors. Increasing the number of phases with the Buss commutated inverter does not increase the number of commutation components; however, it does increase the commutation frequency which will have an affect on the controller efficiency.

All the areas available for improving motor efficiency must be considered with respect to their effect on manufacturing cost. For example, the use of copper rotor bars presents special difficulties in motor manufacture which must be included in the hardware design process.

2. Tachometer Simplification

Precise control of the magnitude and direction of motor shaft torque requires knowledge of the instantaneous value of the motor's slip frequency. By definition, slip is a direct indication of the discrepancy between the inverter output frequency, which determined the speed of the rotating field in the motor, and the actual shaft speed.

The conventional approach is to use a speed transducer coupled to the motor shaft; however, the presence of this transducer spoils the characteristics of ruggedness and mechanical simplicity normally associated with an AC induction motor. This method also requires the use of a rather precise tachometer, since even small relative errors between the two terms of the subtraction greatly affects the difference.

The drawbacks of a tachometer coupled to the motor shaft will, in all probability, be eliminated or greatly reduced in an advanced AC propulsion system. Several techniques to accomplish this are under development, with one technique[31] being to obtain information on the slip

level by signal processing techniques applied to the instantaneous values of the stator voltage and current. In this case, the slip sensor is envisioned as part of the low power control.

3. Integral Motor/Controller Package

Controlling the temperature of the heat engine lubricant was considered by Curtiss-Wright to be an important step in achieving reliable and efficient on/off operation of the heat engine.

One technique for controlling the lubricant temperature at low ambient temperatures is to use the losses generated by the motor and controller to heat the engine lubricant. This system will be discussed further in Section 5.3.5. To limit the maximum lubricant temperature under high ambient conditions, a heat exchanger was envisioned. Estimates made by South Coast Technology indicate that the maximum lubricant temperature at the heat exchanger outlet could be maintained below 65-70°C.

Thyristors are normally rated for operation at a maximum junction temperature of 125 to 140°C. This temperature rating makes it feasible to consider using the engine lubricant to cool both the motor and the main power semiconductors. One approach is to mount the SCR's directly to the aluminum frame of the motor, thereby minimizing system weight and removing the controller from inside the vehicle.

One problem in mounting conventional stud or hockey puck devices directly to the motor frame is maintaining the required isolation between devices. To eliminate this problem, an isolated power hybrid module is envisioned as being an attractive alternative. This approach does allow easy device assembly and replacement, and eliminates the problems associated with isolating the motor frame from each semiconductor.

For such a package, the SCR junction to plate thermal resistance is 0.12°C/W, the estimated interface thermal resistance is 0.08°C/W, and assuming an individual SCR power dissipation of 75 watts under steady

state conditions, the junction temperature rise above the motor frame is 15°C. For a junction temperature of 125°C, the maximum allowable temperature rise of the motor frame above the engine lubricant temperature is 40° to 45°C. Depending on the oil flow rate and the placement of the oil around the motor frame, this temperature rise is considered attainable.

In the hybrid vehicle configuration under study, the motor is to be mounted in line with the transmission. To accomplish this requires a special motor frame design to meet the overall length requirements. The estimated motor dimensions, based on discussions with Gould's electric motor division, are an overall length of 11 inches and an outside diameter of 15 inches for a motor having a standard 60 Hz rating of 10 HP at 1800 RPM.

5.3.4 Transmission

The conceptual design retains the 4-speed automatic transmission with torque converter used in the baseline systems, based on the tradeoffs discussed in Section 4.4.4 . This would provide the best starting point for development in terms of permitting the development effort to be concentrated in the most critical areas, namely, on-off control of the heat engine and the associated emission control strategy, optimization of the overall control strategy, and driveability. It may ultimately be feasible and desirable to utilize a transmission such as the Ford FIOD which has split torque paths in the higher gears to minimize torque converter losses. The feasibility of such a unit will ultimately depend more on driveability characteristics, in particular, the harshness of the engine on-off and off-on transients, than on efficiency considerations. The mechanical torque paths in the higher gears would, of course, tend to increase this harshness relative to a transmission in which all torque is transmitted through the torque converter.

5.3.5 Lubrication and Cooling Systems

One of the problems in the design of a hybrid propulsion system in which the heat engine is operated only intermittently involves temperature maintenance and regulation of the heat engine. One approach to this problem is to use

conventional cooling and lubrication systems for the heat engine which are independent of the other lubrication/cooling systems required for the other propulsion system components. An alternative is to use a single fluid to perform the following functions:

- Lubricate the heat engine.
- Maintain the temperature of the heat engine within certain limits; i.e., during periods of high load on the heat engine, it would meet a portion of the heat engine's cooling requirements, just as the oil in a conventional engine does; and, during periods when the heat engine is off, it keeps its temperature from dropping too low.
- Cool the motor and controller.
- Cool and lubricate the transmission, and provide a source of hydraulic power for the transmission, just as a conventional transmission fluid does.
- (Possibly) provide a source of hydraulic power for the power steering system.

A schematic of such an integrated cooling/lubrication system is shown in Figure 5-16. Note that the heat engine will still require an independent, conventional cooling system. The underlying idea behind the system shown in Figure 5-16 is to utilize the waste heat from the traction motor and transmission to maintain an elevated heat engine temperature during the periods of time when its duty cycle is very light. It is felt that such a system would go a long way toward reducing the startup, driveability, and emissions problems associated with an on-off engine operation, as well as improving engine life by reducing the amount of thermal cycling it has to go through. Other potential benefits include a reduction in package size of the motor controller by using liquid rather than air cooling, and more rapid warm up of the heat engine and transmission from a cold start.

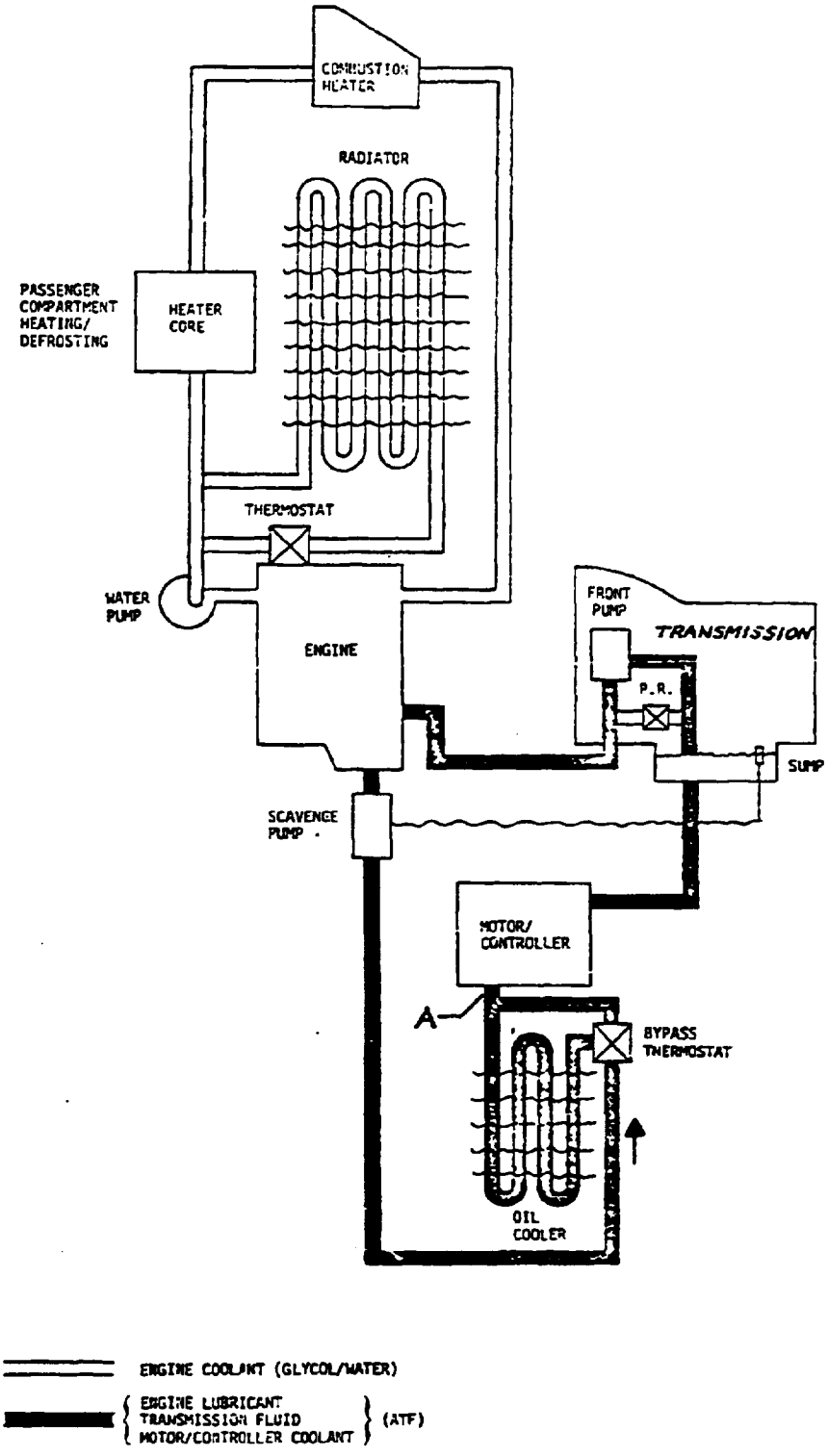

Figure 5-16 INTEGRATED COOLING / LUBRICATION SYSTEM

The fluid used in the system would be a variety of automatic transmission fluid. In particular, the formulation DEXRON-II has been found to be suitable for use as a lubricant in rotary engines. As indicated in Figure 5-16 , the temperature of the inlet fluid to the controller is controlled with a bypass [illegible]. The controller components are the most critical in the entire system, since these are located at the coolest part of the circuit. To maintain [illegible] temperature not in excess of 125°C, it is estimated that the maximum fluid temperature at point A in Figure 5-16 should not exceed about 60°C (140°F). The system flow rate and heat exchanger size must be selected with this in mind. The system utilizes the transmission sump to supply both the engine oil pump and the transmission front pump. If the pressure requirements of the heat engine and transmission are compatible, these could be combined into the same pump. The engine sump is "dry" and is scavenged by a pump which feeds the heat exchanger and the motor/controller. Alternatively, a common wet sump could be used for the engine and transmission, with the sump oil being circulated through the heat exchanger and motor/controller in a separate circuit. Such a common sump might, however, be difficult to implement in an in-line heat engine/motor/transmission arrangement (Section 5.3.6).

5.3.6 System Packaging

Unlike conventional piston engines, the rotary engine is similar to an electric motor in its general conformation, in that it is roughly symmetric about the output shaft centerline. By designing the electric motor with a diameter similar to that of the rotary and a short overall length, the two units can be packaged in-line, with the heat engine engagement clutch between them, achieving a very compact power unit with a minimum of mechanical complexity. This configuration would be suitable for a conventional front engine, rear drive vehicle or, for a front wheel drive. A front drive with a longitudinal engine arrangement in which the power unit and transmission straddle the differential requires an additional gear set to transfer the drive forward to the differential. A transverse configuration is somewhat more difficult to implement with this basic power unit layout than with a piston engine because of the relatively large diameter of the rotary engine and the electric motor. This necessitates a very large offset between the transmission input shaft and the axle half-shafts in

order for the half-shafts to clear the power unit. Consequently, an intermediate gear would be required between the transmission output and the final drive gear, unlike the case of a conventional transverse drive arrangement using a piston engine, in which the final drive pinion is located right on the transmission output shaft. Table 5-2 compares the three arrangements in terms of the number of transfer gears required and the type of final drive; the systems are listed in order of increasing mechanical complexity. The first two entries in the table are probably equivalent in terms of efficiency, since the advantage of the rear drive system in not requiring the additional transfer gear is probably wiped out by the increased losses of a spiral bevel or hypoid final drive. Based on these considerations, the straightforward in-line configuration was chosen for the conceptual design.

Table 5-2. Gearing Requirements of Alternative Drive Configurations

Configuration	Type of Final Drive	Transfer Gears Required
Front engine, rear drive	Spiral bevel or hypoid	0
Transverse front engine, front drive	Helical	1
Longitudinal front engine, front drive	Spiral bevel or hypoid	2

5.4 Projected System Characteristics

The conceptual design for the advanced hybrid propulsion system differs from the baseline used in the design tradeoff studies only in the use of a higher battery discharge limit, D_{BMAX}. As discussed in Section 4.4.2 under "Control Strategy Variations," D_{BMAX} = .8 appears to be a better choice than the value of .6 used in characterizing the baseline design. Apart from making the appropriate adjustments for this parameter change, the various characteristics of the baseline system discussed earlier in this report are also applicable to the conceptual design. In particular, the acceleration and gradeability characteristics are defined by Figures 4-12 and 4-13. The energy consumption figures are as stated in Table 4-4, with the following changes to account for the change in D_{BMAX} :

- Operating range in Mode 1 to D_{BMAX} = .8 is 62.5 km on the urban cycle and 78.1 km on the highway cycle.

- Yearly average fuel consumption is 27.4 g/km and wall plug energy consumption is .221 kwh/km.

In Table 4-6, the total energy consumption and petroleum energy consumption figures for D_{BMAX} = .8 can be used for the conceptual design. The acquisition costs in Table 4-7 need no modification; however, the life cycle cost of 7.17¢/km with $2/gal. gasoline and 7¢/kwh electricity drops slightly to 7.13¢/km.

APPENDIX A - DOCUMENTATION FOR "HYBRID" COMPUTER PROGRAM

PROGRAM DESCRIPTION

HYBRID computes the fuel and energy consumption of a hybrid vehicle with a bi-modal control strategy over specified component driving cycles. Fuel and energy consumption are computed separately for the two modes of operation. The program also computes yearly average fuel and energy consumption using a composite driving cycle which varies as a function of daily travel.

The distribution of daily travel is specified as input data, as well as the weights which the component driving cycles are given in each of the composite cycles.

EQUATIONS FOR "HYBRID" COMPUTER PROGRAM

1. Required Tractive Effort

   1.1 Acceleration

$$F_{AC} = \left(M_T + \frac{I_{DL}}{R_T^2}\right) a_v \qquad (N)$$

   1.2 Rolling Resistance

$$F_R = M_T g \, (C_1 + C_2 V) \qquad (N)$$

   1.3 Aerodynamic Drag

$$F_A = C_D A \cdot 1/2 \rho V^2 \qquad (N)$$

   1.4 Net Tractive Effort

$$F_{NET} = F_A + F_R + F_{AC}$$

2. Final Drive Assembly

   2.1 $T_{DO} = F_{NET} R_T$

   2.2 $$T_{TO} = \begin{cases} T_{DO} / (\mu_D r_D) , & F_{NET} \geq 0 \\ T_{DO} \, \mu_D / r_D , & F_{NET} < 0 \end{cases} \qquad (N\text{-}M)$$

   2.3 $W_{DO} = (60/2\pi) \, v/R_T \quad (RPM)$

   2.4 $W_{TO} = W_{DO} \, r_D$

3. Transmission

   3.1 $$P_{SO} = \begin{cases} \frac{2\pi}{60,000} \, T_{TO} \, \omega_{TO} / \mu_T , & F_{NET} \geq 0 \\ \frac{2\pi}{60,000} \, T_{TO} \, \omega_{TO} \, \mu , & F_{NET} \geq 0 \end{cases} \qquad (KW)$$

4. Heat Engine/Motor/Brakes (Output)

   A. For $F_{NET} \geq 0$, $V > 0$, or $a_V > 0$

   4.1 $P_{BRK} = 0$ (Mode 1 and Mode 2)

   4.2 $P_{GO} = 0$ (Mode 1 and Mode 2)

Equations for "HYBRID" Computer Program (cont'd)

4. (cont'd)

A1. On Mode 1:

4.3
$$P_{EO} = \begin{cases} 0\ , & P_{SO} \leq P_{EOMIN} \\ P_{EOMIN}\ , & P_{EOMIN} < P_{SO} \leq P_{MMAX} + P_{EOMIN} \\ P_{SO} - P_{MMAX}\ , & P_{MMAX} + P_{EOMIN} < P_{SO} \end{cases}$$

4.4
$$P_{MO} = \begin{cases} P_{SO}\ , & P_{SO} \leq P_{EOMIN} \\ P_{SO} - P_{EOMIN}\ , & P_{EOMIN} < P_{SO} \leq P_{MMAX} + P_{EOMIN} \\ P_{MMAX}\ , & P_{MMAX} + P_{EOMIN} < P_{SO} \end{cases}$$

A2. On Mode 2:

4.5
$$P_{EO} = \begin{cases} P_{SO}\ , & P_{SO} \leq P_{HEMAX} \\ P_{HEMAX}\ , & P_{SO} > P_{HEMAX} \end{cases}$$

$$P_{MO} = \begin{cases} 0\ , & P_{SO} \leq P_{HEMAX} \\ P_{SO} - P_{HEMAX}\ , & P_{SO} > P_{HEMAX} \end{cases}$$

B. For $V = a_v = 0$ (Car at Rest, Mode 1 and Mode 2):

4.7 $P_{EO} = P_{MO} = P_{GO} = P_{BRK} = 0$

C. $F_{NET} < 0$ (Deceleration, Mode 1 and Mode 2):

4.8 $P_{MO} = P_{EO} = 0$

4.9
$$P_{GO} = \begin{cases} P_{SO}\ , & P_{SO} \geq P_{MMIN} \\ P_{MMIN}\ , & P_{SO} < P_{MMIN} \end{cases}$$

4.10*
$$P_{BRK} = \begin{cases} 0\ , & P_{SO} \geq P_{MMIN} \\ P_{SO} - P_{MMIN}\ , & P_{SO} < P_{MMIN} \end{cases}$$

* This representation is a bit fictitious in that it models the brakes as being at the transmission input. However, this is of no significance as far as the propulsion system computations are concerned.

Equations for "HYBRID" Computer Program (cont'd)

5. Heat Engine Input (Fuel, Modes 1 and 2)

5.1
$$F_C = \left\{ \begin{array}{l} 0\ , \quad P_{EO} = 0 \\ P_{EO} \cdot BSFC = P_{EO} \cdot f(P_{EO}), \quad P_{EO} \neq 0 \end{array} \right\} \quad (gm/hr)$$

6. Battery Output (Electrical, Modes 1 and 2)

6.1
$$P_B = \left\{ \begin{array}{ll} P_{NLD} + P_{MO}/\mu_m + P_{GO}\ \mu_G\mu_{RG} & \text{(Mode 1)} \\ P_{NLD} + P_{MO}/\mu_m + P_{GO}\ \mu_G\ \mu_{RG2} & \text{(Mode 2)} \end{array} \right.$$

7. Energy and Fuel Over the Interval (0, T) (Mode 1 and Mode 2)

7.1 Rolling Resistance

$$E_R = 10^{-3} \int_0^T P_R dt = 10^{-6} \int_0^T F_R V dt \quad (MJ)$$

7.2 Aerodynamic

$$E_A = 10^{-3} \int_0^T P_A dt = 10^{-6} \int_0^T F_A V dt \quad (MJ)$$

7.3 Final Drive

$$E_D = 10^{-3} \int_0^T /P_T - P_D/dt = 10^{-6} \cdot \frac{2}{60} \int_0^T /T_{TO}\omega_{TO} - T_{DO}\omega_{DO}/dt \quad (MJ)$$

7.4 Transmission

$$E_T = \int_0^T /P_{SO} - P_T/dt = 10^{-3} \int_0^T /P_{SO} - \frac{2}{60{,}000} T_{TO}\omega_{TO}/dt \quad (MJ)$$

7.5 Brakes

$$E_{BRK} = 10^{-3} \int_0^T /P_{BRK}/dt \quad (MJ)$$

** μ_{RG} and μ_{RG2} represent average battery regeneration efficiencies on Modes 1 and 2, respectively. μ_{RG2} is assumed to be higher than μ_{RG} because of the lower average state of charge on Mode 2.

Equations for "HYBRID" Computer Program (cont'd)

7.6 Engine Output

$$E_{EO} = 10^{-3} \int_0^T P_{EO}dt \qquad \text{(MJ)}$$

7.7 Motor/Generator Output

$$E_{MO} = 10^{-3} \int_0^T P_{MO}dt \qquad \text{(MJ)}$$

$$E_{GO} = 10^{-3} \int_0^T P_{GO}dt \qquad \text{(MJ)}$$

7.8 Battery Output

$$E_B = 10^{-3} \int_0^T P_B dt \qquad \text{(MJ)}$$

7.9 Fuel

$$F_{CT} = 1/3600 \int_0^T F_C dt \qquad \text{(g)}$$

NOMENCLATURE FOR "HYBRID"

Parameters		Units	Description
Equation	Program		
	NPWR	-	PHEZ, BSFC matrix size
	PHEZRO	Kw	Heat engine power, nominal
	FCDL	g/Hr	Fuel consumption at idle (unscaled)
	FUELSG	-	Fuel specific gravity
	PHEC(20)	Kw	Heat engine power (unscaled)
BSFC	BSFC(20)	-	Brake Specific fuel consumption
μ_t	EMUT	-	Transmission efficiency
	NDDSCH	-	(DDISCH, CYCLES) matrix size
	CHGEFF	-	Battery charging efficiency
	DDISCH(20)	-	Battery discharge depth
	CYCLES(20)	-	Number of cycles at battery discharge depth
r_o	DRATIO	-	Differential ratio
μ_D	EMUD	-	Differential efficiency
R_T	RTIRE	m	Tire radius
C_1	CTIRE1	-	Rolling resistance coefficient
C_2	CTIRE2	-	Rolling resistance coefficient
	NCYCLE	-	Number of driving cycles
	NTC(3)	-	(TIMC, SPEDC) matrix size
	NPRTC(3)	-	Output printing flag for driving cycles
	NUNITS	-	Miles/Hr to Km/Hr conversion flag
	DTC(3)	sec	Time interval for driving cycles
	TFC(3)	sec	Final time for driving cycles
	TIMC(3,200)	sec	Time on driving cycles
	SPEDC(3,200)	Km/Hr	Speed on driving cycles
	NCOMP	-	(DSUP, DNC, GAMMA) matrix size
	DSTAV	km	Average usage
	DSUP(30)	Km	Max. distance on driving cycle (Travel distribution data)
	DNC(30)	-	Fraction of total distance (Travel distribution data)
	GAMMA(30,3)	-	Driving cycle weights (Travel distribution data)
	NCASE	-	Number of cases

Nomenclature for "HYBRID" (cont'd)

Parameters		Units	Description
Equation	Program		
P_{eomin}	PEOMIN	Kw	Heat engine minimum power
	DBMAX		Battery discharge limit
P_{HEMAX}	PHEMAX	Kw	Heat engine power, maximum
P_{MMAX}	PMMAX	Kw	Motor power, maximum
P_{MMIN}	P_{MMIN}	Kw	Motor power, minimum
μm	EMUM	-	Motor efficiency
μg	EMUG	-	Generator efficiency (of motor)
P_{NLD}	PINNLD	Kw	Motor no-load input
	WB	Kg	Battery weight
	EBMAX	Wh/Kg	Battery energy density
μ_{RG}	EMURG	-	Average generating efficiency (of motor)
μ_{RG2}	EMURG2	-	Maximum generating efficiency (of motor)
M_T	VMASS	Kg	Vehicle mass
I_{DL}	DLI	$kg\text{-}m^2$	Driveline inertia
C_{DA}	CDA	m^2	Drag coefficient * area

Nomenclature for "HYBRID" (cont'd)

Variables		Units	Description
Equation	Program		
	A(3)	m/sec^2	Accelerations
	BLIFE	Km	Battery life (expected)
	DBAR(30)	Km	Interpolated values of driving cycle distances
	DDAV	Km	Avg. distance on driving cycle
	DELT	sec	Time interval size
	DIST(3)	M	Distance on each cycle
	DLOW	Km	Minimum distance on driving cycle
	DT	sec	Time increment
P_B	EB	Mj	Mode 1 battery power output
P_E	EB2	Mj	Mode 2 battery power output
	ECAV	Mj/Km	Yearly average energy consumption
	ECBAR(30)	Mj/Km	Mode 1 composite cycles energy consumption
	ECBAR2(30)	Mj/Km	Mode 2 composite cycles energy consumption
	ECHE(3)	Mj/Km	Heat engine energy consumption, each cycle
	ECMAV(30)	Mj/Km	Mode averaged composite cycles energy consumption
	ECONS(3)	Mj/Km	Mode 1 cycle energy consumption
	ECONS2(3)	Mj/Km	Mode 2 cycle energy consumption
	ECSYS(3)	Mj/Km	System energy consumption each cycle
	EHEAV	Mj/Km	Yr. avg. heat engine energy consumption
	EHEBAR(30)	Mj/Km	Heat engine energy consumption, composite
	EK(80)	-	Runga-Kutta integration variables
	ESYSAV	Mj/Km	Yr. avg. system energy consumption
	ESYBR(30)	Mj/Km	System energy consumption, composite
	FCAV	g/Km	Yearly average fuel consumption
	FCBAR(30)	g/Km	Mode 1 composite cycles fuel consumption
	FCBAR2(30)	g/Km	Mode 2 composite cycles fuel consumption
	FCIDLE	g/Hr	Fuel consumption at idle (scaled)
	FCMAV(30)	g/Km	Mode averaged composite cycles fuel consumption
	FCONS(3)	g/Km	Mode 1, cycle fuel consumption
	FCONS2(3)	g/Km	Mode 2, cycle fuel consumption
	FEAV	Km/L	Yr. avg. fuel economy
	HEEF	-	Heat engine energy fraction
	INT1	-	Function subroutine, 1 dimensional interpolation
	INT2	-	Function subroutine, 2 dimensional interpolation

Nomenclature for "HYBRID" (cont'd)

Variables		Units	Description
Equation	Program		
	K	-	Incremented print flag
	NPRNT	-	Print flag for specified cycle
	NTIME	-	Number of time points for specified cycle
P_{BRK}	PBRK	Kw	Mode 1 braking power output
	PBRK2	Kw	Mode 2 braking power output
	PEO	Kw	Mode 1 engine power output
	PEO2	Kw	Mode 2 engine power output
	PGO	Kw	Mode 1 generator power output
	PGO2	Kw	Mode 2 generator power output
	PHE(20)	Kw	Heat engine power (scaled)
	PMO	Kw	Mode 1 motor power output
	PMO2	Kw	Mode 2 motor power output
	PSO	Kw	System power output
	RANGE(30)	Km	Range for new battery discharge limit
	REFRAC(30)	-	Fraction of total driving cycle
	SKALE	-	Heat engine scale factor
	SPEED(20)	Km/Hr	Speeds for specified driving cycle
	T	sec	Time (incremented for integration)
	TF	sec	Final time for specified cycle
	TIME(200)	sec	Times for specified driving cycle
	TTMP	sec	Time holder
V	V(6)	m/sec	Velocities
M_T	VMASS2	kg	Vehicle inertial mass
	VTMP	m/sec	Velocity hold
	VTMPL	m/sec	Velocity hold
	WPAV	Kw/Km	Yr. avg. wall plug output
E_A	Y(1)	Mj	Aerodynamic energy loss
E_R	Y(2)	Mj	Rolling resistance energy loss
E_D	Y(3)	Mj	Differential energy loss
E_T	Y(4)	Mj	Transmission energy loss
	Y(5)	Mj	System output energy
E_{MO}	Y(6)	Mj	Motor output energy, Mode 1
	Y(7)	Mj	Motor output energy, Mode 2
E_{EO}	Y(8)	Mj	Engine output energy, Mode 1
	Y(9)	Mj	Engine output energy, Mode 2

Nomenclature for "HYBRID" (cont'd)

Variables		Units	Description
Equation	Program		
E_{GO}	Y(10)	Mj	Generator output energy, Mode 1
	Y(11)	m/sec	Velocity
	Y(12)	Km	Distance
	Y(13)	Mj	Generator output energy, Mode 2
E_{BRK}	Y(14)	Mj	Brake output energy, Mode 1
	Y(15)	Mj	Brake output energy, Mode 2
F_{CT}	Y(16)	g	Fuel output energy, Mode 1
	Y(17)	g	Fuel output energy, Mode 2
E_B	Y(18)	Mj	Battery output energy, Mode 1
	Y(19)	Mj	Battery outout energy, Mode 2
	YDOT(20)	-	Runga-Kutta integration variables
	YTMP(20)	-	Runga-Kutta integration variables

SUBROUTINE "VEHIC"

Variables			
Equation	Program	Units	Description
F_A	FA	N	Force of aerodynamic drag
F_{AC}	FAC	N	Force of acceleration
F_C	FC	g/Hr	Mode 1 fuel consumption
	FC2	g/Hr	Mode 2 fuel consumption
F_R	FR	N	Force of rolling resistance
F_{NET}	FNET	N	Net force on wheels
	PA	Kw	Aerodynamic power
P_{BRK}	PBRK	Kw	Mode 1 braking power output
	PBRK2	Kw	Mode 2 braking power output
	PD	Kw	Drive train power
P_{EO}	PEO	Kw	Mode 1 engine power output
	PEO2	Kw	Mode 2 engine power output
P_{GO}	PGO	Kw	Mode 1 generator power output
	PGO2	Kw	Mode 2 generator power output
P_{MO}	PMO	Kw	Mode 1 motor power output
	PMO2	Kw	Mode 2 motor power output
	PR	Kw	Rolling resistance power
P_{SO}	PSO	Kw	System power output
	PT	Kw	Transmission power
W_{DO}	RPMDO	RPM	Drive train output
W_{TO}	RPMTO	RPM	Transmission output
T_{DO}	TDO	NT-M	Drive train output torque
T_{TO}	TTO	NT-M	Transmission output torque
	VMPS	m/sec^2	Velocity ($meters/sec^2$)
	VDOT(20)	-	Variables of integration

INPUT FORMAT

PROGRAM: HYBRID | NAME:
ROUTINE: MAIN PROGRAM | DATE: | PAGE 1 OF 2

TYPE	STATEMENT NO.	CONT	FORTRAN STATEMENT (0 ZERO, 0 ALPHA 0 / 1 ONE, 1 ALPHA 1 / 2 TWO, 2 ALPHA 2)	SERIAL NUMBER
			ENGINE DATA	
		NPWR	PWRECRO ECDL FUELSG	
	PWRC	(1,1)	BSFC(1,1) ... PWRC(NPWR) BSFC(NPWR)	
			TRANSMISSION DATA	
		EMUT		
			BATTERY DATA	
	NDDSCH		CHGEFF	
	DDISC	H(1,1)	CYCLES(1,1) ... DDISCH(NDDSCH) CYCLES(NDDSCH)	
			DIFFERENTIAL AND TIRE DATA	
	DRATIO		EMUD RTIRE CTIRE1 CTIRE2	
			DRIVING CYCLE DATA	
	NCYCLE			
	MTC	(1,1)	NPRTG(1,1) NUNITS DTC(1,1) TFC(1,1) ... NTC(NCYCLE)	
NPRTC(NCYCLE)			NUNITS DTC(NCYCLE) TTC(NCYCLE)	
	TIMC	(1,1)	SPEDC(1,1) ... TIMC(NCYCLE,NT) SPEDC(NCYCLE,NT)	

FORM NO. GRC 109 REV. 1

256

PROGRAM HYBRID | NAME

ROUTINE MAIN PROGRAM | DATE | PAGE 2 OF 2

FORTRAN STATEMENT — 0 = ZERO, 0 = ALPHA 0; 1 = ONE, 1 = ALPHA 1; 2 = TWO, 2 = ALPHA 2

TYPE	STATEMENT NO.	CONT						SERIAL NUMBER
			TRAVEL DISTRIBUTION DATA					
		NCOMP	DSTAV				GAMMA(NCOMP,NCYCLS)	
		DSUP(1)	DNC(1)	GAMMA(1,1)	DSUP(NCOMP)	DNC(NCOMP)		
			RUN DATA					
		NCASE						
		TEMIN	DBMAX	PEOMIN				
			MOTOR/GENERATOR DATA					
		PMMAX	PMMIN	EMUM	EMUG	PINLD		
		WB	EBMAX	EMURG	EMURG2			
			VEHICLE DATA					
		VMASS	DLI	CDA				

FORM NO. GRC 109 REV. 1

Hybrid Flowchart

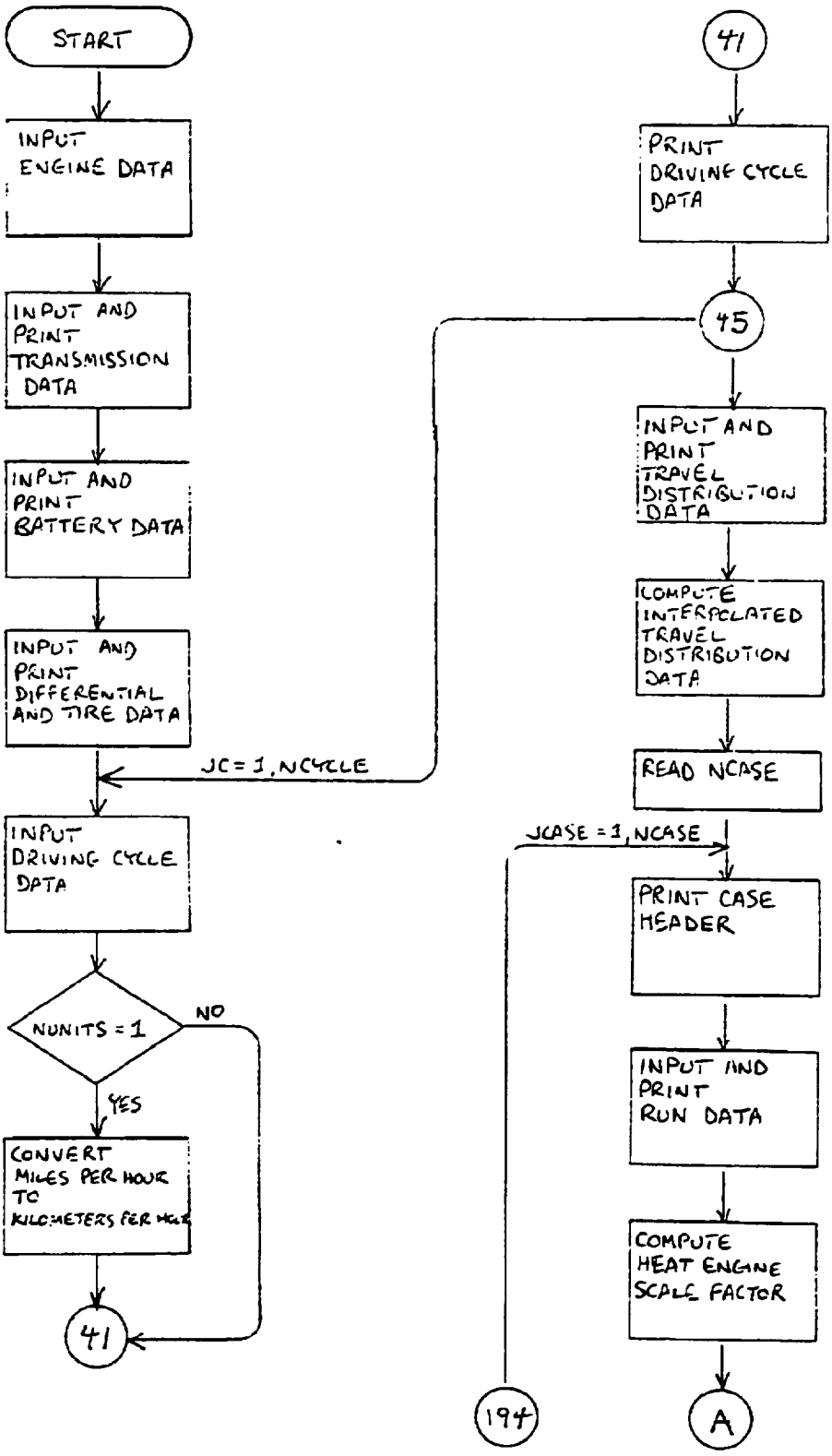

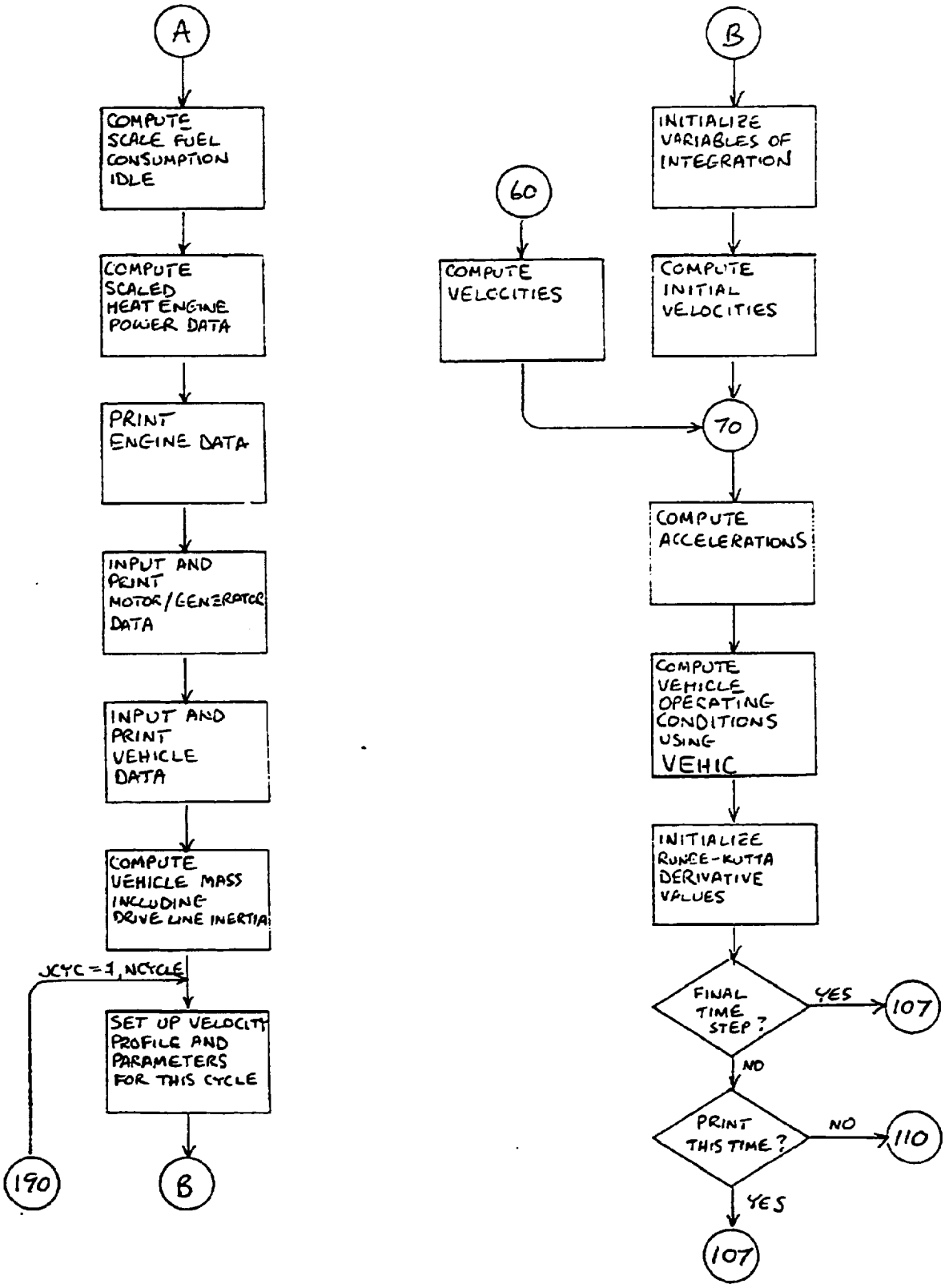
A
COMPUTE SCALE FUEL CONSUMPTION IDLE
COMPUTE SCALED HEAT ENGINE POWER DATA
PRINT ENGINE DATA
INPUT AND PRINT MOTOR/GENERATOR DATA
INPUT AND PRINT VEHICLE DATA
COMPUTE VEHICLE MASS INCLUDING DRIVE LINE INERTIA
JCYC = 1, NCYCLE
SET UP VELOCITY PROFILE AND PARAMETERS FOR THIS CYCLE
190
B
60
COMPUTE VELOCITIES
B
INITIALIZE VARIABLES OF INTEGRATION
COMPUTE INITIAL VELOCITIES
70
COMPUTE ACCELERATIONS
COMPUTE VEHICLE OPERATING CONDITIONS USING VEHIC
INITIALIZE RUNGE-KUTTA DERIVATIVE VALUES
FINAL TIME STEP ?
YES
107
NO
PRINT THIS TIME ?
NO
110
YES
107

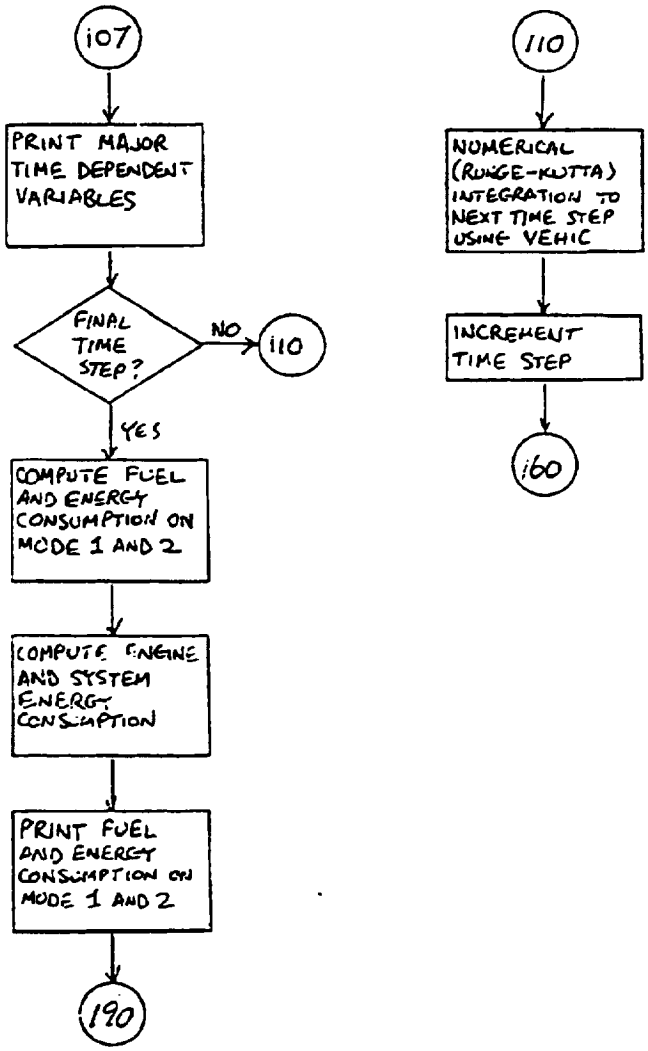
107
PRINT MAJOR TIME DEPENDENT VARIABLES
FINAL TIME STEP?
NO
110
YES
COMPUTE FUEL AND ENERGY CONSUMPTION ON MODE 1 AND 2
COMPUTE ENGINE AND SYSTEM ENERGY CONSUMPTION
PRINT FUEL AND ENERGY CONSUMPTION ON MODE 1 AND 2
190
110
NUMERICAL (RUNGE-KUTTA) INTEGRATION TO NEXT TIME STEP USING VEHIC
INCREMENT TIME STEP
160

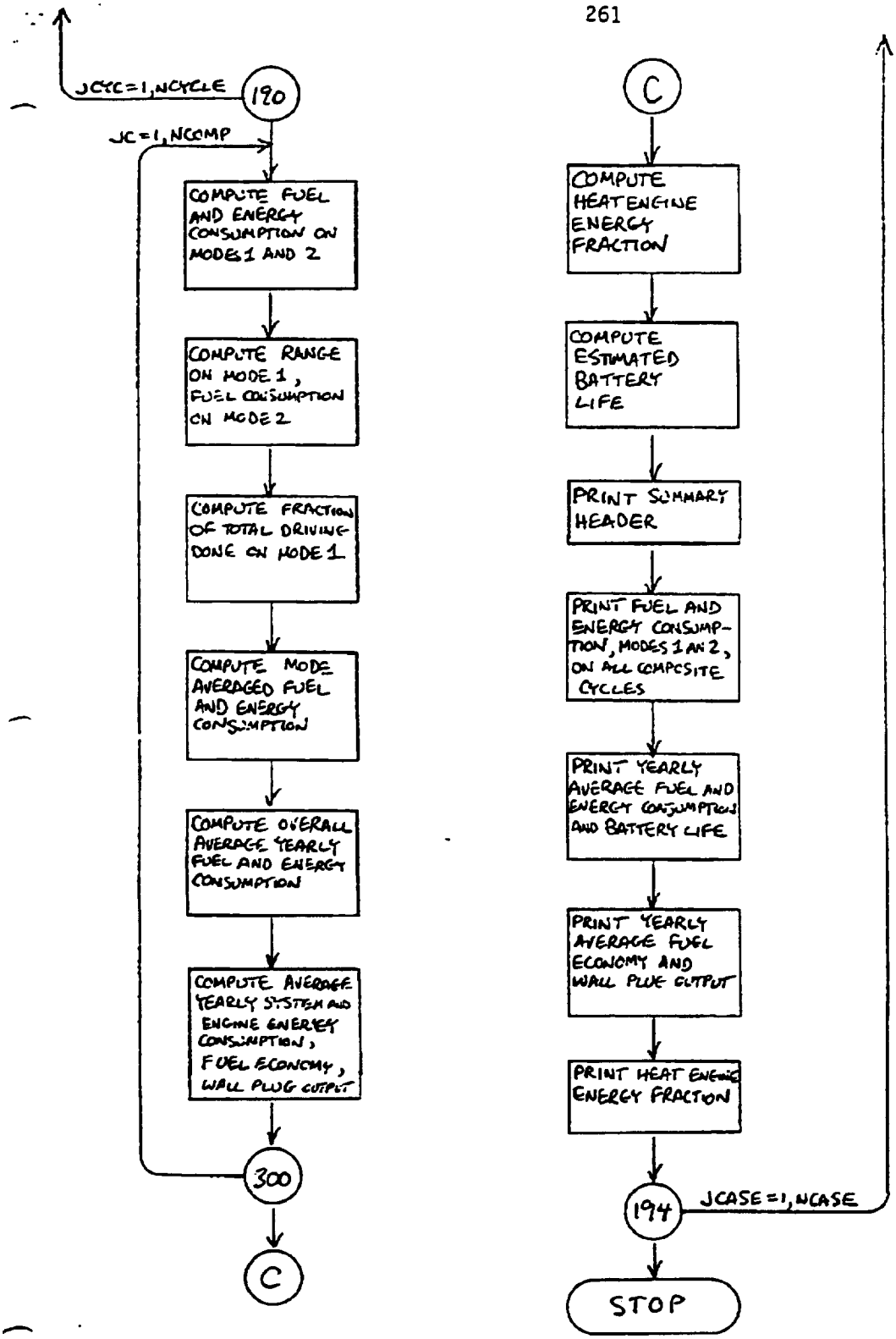
JCYC=1,NCYCLE
190
JC=1,NCOMP
COMPUTE FUEL AND ENERGY CONSUMPTION ON MODES 1 AND 2
COMPUTE RANGE ON MODE 1, FUEL CONSUMPTION ON MODE 2
COMPUTE FRACTION OF TOTAL DRIVING DONE ON MODE 1
COMPUTE MODE AVERAGED FUEL AND ENERGY CONSUMPTION
COMPUTE OVERALL AVERAGE YEARLY FUEL AND ENERGY CONSUMPTION
COMPUTE AVERAGE YEARLY SYSTEM AND ENGINE ENERGY CONSUMPTION, FUEL ECONOMY, WALL PLUG OUTPUT
300
C
C
COMPUTE HEAT ENGINE ENERGY FRACTION
COMPUTE ESTIMATED BATTERY LIFE
PRINT SUMMARY HEADER
PRINT FUEL AND ENERGY CONSUMPTION, MODES 1 AND 2, ON ALL COMPOSITE CYCLES
PRINT YEARLY AVERAGE FUEL AND ENERGY CONSUMPTION AND BATTERY LIFE
PRINT YEARLY AVERAGE FUEL ECONOMY AND WALL PLUG OUTPUT
PRINT HEAT ENGINE ENERGY FRACTION
194
JCASE=1,NCASE
STOP

VEHIC Subroutine Flowchart

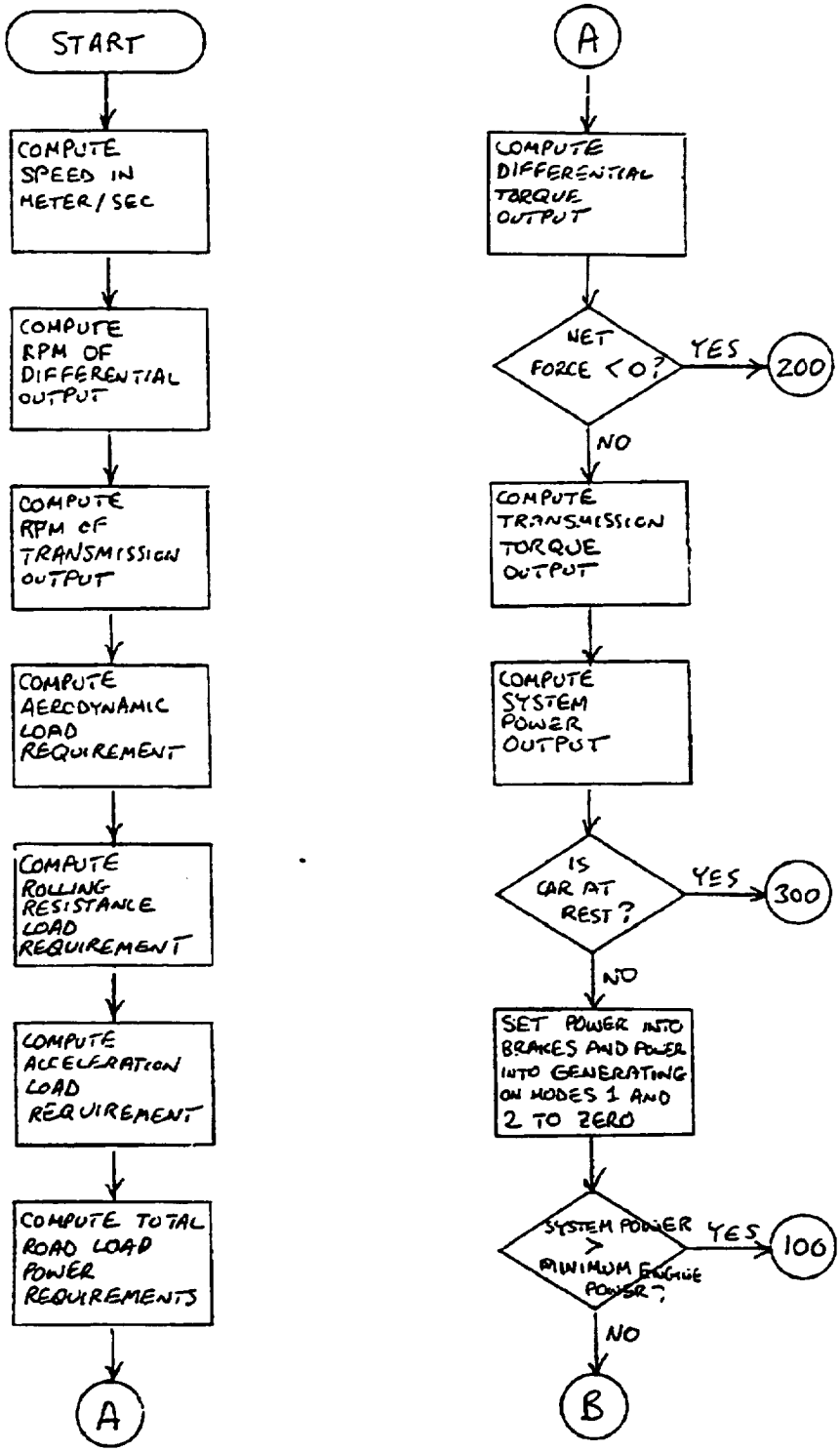

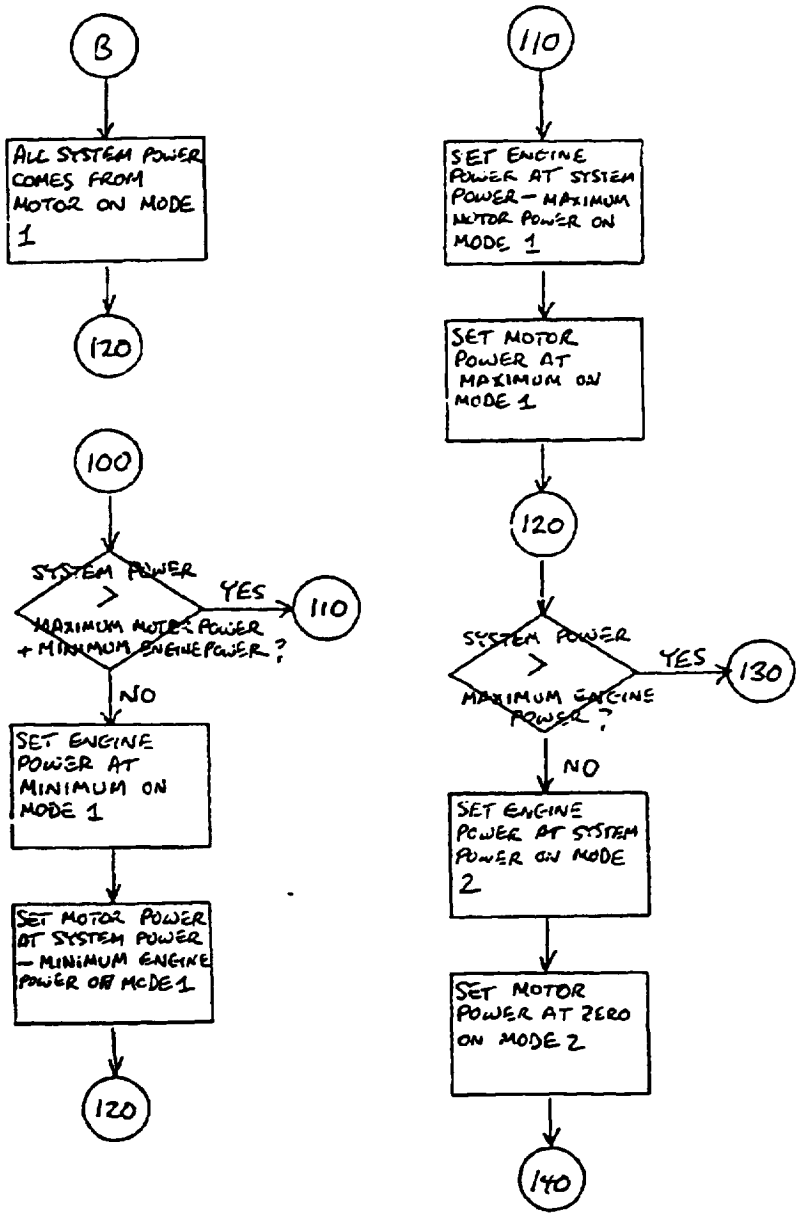
B
ALL SYSTEM POWER COMES FROM MOTOR ON MODE 1
120
100
SYSTEM POWER > MAXIMUM MOTOR POWER + MINIMUM ENGINE POWER ?
YES
110
NO
SET ENGINE POWER AT MINIMUM ON MODE 1
SET MOTOR POWER AT SYSTEM POWER - MINIMUM ENGINE POWER ON MODE 1
120
110
SET ENGINE POWER AT SYSTEM POWER - MAXIMUM MOTOR POWER ON MODE 1
SET MOTOR POWER AT MAXIMUM ON MODE 1
120
SYSTEM POWER > MAXIMUM ENGINE POWER ?
YES
130
NO
SET ENGINE POWER AT SYSTEM POWER ON MODE 2
SET MOTOR POWER AT ZERO ON MODE 2
140

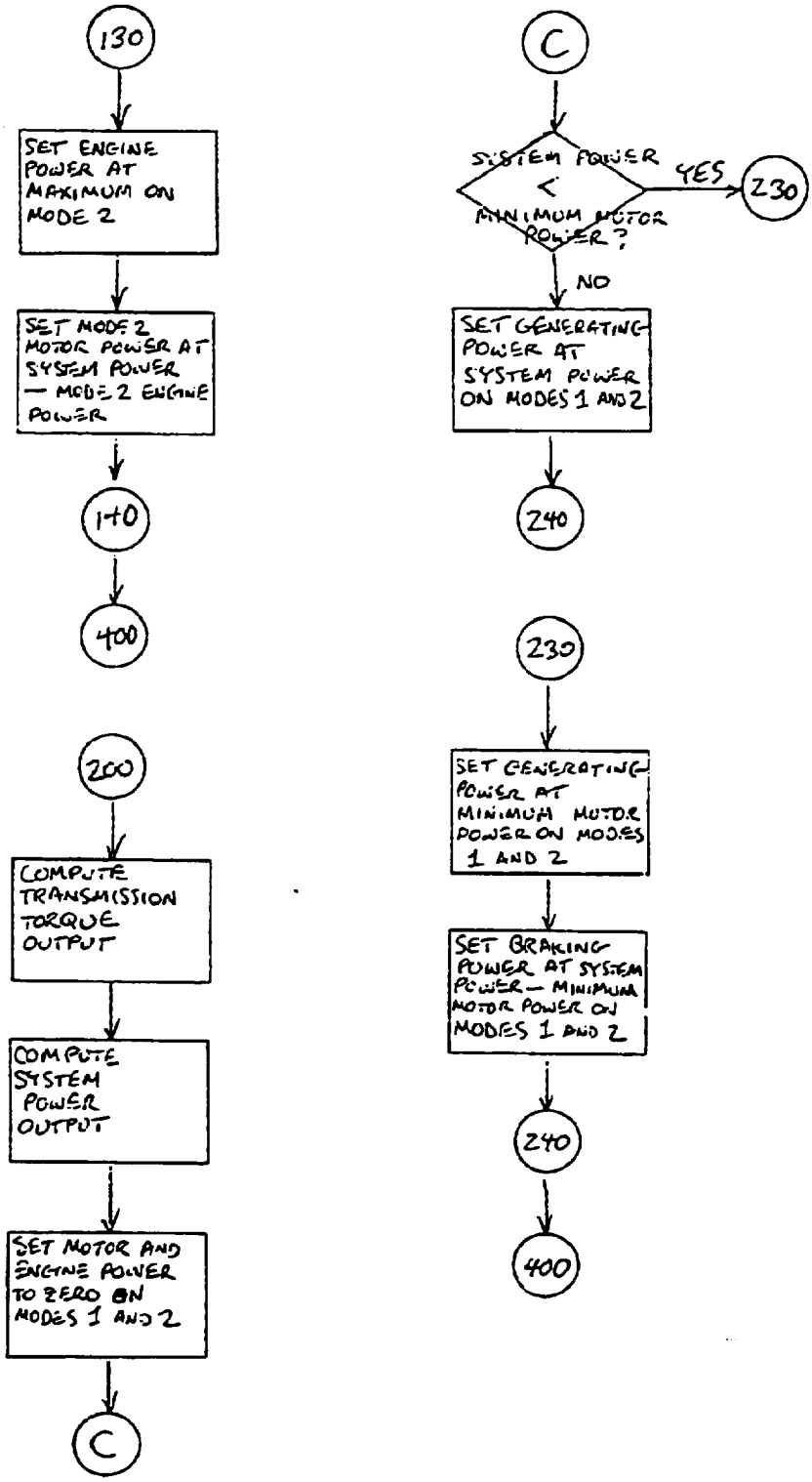
130
SET ENGINE POWER AT MAXIMUM ON MODE 2
SET MODE 2 MOTOR POWER AT SYSTEM POWER — MODE 2 ENGINE POWER
140
400
200
COMPUTE TRANSMISSION TORQUE OUTPUT
COMPUTE SYSTEM POWER OUTPUT
SET MOTOR AND ENGINE POWER TO ZERO ON MODES 1 AND 2
C
C
SYSTEM POWER < MINIMUM MOTOR POWER?
YES
230
NO
SET GENERATING POWER AT SYSTEM POWER ON MODES 1 AND 2
240
230
SET GENERATING POWER AT MINIMUM MOTOR POWER ON MODES 1 AND 2
SET BRAKING POWER AT SYSTEM POWER — MINIMUM MOTOR POWER ON MODES 1 AND 2
240
400

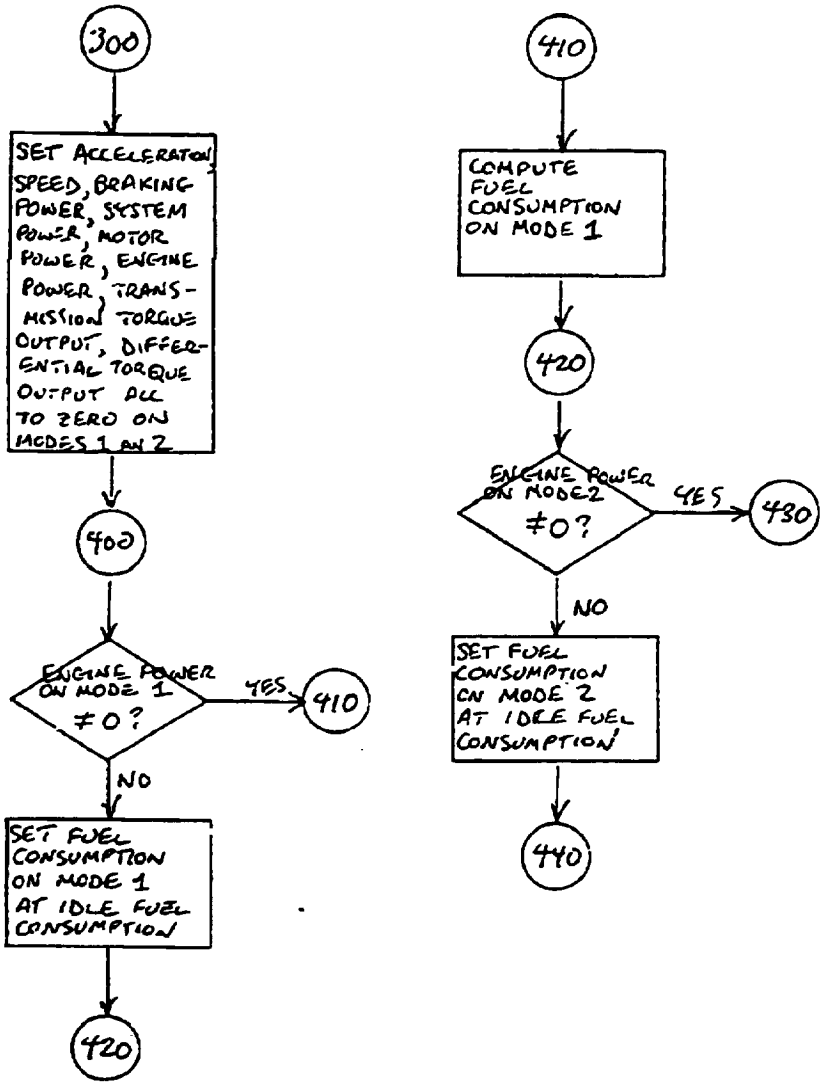
300
SET ACCELERATION, SPEED, BRAKING POWER, SYSTEM POWER, MOTOR POWER, ENGINE POWER, TRANSMISSION TORQUE OUTPUT, DIFFERENTIAL TORQUE OUTPUT ALL TO ZERO ON MODES 1 AND 2
400
ENGINE POWER ON MODE 1 ≠0?
YES
410
NO
SET FUEL CONSUMPTION ON MODE 1 AT IDLE FUEL CONSUMPTION
420
410
COMPUTE FUEL CONSUMPTION ON MODE 1
420
ENGINE POWER ON MODE 2 ≠0?
YES
430
NO
SET FUEL CONSUMPTION ON MODE 2 AT IDLE FUEL CONSUMPTION
440

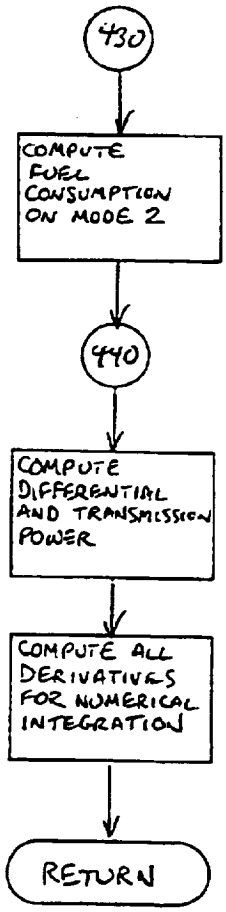
430
COMPUTE FUEL CONSUMPTION ON MODE 2
440
COMPUTE DIFFERENTIAL AND TRANSMISSION POWER
COMPUTE ALL DERIVATIVES FOR NUMERICAL INTEGRATION
RETURN

SUBROUTINE INT1

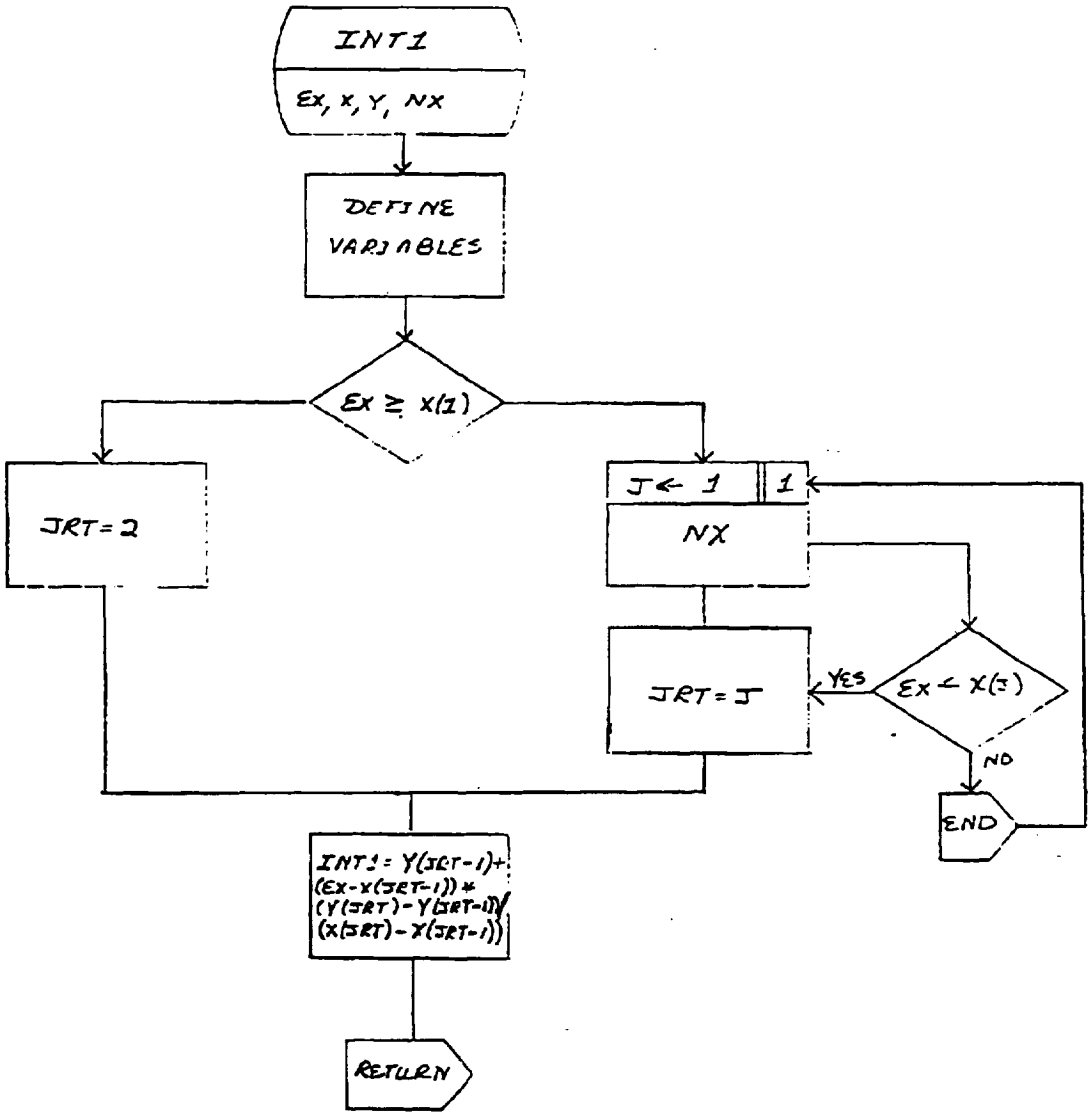

SUBROUTINE INT2

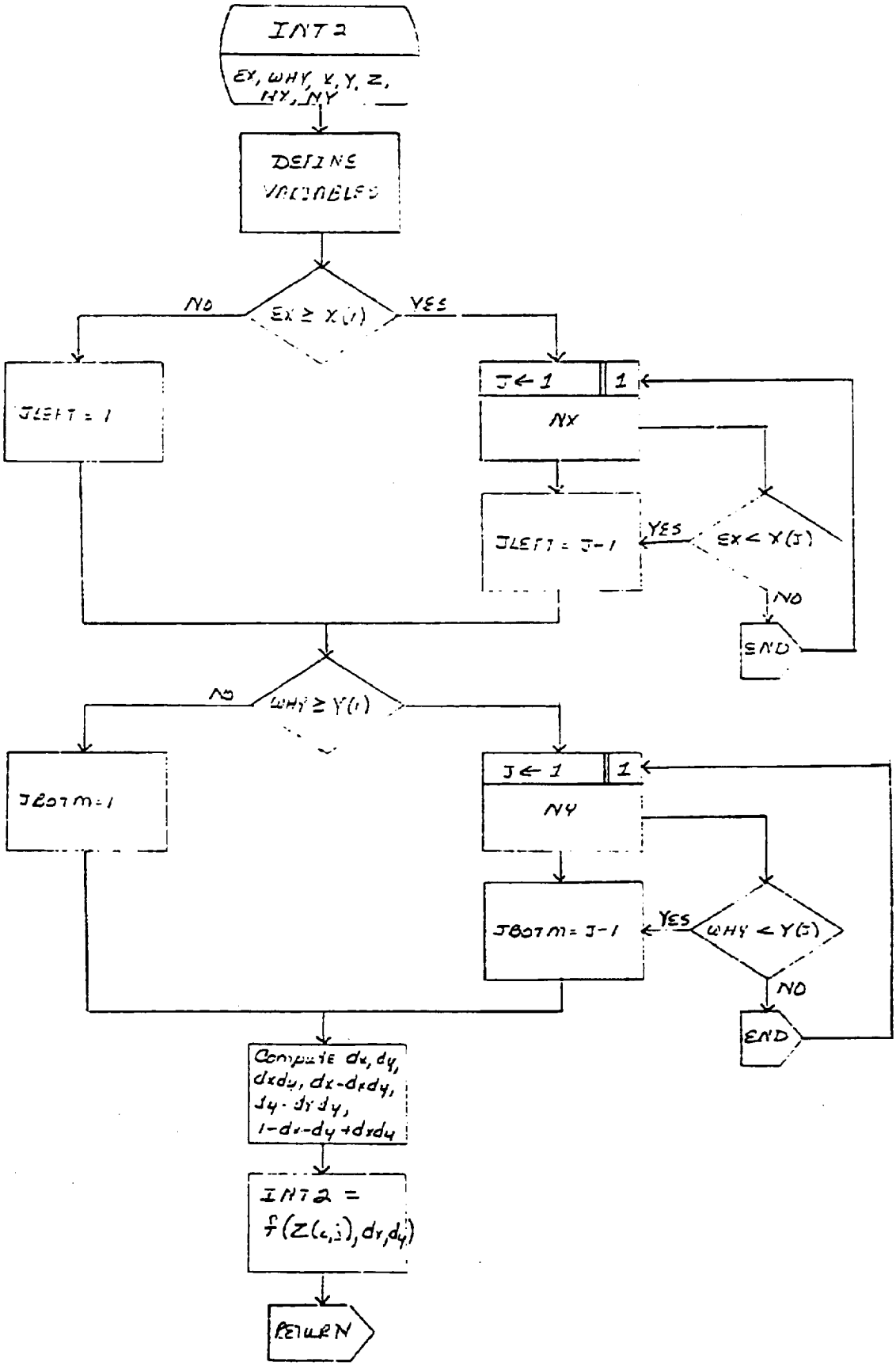

APPENDIX B - DOCUMENTATION FOR "LYFE2" COMPUTER PROGRAM

PROGRAM DESCRIPTION

LYFE2 computes the life cycle cost of a propulsion system over a 10-year span. Included in operating cost are maintenance, repair, fuel, and battery replacement (all mileage dependent). Life cycle cost is operating cost plus propulsion system acquisition costs and minus propulsion system and battery salvage values.

Two versions of this program were developed. Version "A" was used during the Parametric Studies task. It considered two cost cases: Case 1 (minimum mark-up), and Case 2 (maximum mark-up). In Case 1, propulsion system acquisition cost was computed at twice the manufacturing cost of a reference conventional propulsion system plus 1.25 times the differential in manufacturing cost of the hybrid system over the conventional system, and battery acquisition and replacement costs were computed at 1.25 times the battery OEM cost. In Case 2, all acquisition and replacement costs were computed at twice the corresponding manufacturing or OEM cost. Version "A" required the propulsion system manufacturing cost to be computed separately and used as an input. Version "B" was used during the Design Tradeoff Studies task. It incorporated within the program the manufacturing cost vs. power relationships for the heat engine, electric propulsion subsystem, and transaxle. It also used a different set of mark-ups from base manufacturing or OEM costs to acquisition costs, as discussed in Section 4.3 of this report.

EQUATIONS FOR "LYFE2" COMPUTER PROGRAM

(See Nomenclature for explanation of symbols)

I. Version "A"

Acquisition Costs

A. System (not including batteries)

Cost Case 1: PSPP = 2* CMRP + 1.25* (CMH - CMRP)

Cost Case 2: PSPP = 2* CMH

B. Batteries

Cost Case 1: BRC = 1.25* BOEM

Cost Case 2: BRC = 2* BOEM

Operating Costs

A. Maintenance (¢/Km)

1. Heat Engine: $HEMC = PHE^* \frac{.003106}{.746} + .111818$

2. Electric Propulsion Subsystem:

$$EMMC = PM^* \frac{.001242}{.746} + .037273$$

3. Batteries: BMC = WB* .000248

B. Repair (¢/Km)

1. Heat Engine: $HERC = PHE^* \frac{.00497}{.746} + .173939$

2. Electric Propulsion Subsystem:

$$EMRC = PM^* \frac{.00124}{.746} + .05591$$

3. Transaxle: $TRC = (PHE + PM)^* \frac{.000808}{.746} + .031061$

C. Fuel (¢/Km)

1. Gasoline: PFCK = 53* GGPK (corresponds to $2/gal.)

2. Electrical Energy: EFCK = 7* EKWHPK

D. Battery Replacement

(Same as battery acquisition)

Equations for "LYFE2" Computer Program (cont'd)

II. Version "B"

Manufacturing Costs

Note: Program computes manufacturing costs in 1980 $ and divides by 1.28 to get equivalent 1976 $. The following relationships are stated directly in 1976 $.

A. Heat Engine: CHE = PHE*4.36 + 121

B. Electric Propulsion Subsystem: CEP = PM*17.6 + 195

C. Transaxle: CTRANS = (PHE + PM) * 1.31 + 125

Acquisition Costs

A. Heat Engine: RCHE = 2.3 * CHE

B. Electric Propulsion Subsystem: RCEP = 2.2 * CEP

C. Transaxle: RCTRANS = 2.3 * CTRANS

D. Batteries: RCBAT = 1.3 * CBAT

Operating Costs

Same as Version "A"

NOMENCLATURE FOR "LYFE2"

Name	Units	Description
AL	$	System loan amount
ALBR	$	Battery replacement loan amount
ALCCK	$	Average life cycle cost per Km
AOC	$	Annual operating cost (Vector)
AOCK	$	Average operating cost per Km
AP	$	System loan, payment amount
APBR	$	Battery replacement loan, payment amount
AVKT	Km	Average annual vehicle Km traveled (national average)
BMC	¢	Battery maintenance costs
BOEM	$	Battery manufucturing costs
BR	Km	Km tally for battery replacement
BRC	$	Battery replacement costs
BRK	Km	Life expectancy of batteries
BSV	$	Battery salvage value
CMH	$	Manufacturing cost of hybrid propulsion system
CMRP	$	Manufacturing cost of reference conventional propulsion system
CEP	$	Manufacturing cost of electric propulsion subsystem
CHE	$	Manufacturing cost of heat engine
CTRANS	$	Manufacturing cost of transaxle
CBAT	$	OEM cost of batteries
DAOC	$	Discounted annual operating cost (Vector)
DF	-	Discount factor
DLCCK	$	Discounted life cycle cost per Km
DOCK	$	Discounted operating cost per Km
DYLCC	$	Discounted annual life cycle cost
EFCK	¢	Annual electricity cost per Km (Vector)
EKPY	Km	Adjusted annual Km travelled (Vector)
EKT	Km	Average annual vehicle Km travelled - Passenger car forecast, U.S.A. (Vector
EKWHPK	Kwh/Km	Electricity consumption rate
EMMC	¢	Electric motor maintenance cost
EMRC	¢	Electric motor repair cost
FMC	¢	Flywheel maintenance cost
GDPK	Lt/Km	Diesel fuel consumption
GGPK	Lt/Km	Gasoline fuel consumption

Nomenclature for "LYFE2" (cont'd)

Name	Units	Description
HEMC	¢	Heat engine maintenance cost
HERC	¢	Heat engine repair cost
KBR	-	Battery replacement flag (Vector)
NCASE	-	Number of cases to be executed
PDP	-	Percentage down payment
PFCK	¢	Annual petroleum cost per Km (Vector)
PHE	Kw	Heat engine power
PM	Kw	Electric motor power
PSPP	$	Propulsion system purchase price
PSSV	$	Propulsion system salvage value
PV	$	Vehicle price
RCEP	$	Acuisition cost of electric propulsion subsystem
RCHE	$	" " " heat engine
RCTRANS	$	" " " transaxle
RCBAT	$	" " " batteries
RKF	-	Km repair factor
TAOC	$	Total annual operating cost
TDLCC	$	Total discounted life cycle cost
TDOC	$	Total discounted operating cost
TFCK	¢	Total annual fuel cost per Km (Vector)
TK	Km	Total Km (10 years)
TLCC	$	Total life cycle cost
TMCK	¢	Total maintenance cost per Km
TRC	¢	Transmission repair cost
TRCK	¢	Total repair cost per Km
TRCKF	¢	Total repair cost per Km * Km (Vector repair factor
VKT	Km	Annual vehicle Km travelled - National average (Vector
WB	Kg	Battery weight
WV	Kg	Vehicle weight
YLCC	$	Annual life cycle cost (Vector)

INPUT FORMAT

PROGRAM: CYFC2 | NAME:
ROUTINE: | DATE: | PAGE: OF

TYPE	STATEMENT NO.	CONT	FORTRAN STATEMENT (0 = ZERO, O = ALPHA O; 1 = ONE, I = ALPHA I; 2 = TWO, Z = ALPHA Z)	SERIAL NUMBER
		NC	NCASE	
			FOR EACH CASE	
	NY	EARS		
		CAH	CMRP WB PHE PM PDP	
		GGPK	GDPK EKWHPK BOEM BRK	
	VK	T(1)	VKT(NYEARS) AVKT EKT	
	RK	F(1)	RKT(NYEARS)	
			NOTE: FOR VERSION 'B', CMH AND BOEM ARE COMPUTED INTERNALLY,	
			SO ANY VALUE CAN BE GIVEN FOR THESE INPUTS. CMRP IS	
			NOT USED IN VERSION 'B', SO IT ALSO CAN BE GIVEN AN	
			ARBITRARY VALUE.	

FORM NO. GRC 109 REV. 1

LYFE2

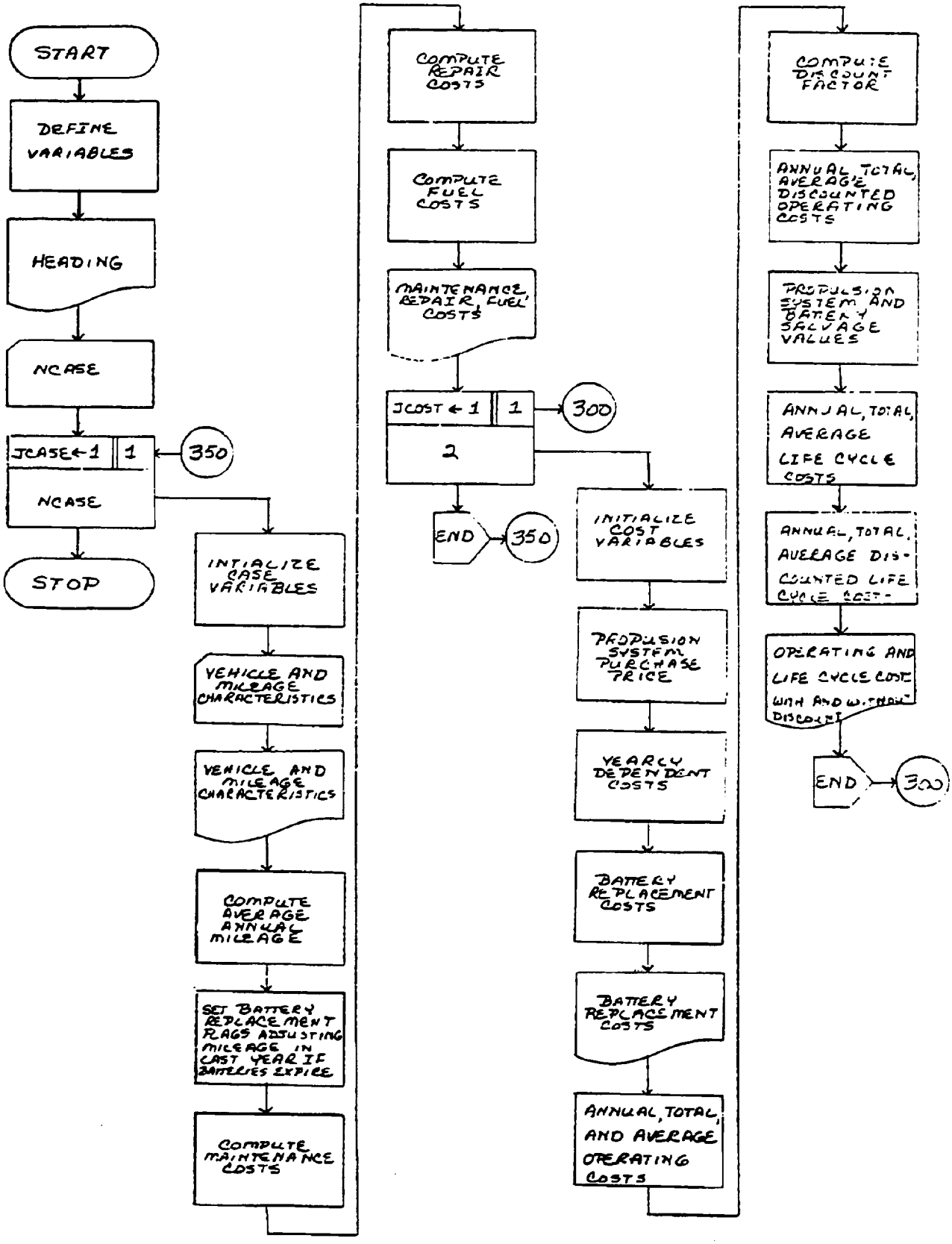
START
DEFINE VARIABLES
HEADING
NCASE
JCASE←1
1
350
NCASE
STOP
INTIALIZE CASE VARIABLES
VEHICLE AND MILEAGE CHARACTERISTICS
VEHICLE AND MILEAGE CHARACTERISTICS
COMPUTE AVERAGE ANNUAL MILEAGE
SET BATTERY REPLACEMENT FLAGS ADJUSTING MILEAGE IN LAST YEAR IF BATTERIES EXPIRE
COMPUTE MAINTENANCE COSTS
COMPUTE REPAIR COSTS
COMPUTE FUEL COSTS
MAINTENANCE, REPAIR, FUEL COSTS
JCOST ← 1
1
300
2
END
350
INITIALIZE COST VARIABLES
PROPULSION SYSTEM PURCHASE PRICE
YEARLY DEPENDENT COSTS
BATTERY REPLACEMENT COSTS
BATTERY REPLACEMENT COSTS
ANNUAL, TOTAL, AND AVERAGE OPERATING COSTS
COMPUTE DISCOUNT FACTOR
ANNUAL, TOTAL, AVERAGE DISCOUNTED OPERATING COSTS
PROPULSION SYSTEM AND BATTERY SALVAGE VALUES
ANNUAL, TOTAL, AVERAGE LIFE CYCLE COSTS
ANNUAL, TOTAL, AVERAGE DISCOUNTED LIFE CYCLE COSTS
OPERATING AND LIFE CYCLE COST WITH AND WITHOUT DISCOUNT
END
300

APPENDIX C - DOCUMENTATION FOR "HYBRID2" COMPUTER PROGRAM

PROGRAM DESCRIPTION

HYBRID2 computes the fuel and energy consumption of a hybrid vehicle with a bi-modal control strategy over specified component driving cycles. Fuel and energy consumption are computed separately for the two modes of operation. The program also computes yearly average fuel and energy consumption using a composite driving cycle which varies as a function of daily travel.

The modelling techniques used include the following:

Heat Engine - Represented by a map of bsfc as a function of bmep and rpm, together with a curve of maximum torque versus rpm. The displacement of the engine for which this data is supplied is used as input; the program has provisions for scaling the data to other displacements.

Electric Motor/Controls - Electrical input represented as a piecewise linear function of mechanical output in both driving and braking modes. Maximum (driving) and minimum (braking) torque as functions of rpm are also required.

Battery - Modelled by a fractional depletion technique using the power averaged over a specified time interval rather than instantaneous power.

Engine Accessory Load - Represented by a curve of torque required vs. system output (torque converter input) rpm. Included in this load is the transmission front pump, in addition to belt-driven accessories.

Torque Converter - Represented by curves of speed and torque ratios (output/input) as functions of an output speed-torque parameter equal to output speed/$\sqrt{\text{output torque}}$. An input speed-torque factor, (input speed)^2/(input torque), at stall must also be specified.

Gearbox - Represented by a set of gear ratios with different efficiencies for each ratio. Spin loss coefficients (exclusive of the front pump) may also be specified.

Differential - Same treatment as gearbox.

Vehicle Road Load - Represented by a combination of an aerodynamic load (proportional to speed squared) and tire rolling resistance. The rolling resistance coefficients can include a constant term and one which is linear with vehicle speed.

The program structure is modular, with the control strategy and shift strategies being contained in separate subroutines. A breakdown of the program routines and their functions is as follows:

1. HYBRID2 (main program)
   - Input of case data
   - Output
   - Numerical integration
   - Computation of yearly average fuel and energy consumption from individual driving cycle results.

2. VEHIC
   - Computation of road loads, power flow through the vehicle system up to the torque converter output.
   - Computation of derivatives of all variables of integration.

3. HYREAD
   - Input of fixed, detailed component data.

4. GRSHFT
   - Controls transmission gear ratio in accord with a pre-set shift strategy.

5. PMOVR
   - Controls heat engine/motor power split in accord with a pre-set control strategy.

6. TQCON
   - Computes torque converter input speed and torque given output conditions, or output torque and input speed given input torque and output speed.

7. FILTER
   - Filters battery output power to provide a smoothed battery output power curve.

8. INT1, INT2
   - One and two dimensional interpolation routines, respectively.

EQUATIONS FOR "HYBRID2"

1. Required Tractive Effort

Acceleration:

(nt) 1.1 $F_{AC} = (M_T + \frac{I_{DL}}{R_T^2}) a_v$

Rolling Resistance:

(nt) 1.2 $F_R = M_T g \cdot (C_1 + C_2 V)$

Aerodynamic Drag:

(nt) 1.3 $F_A = C_D A \cdot 1/2 \rho v^2$

Net Tractive Effort:

(nt) 1.4 $F_{NET} = F_A + F_R + F_{AC}$

2. Final Drive Assembly

(RPM) 2.1 $\omega_{DO} = \frac{60}{2\pi} \frac{V}{R_T}$

(RPM) 2.2 $\omega_{TO} = \omega_{DO} r_D$

Torque loss due to friction (load independent loss):

(N-M) 2.3 $T_{LFD} = C_{D1} + C_{D2} \omega_{TO}$

Output torques: (See equation 3.2)

(nt-m) 2.4

$$T_{DO} = \begin{cases} F_{NET} R_T & F_{NET} \geq 0, \text{ or } F_{NET} < 0 \text{ and } [T_{TCO} \leq T'_{SO} \text{ or } P'_{SO} \geq 0] \\ (T_{TO} - T_{LFD}) r_D / \mu_D & F_{NET} < 0,\ T'_{TCO} > T_{SO} \text{ and } P'_{SO} < 0 \end{cases}$$

Equations for "HYBRID2" (cont'd)

(nt-m) 2.5

$$T_{TO} = \begin{cases} T_{DO}/\mu_D r_D + T_{LFD} & F_{NET} \geq 0 \\ T_{DO}\mu_D/r_D + T_{LFT} & F_{NET} < 0, \text{ and } T'_{TCO} \leq T'_{SO} \text{ or } P'_{SO} \geq 0 \\ (T_{SO} - T_{LFT})r_T/\mu_T & F_{NET} < 0,\ T'_{TCO} > T'_{SO} \text{ and } P'_{SO} < 0 \end{cases}$$

3. Transmission

(RPM) 3.1 $\omega_{SO} = \omega_{TO} r_T$

Torque loss due to friction (load independent loss)

3.2 $T_{LFT} = C_{T1} + C_{T2}\omega_{TO} r_T$

Preliminary computations, input torque and input power: (used only when $F_{NET} < 0$)

3.3X $T'_{SO} = T_{TO}\,\mu_T/r_T + T_{LFT}$

3.4X $P'_{SO} = \frac{2\pi}{60{,}000}\, T'_{SO}\omega_{SO}$

Final computations, input torque and input power: (see equation 4.5X)

(nt-m) 3.3

$$T_{SO} = \begin{cases} T_{TO}/\mu_T r_T + T_{LFT} & F_{NET} \geq 0 \\ T'_{SO} & F_{NET} < 0, \text{ and } T'_{TCO} \leq T'_{SO} \text{ or } P'_{SO} \geq 0 \\ T'_{TCO} & F_{NET} < 0,\ T'_{TCO} > T'_{SO}, \text{ and } P'_{SO} < 0 \end{cases}$$

(kw) 3.4 $P_{SO} = \frac{2\pi}{60{,}000}\, T_{SO}\omega_{SO}$

4. Torque Converter and Accessories (transmission front pump and power steering pump)

$F_{NET} \geq 0$: Input RPM, input torques

(RPM) 4.1

$$\omega_{TCN} = \begin{cases} \omega_{SO}/f(\omega_{SO}/\sqrt{T_{SO}}) & T_{SO} > 0 \text{ and } \omega_{SO} > 0 \\ \omega_{SO} & T_{SO} = 0 \\ \omega_{IDL} & V = 0,\ A = 0 \\ (C_{TC\emptyset} \cdot T_{SO}/T_{QR1})^{1/2} & T_{SO} > 0 \text{ and } \omega_{SO} = 0 \end{cases}$$

Equations for "HYBRID2" (cont'd)

(nt-m) 4.2

$$T_{TCIN} = \begin{cases} T_{SO}/f(\omega_{SO}/\sqrt{T_{SO}}) + T_{ACC}(\omega_{TCN}) & T_{SO} > 0,\ \omega_{SO} > 0 \\ T_{ACC}(\omega_{TCN}) & T_{SO} = 0 \\ (\omega_{IDL})^2/C_{TC\emptyset} + T_{ACC}(\omega_{TCN}) & V = 0,\ A = 0 \\ T_{SO}/T_{QR1} + T_{ACC}(\omega_{TCN}) & T_{SO} > 0,\ \omega_{SO} = 0 \end{cases}$$

$F_{NET} < 0$: Preliminary computations of input RPM, torque and output torque

4.3X

$$\omega'_{TCN}(T_{TCN}, \omega_{SO}) = \begin{cases} \omega_{SO}/f(\omega_{SO}/\sqrt{T_{TCN}}) & T_{TCN} > 0 \text{ and } \omega_{SO} > 0 \\ \sqrt{T_{TCN}C_{TC\emptyset}} & T_{TCN} > 0 \text{ and } \omega_{SO} = 0 \\ \omega_{SO} & T_{TCN} = 0 \text{ and } \omega_{SO} \geq \omega_{IDL} \\ \omega_{IDL} & T_{TCN} = 0 \text{ and } \omega_{SO} < \omega_{IDL} \\ \omega_{SO}f(\omega_{SO}/\sqrt{T_{TCN}}) & T_{TCN} < 0 \text{ and } \omega_{SO} > 0 \\ \omega_{IDL} & T_{TCN} < 0 \text{ and } \omega_{SO} = 0 \end{cases}$$

4.4X $T'_{TCIN} = F(\omega_{SO})$ such that:

$$\omega'_{TCN}(T'_{TCN}, \omega_{SO}) = (T'_{TCIN})$$

where: $\begin{cases} \omega(T) \equiv T^{-1}(T(\omega)) \\ T(\omega) \equiv T_{MMIN}(\omega) - T_{ACC}(\omega) \end{cases}$

4.5X

$$T'_{TCO} = \begin{cases} T'_{TCIN}f(\omega_{SO}/\sqrt{T'_{TCIN}}) & T'_{TCIN} > 0 \text{ and } \omega_{SO} > 0 \\ T'_{TCIN}T_{QR1} & T'_{TCIN} > 0 \text{ and } \omega_{SO} = 0 \\ 0 & T'_{TCIN} = 0 \\ T'_{TCIN} & T'_{TCIN} < 0 \text{ and } \omega_{SO} > 0 \\ (\omega_{IDL})^2/C_{TC\emptyset} & T'_{TCIN} > 0 \text{ and } \omega_{SO} = 0 \end{cases}$$

Equations for "HYBRID2" (cont'd)

$F_{NET} < 0$: Final Computations

(RPM) 4.3

$$\omega_{TCN} = \begin{cases} \omega'_{TCN}(T'_{TCIN}, \omega_{SO}) & T'_{TCO} > T'_{SO} \\ \omega_{SO} f(\omega_{SO}/\sqrt{T_{SO}}) & T'_{TCO} \leq T'_{SO} \text{ and } \omega_{SO} > 0 \\ \omega_{IDL} & T'_{TCO} \leq T'_{SO} \text{ and } \omega_{SO} = 0 \end{cases}$$

(nt-m) 4.4

$$T_{TCIN} = \begin{cases} T'_{TCIN} & T'_{TCO} > T'_{SO} \\ T_{SO} + T_{ACC}(\omega_{TCN}) & T'_{TCO} \leq T'_{SO}, \ \omega_{SO} > 0 \\ (\omega_{IDL})^2/C_{TC\emptyset} + T_{ACC}(\omega_{TCN}) & T'_{TCO} \leq T'_{SO}, \ \omega_{SO} = 0 \end{cases}$$

(nt-m) 4.5

$$T_{TCO} = \begin{cases} T'_{TCO} & T'_{TCO} > T'_{SO} \\ T_{SO} & T'_{TCO} \leq T'_{SO} \text{ and } \omega_{SO} > 0 \\ T_{QRI \quad IDL})^2/C_{TC\emptyset} & T'_{TCO} < T'_{SO} \text{ and } \omega_{SO} = 0 \end{cases}$$

5. Heat Engine, Motor, Brakes (output)

Output Torques

(A) $F_{NET} \geq 0$, $v > 0$, $a_v > 0$

(kw) 5.1 $$P_{COM} = \frac{2\pi}{60,000} T_{TCIN} \omega_{TCN}$$

(kw) 5.2 $$P_{MMAX} = \frac{2\pi}{60,000} \omega_{TCN} T_{MMAX} = \frac{2\pi}{60,000} \omega_{TCN} f(\omega_{TCN})$$

(kw) 5.3

$$P_{NOM} = \begin{cases} P_{EOMIN} & P_{EOMIN} < P_{MMAX} \\ P_{MMAX} & P_{EOMIN} > P_{MMAX} \end{cases}$$

(kw) 5.4

$$P_{HEMIN} = \begin{cases} \frac{2\pi}{60,000} (T_{EOM\emptyset} \omega_{TCN} + \Delta T_{EOM\emptyset}(\omega_{TCN} - \omega_0)) & \omega_{TCN} > \omega_0 \\ \frac{2\pi}{60,000} T_{EOM\emptyset} \omega_{TCN} & \omega_{TCN} \leq \omega_0 \end{cases}$$

(kw) 5.5 $$P_{HEMAX} = \frac{2\pi}{60,000} \omega_{TCN} T_{HEMAX} = \frac{2\pi}{60,000} \omega_{TCN} f(\omega_{TCN})$$

Equations for "HYBRID2" (cont'd)

(A1) On Mode 1

(nt-m) 5.6

$$T_{EO} = \begin{cases} 0 & P_{COM} \leq P_{NOM} \text{ and } V \leq V_{MAX} \\ T_{TCIN} & P_{COM} > P_{NOM} \text{ or } V > V_{MAX},\ P_{COM} \leq P_{HEMIN}, \\ & \quad \text{and } T_{TCIN} < T_{EOMIN} \\ T_{EOMIN} = \frac{60{,}000}{2\pi} P_{HEMIN}/\omega_{TCN} & P_{COM} > P_{NOM} \text{ or } V > V_{MAX}, \\ & P_{COM} \leq P_{HEMIN}, \text{ and } T_{TCIN} \geq T_{EOMIN} \\ T_{TCIN} - T_{MMAX} & P_{COM} > P_{NOM} \text{ or } V > V_{MAX} \text{ and } P_{COM} > P_{HEMIN} \end{cases}$$

(nt-m) 5.7

$$T_{MO} = \begin{cases} T_{TCIN} - T_{EO} & P_{COM} \leq P_{NOM} \text{ and } V \leq V_{MAX}, \\ & \quad \text{or } P_{COM} \leq P_{HEMIN} + P_{MMAX} \\ T_{MMAX} & P_{COM} > P_{NOM} \text{ or } V > V_{MAX}, \\ & \quad \text{and } P_{COM} > P_{HEMIN} + P_{MMAX} \end{cases}$$

(A2) On Mode 2

(nt-m) 5.8

$$T_{EO} = \begin{cases} 0 & P_{COM} \leq P_{HEMIN} \\ T_{HEMAX} & T_{HEMAX} < T_{TCIN} \text{ and } P_{COM} > P_{HEMIN} \\ T_{TCIN} & T_{HEMAX} \geq T_{TCIN} \text{ and } P_{COM} > P_{HEMIN} \end{cases}$$

(nt-m) 5.9

$$T_{MO} = \begin{cases} T_{TCIN} & P_{COM} \leq P_{HEMIN} \\ T_{TCIN} - T_{EO} & P_{COM} > P_{HEMIN} \end{cases}$$

(B) For $v = a_v = 0$ (Car at rest, Modes 1 and 2)

(nt-m) 5.10 $T_{EO} = 0$

(nt-m) 5.11 $T_{MO} = T_{TCIN}$

Equations for "HYBRID2" (cont'd)

(c) For $F_{NET} < 0$ (Decelerating, Modes 1 and 2)

(nt-m) 5.12 $T_{EO} = 0$

(nt-m) 5.13
$$T_{MO} = \begin{cases} 0 & T'_{TCO} > T'_{SO} \text{ or } T_{TCIN} < 0 \\ T_{TCIN} & T'_{TCO} \leq T'_{SO} \text{ and } T_{TCIN} > 0 \end{cases}$$

(nt-m) 5.14
$$T_{GO} = \begin{cases} 0 & T'_{TCO} \leq T'_{SO} \text{ and } T'_{TCIN} > 0 \\ T_{TCIN} & T'_{TCO} \leq T'_{SO} \text{ and } T_{TCIN} \leq 0 \\ T_{MMIN} & T'_{TCO} > T'_{SO} \end{cases}$$

Output RPM and Power

(RPM) 5.15
$$\omega_{EO} = \begin{cases} 0 & P_{COM} \leq P_{NOM} \text{ and } V \leq V_{MAX} \text{ (Mode 1)} \\ \omega_{TCIN} & P_{COM} > P_{NOM} \text{ or } V > V_{MAX} \text{ (Mode 1)} \\ 0 & P_{COM} \leq P_{NOM} \text{ (Mode 2)} \\ \omega_{TCN} & P_{COM} > P_{NOM} \text{ (Mode 2)} \\ 0 & F_{NET} < 0, \text{ or } V = 0 \text{ and } a_v = 0 \end{cases} \Big\} F_{NET} \geq 0$$

(kw) 5.16 $P_{EO} = \frac{2\pi}{60{,}000} T_{EO} \omega_{EO}$

(kw) 5.17 $P_{MO} = \frac{2\pi}{60{,}000} T_{MO} \omega_{TCN}$

(kw) 5.18
$$P_{GO} = \begin{cases} 0 & F_{NET} \geq 0 \\ \frac{2\pi}{60{,}000} T_{GO} \omega_{TCN} & F_{NET} < 0 \end{cases}$$

(kw) 5.19
$$P_{BRK} = \begin{cases} 0 & F_{NET} \geq 0 \text{ or } T'_{TCO} \leq T'_{SO} \\ P_{RW} - P_D = \frac{2\pi}{60{,}000} \omega_{DO}[F_{NET} R_T - T_{DO}] & F_{NET} < 0 \text{ and } T'_{TCO} > T'_{SO} \end{cases}$$

Equations for "HYBRID2" (cont'd)

6. Heat Engine Input (fuel)

(g/hr) 6.1
$$F_C = \begin{cases} 0 & P_{EO} = 0 \\ P_{EO}\ BSFC = P_{EO} f(\omega_{EO}, BMEP) = P_{EO} f(\omega_{EO}, \frac{125.664\ T_{EO}}{displ.}) & P_{EO} \neq 0 \end{cases}$$

7. Battery Output

(kw) 7.1
$$P_B = \begin{cases} P_{NLD} + P_{MO}/\mu_M + P_{GO}\mu_M, & P_{MO} < P' \text{ and } P_{GO} + P' > 0 \\ P_{NLD} + P_{MO}/\mu_M + (P_{MO} - P')(\frac{1}{\mu'_M} - \frac{1}{\mu_M}) + P_{GO}\mu_M, & P_{MO} > P' \text{ and } P_{GO} + P' > 0 \\ P_{NLD} + P_{MO}/\mu_M + P_{GO}\mu_M + (P_{GO} + P')(\mu_M - \mu'_M), & P_{MO} < P' \text{ and } P_{GO} + P' < 0 \\ P_{NLD} + P_{MO}/\mu_M + (P_{MO} - P')(\frac{1}{\mu'_M} - \frac{1}{\mu_M}) + P_{GO}\mu_M + (P_{GO} + P')(\mu_M - \mu'_M), & P_{MO} > P' \text{ and } P_{GO} + P' < 0 \end{cases}$$

8. Energy and Fuel Consumed Over Time Interval (0, T)

Rolling Resistance and Aerodynamic

(mj) 8.1
$$E_R + E_A = 10^{-3} \int_0^T (P_A + P_R)dt = 10^{-6} \int_0^T (F_A + F_R)Vdt$$

8.2 Drivetrain Energy (final drive, transmission, torque converter)

(mj)
$$E_{DT} = 10^{-3} \int_0^T (|P_T - P_D| + |P_{SO} - P_T| + |P_{LTC}|)dt$$

$$= \begin{cases} 10^{-6} \frac{2\pi}{60} \int_0^T (|T_{TO}\omega_{TO} - T_{DO}\omega_{DO}| + |T_{SO}\omega_{SO} - T_{TO}\omega_{TO}| + |T_{TCIN}\omega_{TCN} - T_{SO}\omega_{SO}|)dt & F_{NET} \geq 0 \text{ or } T_{TCO} \leq T_{SO} \\ 10^{-6} \frac{2\pi}{60} \int_0^T (|T_{TO}\omega_{TO} - T_{DO}\omega_{DO}| + |T_{SO}\omega_{SO} - T_{TO}\omega_{TO}| + |T_{MMIN}\omega_{TCN} - T_{SO}\omega_{SO}|)dt & FNET < 0 \text{ and } T_{TCO} > T_{SO} \end{cases}$$

Brakes

(mi) 8.3
$$E_{BRK} = 10^{-3} \int_0^T |P_{BRK}|dt$$

Equations for "HYBRID2" (cont'd)

Engine Output

(mj) 8.4 $$E_{EO} = 10^{-3} \int_0^T P_{EO}dt$$

Motor/Generator Output

(mj) 8.5 $$E_{MO} = 10^{-3} \int_0^T P_{MO}dt \; ; \; E_{GO} = 10^{-3} \int_0^t P_{GO}dt$$

Battery Output

(mj) 8.6 $$E_B = 10^{-3} \int_0^T P_B dt$$

Fuel

(g) 8.7 $$F_{Cf} = \frac{1}{3600} \int_0^T F_C dt$$

9. Fuel and Energy Consumption on Driving Cycle K

Battery Depletion

9.1 $$P'_{MOT}(t) = 10^3 P_B$$

(w) 9.2 $$P_{MOT}(t) = \frac{1}{2\Delta t_f} \int_{t - t_f}^{t + \Delta t_f} P'_{MOT}(t)dt$$

(mj) 9.3 $$E_{RG}(t) = \begin{cases} f\left(\frac{P_{MOT}(t)}{W_B}\right) W_B & P_{MOT}(t) \geq 0 \\ \frac{W_B E_{BMAX}}{\mu_{RG}} & P_{MOT}(t) < 0 \end{cases}$$

$(\frac{1}{km})$ 9.4 $$Depl_K = \frac{1}{3600 D_K} \int_0^T \frac{P_{MOT}(t)}{E_{RG}(t)} dt$$

Fuel Consumption (Mode 1 and Mode 2)

(g/km) 9.6 $$FC_{1_K} = \frac{F_{CT_K}}{D_K} \qquad FC_{2_K} = \frac{F_{CT_K}}{D_K}$$

Equations for "HYBRID2" (cont'd)

Energy Consumption (Mode 1 and Mode 2)

(mj/km) 9.7 $EC_{1_K} = \frac{E_{B_K}}{3.6D_K}$ $EC_{2_K} = \frac{E_{B_K}}{3.6D_K}$

10. Composite Cycles Fuel and Energy (k ranges from 1 to the number of driving cycles; j ranges from 1 the number of composite cycles)

Battery Energy Consumption

(kw) 10.1 $\overline{BD}_j = \sum_{k=1}^{n} \gamma_{jk} Depl_k$

Energy Consumption, Mode 1 and Mode 2

(mj/km) 10.2 $\overline{EC}_{1j} = \sum_{k=1}^{n} \gamma_{jk} EC_{1k}$

(mj/km) 10.3 $\overline{EC}_{2j} = \sum_{k=1}^{n} \gamma_{jk} EC_{2k}$

Fuel Consumption, Mode 1 and Mode 2

(g/km) 10.4 $\overline{FC}_{1j} = \sum_{k=1}^{n} \gamma_{jk} FC_{1k}$

10.5 $\overline{FC}'_{2j} = \sum_{k=1}^{n} \gamma_{jk} FC_{2k}$

(g/km) $\overline{FC}_{2j} = \frac{(\overline{FC}'_{2j} \cdot \overline{EC}_{1j} - \overline{FC}_{1j}\overline{EC}_{2j})}{(\overline{EC}_{1j} - \overline{EC}_{2j})}$ { Corrected for non-zero energy consumption on Mode 2.

Average Velocity

(m/sec.) 10.6 $\overline{V}_j = \frac{1}{\sum_{k=1}^{n} \frac{\gamma_{jk}}{\overline{V}_k}} = \frac{3600}{\sum_{k=1}^{n} \frac{\gamma_{jk} T_k}{D_k}}$

Specific Power

(kw) 10.7 $\overline{P}_{spj} = \frac{10^3 \overline{EC}_{1j} \overline{V}_j}{W_B}$

■

Equations for "HYBRID2" (cont'd)

Range

(km) 10.8 $$R_j = \frac{DB_{max}}{\overline{BD}_j}$$

Fraction of Driving on Mode 1 for Each Composite Cycle

(-) 10.9 $$R_{\phi j} = \begin{cases} 0 & D_{warm} > D_{supj} \\ R_j/\overline{D}_j & D_{warm} \leq D_{supj},\ R_j \leq D_{sup_{(j-1)}} - D_{warm} \\ 1 - \frac{D_{warm}}{\overline{D}_j} & D_{warm} \leq D_{supj},\ R_j > D_{sup_{(j-1)}} - D_{warm},\ R_j > D_{supj} - D_{warm} \\ \frac{R_j}{\overline{D}_j}\left(1 - \frac{(R_j - D_{sup_{(j-1)}} + D_{warm})^2}{2R_j(D_{supj} - D_{sup_{(j-1)}})}\right) & \begin{cases} D_{warm} \leq D_{supj} \\ R_j > D_{sup_{(j-1)}} - D_{warm} \\ R_j \leq D_{supj} - D_{warm} \end{cases} \end{cases}$$

Mode Averaged Fuel and Energy

(g/km) 10.10 $$\underline{FC}_{mj} = R_{\phi j}\overline{FC}_{1j} + (1 - R_{\phi j})\overline{FC}_{2j}$$

(mj/km) 10.11 $$\underline{EC}_{mj} = R_{\phi j}\overline{EC}_{1j} + (1 - R_{\phi j})\overline{EC}_{2j}$$

11. Overall Yearly Averages (fuel and energy)

(g/km) 11.1 $$\underline{FC} = \sum_{j=1}^{N} dj\underline{FC}_{mj}$$

(mj/km) 11.2 $$\underline{EC} = \sum_{j-1}^{N} dj\underline{EC}_{mj}$$

Equations for "HYBRID2" (cont'd)

Battery Life

(km) 11.3 $\underline{D_D} = \dfrac{\underline{EC} \cdot \underline{D_{st}}}{.04W_B}$

(km) 11.4 $\underline{BL} = \underline{Dst}\ f\ (\underline{D_D})$

Fuel Economy

(km/l) 11.5 $\underline{FE} = 10^3 \dfrac{F_{sg}}{\underline{FC}}$

Wall Plug Output

(kw/km) 11.6 $\underline{WP} = \dfrac{\underline{EC}}{\mu_{CH}}$

NOMENCLATURE FOR "HYBRID2"

Parameters Equation	Program	Units	Description
	NPRM	-	Number of RPM's (engine)
	NMEP	-	Number of BMEP's
	FUELSG	g/cc	Fuel specific gravity
	DISPL	cc	Displacement
	SKALE	-	Scale factor for engine
	RPM(20)	rpm	RPM (engine)
	TQMAX(20)	ntm	Maximum torque (engine)
	BMEP(20)	bar	Brake mean effective pressure
	BSFC(20,20)	gw/kw-hr	Brake specific fuel consumption
	NOP	-	Number of engine powers
	RPMBST	rpm	Best operating speed (engine)
	PBEST	kw	Best operating power (engine)
	PEOP(20)	kw	Engine power
	RPMEOP(20)	rpm	Optimum engine speed at specified power
	NSPMO	-	Number RPM's (motor)
	EMUM	-	Motor efficiency
	EMUG	-	Generator efficiency
	TMSKL	-	Scale factor for motor
	PINNLD	kw	No load input power (motor)
	RPMIDL	rpm	Idle speed (motor)
	RPMOPM	rpm	Best operating speed (motor) (used with CVT)
	SPMO(20)	rpm	RPM (motor)
	TMOMAX(20)	ntm	Maximum torque (motor)
	TMOMIN(20)	ntm	Minimum torque (motor)
	JCVT	-	= 1 → Continuously variable transmission (CVT)
	EMUCVT	-	Efficiency (CVT)
	RATUP	-	Speed up ratio (CVT)
	RATDN	-	Slow down ratio (CVT)
	NTSP	-	Number of TSP's, TQR's and SPR's
	CTCCRP	rpm^2/ntm	NI**2/TI(STALL)
	TSP(20)	rpm/ ntm	$NO/\sqrt{TO}$
	TSP2(20)		$NO/\sqrt{TI}$
	TQR(20)	-	TO/TI
	SPR(20)	-	NO/NI

(used with CVT)

Nomenclature for "HYBRID2" (cont'd)

Parameters		Units	Description
Equation	Program		
	NGEAR	-	Number of gears
	NTH	-	Number of THSET's, UPSHIFT's, and DNSHFT's
	UPSEL	rpm	Shift up for electric operation
	DNSEL	rpm	Shift down for electric operation
	NLOCK(5)	-	Lock-up (gearbox)
	TRATIO(5)	-	Ratio (gearbox)
	CT1(5)	ntm	Spin loss coefficient (gearbox)
	CT2(5)	ntm/rpm	Spin loss coeffient (gearbox)
	EMUT(5)	-	Torque efficiency (gearbox)
	THSET(5)	kw	Set of powers defining shift function
	UPSHFT(5)	rpm	Upshift RPM
	DNSHFT(5)	rpm	Downshift RPM
	NDDSCH	-	Number discharge depths (battery)
	NDENS	-	Number of specific powers (battery)
	WB	kg	Battery mass
	EBMAX	wh/kg	Energy density (battery)
	EMURG	-	Average regeneration efficiency (battery)
	EMURG2	-	Maximum regeneration efficiency (battery)
	CHGEFF	-	Recharge efficiency (battery)
	DDISCH(20)	-	Discharge depth (battery)
	CYCLES(20)	-	Cycle life (battery)
	PDENS(20)	kw	Specific power (battery)
	EDENS(20)	mj	Specific energy (battery)
	DRATIO	-	Differential ratio
	CD1	ntm	Spin loss coefficient (differential)
	CD2	ntm/rpm	Spin loss coefficient (differential)
	EMUD	-	Torque efficiency (differential)
	RTIRE	m	Rolling radius (tire)
	CTIRE1	-	Rolling resistance coefficient (tire)
	CTIRE2	1/(km/hr)	Rolling resistance coefficient (tire)
	NAX	-	Number speeds and torques (accessory load)
	RPMAX(20)	rpm	Speed (accessory load)
	TAX(20)	nt-m	Torque (accessory load)
	VMASS	kg	Vehicle mass
	DLI	$kg \cdot m^2$	Driveline inertia

Nomenclature for "HYBRID2" (cont'd)

Parameters			
Equation	Program	Units	Description
	CDA	m^2	Drag coefficient * area
	NCYCLE	-	Number of driving cycles
	NTC(3)	-	TIMC, SPEDC matrix size
	NPRTC(3)	-	Output print flag for driving cycle
	NUNITS	-	Miles/hr to km/hr conversion flag
	DTC(3)	sec	Time interval for driving cycles
	TFC(3)	sec	Final time for driving cycles
	TIMC(3,200)	sec	Time } driving cycle
	SPEDC(3,200)	km/hr	Speed }
	NCOMP	-	DSUP, DNC, GAMMA matrix size
	DSTAV	-	Average usage } travel distribution data
	DWARM	km	Warm up distance }
	DSUP(30)	km	Maximum distance - driving cycle } travel distribution data
	DNC(30)	-	Fraction of total distance }
	GAMMA(30,3)	-	Driving cycle weights }
	NCASE	-	Number of cases
	TEOMIN	nt·m	Minimum engine torque (Mode 1)
	TEOMN2	nt·m	Minimum engine torque (Mode 2)
	DBMAX	-	Battery discharge limit
	PEOMIN	kw	Heat engine minimum power
	VMAX	km/hr	Transition speed
	DTFLTR	-	Low-pass filter sub-interval length

Nomenclature for "HYBRID2" (cont'd)

Variables			
Equation	Program	Units	Description
	A(3)	m/sec^2	Vehicle acceleration motor
	ABPI	j	Absolute value battery power
	BDBAR(30)	kw	Battery energy consumption - composite cycle
	BLIFE	km	Battery life (expected)
	BPI	j	Battery power
	DBAR(30)	km	Interpolated values of driving cycle distances
	DDAV	km	Average distance on driving cycle
	DELT	sec	Time interval size
	DEPL(3)	l/km	Battery depletion on each cycle
	DIST(3)	m	Distance on each cycle
	DLOW	km	Minimum distance on driving cycle
	DT	sec	Time increment
	EB	mj	System output energy - Mode 1
	EB2	mj	System output energy - Mode 2
	EBMAX	wh/kg	Energy density (battery)
	ECAV	mj/km	Yearly average energy consumption
	ECBAR(30)	mj/km	Composite cycles energy consumption - Mode 1
	ECBAR2(30)	mj/km	Composite cycles energy consumption - Mode 2
	ECHE(3)	mj/km	Cycle heat engine energy consumption
	ECMAV(30)	mj/km	Composite cycles mode averaged energy consumption
	ECONS(3)	mj/km	Cycle energy consumption - Mode 1
	ECONS2(3)	mj/km	Cycle energy consumption - Mode 2
	ECSYS(3)	mj/km	Cycle system energy consumption
	EHEAV	mj/km	Yearly avg. heat engine energy consumption
	EHEBAR(30)	mj/km	Composite cycles heat engine energy consumption
	EK(80)	-	YDOT hold vector
	EKIN	mj	Kinetic energy
	ERG(2800)	mj	Battery specific energy
	ESYSAV	mj/km	Yearly average system energy consumption
	ESYSBR(30)	mj/km	Composite cycles system energy consumption
	FCAV	g/km	Yearly average fuel consumption
	FCBAR(30)	g/km	Composite cycles fuel consumption - Mode 1
	FCBAR2(30)	g/km	Composite cycles fuel consumption - Mode 2
	FCMAV(30)	g/km	Composite cycles mode averaged fuel consumption
	FCONS	g/km	Cycle fuel consumption, Mode 1
	FCONS2	g/km	Cycle fuel consumption, Mode 2

Nomenclature for "HYBRID2" (cont'd)

Variables		Units	Description
Equation	Program		
	FEAV	km/l	Yearly averaged fuel economy
	HEEF	-	Heat engine energy fraction
	IBP(20)	-	Storage for cycle battery power distribution
	IFLAG	-	Denotes when gearshift has occurred
	INT1	-	Interpolation subroutine (1 dimensional)
	INT2	-	Interpolation subroutine (2 dimensional)
	ITIBP	-	Total number of cycle time iterations
	K	-	Print skip control counter
	NPRNT	-	Number of skips between successive prints
	NTIME	-	Number of TIME's and SPEED's
	PBRK	kw	Braking power
	PEO	kw	Engine output power
	PEO2	kw	Engine output power 2
	PEOP	kw	Set of powers for optimum power curve
	PGO	kw	Regenerative output power
	PMO	kw	Motor output power
	PMO2	kw	Motor output power 2
	PMOT(2800)	w	Storage for cycle specific battery powers
	PRW	kw	Rear wheel power
	PSO	kw	Hybrid system output power
	PSO2	kw	Hybrid system output power 2
	RANGE(30)	km	Range for new battery discharge limit
	RFRAC(30)	-	Composite cycles fraction of total driving distance
	RPMTC1	rpm	Torque converter RPM - Mode 1
	RPMTC2	rpm	Torque converter RPM - Mode 2
	SPEED(200)	km/hr	Driving cycle speed
	SPENG(25)	mj	Composite cycle specific energy - Mode 1
	SPPWR(25)	kw	Composite cycles specific power - Mode 1
	T	sec	Time in simulation
	TIME(200)	sec	Driving cycle time
	TTMP	sec	Time holder
	V(6)	km/hr	Vehicle speed vector
	VAVG(3)	m/sec	Average velocity
	VBAR(25)	m/sec	Composite cycles average speed
	VMASS2	kg	Effective vehicle inertial mass
	VMPS	m/sec	Vehicle speed

Nomenclature for "HYBRID2" (cont'd)

Variables			
Equation	Program	Units	Description
	VRECIP	sec/m	Reciprocal of avg. velocity for composite cycle
	VTMP	m/sec	Velocity hold
	VTMPL	m/sec	Velocity hold
	WPAV	kw/km	Yearly average wall plug output
	Y(1)	mj	Aerodynamic + rolling resistance energy loss
	Y(2)	mj	Drivetrain energy output - Mode 1
	Y(3)	mj	Drivetrain energy output - Mode 2
	Y(4)	mj	Braking output energy
	Y(5)	mj	System output energy - Mode 1
	Y(6)	mj	System output energy - Mode 2
	Y(7)	mj	Engine output energy - Mode 1
	Y(8)	mj	Engine output energy - Mode 2
	Y(9)	mj	Motor shaft output energy - Mode 1
	Y(10)	mj	Motor shaft output energy - Mode 2
	Y(11)	m/sec	Velocity
	Y(12)	km	Distance
	Y(13)	mj	Generator output energy
	Y(14)	sec	Heat engine on time - Mode 1
	Y(15)	sec	Heat engine on time - Mode 2
	Y(16)	g	Fuel output energy - Mode 1
	Y(17)	g	Fuel output energy - Mode 2
	Y(18)	mj	System output energy - Mode 1
	Y(19)	mj	System output energy - Mode 2
	YDOT(20)	-	Runga-Kutta integration variables
	YTMP(20)	-	Runga-Kutta integration variables
	MOT	-	Number of entries in vector PMOT after power function smoothed
	JGEAR	-	Gear Mode 1 currently in
	JGEAR2	-	Gear Mode 2 currently in
	NTM	-	Number of entries in vector PMOT
	TF	sec	Final time in simulation of cycle

Nomenclature for "VEHIC"

Variables			
quation	Program	Units	Description
	BRMEP	bar	Brake mean effective pressure
	BRMEP2	bar	Brake mean effective pressure 2
	FA	nt	Aerodynamic drag force
	FAC	nt	Acceleration force on vehicle
	FC	g/hr	Engine fuel rate - Mode 1
	FC2	g/hr	Engine fuel rate - Mode 2
	FG	nt	Road grade force
	FNET	nt	Net vehicle force
	FR	nt	Rolling resistance force
	PA	kw	Aerodynamic drag power
	PD	kw	Differential output power
	PLTC	kw	Power load on torque converter - Mode 1
	PLTC2	kw	Power load on torque converter - Mode 2
	PR	kw	Rolling resistance power
	PRW	kw	Rear wheel power
	PT	kw	Transmission output power
	RPMDO	rpm	Differential output rpm
	RPMEO	rpm	Engine output rpm
	RPMEO2	rpm	Engine output rpm 2
	RPMSO	rpm	Hybrid system output rpm
	RPMSO2	rpm	Hybrid system output rpm 2
	RPMTO	rpm	Transmission output rpm
	SFC	g/kwh	Specific fuel consumption
	TDO	nt·m	Differential output torque
	TEO	nt·m	Engine output torque
	TEO2	nt·m	Engine output torque 2
	TLFD	nt·m	Differential torque loss
	TLFT	nt·m	Transmission torque loss
	TLFT2	nt·m	Transmission torque loss 2
	TSO	nt·m	Hybrid system output torque
	TSO2	nt·m	Hybrid system output torque 2
	TTO	nt·m	Transmission output torque
	NLCK	-	Gear lock-up flag, Mode 1
	NLCK2	-	Gear lock-up flag, Mode 2

Nomenclature for "PMOVR"

Variables		Units	Description
Equation	Program		
	CC	mw/(ntm·rpm)	(rad/sec)/(1000 rpm)
	PCOM	kw	System power command
	PHEMAX	kw	Maximum heat engine power
	PHEMIN	kw	Minimum heat engine power
	PMMAX	kw	Maximum motor power
	PNOM	kw	Nominal power
	RPMTC	rpm	Torque converter rpm
	RPMTCN	rpm	Torque converter input rpm
	RPMTCO	rpm	Torque converter output rpm
	TACC	nt·m	Accessory output torque
	TGO	nt·m	Generator output torque
	THEMAX	nt·m	Maximum heat engine torque
	TMMAX	nt·m	Maximum motor torque
	TMMIN	nt·m	Minimum motor torque
	TMO	nt·m	Motor output torque
	TMO2	nt·m	Motor output torque 2
	TTCIN	nt·m	Torque converter input torque
	TTCN1	nt·m	Torque converter input torque - Mode 1
	TTCN2	nt·m	Torque converter input torque - Mode 2
	TTCO	nt·m	Torque converter output torque
	JBRK	-	Braking (not) required flag

Nomenclature for "TQCON"

Variables		Units	Description
Equation	Program		
	SPRAT	-	Speed ratio
	TQRAT	-	Torque ratio
	TSPAR	rpm/$\sqrt{nt \cdot m}$	Torque-speed parameter (output/output)
	TSPAR2	rpm/$\sqrt{nt \cdot m}$	Torque-speed parameter (input/output)

INPUT FORMAT

PROGRAM	HYBRID2	NAME	
ROUTINE	MAIN PROGRAM	DATE	PAGE OF

TYPE	STATEMENT NO	COMMENT	FORTRAN STATEMENT (0 ZERO, 0 = ALPHA O; 1 = ONE, 1 = ALPHA I; 2 = TWO, 2 = ALPHA Z)	SERIAL NUMBER
			RUN DATA	
		NCASE		
			CASE DATA	
		TEOMIN	TEOMAX DAMAX PEOMIN VMAX	
		DT FLTR		

PROGRAM HYBRID2 | NAME

ROUTINE HYREAD | DATE | PAGE 1 OF 3

FORTRAN STATEMENT — 0 = ZERO, O = ALPHA O; 1 = ONE, I = ALPHA I; 2 = TWO, Z = ALPHA Z

TYPE	STATEMENT NO.	CONT.	
			ENGINE DATA:
			NRPM, NMEP, FUELSG, DISPL, SKALE
			RPM(1), TQMAX(1), ..., RPM(NRPM), TQMAX(NRPM), BMEP(1), ...
			BMEP(NMEP), BSFC(1,1), ..., BSFC(NRPM,NMEP)
			NOP, RPMBST, PBEST
			PEOP(1), RPMEOP(1), ..., PEOP(NOP), RPMEOP(NOP)
			MOTOR/GENERATOR DATA
			NSPMO, EMUM, EMUG, TMSKL, PINNLD, RPMIDL, RPMDPM
			SPMO(1), TMOMAX(1), TMOMIN(1), ..., SPMO(NSPMO), TMOMAX(NSPMO), TMOMIN(NSPMO)
			JCVT
			CONTINUOUSLY VARIABLE TRANSMISSION DATA
			EMUCVT, RATIOP, RATION
			TORQUE CONVERTER DATA
			NTSP
			CT, CZRO, TSP(1), TQR(1), SPR(1), ..., TSP(NTSP), TQR(NTSP)
			SPR(NTSP)

SERIAL NUMBER

301

FORM NO. GRC 109 REV. 1

PROGRAM	HYBRID2	NAME	
ROUTINE	HYREAD	DATE	PAGE 2 OF 3

TYPE	STATEMENT NO	CONT	FORTRAN STATEMENT (0 = ZERO, 0 = ALPHA 0; 1 = ONE, 1 = ALPHA 1; 2 = TWO, 2 = ALPHA 2)	SERIAL NUMBER
			TIRE/SET DATA	
		NGEAR	NTH	UPSEL	DNSEL				
	NLOCK	(1)	TIRED(1)	UPSHFT(1)	DNSHFT(1)			NLOCK(NGEAR)	
	NRATIO	(NGEAR)	GI1(NGEAR)	GI2(NGEAR)	EMUT(NGEAR)				
	TIRSET	(1)	UPSHFT(1)	DNSHFT(1)		TIRSET(NTH)	UPSHIFT(NTH)	DNSHFT(NTH)	
			BATTERY DATA						
	NDDSCH		NDENS	WB	EBMAX	EMURG	EMURG2	CHGEFF	
	DDISCH	(1)	CYCLES(1)		DDISCH(NDDSCH)	CYCLES(NDDSCH)			
	PDENS	(1)	EDENS(1)		PDENS(NDENS)	EDENS(NDENS)			
			DIFFERENTIAL AND TIRE DATA						
	DRATIO		CD2	CD3	EMUD	RATIOE	CTIRE1	CTIRE2	
			ACCESSORY DATA						
	RPMAX	NAX (1)	TAX(1)		RPMAX(NAX)	TAX(NAX)			
			VEHICLE DATA						
		VMASS	DLI	CDA					
			DRIVING SCHEDULE DATA						
	NCYCLE								
	NTC	(1)	NPRTC(1)	NUNITS	DTC(1)	TTC(1)		NTC(NCYCLE	
	NPRTC	(NCYCLE)	NUNITS	DTC(NCYCLE)	TTC(NCYCLE)				
	TIMC	(1,1)	SPEEDC(1,1)		TIMC(NCYCLE,NT	SPEEDC(NCYCLE,NT			

FORM NO. GRC 109 REV. 1

PROGRAM HYBRID2 | NAME

ROUTINE HYREAD | DATE | PAGE 3 OF 3

FORTRAN STATEMENT

0 - ZERO
O - ALPHA O
1 = ONE
I = ALPHA I
2 = TWO
Z = ALPHA Z

TYPE	STATEMENT NO.	CONT	FORTRAN STATEMENT	SERIAL NUMBER
			TRUE DISTRIBUTION LAMB	
		N	COMP DSTAV DWARM	
	DS		P(1) DNC(1) GAMMA(1,1) DSUPS DNC(NCDME GAMMA(NCOATNCOVE	

303

HYBRID 2

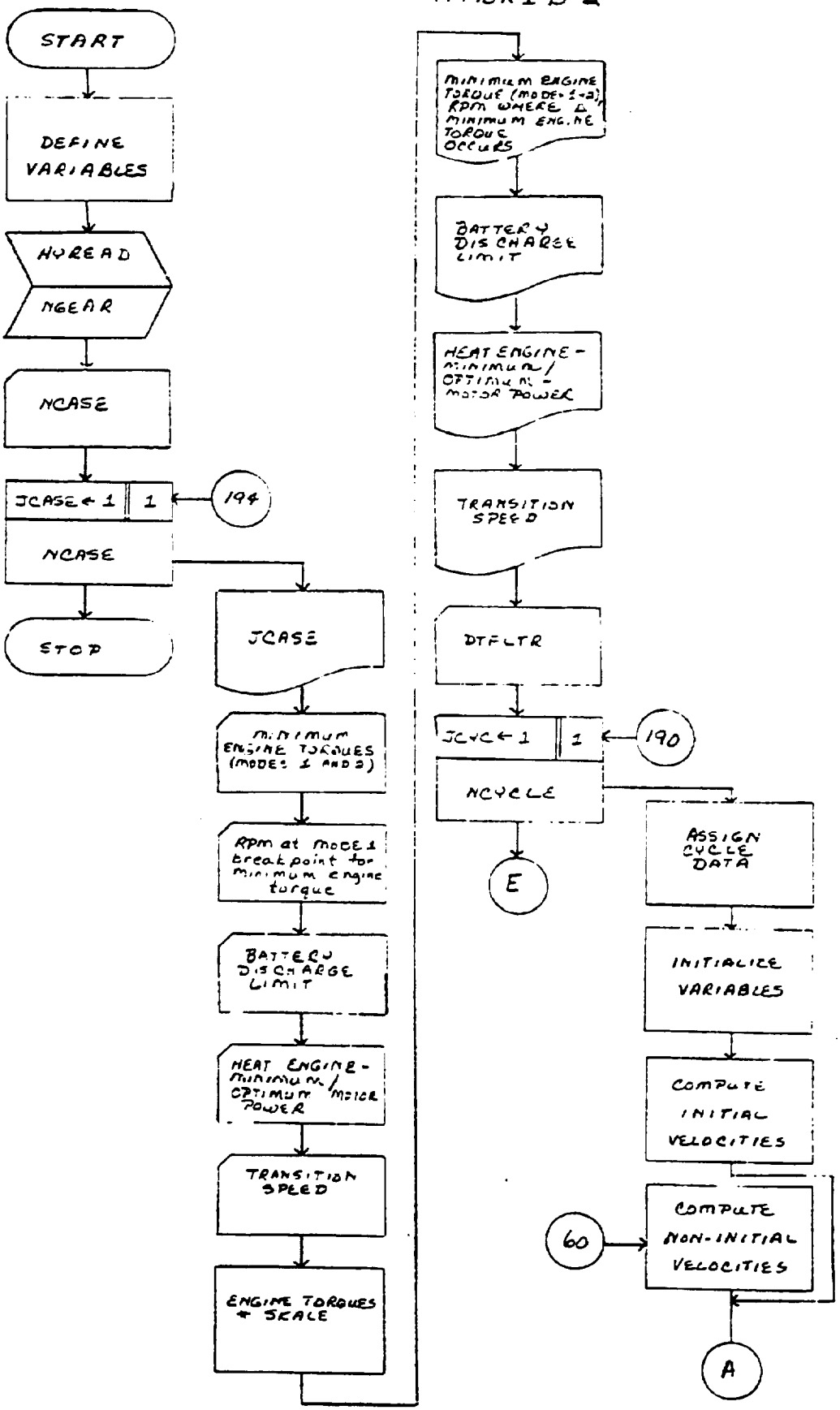
START
DEFINE VARIABLES
HYREAD
NGEAR
NCASE
JCASE ← 1
1
194
NCASE
STOP
JCASE
MINIMUM ENGINE TORQUES (MODES 1 AND 2)
RPM at MODE 1 breakpoint for minimum engine torque
BATTERY DISCHARGE LIMIT
HEAT ENGINE - MINIMUM / OPTIMUM - MOTOR POWER
TRANSITION SPEED
ENGINE TORQUES ← SCALE
MINIMUM ENGINE TORQUE (MODES 1-2), RPM WHERE A MINIMUM ENG. NE TORQUE OCCURS
BATTERY DISCHARGE LIMIT
HEAT ENGINE - MINIMUM / OPTIMUM - MOTOR POWER
TRANSITION SPEED
DTFLTR
JCYC ← 1
1
190
NCYCLE
E
ASSIGN CYCLE DATA
INITIALIZE VARIABLES
COMPUTE INITIAL VELOCITIES
60
COMPUTE NON-INITIAL VELOCITIES
A

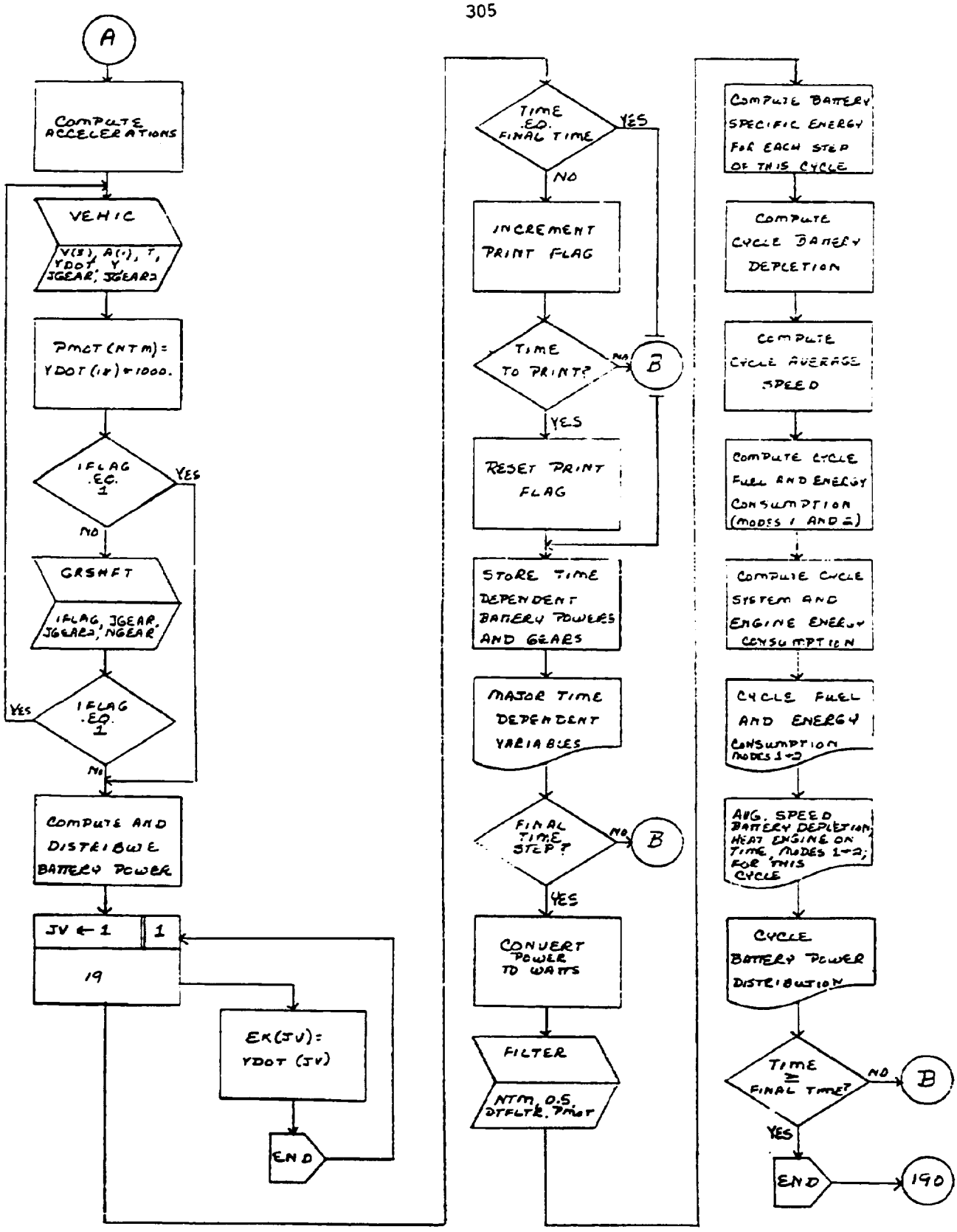
A
COMPUTE ACCELERATIONS
VEHIC
V(I), A(I), T, YDOT, Y, JGEAR, JGEAR2
PMOT(NTM) = YDOT(IP) * 1000.
IFLAG .EQ. 1
YES
NO
GRSHFT
IFLAG, JGEAR, JGEAR2, NGEAR
IFLAG .EQ. 1
YES
NO
COMPUTE AND DISTRIBUTE BATTERY POWER
JV ← 1
1
19
EK(JV) = YDOT(JV)
END
TIME .EQ. FINAL TIME
YES
NO
INCREMENT PRINT FLAG
TIME TO PRINT?
NO
B
YES
RESET PRINT FLAG
STORE TIME DEPENDENT BATTERY POWERS AND GEARS
MAJOR TIME DEPENDENT VARIABLES
FINAL TIME STEP?
NO
B
YES
CONVERT POWER TO WATTS
FILTER
NTM, 0.5, DTFLTR, PMOT
COMPUTE BATTERY SPECIFIC ENERGY FOR EACH STEP OF THIS CYCLE
COMPUTE CYCLE BATTERY DEPLETION
COMPUTE CYCLE AVERAGE SPEED
COMPUTE CYCLE FUEL AND ENERGY CONSUMPTION (MODES 1 AND 2)
COMPUTE CYCLE SYSTEM AND ENGINE ENERGY CONSUMPTION
CYCLE FUEL AND ENERGY CONSUMPTION MODES 1-2
AVG. SPEED, BATTERY DEPLETION, HEAT ENGINE ON TIME, MODES 1-2; FOR THIS CYCLE
CYCLE BATTERY POWER DISTRIBUTION
TIME ≥ FINAL TIME?
NO
B
YES
END
190

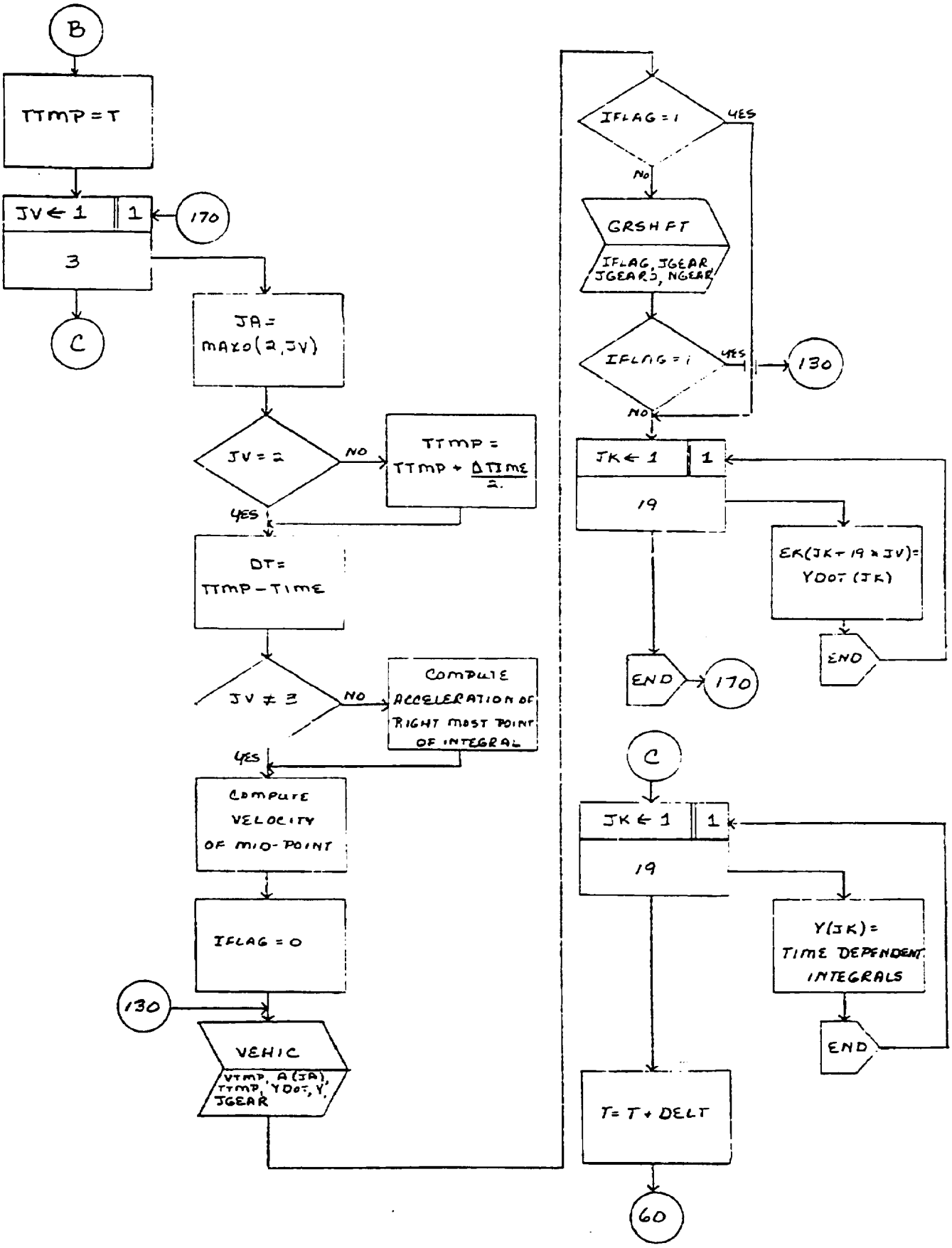
B
TTMP = T
JV ← 1
1
3
170
C
JA = MAX0(2,JV)
JV = 2
NO
TTMP = TTMP + ΔTIME/2.
YES
DT = TTMP - TIME
JV ≠ 3
NO
COMPUTE ACCELERATION OF RIGHT MOST POINT OF INTEGRAL
YES
COMPUTE VELOCITY OF MID-POINT
IFLAG = 0
130
VEHIC
VTMP, A(JA), TTMP, YDOT, Y, JGEAR
IFLAG = 1
YES
NO
GRSHFT
IFLAG, JGEAR, JGEAR5, NGEAR
IFLAG = 1
YES
130
NO
JK ← 1
1
19
YK(JK+19*JV) = YDOT(JK)
END
END
170
C
JK ← 1
1
19
Y(JK) = TIME DEPENDENT INTEGRALS
END
T = T + DELT
60

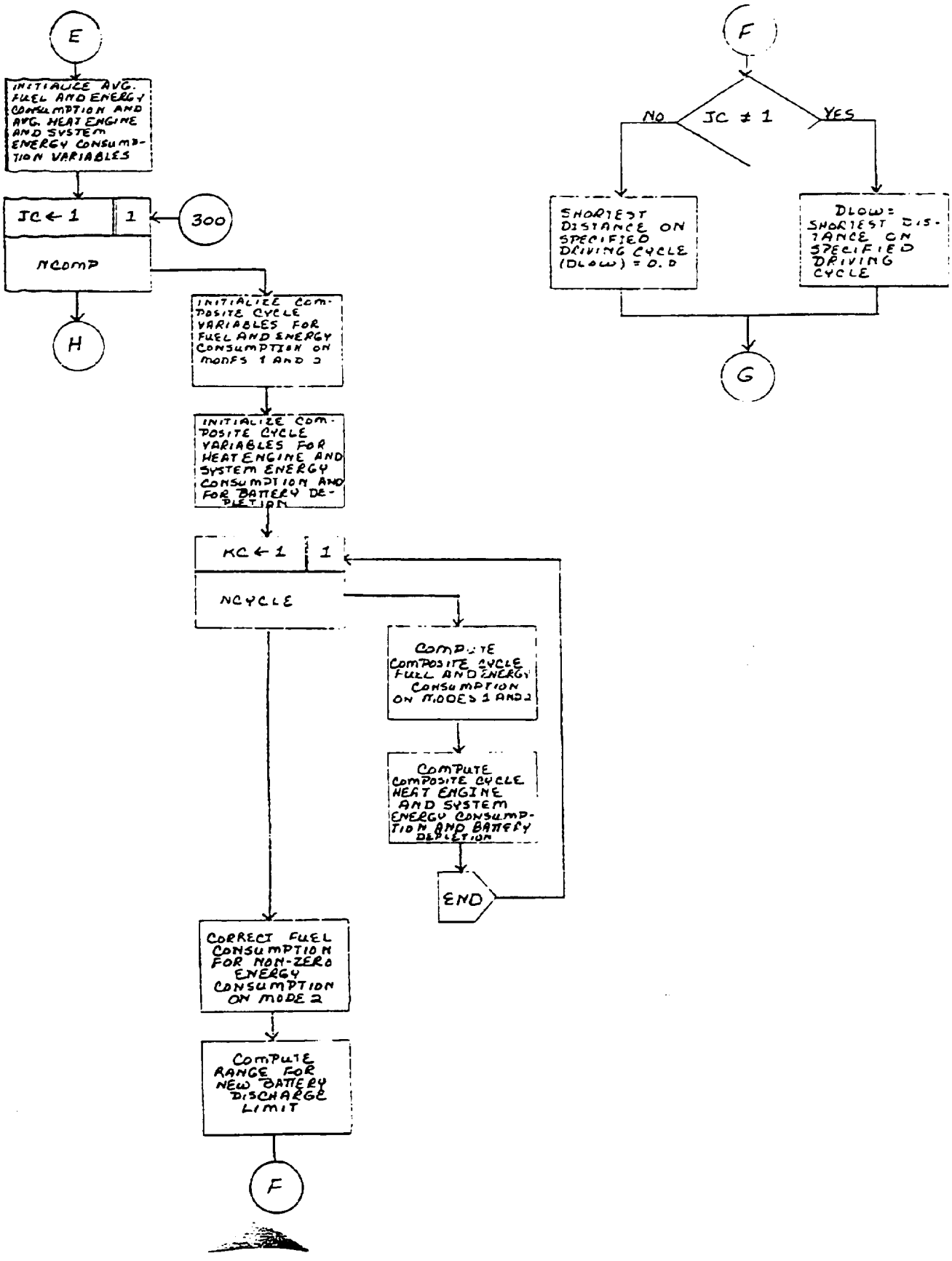
E
INITIALIZE AVG. FUEL AND ENERGY CONSUMPTION AND AVG. HEAT ENGINE AND SYSTEM ENERGY CONSUMPTION VARIABLES
JC ← 1
1
300
NCOMP
H
INITIALIZE COMPOSITE CYCLE VARIABLES FOR FUEL AND ENERGY CONSUMPTION ON MODES 1 AND 2
INITIALIZE COMPOSITE CYCLE VARIABLES FOR HEAT ENGINE AND SYSTEM ENERGY CONSUMPTION AND FOR BATTERY DEPLETION
KC ← 1
1
NCYCLE
COMPUTE COMPOSITE CYCLE FUEL AND ENERGY CONSUMPTION ON MODES 1 AND 2
COMPUTE COMPOSITE CYCLE HEAT ENGINE AND SYSTEM ENERGY CONSUMPTION AND BATTERY DEPLETION
END
CORRECT FUEL CONSUMPTION FOR NON-ZERO ENERGY CONSUMPTION ON MODE 2
COMPUTE RANGE FOR NEW BATTERY DISCHARGE LIMIT
F
F
JC ≠ 1
NO
YES
SHORTEST DISTANCE ON SPECIFIED DRIVING CYCLE (DLOW) = 0.0
DLOW = SHORTEST DISTANCE ON SPECIFIED DRIVING CYCLE
G

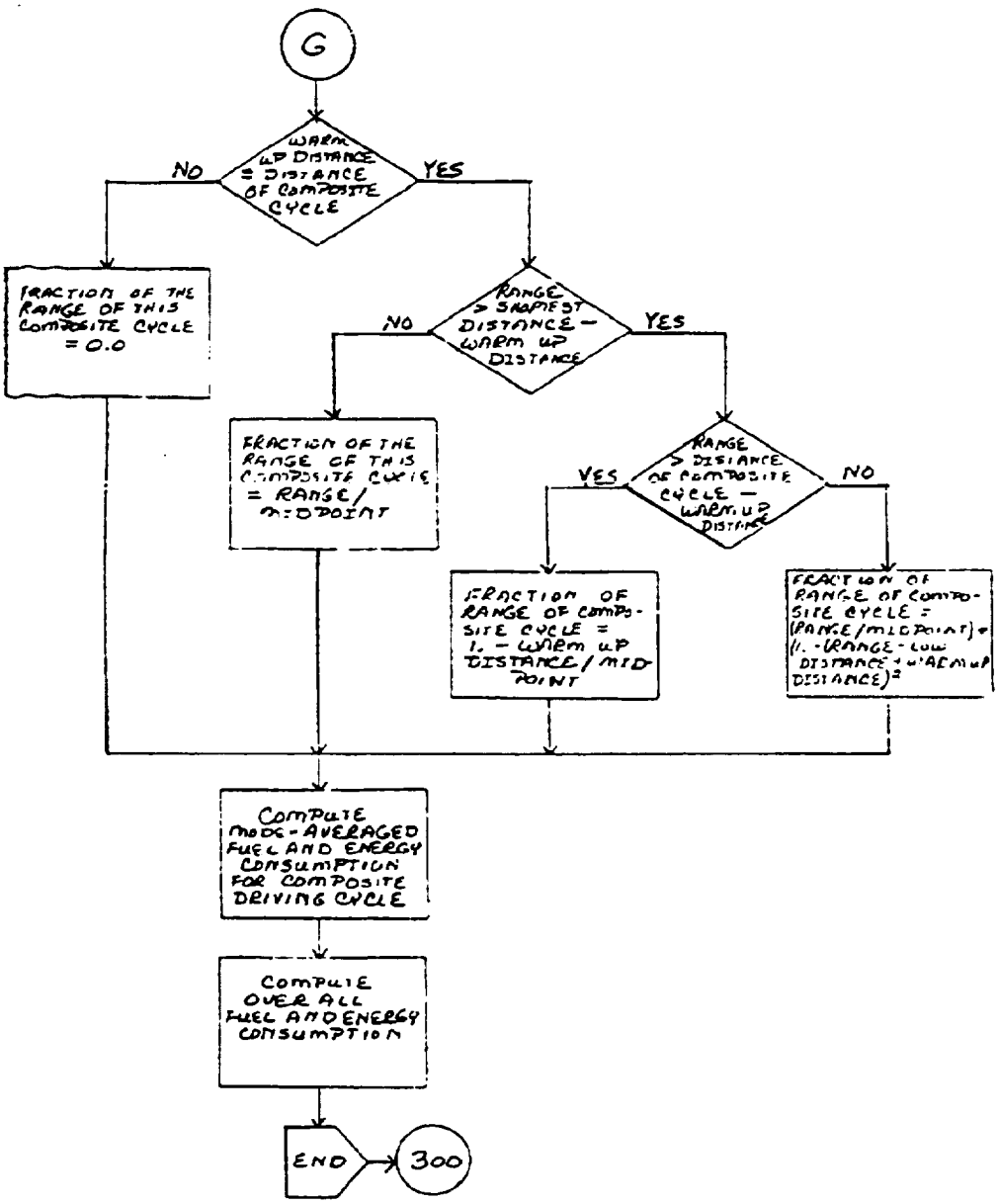
G
WARM UP DISTANCE = DISTANCE OF COMPOSITE CYCLE
NO
YES
FRACTION OF THE RANGE OF THIS COMPOSITE CYCLE = 0.0
RANGE > SHORTEST DISTANCE - WARM UP DISTANCE
NO
YES
FRACTION OF THE RANGE OF THIS COMPOSITE CYCLE = RANGE / MIDPOINT
RANGE > DISTANCE OF COMPOSITE CYCLE - WARM UP DISTANCE
YES
NO
FRACTION OF RANGE OF COMPOSITE CYCLE = 1. - WARM UP DISTANCE / MIDPOINT
FRACTION OF RANGE OF COMPOSITE CYCLE = (RANGE/MIDPOINT) * (1. - (RANGE - LOW DISTANCE - WARM UP DISTANCE)^2
COMPUTE MODE-AVERAGED FUEL AND ENERGY CONSUMPTION FOR COMPOSITE DRIVING CYCLE
COMPUTE OVER ALL FUEL AND ENERGY CONSUMPTION
END
300

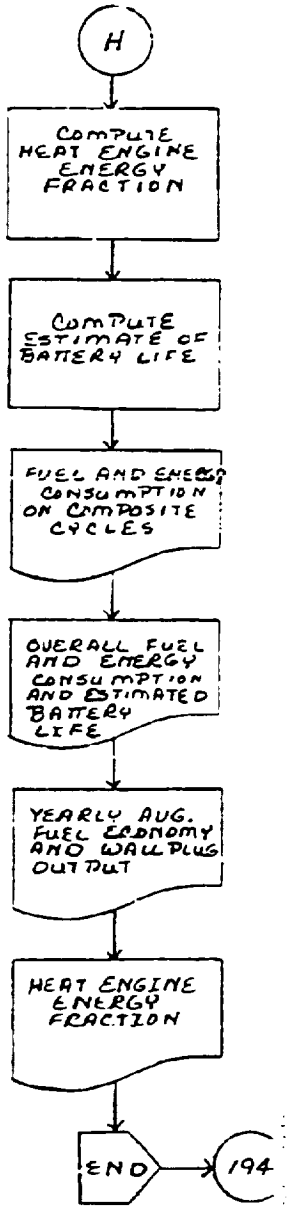
H
COMPUTE HEAT ENGINE ENERGY FRACTION
COMPUTE ESTIMATE OF BATTERY LIFE
FUEL AND ENERGY CONSUMPTION ON COMPOSITE CYCLES
OVERALL FUEL AND ENERGY CONSUMPTION AND ESTIMATED BATTERY LIFE
YEARLY AVG. FUEL ECONOMY AND WALL PLUG OUTPUT
HEAT ENGINE ENERGY FRACTION
END
194

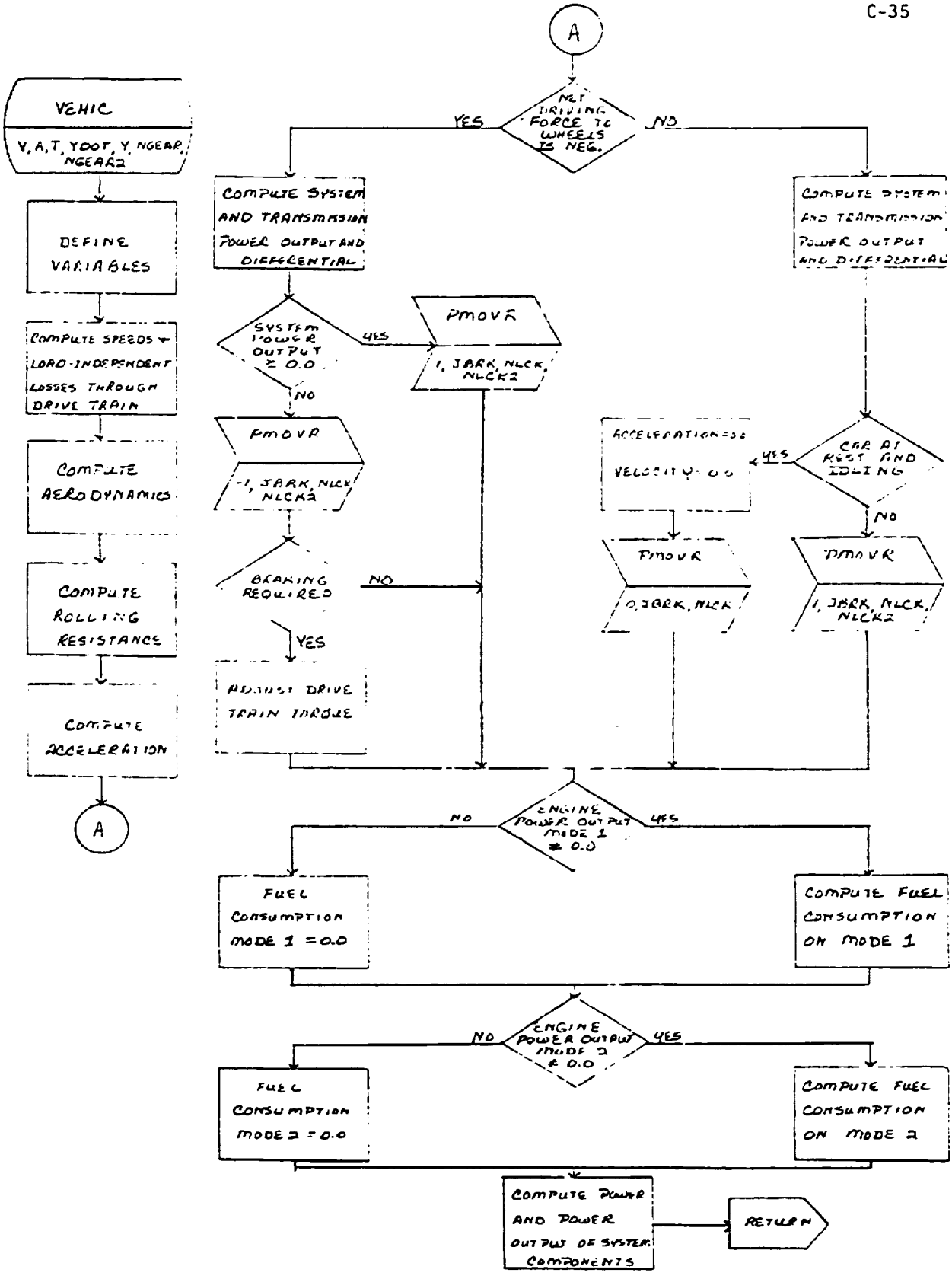
VEHIC
V, A, T, YDOT, Y, NGEAR, NGEAR2
DEFINE VARIABLES
COMPUTE SPEEDS - LOAD-INDEPENDENT LOSSES THROUGH DRIVE TRAIN
COMPUTE AERODYNAMICS
COMPUTE ROLLING RESISTANCE
COMPUTE ACCELERATION
A
A
NET DRIVING FORCE TO WHEELS IS NEG.
YES
NO
COMPUTE SYSTEM AND TRANSMISSION POWER OUTPUT AND DIFFERENTIAL
SYSTEM POWER OUTPUT ≥ 0.0
YES
PMOVR
1, JBRK, NLCK, NLCK2
NO
PMOVR
-1, JBRK, NLCK, NLCK2
BRAKING REQUIRED
NO
YES
ADJUST DRIVE TRAIN TORQUE
COMPUTE SYSTEM AND TRANSMISSION POWER OUTPUT AND DIFFERENTIAL
ACCELERATION=0.0 VELOCITY=0.0
YES
CAR AT REST AND IDLING
NO
PMOVR
0, JBRK, NLCK
PMOVR
1, JBRK, NLCK, NLCK2
ENGINE POWER OUTPUT MODE 1 ≠ 0.0
NO
YES
FUEL CONSUMPTION MODE 1 = 0.0
COMPUTE FUEL CONSUMPTION ON MODE 1
ENGINE POWER OUTPUT MODE 2 ≠ 0.0
NO
YES
FUEL CONSUMPTION MODE 2 = 0.0
COMPUTE FUEL CONSUMPTION ON MODE 2
COMPUTE POWER AND POWER OUTPUT OF SYSTEM COMPONENTS
RETURN

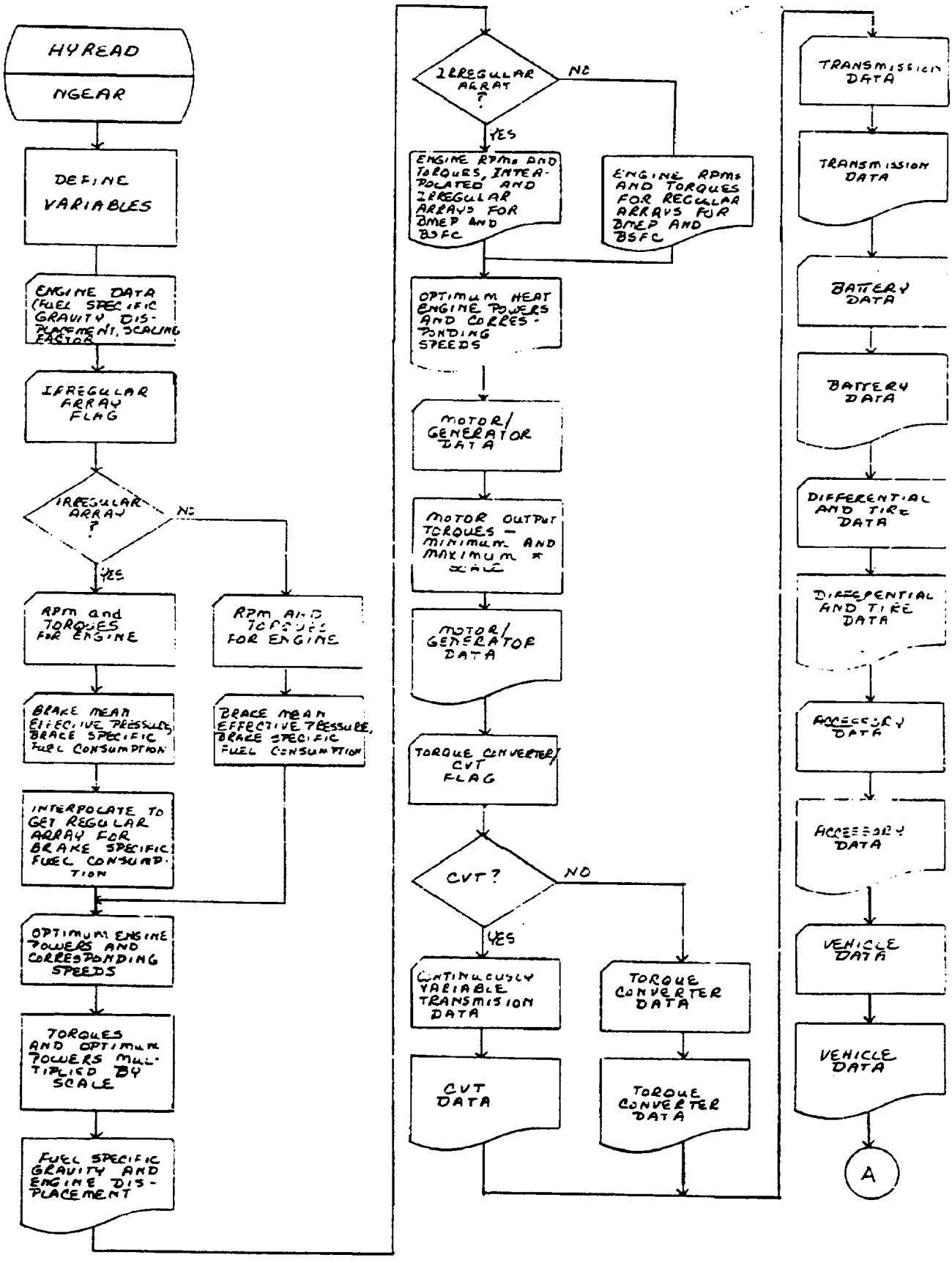
HYREAD
NGEAR
DEFINE VARIABLES
ENGINE DATA (FUEL SPECIFIC GRAVITY, DISPLACEMENT, SCALING FACTOR
IRREGULAR ARRAY FLAG
IRREGULAR ARRAY ?
NO
YES
RPM and TORQUES FOR ENGINE
BRAKE MEAN EFFECTIVE PRESSURE, BRAKE SPECIFIC FUEL CONSUMPTION
INTERPOLATE TO GET REGULAR ARRAY FOR BRAKE SPECIFIC FUEL CONSUMPTION
RPM AND TORQUES FOR ENGINE
BRAKE MEAN EFFECTIVE PRESSURE, BRAKE SPECIFIC FUEL CONSUMPTION
OPTIMUM ENGINE POWERS AND CORRESPONDING SPEEDS
TORQUES AND OPTIMUM POWERS MULTIPLIED BY SCALE
FUEL SPECIFIC GRAVITY AND ENGINE DISPLACEMENT
IRREGULAR ARRAY ?
NO
YES
ENGINE RPMs AND TORQUES, INTERPOLATED AND IRREGULAR ARRAYS FOR BMEP AND BSFC
ENGINE RPMs AND TORQUES FOR REGULAR ARRAYS FOR BMEP AND BSFC
OPTIMUM HEAT ENGINE POWERS AND CORRESPONDING SPEEDS
MOTOR/GENERATOR DATA
MOTOR OUTPUT TORQUES - MINIMUM AND MAXIMUM * SCALE
MOTOR/GENERATOR DATA
TORQUE CONVERTER/CVT FLAG
CVT ?
NO
YES
CONTINUOUSLY VARIABLE TRANSMISION DATA
CVT DATA
TORQUE CONVERTER DATA
TORQUE CONVERTER DATA
TRANSMISSION DATA
TRANSMISSION DATA
BATTERY DATA
BATTERY DATA
DIFFERENTIAL AND TIRE DATA
DIFFERENTIAL AND TIRE DATA
ACCESSORY DATA
ACCESSORY DATA
VEHICLE DATA
VEHICLE DATA
A

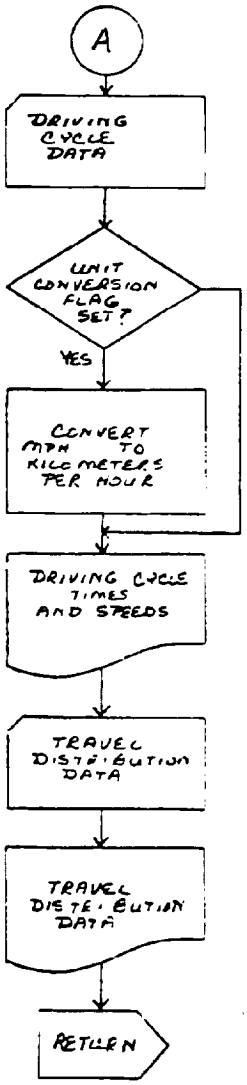
A
DRIVING CYCLE DATA
UNIT CONVERSION FLAG SET?
YES
CONVERT MPH TO KILOMETERS PER HOUR
DRIVING CYCLE TIMES AND SPEEDS
TRAVEL DISTRIBUTION DATA
TRAVEL DISTRIBUTION DATA
RETURN

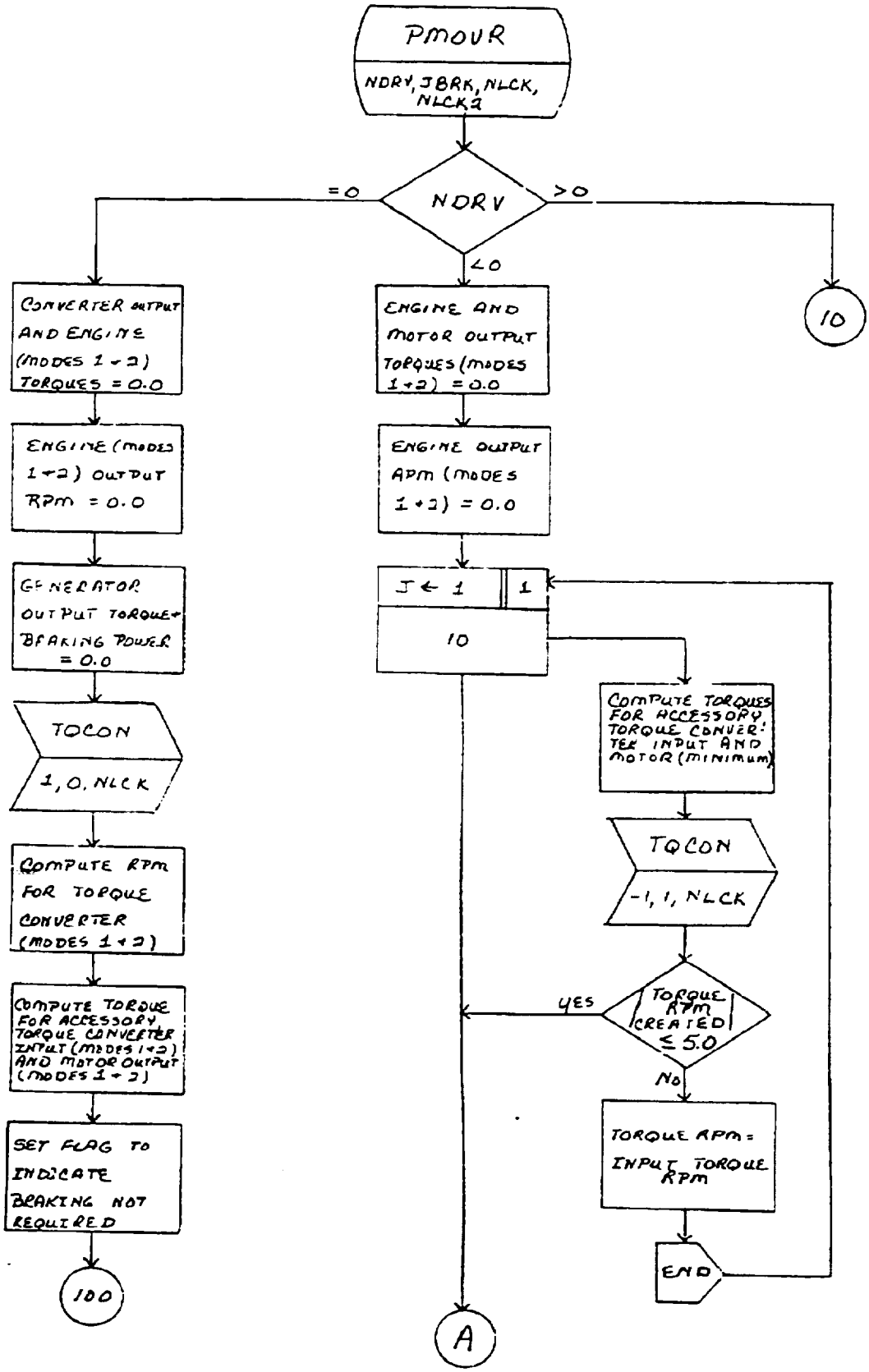
PMOVR
NDRV, JBRK, NLCK, NLCK2
NDRV
=0
<0
>0
CONVERTER OUTPUT AND ENGINE (MODES 1+2) TORQUES = 0.0
ENGINE (MODES 1+2) OUTPUT RPM = 0.0
GENERATOR OUTPUT TORQUE+ BRAKING POWER = 0.0
TOCON
1, 0, NLCK
COMPUTE RPM FOR TORQUE CONVERTER (MODES 1+2)
COMPUTE TORQUE FOR ACCESSORY TORQUE CONVERTER INPUT (MODES 1+2) AND MOTOR OUTPUT (MODES 1+2)
SET FLAG TO INDICATE BRAKING NOT REQUIRED
100
ENGINE AND MOTOR OUTPUT TORQUES (MODES 1+2) = 0.0
ENGINE OUTPUT RPM (MODES 1+2) = 0.0
J ← 1
1
10
A
10
COMPUTE TORQUES FOR ACCESSORY TORQUE CONVERTER INPUT AND MOTOR (MINIMUM)
TQCON
-1, 1, NLCK
YES
TORQUE RPM CREATED ≤ 5.0
No
TORQUE RPM = INPUT TORQUE RPM
END

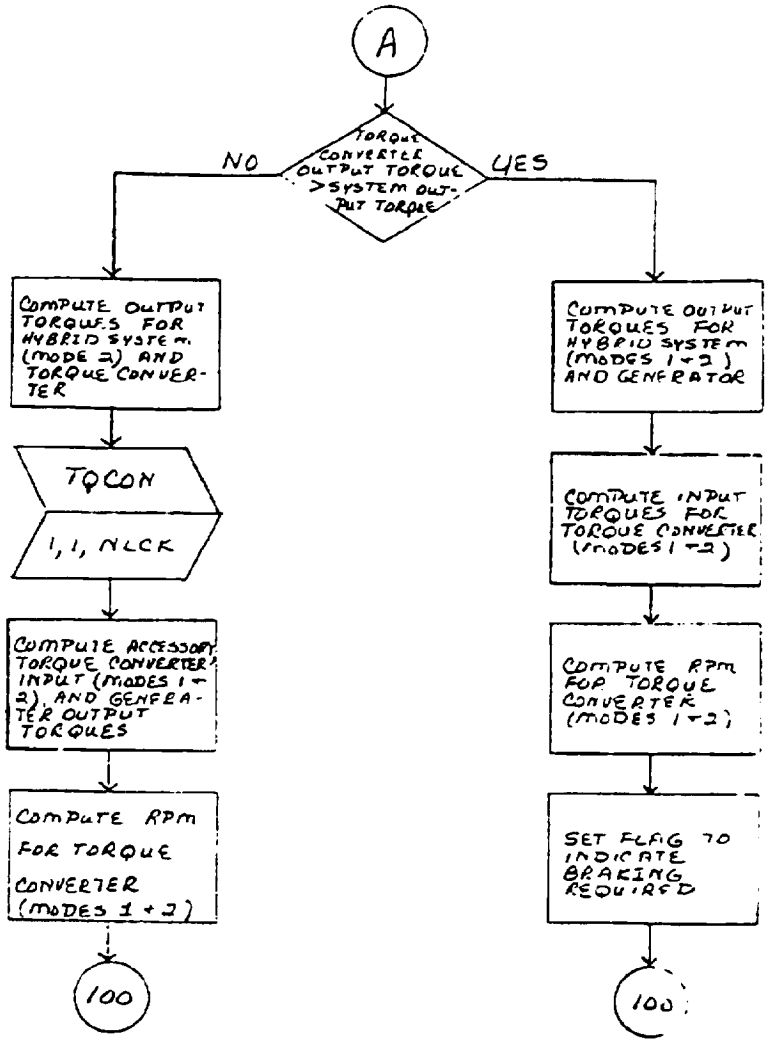
A
TORQUE CONVERTER OUTPUT TORQUE > SYSTEM OUTPUT TORQUE
NO
YES
COMPUTE OUTPUT TORQUES FOR HYBRID SYSTEM (MODE 2) AND TORQUE CONVERTER
TQCON
1, 1, NLCK
COMPUTE ACCESSORY TORQUE CONVERTER INPUT (MODES 1 + 2) AND GENERATOR OUTPUT TORQUES
COMPUTE RPM FOR TORQUE CONVERTER (MODES 1 + 2)
100
COMPUTE OUTPUT TORQUES FOR HYBRID SYSTEM (MODES 1 + 2) AND GENERATOR
COMPUTE INPUT TORQUES FOR TORQUE CONVERTER (MODES 1 + 2)
COMPUTE RPM FOR TORQUE CONVERTER (MODES 1 + 2)
SET FLAG TO INDICATE BRAKING REQUIRED
100

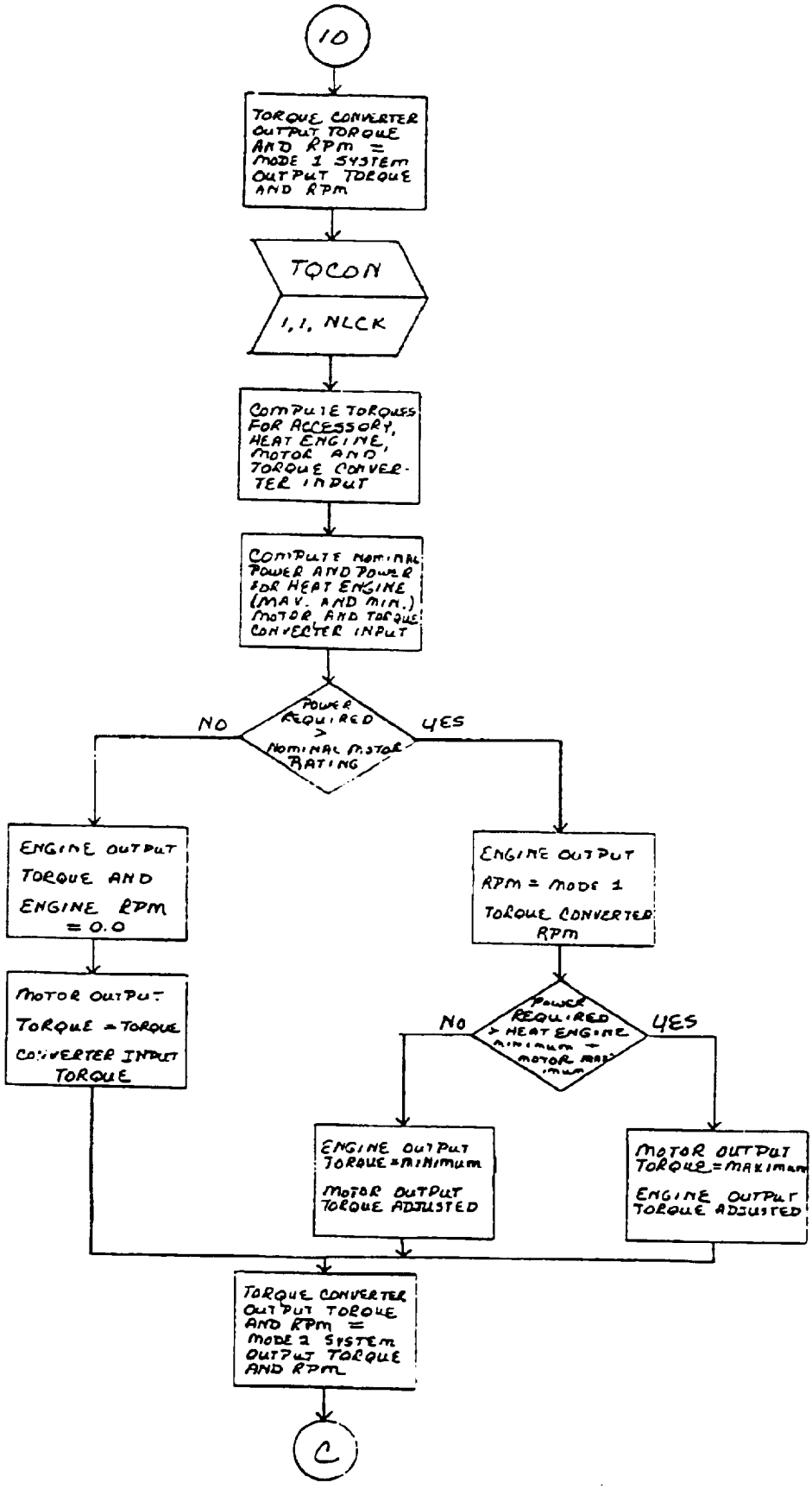
10
TORQUE CONVERTER OUTPUT TORQUE AND RPM = MODE 1 SYSTEM OUTPUT TORQUE AND RPM
TQCON
1, 1, NLCK
COMPUTE TORQUES FOR ACCESSORY, HEAT ENGINE, MOTOR AND TORQUE CONVERTER INPUT
COMPUTE NOMINAL POWER AND POWER FOR HEAT ENGINE (MAX. AND MIN.) MOTOR AND TORQUE CONVERTER INPUT
POWER REQUIRED > NOMINAL MOTOR RATING
NO
YES
ENGINE OUTPUT TORQUE AND ENGINE RPM = 0.0
MOTOR OUTPUT TORQUE = TORQUE CONVERTER INPUT TORQUE
ENGINE OUTPUT RPM = MODE 1 TORQUE CONVERTER RPM
POWER REQUIRED > HEAT ENGINE MINIMUM + MOTOR MAXIMUM
NO
YES
ENGINE OUTPUT TORQUE = MINIMUM
MOTOR OUTPUT TORQUE ADJUSTED
MOTOR OUTPUT TORQUE = MAXIMUM
ENGINE OUTPUT TORQUE ADJUSTED
TORQUE CONVERTER OUTPUT TORQUE AND RPM = MODE 2 SYSTEM OUTPUT TORQUE AND RPM
C

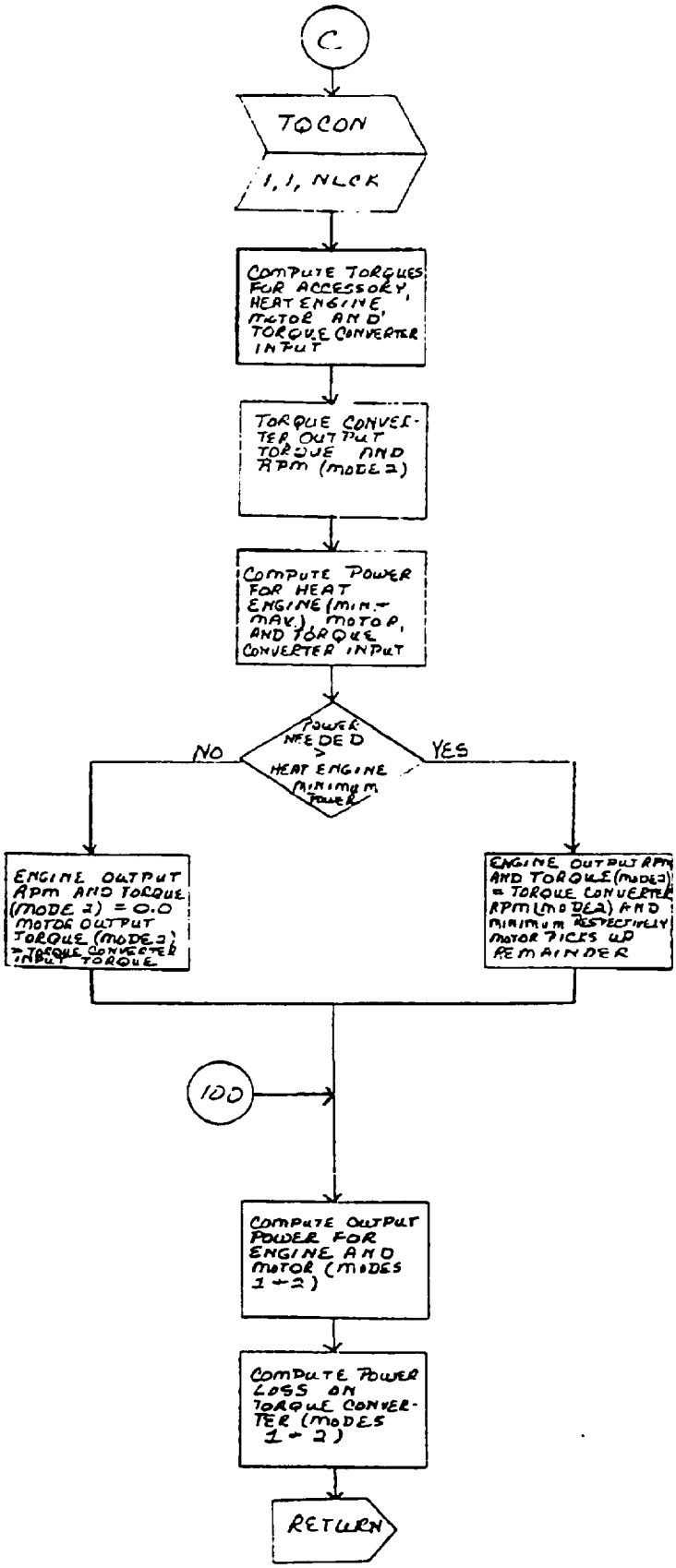
C
TQCON
1, 1, NLCK
COMPUTE TORQUES FOR ACCESSORY, HEAT ENGINE, MOTOR AND TORQUE CONVERTER INPUT
TORQUE CONVERTER OUTPUT TORQUE AND RPM (MODE 2)
COMPUTE POWER FOR HEAT ENGINE (MIN. - MAX.), MOTOR, AND TORQUE CONVERTER INPUT
POWER NEEDED > HEAT ENGINE MINIMUM POWER
NO
YES
ENGINE OUTPUT RPM AND TORQUE (MODE 2) = 0.0 MOTOR OUTPUT TORQUE (MODE 2) = TORQUE CONVERTER INPUT TORQUE
ENGINE OUTPUT RPM AND TORQUE (MODE 2) = TORQUE CONVERTER RPM (AND DEL 2) AND MINIMUM RESPECTIVELY MOTOR TAKES UP REMAINDER
100
COMPUTE OUTPUT POWER FOR ENGINE AND MOTOR (MODES 1-2)
COMPUTE POWER LOSS ON TORQUE CONVERTER (MODES 1-2)
RETURN

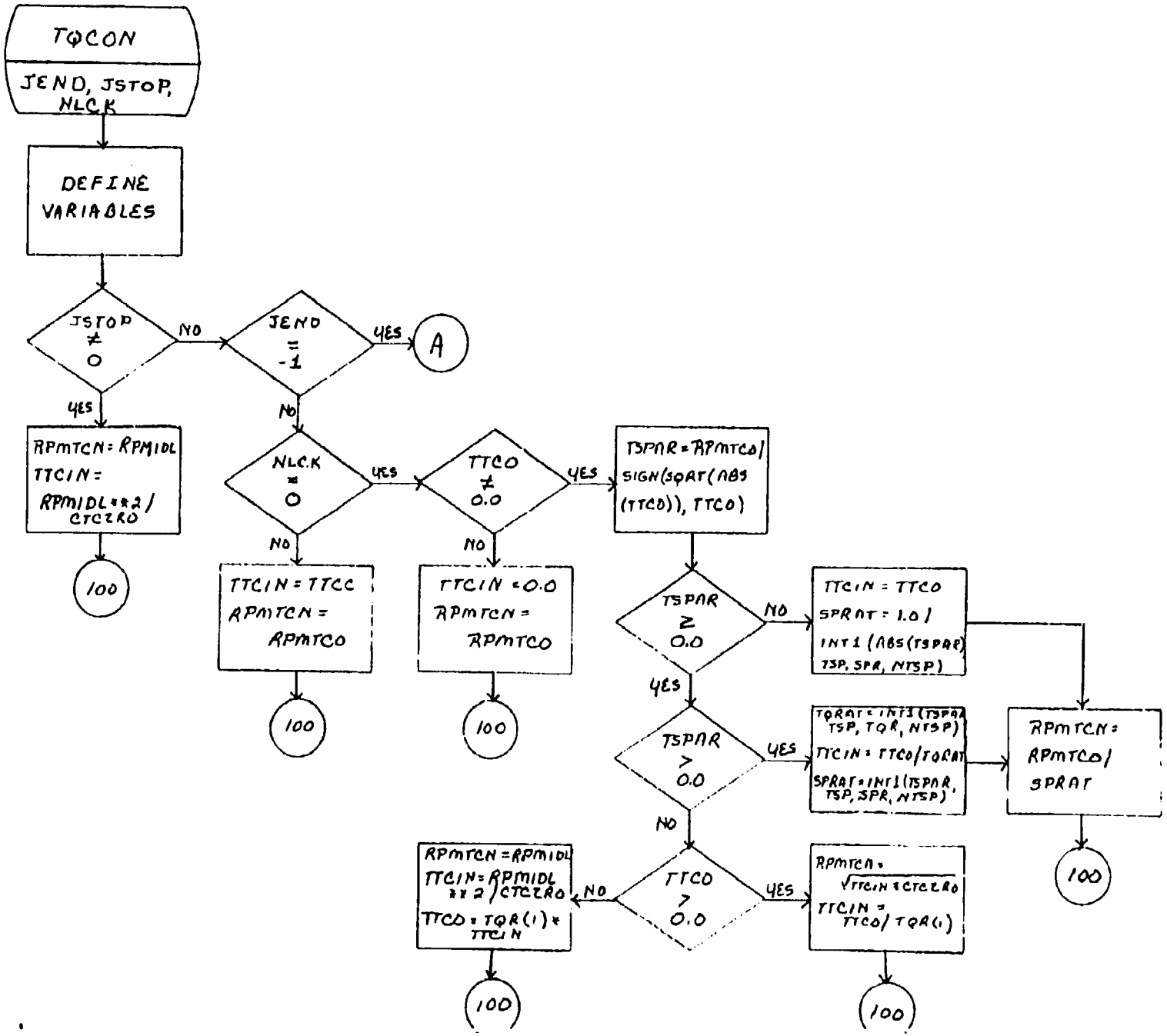
TQCON
JEND, JSTOP, NLCK
DEFINE VARIABLES
JSTOP ≠ 0
NO
JEND = -1
YES
A
YES
RPMTCN = RPMIDL
TTCIN = RPMIDL**2 / CTCZRO
100
NO
NLCK = 0
YES
TTCO ≠ 0.0
YES
TSPAR = RPMTCO / SIGN(SQRT(ABS(TTCO)), TTCO)
NO
TTCIN = TTCO
RPMTCN = RPMTCO
100
NO
TTCIN = 0.0
RPMTCN = RPMTCO
100
TSPAR ≥ 0.0
NO
TTCIN = TTCO
SPRAT = 1.0 / INT1(ABS(TSPAR), TSP, SPR, NTSP)
YES
TSPAR > 0.0
YES
TQRAT = INT1(TSPAR, TSP, TQR, NTSP)
TTCIN = TTCO / TQRAT
SPRAT = INT1(TSPAR, TSP, SPR, NTSP)
RPMTCN = RPMTCO / SPRAT
100
NO
TTCO > 0.0
NO
RPMTCN = RPMIDL
TTCIN = RPMIDL**2 / CTCZRO
TTCO = TQR(1) * TTCIN
100
YES
RPMTCN = SQRT(TTCIN * CTCZRO)
TTCIN = TTCO / TQR(1)
100

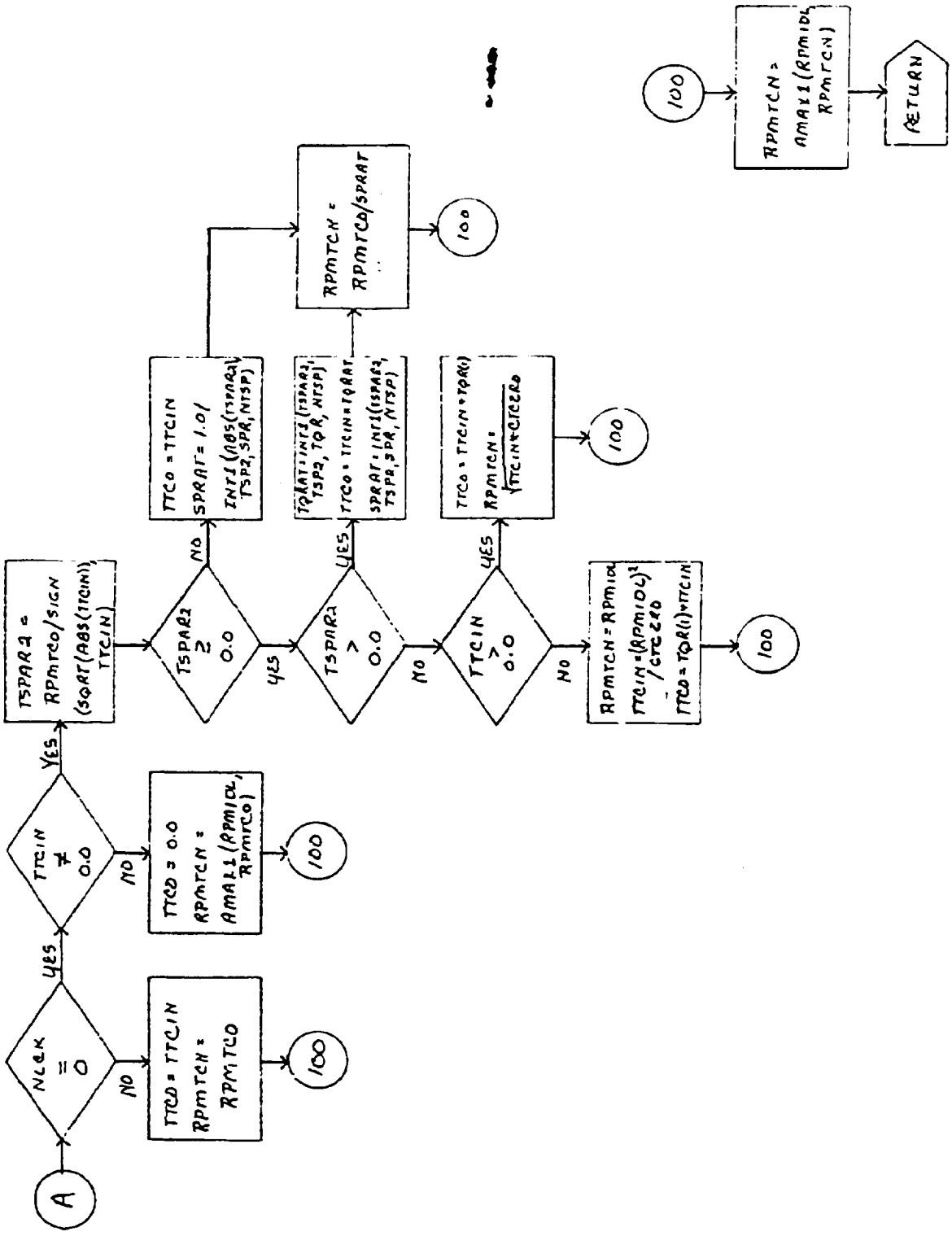
A
NLEK = 0
YES
NO
TTCD = TTCIN
RPMTCN = RPMTCO
100
TTCIN ≠ 0.0
YES
NO
TTCD = 0.0
RPMTCN = AMAX1(RPMICL, RPMTCO)
100
TSPAR2 = RPMTCO/SIGN (SQRT(ABS(TTCIN)), TTCIN)
TSPAR2 ≥ 0.0
YES
NO
TTCD = TTCIN
SPRAT = 1.0/INT1(ABS(TSPAR2), TSP2, SPR, NTSP)
TSPAR2 > 0.0
YES
NO
TQRAT = INT1(TSPAR2, TSP2, TQR, NTSP)
TTCD = TTCIN*TQRAT
SPRAT = INT1(TSPAR2, TSP8, SPR, NTSP)
TTCIN > 0.0
YES
NO
TTCD = TTCIN*TQR(1)
RPMTCN = √(TTCIN*CTE20)
RPMTCN = RPMICL
TTCIN = (RPMICL)²/CTE20
TTCD = TQR(1)*TTCIN
RPMTCN = RPMTCO/SPRAT
100
100
100
RPMTCN = AMAX1(RPMICL, RPMTCN)
RETURN

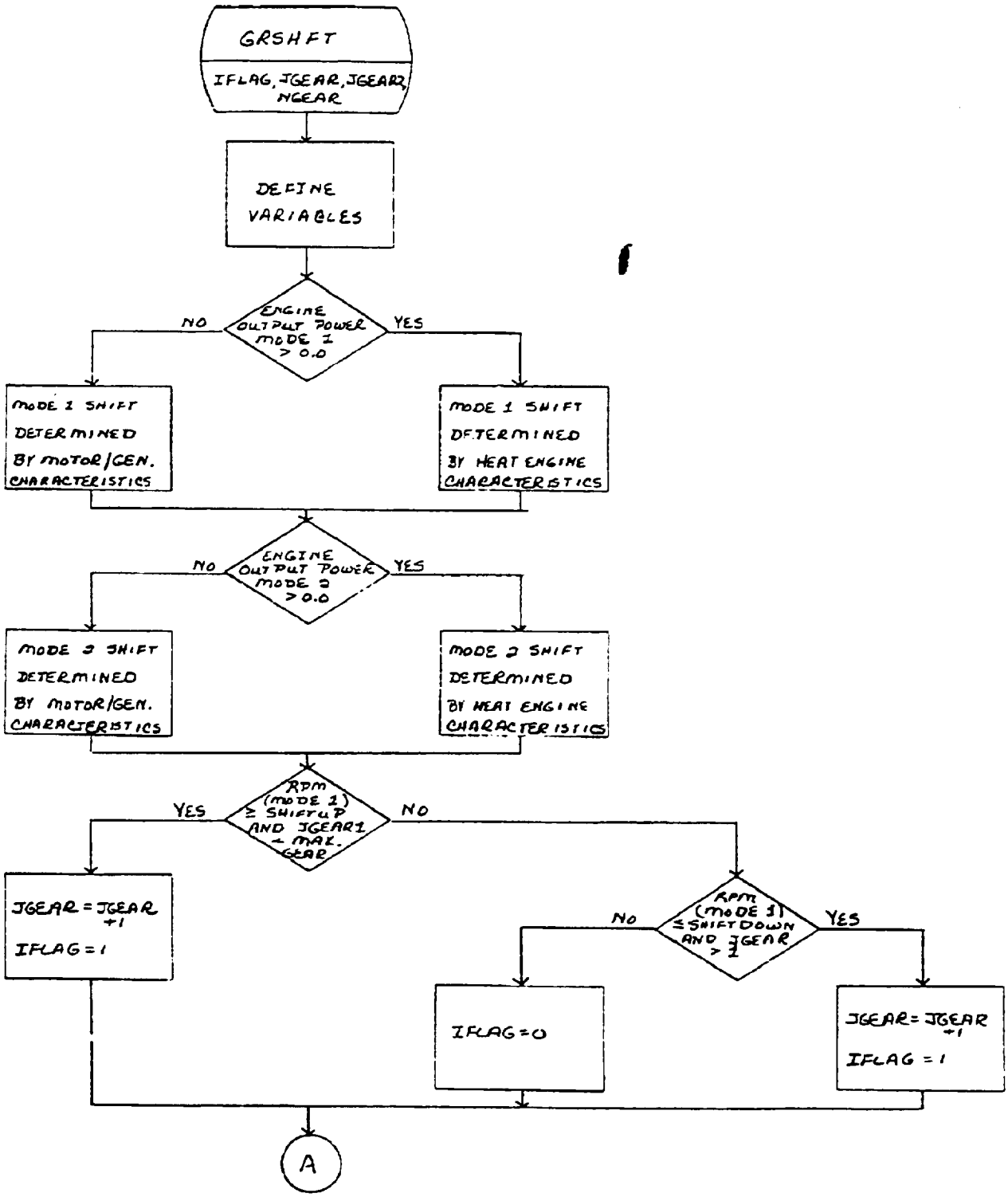
GRSHFT
IFLAG, JGEAR, JGEAR2, NGEAR
DEFINE VARIABLES
ENGINE OUTPUT POWER MODE 1 > 0.0
NO
YES
MODE 1 SHIFT DETERMINED BY MOTOR/GEN. CHARACTERISTICS
MODE 1 SHIFT DETERMINED BY HEAT ENGINE CHARACTERISTICS
ENGINE OUTPUT POWER MODE 2 > 0.0
NO
YES
MODE 2 SHIFT DETERMINED BY MOTOR/GEN. CHARACTERISTICS
MODE 2 SHIFT DETERMINED BY HEAT ENGINE CHARACTERISTICS
RPM (MODE 1) ≥ SHIFTUP AND JGEAR1 ≠ MAX. GEAR
YES
NO
JGEAR = JGEAR +1
IFLAG = 1
RPM (MODE 1) ≤ SHIFTDOWN AND JGEAR > 1
NO
YES
IFLAG = 0
JGEAR = JGEAR +1
IFLAG = 1
A

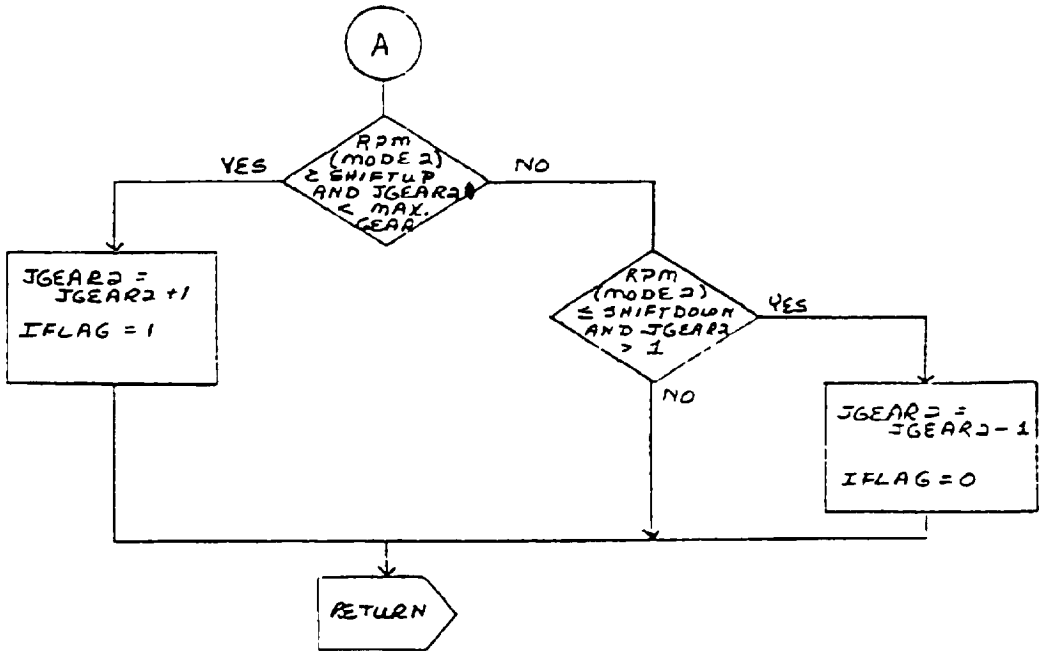
A
RPM (MODE 2) ≥ SHIFTUP AND JGEAR2 < MAX. GEAR
YES
NO
JGEAR2 = JGEAR2 + 1
IFLAG = 1
RPM (MODE 2) ≤ SHIFTDOWN AND JGEAR2 > 1
YES
NO
JGEAR2 = JGEAR2 - 1
IFLAG = 0
RETURN

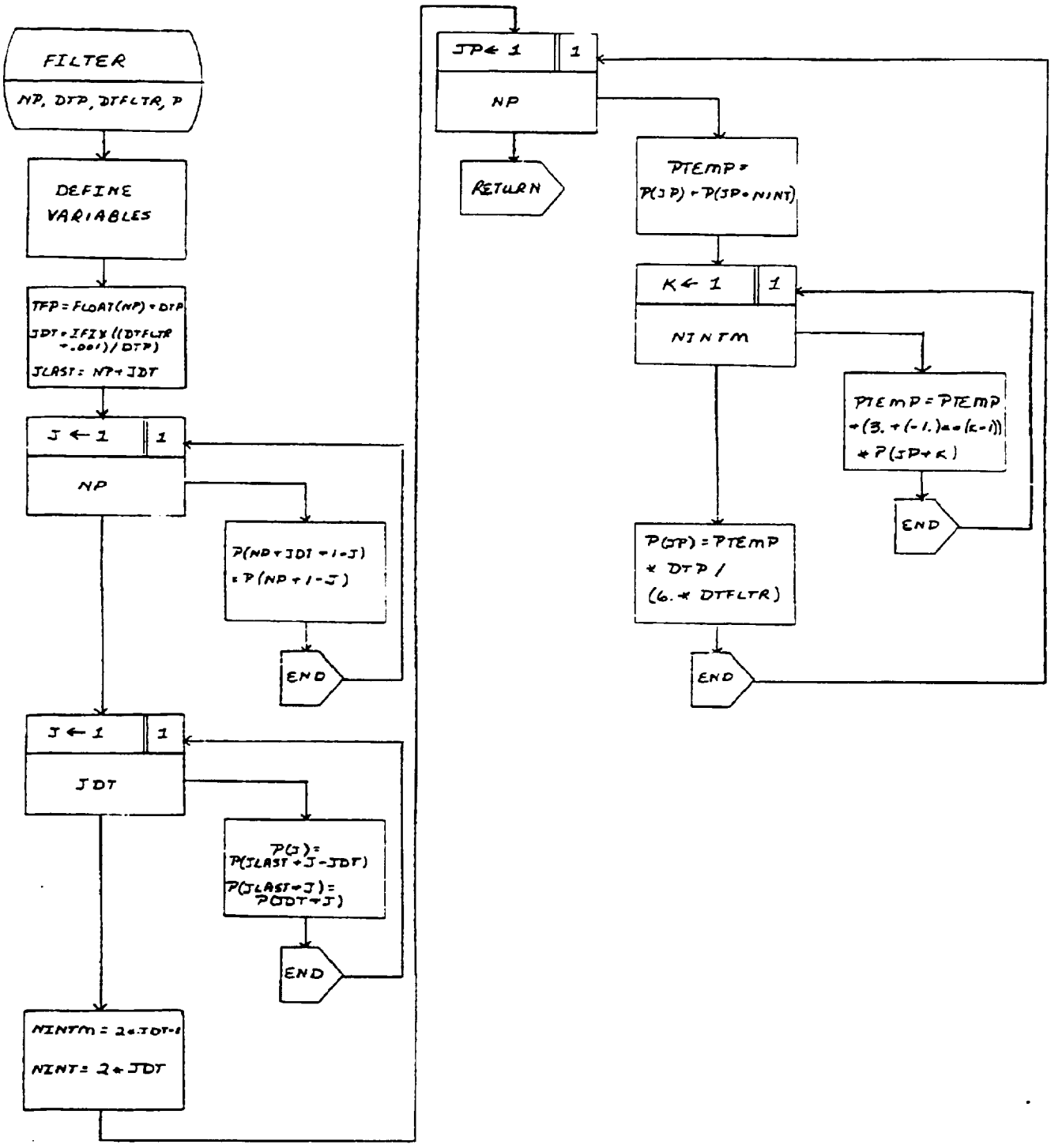
FILTER
NP, DTP, DTFLTR, P
DEFINE VARIABLES
TFP = FLOAT(NP) * DTP
JDT = IFIX ((DTFLTR -.001)/DTP)
JLAST = NP - JDT
J ← 1
1
NP
P(NP - JDT + 1 - J) = P(NP + 1 - J)
END
J ← 1
1
JDT
P(J) = P(JLAST + J - JDT)
P(JLAST + J) = P(JDT + J)
END
NINTM = 2 * JDT - 1
NINT = 2 * JDT
JP ← 1
1
NP
RETURN
PTEMP = P(JP) + P(JP + NINT)
K ← 1
1
NINTM
PTEMP = PTEMP + (3. + (-1.) ** (K-1)) * P(JP + K)
END
P(JP) = PTEMP * DTP / (6. * DTFLTR)
END

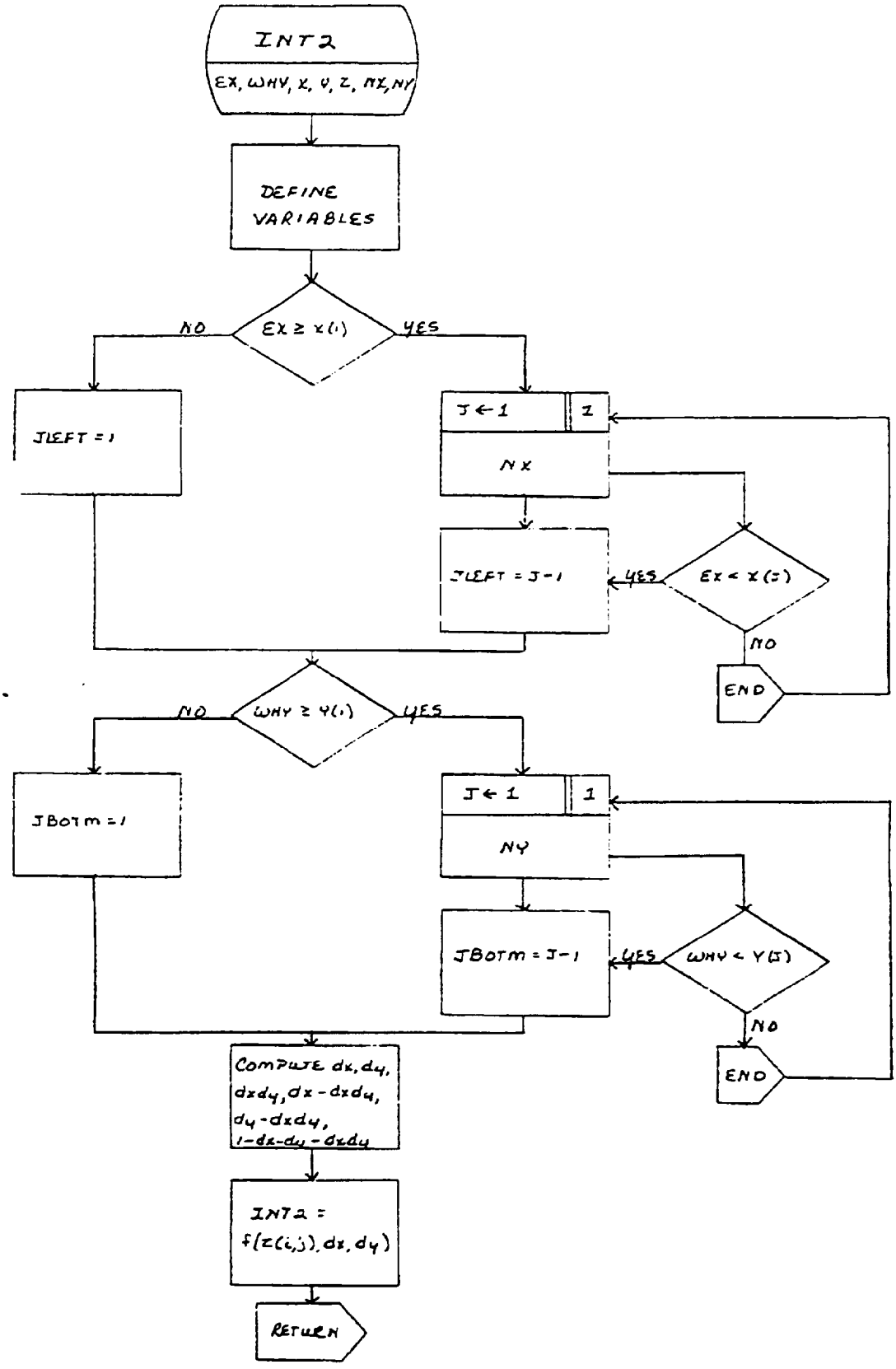
INT2
EX, WHY, X, Y, Z, NX, NY
DEFINE VARIABLES
EX ≥ X(1)
NO
YES
JLEFT = 1
J ← 1
1
NX
JLEFT = J-1
YES
EX < X(J)
NO
END
WHY ≥ Y(1)
NO
YES
JBOTM = 1
J ← 1
1
NY
JBOTM = J-1
YES
WHY < Y(J)
NO
END
COMPUTE dx, dy, dxdy, dx - dxdy, dy - dxdy, 1 - dx - dy - dxdy
INT2 = f(z(i,j), dx, dy)
RETURN

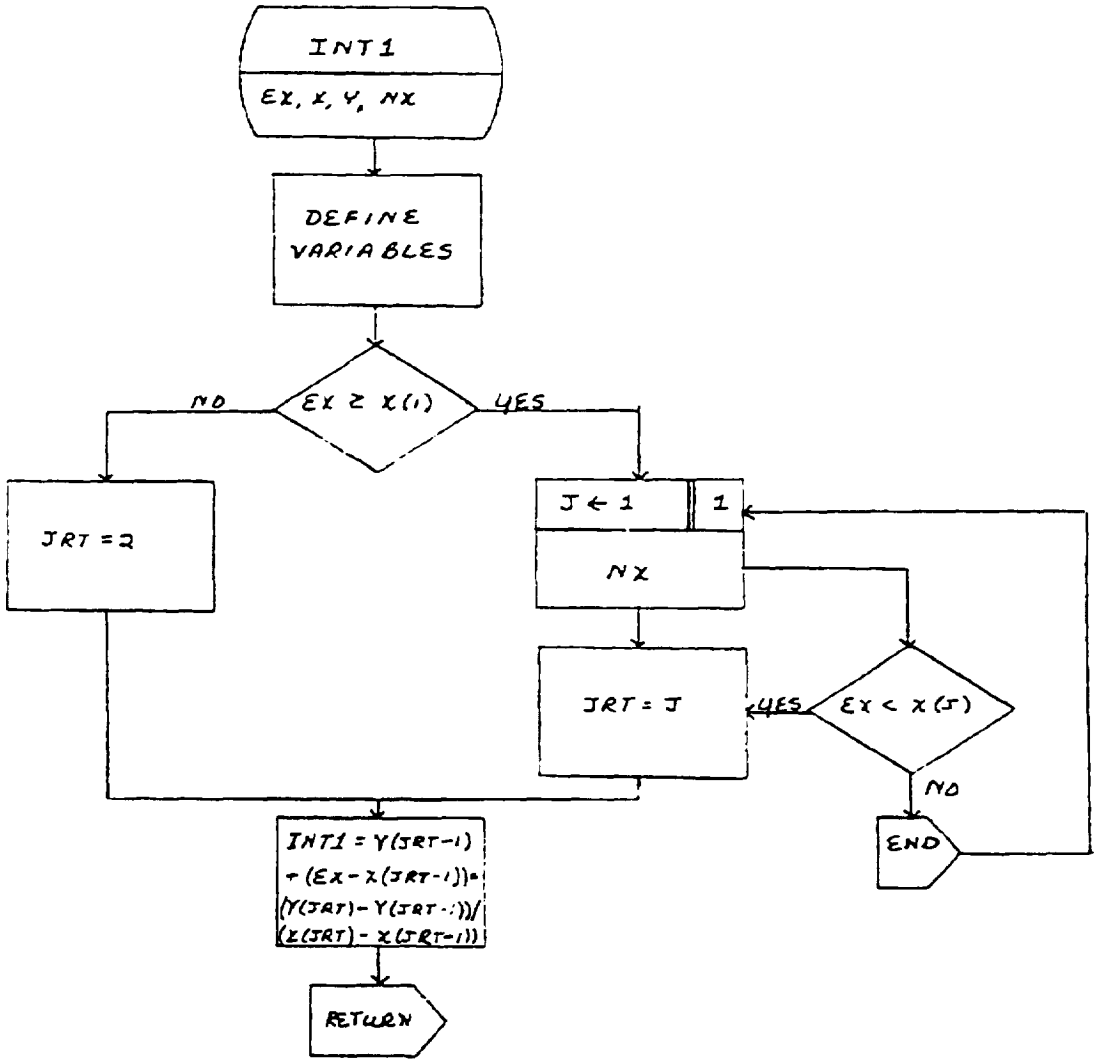
INT1
EX, X, Y, NX
DEFINE VARIABLES
EX ≥ X(1)
NO
YES
JRT = 2
J ← 1
1
NX
JRT = J
YES
EX < X(J)
NO
END
INT1 = Y(JRT-1) + (EX - X(JRT-1))* (Y(JRT) - Y(JRT-1))/ (X(JRT) - X(JRT-1))
RETURN

REFERENCES

1. Near Term Hybrid Vehicle Program, Phase I, Final Report, Jet Propulsion Laboratory Contract No. 955189, South Coast Technology, Inc., Sept., 1979.

2. Hybrid Vehicle Potential Assessment Interim Progress Report, Appendix C, Electric and Hybrid Cost Handbook, R. Heft, S. Heller, Draft #5030-162, Jet Propulsion Laboratory, Pasadena, CA.

3. C. Hu, "A Parametric Study of Power Mosfets," IEEE Power Electronics Specialist Conference, June, 1979.

4. E.O. Johnson, "Physical Limitations on Frequency and Power Parameter of Transistors," RCA Review, Vol. 26, pp. 163-177, June, 1965

5. P.L. Hower, J.B. Brewster, and M. Morozowich, "A New Method of Characterizing the Switching Performance of Power Transistors," 1978 Industrial Applications Conference Proceedings, pp. 1044-1049.

6. P.L. Hower, "Power Transistor Performance Tradeoffs," IEEE Power Electronics Specialist Conference, 1975.

7. S. Krishna and A.J. Yerman, "The Development of a Power Darlington Transistor and Hybrid Integrated Circuit for a DC to DC Converter," IEEE Power Electronic Specialist Conference, 1979, pp. 55-61.

8. Application Data, "Power Switching Transistors, D60T," Westinghouse, May, 1979.

9. W.E. Newell, "A Design Tradeoff Relationship Between Thyristor Ratings," IEEE Transaction on Industry Applications, pp. 397-405, July/August, 1976.

10. A. Abbondanti and P. Wood, "A Criterion for Performance Comparison Between High Power Inverter Circuits," IEEE Transactions on Industry Applications, pp. 154-160, March/April, 1977.

11. A.J. Humphrey, "Inverter Commutation Circuits," IEEE Transactions on Industry and General Applications, pp. 104-110, Jan./Feb., 1968.

12. P. Wood, "DC/AC Power Conditioning and Control Equipment for Advanced Conversion and Storage Technology," Final Report, EPRI Contract EM-271, November, 1976, Westinghouse Electric Corporation.

13. S.B. Dewan and D.L. Duff, "Optimum Design of an Input Commutated Inverter For AC Motor Control," IEEE Transactions on Industry and General Applications, pp. 699-705, Nov./Dec., 1969.

14. R.M. Davis, "Power Diode and Thyristor Circuits," IEEE Monograph Series 7, Copyright 1971, Peter Peregrinus Ltd. Publisher.

15. K.Y.G. Li, "New 3-Phase Inverter Circuit," IEEE Proceedings, Volume 115, No. 11, pp. 1677-1683, November, 1968.

16. S. Martinez and F. Aldana, "Current Source Double DC-Side Forced Commutated Inverter," IEEE Transactions on Industry Applications, pp. 581-593, Nov./Dec., 1978.

17. T. Kume and R.G. Hoft, "Thyristor DC Side Switch Inverter," IEEE Transactions on Industry Applications, pp. 257-277, May, June, 1972.

18. B.D. Bedford and R.G. Hoft, "Principles of Inverter Circuits," Copyright 1964, John Wiley and Sons, Inc.

19. W.T. McLyman, "Transformer and Inductor Design Handbook," Copyright 1978, Marcel Dekker, Inc.

20. P.B. Bhagwat, V. Stefanovic, "Some New Aspects in the Design of PWM Inverters," IEEE Industry Application Conference Proceedings, 1979, pp. 383-393.

21. Vendor Quote, SCR Cost Estimate and Production Capability, April, 1979, Westinghouse.

22. E.P. Cornell, R.H. Guess and F.G. Turnbull, "Advanced Motor Developments for Electric Vehicles," IEEE Transactions on Vehicular Technology, Vol. VT-26, No. 2, May, 1977, pp. 128-134.

23. "Near Term Electric Vehicle Program, Phase I," Final Report, General Electric Corporate Research and Development, August, 1977, Contract EY-76-C-03-1294.

24. Technical Data, ISOSYN Motors, Brown Broveri Corporation, Technical Bulletin FME 902E, 9/79.

25. MA. Rahman, "High Efficiency Permanent Magnet Synchronous Motors," Industrial Applications Conference Proceedings, 1979, pp. 561-564.

26. W. Volkrodt, "Machines of Medium-High Rating with a Ferrite Magnet Field," Siemens Review XLIII, 1976, No. 6, pp. 248-254.

27. A.B. Plunkett, F.G. Turnbull, "Load Commutated Inverter/Synchronous Motor Drive Without a Shaft Position Sensor," General Electric Report No. 78CRD020.

28. G.W. McLean and S.R. Alwash, "Performance and Design of Induction Motors with Square Wave Excitation," Proc. IEEE, Vol. 116, No. 8, August, 1969, pp. 1405-1411.

29. E.E. Ward and H. Harer, "Preliminary Investigation of an Inverter-Fed Five Phase Induction Motor, Proc. IEEE, Vol. 116, No. 6, June, 1969, pp. 980-984.

30. J.E. Long, "Optimum Stator Windings for Inverter Driven Induction Motors," Master Thesis, University of Missouri.

31. A. Abbondanti, M.B.Brennen, "Variable Speed Induction Motor Drives Using Electronic Slip Calculator Based on Motor Voltages and Currents" IEEE Transactions on Industry Applications, Sept./Oct., 1975.

1. Report No.	2. Government Accession No.	3. Recipient's Catalog No.
NASA CR-159773		

4. Title and Subtitle	5. Report Date
Advanced Hybrid Vehicle Propulsion System Study	May 1982
	6. Performing Organization Code 778-36-06
7. Author(s)	8. Performing Organization Report No.
Robert Schwarz	
9. Performing Organization Name and Address	10. Work Unit No.
South Coast Technology, Inc. Ann Arbor, Michigan	11. Contract or Grant No. DEN 3-93
12. Sponsoring Agency Name and Address	13. Type of Report and Period Covered Contractor Report
U. S. Department of Energy Office of Vehicle and Engine R&D Washington, D. C. 20545	14. Sponsoring Agency Code Report No. DOE/NASA/0093-1

15. Supplementary Notes

Final report. Prepared under Interagency Agreement DE-AI01-77CS51044. Project Manager, Miles O. Dustin, Transportation Propulsion Division, NASA Lewis Research Center, Cleveland, Ohio 44135.

16. Abstract

Results are presented of a study of an advanced heat engine/electric automotive hybrid propulsion system. The system uses a rotary stratified charge engine and an ac motor/controller in a parrallel hybrid configuration. The three tasks of the study were (1) parametric studies involving five different vehicle types, (2) design trade-off studies to determine the influence of various vehicle and propulsion system parameters on system performance fuel economy and cost, and (3) a conceptual design establishing feasibility of the selected approach. Energy consumption for the selected system was .034 l/km (61.3 mpg) for the heat engine and .221 kWh/km (.356 kWh/mi) for the electric power system over a modified J227a schedule D driving cycle. Life cycle costs were 7.13 ¢/km (11.5 ¢/mi) at $2/gal gasoline and 7 ¢/kWh electricity for 160,000 km (100,000 mi) life.

17. Key Words (Suggested by Author(s))	18. Distribution Statement
Electric Hybrid Automotive battery	Unclassified - unlimited STAR Category 85 DOE Category UC-96

19. Security Classif. (of this report)	20. Security Classif. (of this page)	21. No. of Pages	22. Price*
Unclassified	Unclassified	330	A15

* For sale by the National Technical Information Service, Springfield, Virginia 22161